THÈSE POUR OBTENIR LE GRADE DE DOCTEUR DE L'UNIVERSITÉ DE MONTPELLIER

En Informatique et sciences du vivant

École doctorale I2S Information Structures Systèmes

Unité de recherche Laboratoire d'Informatique, de Robotique et de Microélectronique de Montpellier

Micro-Imaging with Micro-CT and High-Field MRI for Post-Mortem Fetal Anatomy in the First Trimester: Advancing Toward Clinical Application

Présentée par Audrey LAMOUROUX

Le 11 avril 2025

Sous la direction de Guillaume CAPTIER et Christophe GOZE BAC

Devant le jury composé de

Sophie COLLARDEAU-FRACHON, PUPH, Institut de pathologie multisite, HCL	Présidente du jury
Owen ARTHURS, Professor of radiology, Great Ormond Street Hospital, London	Examinateur
Christophe FIORIO, PU, ICAR LIRMM, UM	Examinateur
Gérard SUBSOL, Chargé de recherche CNRS, ICAR, LIRMM, CNRS, UM	Encadrant
Alexandra BENACHI, PUPH, Université Paris Saclay	Rapporteure
Emmanuel BRUN, Directeur de recherche, INSERM UA7 STROBE, Grenoble	Rapporteur
Guillaume CAPTIER, PUPH, Laboratoire d'anatomie Faculté de médecine Montpellier, UM	Directeur de thèse
Christophe GOZE-BAC, Directeur de recherche CNRS, L2C, BNIF, CNRS, UM	Co-directeur de thèse

UNIVERSITÉ DE MONTPELLIER

TABLE OF CONTENTS

Accessible Summary for the General Public 7

Summary 8

Graphical abstract 10

General Introduction 11

1. Introduction to fetal medicine and prenatal diagnosis 11
2. Fetal Post-Mortem Examination 14
3. Fetal Post-Mortem Examination Acceptance 15
4. Post-Mortem imaging techniques 16
5. Post-Mortem micro-imaging techniques 17
6. Other recent high-resolution imaging techniques 18
7. Objectives of the thesis 18

Part I - Current state of Post-Mortem fetal imaging 20

1. Introduction 20
2. Historical background 21
3. Conventional clinical imaging techniques 23
   - **A) Post-Mortem Radiographs** 23
   - **B) Post-Mortem Computed Tomography** 24
   - **C) Post-mortem Magnetic Resonance Imaging** 24
   - **D) Post-mortem Ultrasound** 25
4. Higher resolution imaging techniques 25
   - **A) Micro Computed Tomography** 26
   - **B) High-field Magnetic Resonance Imaging** 30
5. Autopsy in addition to Less Invasive Autopsy 32
6. Tissue sampling following early pregnancy loss. 32
7. Challenges for implementation 33
8. Future directions, other developments 35
9. Conclusions 35

Part II - Methodology - Sample preparation _____ 36

1. FETTAL Project _____ 37

2. Staining bath comparison _____ 39

A) Introduction **39**

B) Methods **39**

a. Micro-CT acquisition and post-treatment 39
b. Staining protocols 39
c. Staining protocol choice: blind qualitative comparison. 41
d. Staining protocol choice: quantitative comparison. 41

C) Results **42**

D) Discussion **44**

E) Conclusion **45**

3. Staining agent diffusion and staining bath duration. _____ 46

A) Background **46**

B) Methods **47**

a. Inclusion criteria and ethics 47
b. Dice-Micro-CT acquisition and post-treatment 47
c. Dynamical study of the staining agent diffusion and its quantification. 48
d. Modelling Signal Evolution Using Stretched Exponential and Double stretched exponential 49
e. Staining time according to fetal size 49

C) Results **51**

a. Dynamical study of the staining agent diffusion and its quantification. 51
b. Staining bath duration according to the fetal characteristics 55

D) Discussion **56**

E) Conclusion **58**

Part III - Micro-imaging for studying fetal anatomy _____ 59

1. Micro-imaging at 8 weeks of gestation. _____ 59

A) Introduction **59**

B) Methods **62**

a. Micro-CT 62
b. HF-MRI 63
c. Image processing 64
d. Histology sections 66

C) Results **66**

a. Micro-imaging 66
b. Histology 70

D) Discussion **71**

2. Micro-imaging at 12 weeks of gestation. _____ 75

A) Method **75**

a. Micro-CT 75
b. HF-MRI 76
c. Image processing 77
d. Statistical Analysis 78

B) Results 78

C) Discussion 84

Part IV - Post-mortem Micro-CT : Clinical applications and insights. 86

1. Introduction 86
2. Methods 88

A) Study design 88

B) Procedures and definitions 88

C) Fetal Post-Mortem Examination contribution to the diagnosis 89

D) Micro-CT Imaging protocol 90

E) Conventional autopsy 90

F) Statistical Analysis 91

3. Results 91

A) Performance times 94

B) Fetal Post-Mortem Examination contribution 94

C) Micro-CT contribution 95

D) Overall contribution and cause of death 98

4. Discussion 101
5. Conclusion 103

General discussion 104

1. Summary of findings 104
2. Future development 106

A) Research 106

B) Clinical application in France 107

3. Shifting paradigms in genetics. 109

Conclusion 111

Thèse en français : Micro-imagerie par Micro-TDM et IRM à haut champ pour l'étude anatomique post-mortem du fœtus humain au premier trimestre vers une utilisation en fœtopathologie. 112

Résumé de thèse vulgarisé pour le grand public 113

Résumé de la thèse 114

Résumé Substantiel Introduction générale 116

Partie I - État des connaissances de l'imagerie fœtale post-mortem. 119

1. Les techniques d'imagerie conventionnelle 119
2. Les techniques d'imagerie à haute résolution 119

Partie II - Méthodologie – préparation des échantillons avant Micro-TDM 121

1. Le projet FETTAL 121
2. Comparaison des bains de contraste 121
3. Diffusion du contraste et durée des bains de contraste. 121

Partie III - Micro-imagerie pour étude de l'anatomie fœtale 123

1. Micro-imagerie à 8 SA 123
2. Micro-imagerie à 12 SA 124

Partie IV - Micro-TDM Post-mortem : application clinique. 125

Conclusion 127

Abbreviations 128

References 129

Tables and Figures 141

Annexe 1 146

Simcock IC, Lamouroux A, Sebire NJ, Shelmerdine SC & Arthurs OJ. Less-invasive autopsy for early pregnancy loss. Prenatal Diagnosis 2023. Jun 1;43(7):937–49. 146

Annexe 2 _____ 160

Lamouroux A, Cardoso M, Bottero C, Fuchs F, Mousty E, Genevieve D, Subsol G, Goze-Bac C & Captier G. Modelling of staining in post-mortem diffusible iodine-based contrast enhanced (Dice) micro-CT imaging of non-macerated first-trimester human fetuses submitted in BMC Medical Imaging _____ 160

Annexe 3 _____ 182

Lamouroux A, Cardoso M, Bottero C, Gallo M, Duraes M, Salerno J, Bertrand M, Rigau V, Fuchs F, Mousty E, Genevieve D, Subsol G, Goze-Bac C, & Captier G. Micro-CT and high-field MRI for studying very early post-mortem human fetal anatomy at 8 weeks of gestation. Prenat Diagn 2024; 44: 3–14. _____ 182

Annexe 4 _____ 195

Simcock IC, Lamouroux A, Shelmerdine SC, Sebire NJ, Hutchinson CJ & Arthurs OJ. Fetal post-mortem imaging using microfocus computed tomography: single centre retrospective clinical experience. Submitted in American Journal of Obstetrics and Gynecology _____ 195

ACCESSIBLE SUMMARY FOR THE GENERAL PUBLIC

In cases of fetal death, whether spontaneous or induced by serious conditions, post-mortem examinations help couples understand the risk of recurrence. Less-invasive imaging-based approaches are generally better accepted than conventional autopsy due to its invasiveness. Unlike conventional post-mortem imaging techniques, micro-Computed tomography (CT) and high-field MRI (>3 Tesla) offer isotropic resolution <100 μm suitable for exploring fetal anatomy as early as the first trimester. Before micro-CT scanning, the fetus is immersed in iodine baths for a duration tailored to its size. Micro-CT provides superior contrast images compared to MRI, though tissue shrinkage may occur, requiring specific biometric standards. In clinical practice, comprehensive post-mortem exploration using micro-CT leads to accurate diagnoses in 51% of cases and reduces the need for conventional autopsy by 96%.

SUMMARY

In cases of fetal death, whether spontaneous (miscarriage or *in utero* death) or induced due to serious conditions (termination of pregnancy) such as congenital malformations (3.2% of pregnancies), conventional autopsy remains the gold standard for determining the cause of death. However, its invasive nature often leads to parental refusal. This thesis aims to explore the use of Micro-CT and High-Field MRI for post-mortem fetal imaging in the first trimester, providing detailed anatomical insights and advancing toward clinical application.

This thesis begins by reviewing the current state of less-invasive fetal autopsy (***Simcock IC, Lamouroux A, et al. Less-invasive autopsy for early pregnancy loss. Prenat Diagn. 2023 Jun 1;43(7):937–49.***). Conventional post-mortem (PM) imaging techniques - radiography, CT, MRI, and ultrasound - offer limited diagnostic accuracy before 20 weeks of gestation (WG). In contrast, advanced micro-imaging techniques, such as micro-CT (MCT) and high-field MRI (HF-MRI) using a magnetic field strength exceeding 3 Tesla provide an isotropic resolution under 100 µm and superior visualization of early pregnancy losses.

The second part outlines a methodology for enhancing image quality in MCT imaging by modelling the staining diffusion process and optimizing sample preparation prior to MCT acquisition (***Lamouroux A, et al. Modelling of staining in post-mortem diffusible iodine-based contrast enhanced (Dice) micro-CT imaging of non-macerated first-trimester human fetuses submitted in BMC Medical Imaging***). Our study examined diffusible iodine-based contrast-enhanced (Dice) staining solution, composed of 4% paraformaldehyde and Lugol's iodine (63.25 mg/ml total iodine content) in a 1:1 ratio. Contrast diffusion follows a stretched exponential model, except in the liver. The optimal staining duration - ensuring a contrast-to-noise ratio exceeding 5 (Rose criterion) – varies by fetal size, such as crown-rump length (CRL) or weight. For instance, a non-macerated fetus with a 50 mm CRL or 20 g weight requires at least 96 hours of staining for optimal contrast. Tailoring staining duration based on fetal size maximizes imaging quality.

MCT and HF-MRI are used in the third part to assess critical anatomical structures at 8 and 12 WG (***Lamouroux A, et al. Micro-CT and high-field MRI for studying very early post-mortem human fetal anatomy at 8 weeks of gestation. Prenat Diagn. 2024 Jan;44(1):3–14***). Dice MCT provided superior contrast compared to MRI at 8 WG, while biometric standards were established at 12 WG to account for tissue shrinkage. Given its higher resolution and diagnostic value, MCT appears better suited for clinical application than HF-MRI.

The fourth part offers valuable perspectives on the future integration of PM-MCT into routine clinical practice and less-invasive autopsy. This large-scale clinical study involves over 1,000 fetuses with an average turnaround time of under 21 days (***Simcock IC, Lamouroux A, et al. Fetal post-mortem imaging using microfocus computed tomography: single centre retrospective clinical experience, submitted in American Journal of Obstetrics and Gynecology)***. A cause of death was identified in 47% of cases - 21% fetal-related and 26% placental - while 49% remained unexplained, particularly in in *utero* deaths (69%) and severely macerated cases (86%). Integrated routine external examination (diagnostic contributor in 21% of cases), placental analyses (35%), and MCT imaging (19%) led to a 96% autopsy avoidance rate, in line with parental consent.

In conclusion, while conventional autopsy remains the gold standard, its invasiveness often limits acceptance. Less invasive autopsy, using Dice MCT and HF-MRI with optimized sample preparation, enables high-resolution fetal imaging even in early gestation. Combining MCT with external and placental examinations significantly reduced the need for conventional autopsy, while maintaining high parental consent rates.

GRAPHICAL ABSTRACT

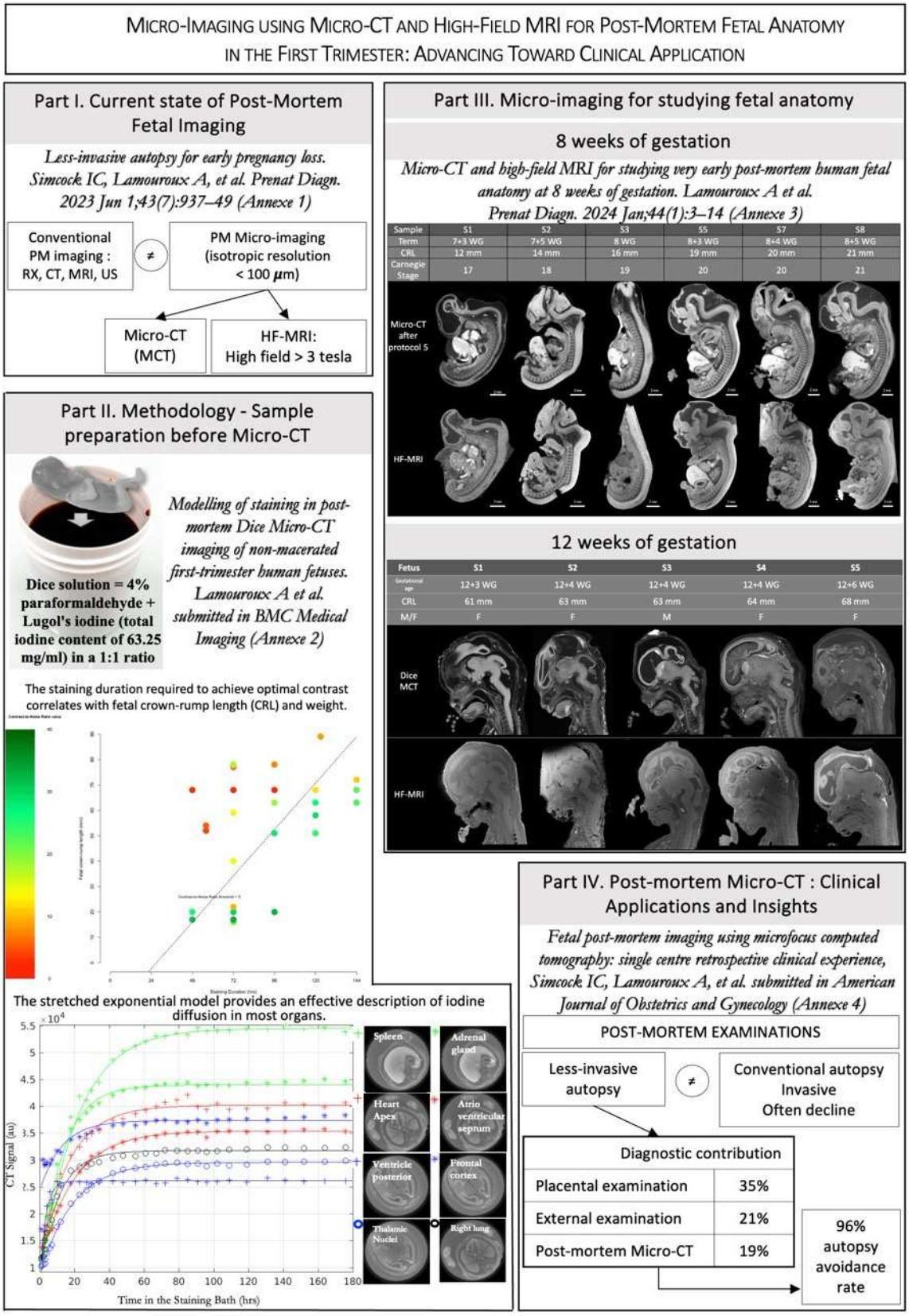

GENERAL INTRODUCTION

1. Introduction to fetal medicine and prenatal diagnosis

Fetal medicine encompasses multidisciplinary clinical, biological, and imaging-based medical practices dedicated to diagnosing, assessing prognosis, and, when possible, treating conditions that may significantly impact the health and development of the fetus or unborn child[1]. The detection of congenital malformations is a significant public health concern, as these anomalies account for 3.2% of births in France[2]. Globally, the World Health Organization estimates that congenital anomalies contribute to approximately 10% of neonatal deaths[3].

During the pregnancy, non-invasive imaging modalities such as ultrasound (US), magnetic resonance imaging (MRI), and computed tomography (CT) can be used to assess fetal development and maternal health. From the landmark 1958 publication in the *Lancet* by Ian Donald[4], US technology has undergone remarkable advancements, including real-time imaging, transvaginal sonography, colour and power Doppler (Figure GI.1), 3D and video (4D) imaging (Figure GI.2). These innovations have greatly enhanced diagnostic capabilities, particularly in the first trimester[5,6]. Similarly, fetal MRI has evolved significantly since its initial applications in the 1980s, offering improved resolution and anatomical detail[7].

Figure GI.1 – Ultrasound scan at 12+1 weeks of gestation (WG) highlighting crown-rump length (CRL) and nuchal translucency measurement as well as morphological evaluation of cephalic pole with plexus choroids, heart using colour doppler, femoral length and foot (Dr Lamouroux)

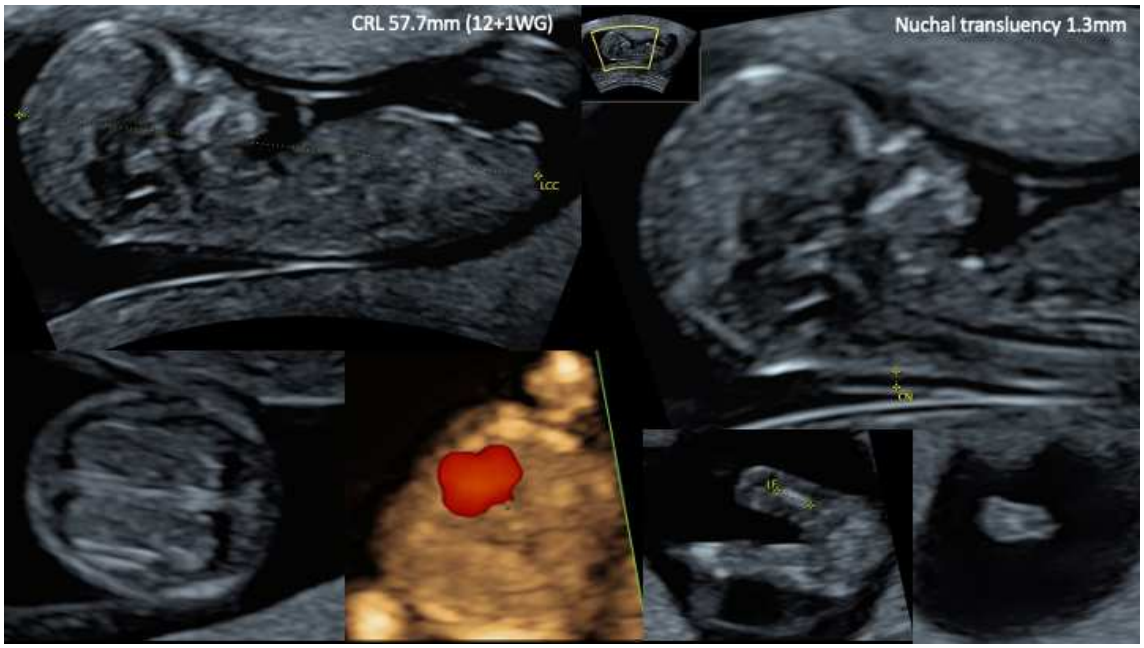

Figure GI.2 – Ultrasound scan using 3D imaging at 12+6 weeks of gestation (Dr Lamouroux)



In France, three screening US are recommended for pregnant women at low risk, typically performed around 12, 22, and 32 weeks of gestation (WG)[8]. The first-trimester US, performed around 12 WG, primarily serves to date the pregnancy using crown-rump length (CRL) measurement and to assess nuchal translucency as part of trisomy 21 screening (Figure GI.1). Advances in imaging technology have significantly improved examination quality, enabling earlier and more detailed morphological assessments (Figure GI.1). As a result, major congenital anomalies, such as anencephaly, holoprosencephaly, and severe congenital heart defects, can now be detected at this stage[9,10]. In parallel, breakthroughs in genetic testing, including next generation sequencing (NGS), have further enhanced early diagnostic precision[11,12].

In France, termination of pregnancy (ToP) for fetal reason (FR) may be performed at any gestational age if two specialists from a center for prenatal diagnosis and counselling confirm a high probability that the fetus has a particularly serious and currently incurable condition[13]. In 2016, such conditions were certified in 9.1 per 1,000 pregnancies[14].

During the discussion about ToP for FR, the medical team may recommend a fetal post-mortem examination (FPME) to further investigate fetal abnormalities[13]. This FPME may also be indicated in case of severe obstetric complications, such as *in utero* death (IUD) or miscarriage, with the obstetrician proposing it to investigate the causes of death and provide insights for genetic counselling and future pregnancies[15].

2. Fetal Post-Mortem Examination

The FPME protocol[15–17] includes a systematic series of diagnostic procedures, beginning with post-mortem (PM) standard radiography of the fetus and, if necessary, complementary imaging such as US[18], CT scan, or MRI[15]. Photographs are also taken to document external features. The external examination (EE)[19] involves a detailed evaluation of dysmorphism, biometric measurements, including weight, crown-rump length, crown-heel length, head circumference and foot length, and the evaluation of external malformations with special attention to craniofacial structures such as the mouth, palate, choanal, eyes and extremities abnormalities (Figure GI.3). The internal examination, or conventional autopsy (CA), consist of a thorough macroscopic analysis of fetal organs, detailing their position, situs, potential malformations, and weight, along with histological sampling of key organs such as heart, lungs, thymus, liver, spleen, kidneys, and brain (Figure GI.3). Additionally, placental examination provides crucial insights into fetal pathology[20–22].

FPME is the gold standard for clarifying the fetal phenotype, enhancing prenatal diagnoses, informing genetic counselling to assess recurrence risks (Figure GI.3), and recommending diagnostic strategies for future pregnancies[15–17,23]. However, autopsy at early gestational age is challenging due to rapid tissue degradation and microdissection. In some cases, delaying ToP for a few weeks may be considered to improve the like hood of obtaining useful histopathological and genetic data, ultimately benefiting genetic counselling. In case of ToP between 11 and 16WG, autopsy results modified genetic counselling in 20.6% of cases[23,24]. Conversely, first-trimester miscarriages before 14WG remain largely unexplored due to the frequent tissue loss, small fetal size, and logistical constraints[25–27].

Figure GI.3 – Illustrative clinical case of a fetal post-mortem examination
A- Prenatal ultrasound imaging (2D and 3D) at 25+5 weeks of gestation (WG) highlighting suspected arthrogryposis with reduced fetal movements and bilateral club feet. Further assessment at 27+1 WG highlighted severe camptodactyly (Dr Frédéric Richard)
B- External examination confirming arthrogryposis. (Dr Audrey Lamouroux)
C- Macroscopic neuropathological examination revealing porencephaly (black arrow) and unilateral ventriculomegaly (white arrowhead) (Dr Constance Wells)
This phenotype prompted whole-exome sequencing, which identified a probably pathogenic variant (ACMG class 4) in the *HECW2* gene, known to cause neurodevelopmental disorder with hypotonia, seizures, and absent language.

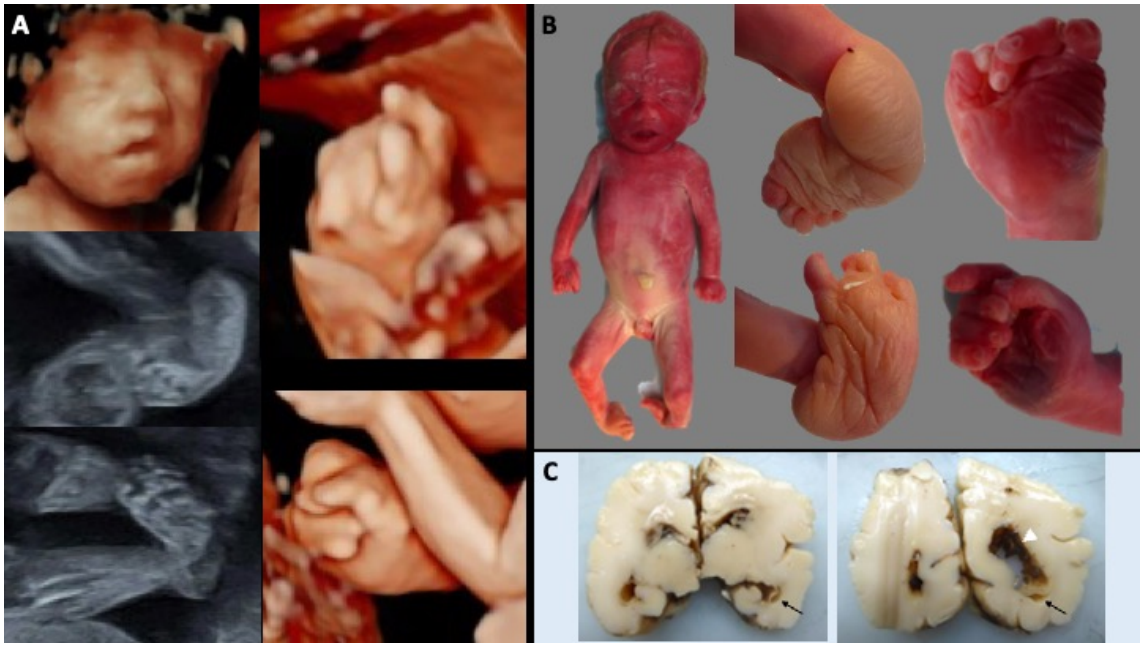

3. Fetal Post-Mortem Examination Acceptance

The acceptance of FPME is influenced by multiple factors, including the type of stillbirth[28], the parental medical history – particularly whether it is a first event or a recurrent pregnancy loss [29] – and personal motivations. Parents may seek autopsy to exclude self-blame[28], while others decline it to avoid funeral delays[30]. Contributions to medical knowledge[31] can also be an important consideration for some families. Religious beliefs[29], cultural barriers, and public perception, particularly in response to media scandals[32], may also play a role. In addition, the way the medical team recommends the conduct of an autopsy is crucial. Factors such as the time spent[33] explaining the procedure, the training and expertise of the staff in prenatal diagnosis[30],

and the organization of the hospital—such as whether the fetus must be transferred to another facility for the autopsy[34]—can all affect parental decisions.

To address these challenges, less-invasive autopsy (LIA) has been introduced, significantly improving acceptance compared to CA[35]. LIA using PM imaging techniques offers multiple benefits, including non-invasiveness, rapid and reproducible data acquisition, and reduced operator-dependent variability. Additionally, PM imaging enables high-quality brain visualization, minimizing technical artifacts seen in traditional dissection[36–38].

4. Post-Mortem imaging techniques

Since 2010, PM fetal imaging has been studied by comparing PM-CT and PM-MRI with superior diagnostic accuracy using PM-MRI[39,40], particularly for maceration[41] and distinguishing between intrauterine and neonatal deaths[42,43]. Research indicates that in 41% of cases, CA was unnecessary when PM-MRI was performed, achieving a diagnostic rate exceeding 99%[44]. However, the diagnostic accuracy of PM-MRI[36,37] varies by anatomical region.

For extra-cardiac thoracic abnormalities, PM-MRI has a sensitivity of 39.6% and a specificity of 85.5%, with limited effectiveness in detecting pulmonary infections[45]. For abdominal abnormalities, PM-MRI offers better accuracy, with sensitivity and specificity of 72.5% and 90.8%, respectively[46]. Agreement rates between PM-MRI and CA are high: 92.2% for neurological abnormalities, 93.7% for thoracic, 91.1% for musculoskeletal, and 89.4% for abdominal abnormalities[47]. When prenatal US findings align with whole-body PM-MRI results, the need for CA is minimal[48]. Moreover, the calculation of volume ratios obtained by semi-automated methods in MRI correlates well with weight ratios in autopsy [49]. However, PM-MRI and PM-CT still face limitations, particularly in early gestations[44,50,51] especially under 24 WG[39,52]. The resolution of these imaging modalities is insufficient to provide reliable results at this stage of development.

PM-US is a highly accessible technique that enables detailed visualization of many common malformations[53–55]. The rate of non-diagnostic FPME with PM-US is higher before 20 WG[56], higher than PM-MRI[57,58] and correlates with maceration, particularly for cardiac and cerebral assessments, whereas the delay between delivery and FPME does not[59]. When PM-US quality is compatible with diagnostic, the diagnostic rate is similar to PM-MRI[57,58].

5. Post-Mortem micro-imaging techniques

To address these challenges, micro-imaging techniques with an isotropic resolution of <100 µm have been developed: high-field MRI (HF-MRI), and Micro-CT (MCT)[41,51,52,60–63]. MCT, initially used for human bone evaluation in 1989[64], has become an essential tool in research[65–67] and clinical applications[61,68]. It offers rapid image acquisition, cost-effectiveness, and an isotropic resolution as fine as 10 µm[52,69–71]. Both clinical CT and MCT rely on X-ray attenuation principles, where an X-ray source and detectors are positioned on opposite sides of the specimen. In MCT, the X-ray components rotate around the stationary subject, or the specimen can be rotated while the X-ray components remain static. Highly detailed images are obtained by capturing X-ray projections at multiple angles, and processing them using advanced algorithms into detailed 3D tomographic images[63,69].

HF-MRI, with magnetic field strengths exceeding 3 Tesla, enables submillimetre spatial resolution[52,62] in the three directions (isotropic) and provides excellent spontaneous soft-tissue contrast[52], making it a valuable alternative for fetal imaging. In recent applications of MCT in PM fetal imaging, the technique has demonstrated high diagnostic yield, with a 97.5% agreement with CA findings before 20 WG[60]. Additionally, MCT eliminated the need for CA in 86.9% of cases and provided additional findings in 81.9% of cases, particularly in cardiac, soft-tissue, and genital anomalies[61].

These advancements in PM micro-imaging technologies highlight the growing potential of less invasive and high-resolution alternatives to conventional FPME.

6. Other recent high-resolution imaging techniques

High-resolution imaging in biological fundamental research have seen the development of three advanced modalities revolutionizing the field.

Phase-contrast X-ray imaging using synchrotron technology enhances the visibility of soft biological tissues by exploiting the phase shifts of X-rays passing through the sample, rather than relying solely on absorption differences[72]. It also reach an histological resolution as shown on placenta[73], heart[74], lung[72] or osteo articular view of a cadaveric hand[75].

Light-sheet microscopy uses a thin sheet of laser light to illuminate samples and a perpendicular objective to collect fluorescence, enabling high-speed, high-resolution imaging with minimal photodamage[76]. It is particularly valuable for visualizing dynamic biological processes in vivo, from subcellular structures to whole-organism development[76] such as zebrafish embryo development[77,78].

Cryogenic contrast-enhanced micro-CT combines sample staining with a contrast-enhancing agent and freezing at an optimal rate to enable high-resolution 3D visualization of soft biological tissues, leveraging the segregation between the contrast agent and water upon ice crystallization[1,2]. This technique is applied to various tissues, including muscle, tendon, cardiac[79], and kidney tissues[80], providing detailed structural analysis and detecting pathology-induced microstructural changes while preserving tissue integrity and avoiding shrinkage and deformation.

7. Objectives of the thesis

This thesis aims to explore the use of Micro-CT and High-Field MRI for post-mortem fetal imaging in the first trimester, providing detailed anatomical insights and advancing toward clinical application.

This thesis begins by reviewing the current state of less-invasive fetal autopsy, focusing on both conventional and high-resolution PM imaging techniques (*Simcock IC, Lamouroux A,*

Sebire NJ, Shelmerdine SC, Arthurs OJ. Less-invasive autopsy for early pregnancy loss. Prenat Diagn. 2023 Jun 1;43(7):937–49.)

The second part outlines a methodology for enhancing MCT image quality by modelling the staining diffusion process and determining the optimal duration of contrast baths tailored to fetal size (*A. Lamouroux, et al. Modelling of staining in post-mortem diffusible iodine-based contrast enhanced (Dice) micro-CT imaging of non-macerated first-trimester human fetuses submitted in BMC Medical Imaging*).

MCT and HF-MRI are used in the third part to assess critical anatomical structures at 8 and 12 WG, evaluating their visualization and measurement accuracy (*Lamouroux A, Cardoso M, Bottero C, et al. Micro-CT and high-field MRI for studying very early post-mortem human fetal anatomy at 8 weeks of gestation. Prenat Diagn. 2024 Jan;44(1):3–14*).

The fourth part offers valuable perspectives on the future integration of PM-MCT into routine clinical practice and less-invasive autopsy, supported by a large-scale clinical study involving over 1,000 fetuses. (*Simcock IC, Lamouroux A, et al. Fetal post-mortem imaging using microfocus computed tomography: single centre retrospective clinical experience, submitted in American Journal of Obstetrics and Gynecology)*.

Finally, the discussion integrates these findings with the ongoing genetic revolution, projecting their combined impact on shaping future clinical practices.

PART I - CURRENT STATE OF POST-MORTEM FETAL IMAGING

Since 2010, a team from Great Ormond Street hospital, including Owen Arthurs, Susan Shelmerdine, Ciaran Hutchinson, Ian Simcock and their colleagues, has been at the forefront of advancing PM fetal imaging. As part of my mobility program from November 2022 to November 2023, I had the opportunity to be hosted at the Great Ormond Street Hospital for Children NHS Foundation Trust in London under the supervision of Dr Owen Arthurs. The first publication resulting from this collaboration is a comprehensive paper surveys both conventional and advanced PM imaging techniques, offering a detailed comparison of their respective advantages and limitations. I contributed significantly to the drafting and editing of the manuscript.

Simcock IC, Lamouroux A, Sebire NJ, Shelmerdine SC & Arthurs OJ.
Less-invasive autopsy for early pregnancy loss.
Prenatal Diagnosis 2023. Jun 1;43(7):937–49.

(Annexe 1)

1. Introduction

Pregnancy loss is a common event with an estimated 23 million miscarriages (<24 WG) and nearly 2 million stillbirths (>24 WG) occurring worldwide every year[25,81]. These numbers are increasing and could be far higher as many women may not present to the health services and data is therefore often based on approximate estimates[26,82,83].

Any pregnancy loss can be traumatic for the family and can lead to prolonged grief, depression, anxiety, and post-traumatic stress, with effects possibly lasting for several years[31,84–87]. Alongside this, miscarriage is little understood by both the general public and healthcare professionals and has been recognised as an under investigated area of medicine[25,88]. Compounding these issues around awareness, parents often believe that they are somehow at fault, which can stop them seeking help and support from healthcare professionals, preventing the true number of miscarriages in the community to be identified[82,89]. In this traumatic context, the delivery of information and its reception by the couple is particularly challenging. So, providing

support and a supportive environment where families can make an informed and appropriate choice for themselves is key.

Investigating the possible causes of pregnancy loss has multiple advantages including guiding future pregnancies and advancing medical knowledge[33,90,91], but helping bereaved parents understand the implications of their choices at this difficult time can be extremely challenging[92]. Staff training is key to imparting often complex information at this difficult time, and experience and guidance in this area for staff is important to clearly convey key complex information[30,33]. This training should come in differing formats including formal courses, case discussions and being involved in multidisciplinary meetings to raise awareness of the impact autopsy, and alternative less invasive investigations can make[30,93].

2. Historical background

CA is the traditional reference standard investigation into pregnancy loss and consists of multiple investigations also called fetal and placental examination including a review of the clinical history, an EE with photography, internal macroscopic examination and histological analysis, tissue sampling for genetic testing and macroscopic/microscopic examination of the placenta[23,91]. Together these investigations provide new clinical information in 40-70% of cases, depending on the clinical question to be answered[91,94–96].

Most perinatal and fetal autopsies are carried out with parental consent for diagnostic purposes, rather than being directed by the coroner/medical examiner for forensic purposes. Involving parents in the decision-making process is essential to increase uptake rates and provide care for the families[97,98]. Some parents choose CA as the "reference standard" or maximum level of investigation possible as they wish to be sure they have excluded all possible causes for their loss[28,91], but this may not be appropriate for all cases: there remains a significant proportion of pregnancy losses where the cause is still 'undetermined' despite full investigation[91,99,100]. Others decline all autopsy investigations as they wish to avoid 'further harm' to their child and are not

prepared to undergo more mental turmoil at this challenging time but can later regret this decision[28,29,33,92,101].

Parents choose to investigate their loss for multiple reasons, including to understand their child's death more fully[102], the recurrence risk for future pregnancies[103], to advance scientific knowledge[104], for a degree of 'closure' after their loss[105] and to rule out self-blame[28,91].

However, autopsy uptake has been declining for many years[30,31,34,96,106–109] with parental reasons for declining including wishing to protect the baby, practical aspects over transfer to a specialist hospital, misconceptions regarding the benefits of autopsy, poor communication between families and healthcare professionals, an uncertainty about the value of the procedure, a mistrust of the hospital system, religious and personal beliefs, and the invasiveness of the procedure[31,33,110,111]. Added to this, there is now a relatively low number of specialist paediatric pathologists (relative to the number of deaths to be investigated[112]) meaning access to specialist paediatric pathology services in the UK is becoming less accessible.

To challenge the declining consent rate, less-invasive autopsy (LIA) techniques, such as laparoscopic examination of the internal organs through smaller incisions or imaging techniques alone have been developed in recent years, providing greater, more acceptable choice to parents[29,31,33,35,97,101,109,111,113–115]. Significant challenges remain in identifying the cause of fetal demise <20 WG or <500 g, as routine imaging techniques, (magnetic resonance imaging (MRI), computed tomography (CT), ultrasound, radiographs) cannot provide sufficient resolution, tissue contrast or soft tissue detail[51,113,116–119]. It should also be noted that identifying abnormalities in early gestation through CA also remains challenging[39,45,46,51,52,58,118,120–122]. Several terms are commonly used to describe the different PM approaches towards diagnosis, and it is important to understand the investigations each term refers to and what can be achieved (Table I.1).

Table I.1 – Four terms used to describe the different post-mortem investigational approaches.

Key terminology				
Term	**Explanation**	**Includes**	**Histology**	**Genetics**
Conventional autopsy	Collection of investigations and gold standard for identifying the cause of fetal demise	Review of the clinical history, external examination with photographs, internal macroscopic examination and placental examination	Yes, all target organs as recommended in guidelines of the Royal College of Pathologists	Tissue samples from target organs for genetic testing
Less-invasive autopsy	Umbrella term including any autopsy procedure (CA or imaging) that is performed with smaller, less or no incisions than CA	Minimally invasive autopsy, non-invasive autopsy and placental examination	Yes, most organs with focal biopsy via minimally invasive autopsy approach	Tissue samples from target organs for genetic testing
Minimally invasive autopsy	Combination of imaging investigations, utilizes smaller incisions than for CA	Laparoscopic or image-guided needle-biopsy approach and placental examination	Yes, most organs with focal biopsy	Tissue samples from target organs for genetic testing
Non-invasive autopsy	Imaging only, no incisions required	External examination, placental examination and all non-invasive imaging investigations	No histology available	No genetic testing available

In this narrative review article, we aim to focus on the developments of high-resolution, non-invasive imaging techniques to identify the possible causes of early pregnancy loss in this challenging area. We defined up to 20 WG as "early" gestation but clarify according to the published literature. Articles published in the last 15 years were identified in December 2022. As there is no definitive gestation related to many of the investigations described, we aim to include, 20 weeks, but will identify specific gestations where the literature allows. Articles were identified in December 2022 through a search of MEDLINE and PubMed, using a Boolean search strategy with word variations relating to 'autopsy', 'conventional', less invasive', minimally invasive', 'non-invasive', 'imaging', 'early gestation', and 'fetus'.

3. Conventional clinical imaging techniques

A) Post-Mortem Radiographs

Fetal PM radiographs (PM-XR) are cheap, quick, widely available, easy to perform, and largely used to estimate gestational age and assess the developing skeleton[51]. As most skeletal dysplasia and abnormalities are now typically identified through ante-natal ultrasound[123], PM-XR

of all fetuses have been shown to add diagnostically useful information in less than 1% of routine cases[124]. Whilst PM-XR are diagnostic in suspected skeletal dysplasia, improvements in antenatal diagnosis means that these abnormalities are being detected earlier at earlier gestations, when the bones are less ossified, and therefore PM-XR are less discriminatory[125–127].

B) Post-Mortem Computed Tomography

PM-CT is also widely available, cheap, and quick to perform[51,128] but the combination of small size and poor soft-tissue contrast limits it's diagnostic ability in small fetuses[39,129,130]. Although PM-CT angiography can increase the soft tissue contrast, large validation studies are still required[39,131,132]. PM-CT can also provide information on dysplasia imaging through 3D reconstructions, but with limited additional diagnostic utility due to limited ossification at early gestations negating this advantage in early pregnancy[39].

C) Post-mortem Magnetic Resonance Imaging

PM-MRI is widely available and provides excellent soft-tissue information. However, due to the increasing clinical pressures, combined with the time required to perform detailed PM-MRI (approx. 60 minutes)[121,133], there is often difficulty in accessing these scanners for PM imaging.

The main challenge for PM-MRI at field strengths below 3T is the low spatial resolution and subsequent difficulty in visualising structures in <20 WG, due to poor tissue contrast and low signal-to-noise[45,46,113,116,121,134]. PM-MRI at 3T field strength provides fewer non-diagnostic scans than 1.5T for fetuses <20 WG through better image contrast, with higher sensitivity (34.6% vs 17.3%)), specificity (65.1% vs 45.3%), and concordance (55.1% vs 36.1%) with CA[121]. Field strengths above 3T have reported further improvement for fetuses <20 WG[119,122,135]. Soft tissue contrast and signal-to-noise ratio (SNR) can be improved through immersion of smaller fetuses in a Gadolinium/formaldehyde solution prior to scanning at 3T, but this technique has not been

optimised for clinical use[120]. Overall, conventional PM-MRI has limited diagnostic accuracy below 20 WG[57,62,113,121].

D) Post-mortem Ultrasound

PM-US may be a suitable alternative when cross-sectional imaging techniques are less available. It can provide information on a wide array of body systems including head, neck, spine, cardiac and vascular imaging, thorax and abdomen, musculoskeletal and soft tissue malformations[53].

It may also be better understood by parents when consenting for PM imaging having already undergone ante-natal ultrasound scanning and is also unaffected by tissue fixation[54–57,126,136]. PM-US also has the advantage of being able to direct needle biopsies for tissue sampling[51,53,59,137–139]. However, PM-US is operator dependent, requiring specialist training to develop the skills and experience to accurately identify possible causes of pregnancy loss in these smaller fetuses[51,55,58,126].

A high-resolution linear or curvilinear probe is advised given the small fetal size. Loss of normal live tissue rigidity can lead to slumping and difficulty maintaining contact with the ultrasound probe, and so a 'water bath' technique has been described, where the whole fetus is fully immersed within a cold, still water bath with a gel stabilising pad[55]. Alternatively, ultrasound transmission gel can be used to generate a stand-off, although cleaning the body afterwards is more challenging and may lead to fungal growth in residual gel[126].

Although relatively high sensitivities and specificities have been reported from multiple studies (ranging from 73 to 97%, similar to 1.5T PM-MRI), most studies have found lower diagnostic rates and higher yield of non-diagnostic imaging in fetuses below 20 WG[54,56–58,126].

4. Higher resolution imaging techniques

More advanced PM imaging techniques including Ultra High-field PM-MRI (PM-HF-MRI) and MCT imaging[62,69,120,140] have been developed for early fetal loss, primarily to address

the combined issues of poor resolution, and low signal and contrast-to-noise ratios[52,57,60–62,65,113,117,119,122,126,140–142].

A) Micro Computed Tomography

MCT provides non-invasive micron-level resolution imaging (figure 1), with increased spatial resolution as fetal size decreases (figure 2), making it ideal for early GA pregnancy loss and providing isotropic datasets which can be reconstructed for visualisation in different planes[60,61,66,67,69,113,122,141,143–147].

Figure I.1 – Coronal post-mortem iodinated Micro-CT image of 15-weeks' gestation fetus, resolution 60μm (A), axial images at the level of the ventricles of the brain (B), and heart (C) and the liver (D) demonstrating the high-resolution imaging Micro-CT provides for early gestation pregnancy losses. Figure adapted from Shelmerdine et al. 2020 with permission[60,61,66,69,113,118,122,141,143–146,148,149]

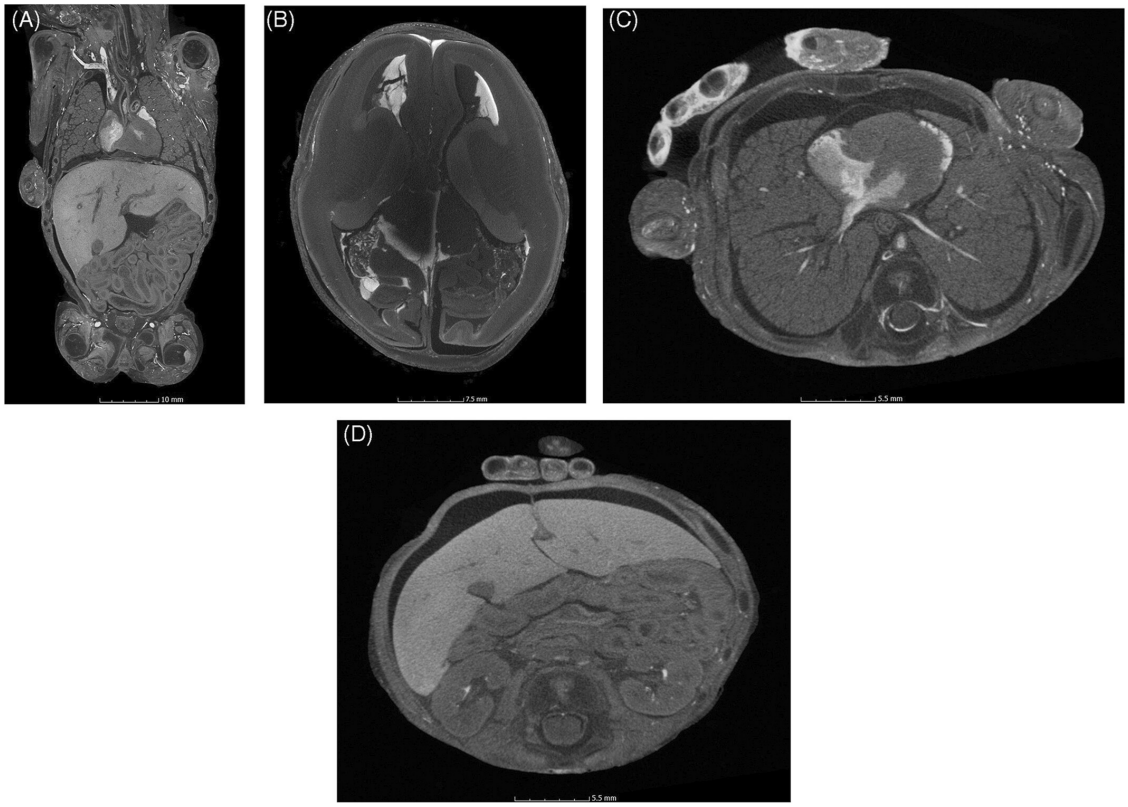

Figure I.2 – (A) Volume rendered a 3-dimensional image of a 7-weeks' gestation embryo demonstrating early eyelid and external ear development along with individual digits of the hand and toe notches. (B) A sagittal post-mortem Micro-CT of the same embryo at 9.7 μm with (C) corresponding histopathological section stained with haematoxylin and eosin staining demonstrating the equivalent internal detail attainable with both Micro-CT and histopathology. Figure adapted from Shelmerdine et al.2018 with permission[66].

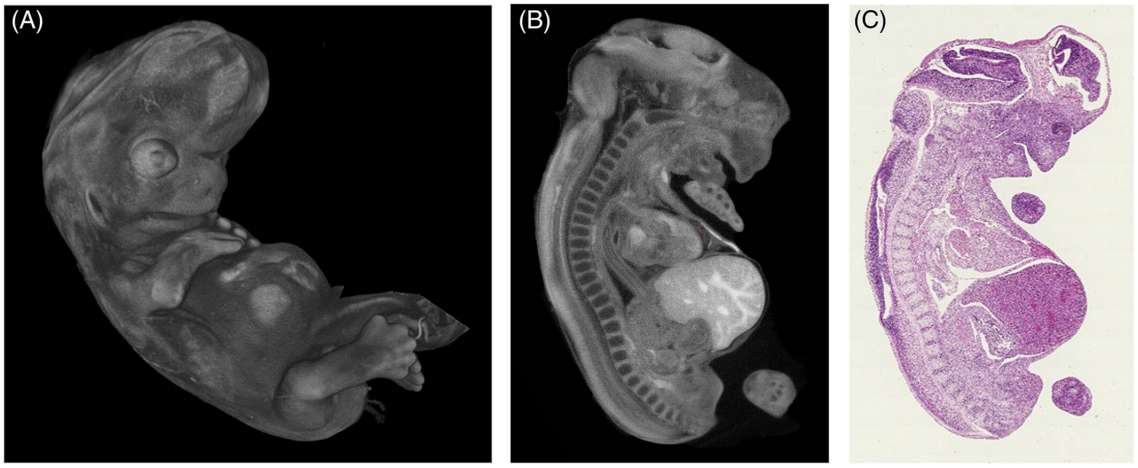

To provide adequate soft tissue contrast however, an exogenous contrast agent is required, typically potassium tri-iodide (I2KI) which stains the soft tissue through cellular diffusion[69,117,141]. Sufficient time must be allowed for complete diffusion, which can take several days or weeks and is dependent on the size of the fetus (figure 3) [69,141,147,150,151].

Figure I.3 – Iodination of the fetus occurs as iodine solution diffuses towards the interior of the fetus over time as demonstrated by (a) pre-iodination, (b-d) progressive iodination seen with iodination from the external surface of the fetus towards the centre, until (e) full iodination occurs. Figure adapted from Docter et al. 2022 with permission [117].

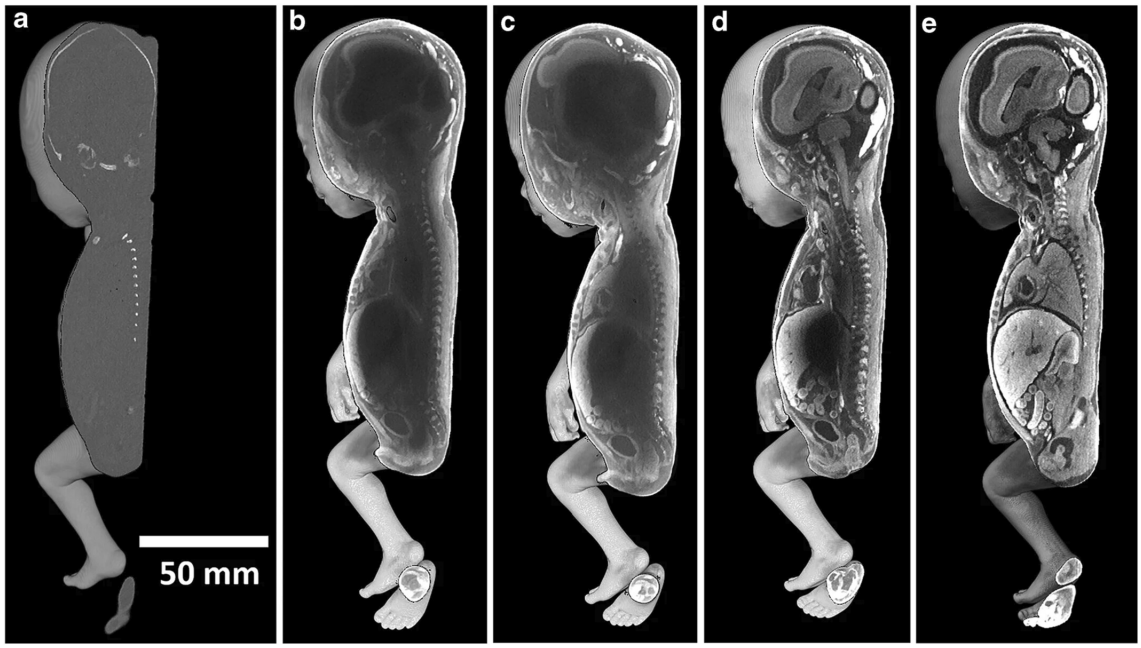

One downside is that concentrated I_2KI may result in tissue distortion, although this can be minimised by using a buffered solution[62,117,141,142,152]. Endovascular staining using various contrast agents have also been investigated[153–155], and may offer opportunities to iodinate larger fetuses in a reduced timeframe in the future[117].

Iodination can cause visible darkening of the fetus which should be discussed with parents during the consent process and may be initially undesirable but can be partially reversed by sodium thiosulphate solution (figure 4) [69,117]. This does not necessarily remove the iodine from all body tissues, however in many cases it is sufficient to just de-stain the skin for cosmetic purposes prior to returning the body to the parents.

MCT has shown a high level of agreement with CA across multiple organ systems for between 11 – 21 WG, of 21 fetuses, with overall sensitivities and specificities of 93.8% and 100%. Although non-diagnostic rates were higher for <14 WG than above (12% vs 4.7%), there were fewer non-diagnostic indices <14 WG, with higher positive predictive values, 97.3% vs 85.7% [60].

A large study analysing 268 MCT scans (11 – 24 WG) demonstrated that sensitivity and specificity were 92.3% and 98% respectively for fetuses up to 24 WG, and pathologists deemed invasive autopsy was unnecessary in 86.9% of cases[61].

Maceration, the breakdown of tissue structure due to immersion within a fluid filled cavity (amniotic fluid) combined with autolysis following fetal demise, is a major challenge in identifying the cause of early pregnancy loss both through imaging and CA[59,99,135,156]. Through the late diagnosis of a miscarriage and a delay between fetal demise, identifying pregnancy loss and delivery of the fetus, it is exposed to an often-unknown intra-uterine retention time. Maceration affects many early pregnancy losses and can affect the accuracy of PMUS even within 48 hours, with between 25 and 40% of scans becoming non-diagnostic due to severe maceration[18,54,57,59,137,157,158]. Equally, in-utero maceration deteriorates image quality for MCT, yet high quality is still possible in over 95% of cases despite the presence of a range of maceration states[68].

Figure I.4 – A 14- weeks' gestation fetus (a) having been refrigerated post-delivery, (b) following immersion in a mixture of potassium tri-iodide solution and 10% formalin to achieve fixation and full iodination where the skin is stained a darker shade, and (c) following immersion in thiosulphate solution prior to being returned to the parents, where the skin colour is returned to close to its original colour.

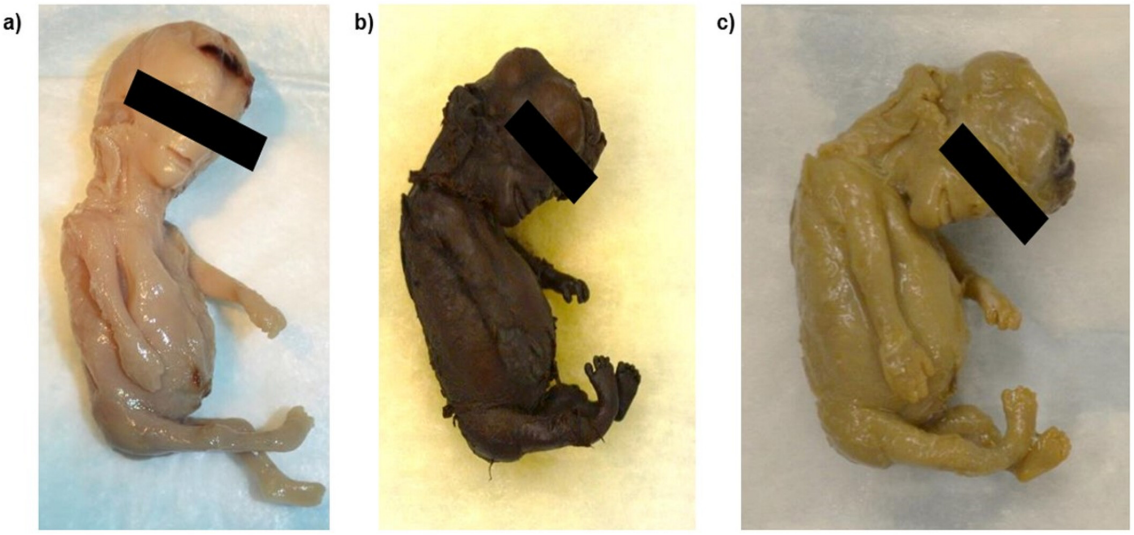

MCT can also be used as an adjunct to CA providing high resolution imaging of excised organs, for example of the kidney[159], brain[145] and heart[122,143,146,160]. Diagnostic accuracy of ex-vivo

imaging is also high, for example for congenital heart disease equal to CA and superior for smaller specimens[160] and has been used to assess cardiac anatomy between 8 – 13 WG to validate prenatal diagnosis following TOP for cardiac anomalies[122].

One practical limitation of MCT is that due to the high-resolution of the technique, the data files are large (approximately 50 GB per clinical patient) requiring large provision of storage for clinical use relative to other suitable techniques (ultra-high-field PMMRI <1GB per patient)[69,141].

Overall, due to the relative higher-resolution, low cost, and quick scan times, MCT has clear advantages[62] and is an excellent alternative to CA[61,118,122]. It can be used to create detailed scale 3D models or augmented virtual reality to aid parental counselling and education of congenital anomalies/fetal development[60,61,66,69,113,122,141,143–148,161], with a range of fetal gestations scanning from 6 weeks[65] to 24 weeks[61] with relatively short scanning times[69].

B) High-field Magnetic Resonance Imaging

Despite the numerous studies and multiple technical advances in recent years, the main disadvantage for PM-MRI is the low image quality below <20 WG or 300 g[119,135,162]. To overcome this, HF-MRI (7T and above) offers a significant increase in the SNR which can either improve the resolution or decrease the scan time, whilst also offering superior soft tissue contrast, whilst reducing the complexity of introducing an exogenous contrast agent[52,135,141,162–164].

HF-MRI images are able to accurately identify anatomical structures, particularly of the heart, below 20 WG[119] albeit with a lower resolution than seen with MCT (137 µm in HF-MRI vs 22 µm in MCT)[62], whilst a high concordance between HF-MRI and CA is seen for a range of anatomical structures with sensitivity (94.6%), specificity (97.6%) and positive and negative predictive values respectively (93% and 98.2%)[164]. One study comparing CA with 9.4T and 1.5T PM-MRI of the brain demonstrated that CA provided no additional information to that of HF-MRI and where CA was non-diagnostic, HF-MRI could provide diagnostic information in 69% of cases[135]. HF-MRI provided greater spatial resolution, higher tissue contrast and better

diagnostic information than 1.5T and was equivalent to CA when there was minimal maceration[135].

PM-MCT can also provide increased SNR and CNR than PM- HF-MRI (7T) for human fetal scanning (4 fetuses, 13-18 WG, 17 – 137 g) with a greater ability to identify anatomical structures in MCT, (figure 5) [62].

Figure I.5 – Coronal slices demonstrating the high-resolution imaging possible of internal anatomy including liver and stomach (a and c) and primary bronchi and lungs (b and d) for both Micro-CT (a and b) and high-field MRI 7T (c) and 3T (d). Figure adapted from Dawood et al. 2021 with permission[62].

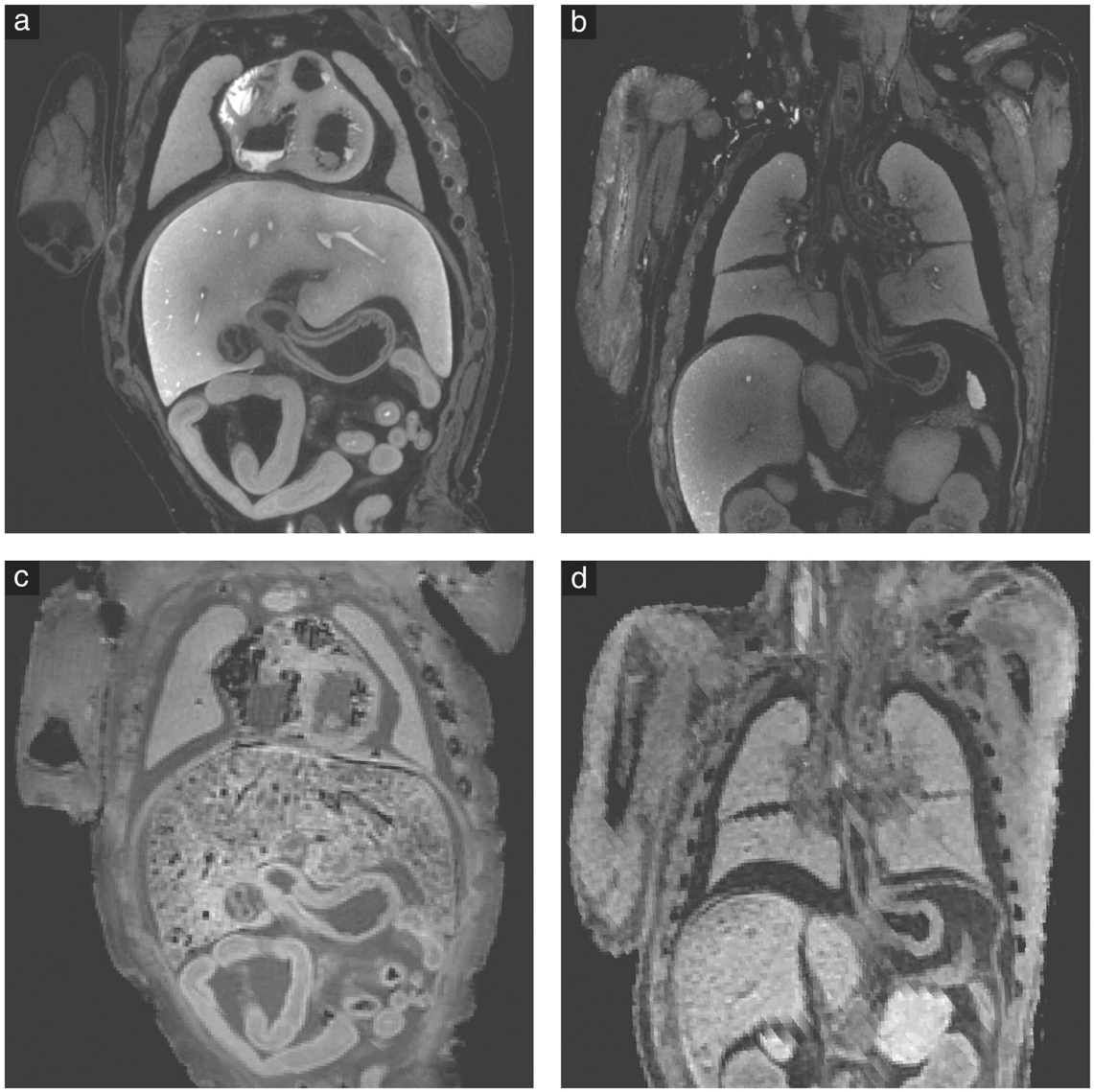

UHF-MRI typically takes longer scanning times, (>18 hours), making it difficult to implement in a clinical setting[51,52,69,135], and may be more expensive than MCT (400 Euros per

patient in comparison to 200 Euros for MCT)[62]. Most UHF-MRI scanners have a small-bore size (16-30 cm diameter), thus limiting the field-of-view, to smaller fetuses [52]. The smaller the fetus, the more likely that MCT would be a better imaging modality, as even higher spatial resolution should be possible by positioning the fetus closer to the X-ray source [62,69], whilst also maintaining shorter scanning times[52].

Overall, as with MCT, most UHF-MRI scanners are research based with limited clinical availability[35,52,126,135]; Relative to UHF-MRI, MCT provides greater cost efficiencies and higher resolution[62].

5. Autopsy in addition to Less Invasive Autopsy

Whilst LIA techniques are proven to provide answers to parents, it is important to identify whether any additional yield would be possible from completing an invasive autopsy[48]. Shelmerdine et al., demonstrated that when there was concordance between PM-MRI and prenatal ultrasound, additional clinically significant information was found at autopsy in only 4.5% (2/44) of cases, where prenatal ultrasound and PM-MRI reported ventriculomegaly, whilst autopsy was non-diagnostic due to brain autolysis[48].

6. Tissue sampling following early pregnancy loss.

Laparoscopic autopsy allows evaluation and tissue sampling of all internal organs via a smaller incision than employed in CA, thus is more cosmetically acceptable to parents[29,97,111]. It has been shown to be useful in fetuses as early as 15 WG but is more difficult with smaller fetuses[51,139]. It also provides similar tissue sampling success (>80%) when compared with more invasive approaches and comparable results to CA in identifying a cause of death[139]. Ultrasound-guided needle biopsy of organs is also a feasible way of tissue sampling, providing biopsy rates of around 85% organ success, and improved accuracy compared to 'blind' tissue sampling (76% vs <52%)[138]. The INTACT (Incisionless Targeted Core Tissue)[138] approach, tissue biopsy through

the umbilicus, is particularly appealing as it combines tissue sampling without making an incision, leaving the fetus cosmetically intact, although not all organs (brain, thyroid, thymus) could be sampled by this approach[138]. Ultrasound guided tissue sampling at PM has obvious implications for the developing world, for example for microbiological assessment in infectious outbreaks in children[165].

7. Challenges for implementation

Although PM imaging guidance can be used to optimise perinatal investigation and pregnancy loss[140], and has been embedded within specific autopsy protocols from the UK Royal College of Pathologists for infants and second/third trimester pregnancies, there is no specific guidance currently available for first trimester loss. A stepwise approach has been suggested for FPME with imaging used to triage further investigations[113], whilst further advice is offered for fetuses <500 g when more specialised investigations are available (UHF-MRI and MCT) (figure 6 and 7)[51]. The developing role of imaging means that new guidelines and referral pathways would be welcome, and are likely to support investment and raise awareness for PM investigations following early pregnancy loss[140].

Figure I.6 – A demonstration of when Micro-CT and high-field MRI can provide superior imaging for early gestation fetuses relative to other imaging modalities. Figure adapted from Shelmerdine et al. 2021 with permission[128].

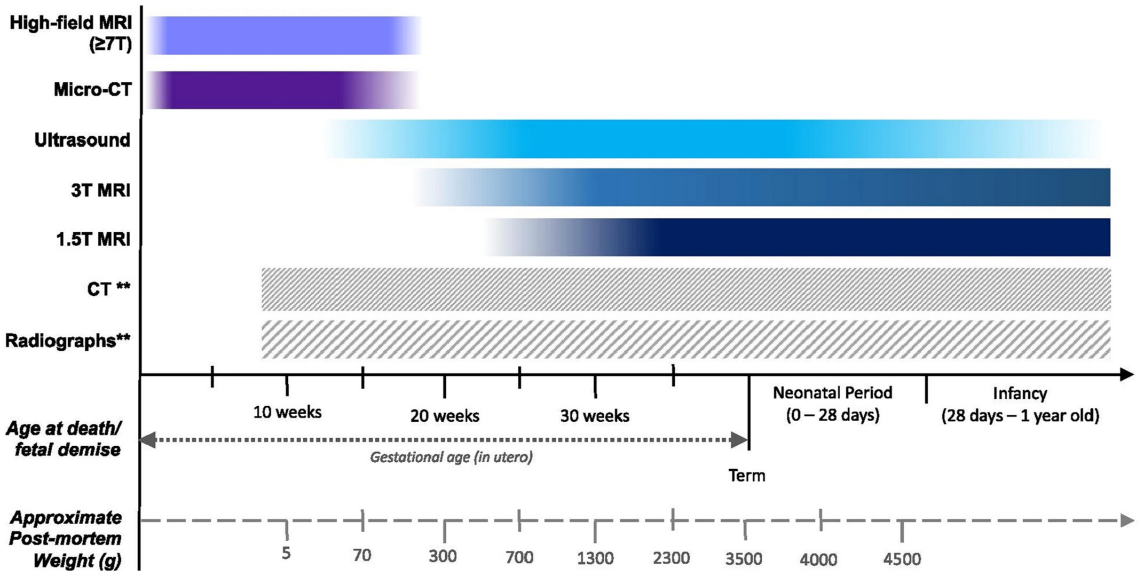

Figure I.7 – A stepwise flowchart for non-invasive investigation of perinatal loss including options for Micro-CT and high-field MRI. Figure adapted from Shelmerdine et al. 2021 with permission[128].

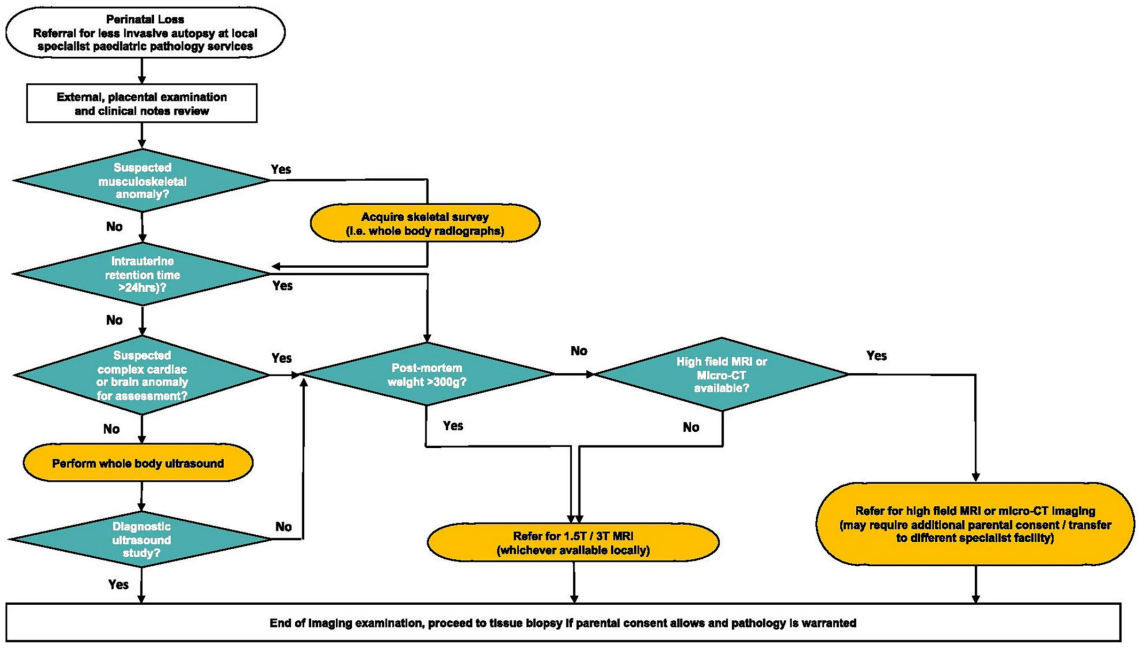

8. Future directions, other developments

Major challenges for the implementation of both MCT and UHF-MRI for investigating early pregnancy loss is the lack of availability for both scanning techniques within a clinical setting, along with staff training in image acquisition and interpretation. Limited funding for these types of services in specific jurisdictions will further limit clinical experience and patient access. Alongside this, referrers and parents should be educated on the benefits of PM investigations and what these innovative techniques can yield. Similarly, national guidance is required to determine their economic role in the wider service provision, at a time of acute shortage of paediatric pathologists.

A detailed health economic assessment is needed, weighing up the costs of scanning against the benefit of helping the grieving process, and a potential reduction in the future burden of mental health issues and ongoing pregnancy losses[140]. Important features of this process includes providing the information in sensitive, easily understood terms according to the families personal situation, with time spent answering questions to ensure parents can make decisions that they do not later regret, whilst providing unbiased support in the decision making process[33,93,103,166].

9. Conclusions

LIA investigations are preferred by parents for a variety of reasons, and through greater provision and choice there will be an uptake in parental consent. MCT and UHF-MRI offer superior PM image quality for early pregnancy loss through increased resolution and CNR when compared to more established NIA techniques. Wider adoption of these investigations will increase the societal awareness surrounding miscarriage and reduce the emotional cost for parents by investigating their loss in a more acceptable personalised manner.

PART II - METHODOLOGY - SAMPLE PREPARATION

MCT is a high-resolution imaging technique that provides precise morphological data, but requires careful sample preparation, as previously detailed. We conducted a comparative study of different preparation protocols. Furthermore, we investigated the diffusion of iodine-based contrast agents in fetal tissues. By fitting mathematical models to our data, we demonstrated that diffusion rates vary significantly between organs, likely influenced by factors such as tissue position and density. Based on these findings, we optimized staining durations for non-macerated fetuses, focusing on enhancing contrast between the lung and liver.

1. FETTAL Project

The Fetal Enhanced Three-dimensional and Translational Anatomical Landscape (FETTAL)[167,168] project is a collaborative effort between three key institutions supported by the University of Montpellier[169] (UM, Montpellier, France) :

- The fetopathologic unit in clinical genetic teams at Montpellier university hospital: provide clinical expertise and access to fetal specimens.
- The ICAR research team at LIRMM (Laboratoire d'Informatique, de robotique et de microélectronique de Montpellier): Contributing expertise in image and visual data analysis, drawing upon the combined strengths of robotics and computer science departments.
- The BioNanoImaging Foundry (BNIF)[170] Technology Platform at the University of Montpellier is equipped with advanced instrumentation that is collaboratively exploited and continuously enhanced by research teams in diverse fields such as instrumentation, image processing, and health biology. This platform offers access to X-ray microtomographs SkyScan 1276 (Bruker) and Agilent 9.4 Tesla MRI scanner

This multidisciplinary collaboration, encompassing medical, computational, and physical sciences, underscores the interdisciplinary nature of the FETTAL project, addressing complex challenges in healthcare and technology. The French BioMedicine Agency (ABM) approved the FETTAL project in April 2015.

FETTAL project follows a cohort pregnant woman who are consulting for voluntary abortion, early spontaneous miscarriage or ToP. Information sheets are given to the women during their consultation with the gynecologist or midwife. Written informed consent is obtained from each woman. All consents are revocable at any time. The criteria for non-inclusion are age < 18 years or unable to give informed consent such as under guardianship or language barrier.

Since 2016, we included 28 non-macerated non-malformed fetuses of various gestational age as detailed in Table II.1.

Table II.1 – Inclusions in the FETTAL Project since 2016 with their characteristics and their corresponding numbers in the different studies

FETTAL Inclusion number	Fetal Characteristics							Fetuses related to the different studies			
	female or male	weight (g)	CRL (mm)	Gestational age according to Robinson formula (WG)	BPC (mm)	Foot length (mm)	Carnegie stage	Staining bath comparison	Technical note	8WG	12WG
F72			8	6+5			16				
F97			17	8+1			19			S4	
F86			8	6+5			16				
F58		1,00	22	8+5			21			S9	
F79		0,30	12	7+3			17	S1		S1	
F45		0,29	16	8			18	S2	S1	S3	
F95		0,24	14	7+5			18	S3		S2	
FE1	F	34,00	78	13+4	23	12			S17		
FE2	F	20,45	54	11+6	22	9			S9		
FE3	M	15,13	52	11+5	18	8			S8		
FE4		0,68	20	8+3			20		S3	S5	
FE5	F	17,14	63	12+4	19	8			S12		S2
FE6	F	7,95	51	11+4	15	6			S7		
FE7	F	19,60	68	12+6	19	9			S14		S5
FE8	F	28,00	77	13+3	24	11			S16		
FE10		1,05	22	8+5			21		S5	S8	
FE11		0,70	20	8+4			20	S4		S6	
FE12	F	16,00	59	12+2	17	9			S11		
FE14	F	27,20	79	13+4	22	11					
FE15			10	6+6							
FE17			7	6+3							
FE18		0,51	17	8+1			19		S2		
FE20	F	46,24	89	14+2	25	14			S18		
FE23		3,55	40	10+5	12	6			S6		
FE24	M	27,72	72	13+1	24	11					
FE25	M	30,40	72	13+1	25	11			S15		
FE27	F	30,06	80	13+5	22	14			S0		
FE28	F	14,10	58	12+1	19	8,5			S10		S1
FE29	F	51,70	92	14+3	29	16					
FE30		0,67	20	8+4	6				S4	S7	
FE31	M	17,80	63	12+4	19	9			S13		S3
FE32	F	16,86	65	12+4	20	10					S4
FE33	M	72,08	100	14+6	30	18					

2. Staining bath comparison

A) Introduction

MCT demands careful sample preparation. Tissue staining allows to visualize soft organs[69,117,141,171]. In 2016, in their literature review, Gignac et al recommended initial fixation before staining[172]. In the literature, we found five different staining protocols to obtain satisfactory contrast-enhanced MCT images (Table II.2.1). These staining protocols are based on different contrast agents, solvents and staining duration[60,61,66,68,69,143–145,159,173–175]. This unpublished study aimed to compare staining protocols effectiveness.

B) Methods

a. Micro-CT acquisition and post-treatment

MCT images were acquired using a Skyscan 1276 (Bruker) X-ray microtomography. The settings (spatial resolution, X-ray attenuation, power, best filter) were carefully determined and adjusted to the sample features to optimize contrast according to the manufacturer recommendations. Then, the serial X-ray views (native images) were transformed into CT images using the N-RECON software (Skyscan, Brucker). MCT images in DICOM and in TIFF format were collected, post-processed, regions of interest (ROIs) were manually defined, and ROI features were collected and viewed using CTVOX, DATAVIEWER, FIJI ImageJ and Myrian.

b. Staining protocols

All samples were fixed in 4% paraformaldehyde (PFA) for at least 72 hours and stored at +5 °C[172]. Table II.2.1 describes the five staining protocols, named P1 to P5. They used different contrast agents [potassium triiodide, Lugol's iodine (I_2KI), iodine dissolved in 100% ethanol, and phosphotungstic acid (PTA)] that were dissolved in ethanol, water, or 4% PFA. To compare the four protocols based on iodine or PTA, the same fetus was stained successively with two different staining solutions (Table II.2.2).

Table II.2.1 – Staining protocols analysed in this study published by Metscher[173,174], by Owen Arthurs' teams [60,61,66,68,69,144], by Lombardi et al.[143,145], and by Vymazalovà et al.[175] (E = ethanol; FA = formaldehyde; I2 = iodine; PFA = paraformaldehyde; PTA = phosphotungstic acid; stage = Carnegie stage; WG = weeks of gestation).

Protocol	Authors (references)	Samples	Dilution protocol	Contrast agent	Conservation solvent	Washing / Fixation	Staining duration	Staining duration chosen for our study (in hours)
P1	Metscher	Chick embryos stage 24	1% (w/v) I2 in 100% E (I2E)	I_2	Any fixation	Wash in E	30min to overnight	12 h
P2			PTA solution = 1% (w/v) PTA in water. Mix 30% PTA solution, 70% E	PTA		Wash in 70% E	2h to overnight	48 h
P3	Owen Arthurs et al.	Human fetuses (11 – 21WG)	Solution of 10% FA and potassium triiodide (I_2KI/Lugol' s I2), with a total I2 content of 63.25mg/mL (iodine mass, 2.49" 10^{-4} mol/mL), in a 1 :1 ratio	I_2KI	4% para FA	Wash in water and drying with gauze	72h	72 h
P4	Claudio Lombardi et al.	Human fetuses (7 – 17WG)	10 g potassium iodide and 5 g I2 in 100mL water (I2KI), diluted 25% or 50% in demineralized water. Stain in 10mL staining solution for every gram of pre-stained specimen weight	I_2KI	4% buffered FA	Wash in E	48 to 72h	48 h
P5	Vymazalová et al.	Human fetuses (9WG)	Progressive dehydration in E series (5–6 h in 30%, then 50%, and finally 70% E). EPTA bath: 5 mL PTA dissolved in 70% ethanol	PTA	40% aqueous FA solution	Fixation with 0.5% agarose	1 – 4 days	48 h

Table II.2.2 – Qualitative and quantitative comparisons of the studied staining protocols (CRL = crown-rump length; SNR = signal to noise ratio; CNR = contrast to noise ratio).

Samples	CRL (mm)	Protocol	Staining time (hours)	Micro-CT resolution (µm)	Source voltage (kV)	Source current (µA)	Filter	Expert blind evaluation	SNR Cerebral vesicle	SNR Cerebro-spinal liquid	**CNR Brain**	SNR Stomach wall	SNR Peritonium or stomach content	**CNR Abdomen**
S1	12	P1	12	13	66	160	Al 0.25	2	9,23	4,52	**6,19**	9,12	5,51	**5,63**
		P3	72	15	87	175	Al 0.5	8	9,85	6,00	**7,39**	10,73	4,81	**8,05**
S2	16	P4	48	18	65	160	Al 0.25	3	18,25	7,03	**7,58**	9,14	7,80	**4,14**
		P3	72	18	94	155	Al 0.5	7	20,26	7,32	**7,60**	15,22	6,61	**5,03**
S3	15	P3	72	15	95	166	Al 0.5	10	14,61	5,64	**9,73**	9,94	8,97	**6,29**
		P5	48	18	62	167	Al 0.25	0	12,39	7,52	**3,50**	7,55	6,90	**2,66**
S4	20	P2	48	18	73	156	Al 0.25	na	10,10	5,75	**7,44**	7,93	6,02	**5,02**
Mean (standard deviation)				16,4 (2)	77,4 (14,2)	162,7 (7)								

Briefly, after fixation, the sample was immersed in the first iodine-based staining solution for the indicated time followed by MCT image acquisition. Then, the sample was deiodinated by immersion in a solution of sodium thiosulfate pentahydrate in water (4%wt/vol) for at least 12 hours[60]. This was followed by immersion in the second iodine- or PTA-based staining solution

for the indicated time and MCT image acquisition (Table II.2.2). In Table II.2.2, the protocols are listed in their order of execution.

c. Staining protocol choice: blind qualitative comparison.

Two experts (an anatomist and a fetal pathologist) analysed the quality of the obtained images while blinded to the staining protocol used. The evaluation grid for each sample included five MCT volume rendering and slice images. For each of the five images for the two staining protocols, the experts chose the one in which the specified anatomical feature was easiest to visualize with the least tissue shrinkage. Their two answers were added to obtain a score going from 0 to 10 (Table II.2.2).

d. Staining protocol choice: quantitative comparison.

For the quantitative comparison, images were reconstructed using the NRECON software and post-processed with the FIJI software. The mean signals (MS) were determined for the following ROIs: brain parenchyma of cerebral vesicles, cerebrospinal liquid, stomach wall, and abdominal liquid (peritoneal or stomach content).

In the literature, the noise, and its standard deviation (SD) are calculated using a ROI in the air around the sample[176]. However, in our MCT images, due to the post-processing method, this approach is not recommended because it gives very variable MS and SD. Consequently, the noise and its SD were evaluated using a reference outside the sample: the cradle. The cradle MS and SD were determined over the entire acquisition volume.

The signal-to-noise ratio (SNR) for a given target organ was the MS of this organ divided by the cradle SD. The contrast-to-noise ratio (CNR) for a given region (i.e. brain or abdomen) was the difference between the MS of two neighbouring organs in this region divided by the cradle SD. Then, SNR and CNR were compared between staining protocols using the Wilcoxon rank sum exact test in *R*++ (version 1.6.04) after effect sizes labelled following Funder's (2019) recommendations.

C) Results

Between January 2016 and July 2023, 4 fetuses (S1 to S4) from 7+3 to 14+2 WG, according to Robinson formula[177], were collected for this study.

Staining protocol P3 always received the highest score (Table II.2.2) in the blinded expert comparison (Figure II.2.1).

The quantitative comparison of SNR differences between brain and abdomen were labelled following Funder's (2019) recommendations mean SNR ±SD: 10 ± 4.60 versus 8.75 ±SD 3.6. The Wilcoxon rank sum exact test testing the difference in ranks between protocol P3 and the other protocols suggests that the effect is negative, statistically not significant, and small (W = 62.00, p = 0.590; r (rank biserial) = -0.14, 95% CI [-0.55, 0.32]). Conversely, the Wilcoxon rank sum exact test testing the difference in ranks between CNR and Bath (mean in group Other = 4.95 (SD 1.84), mean in group Hutch = 7.35 (SD 1.60) suggests that the effect is statistically significant (W=5, p = 0.041).

The S4 sample was stained using protocol P2 (i.e., the PTA-based staining protocol by Metscher[174]) (Tables II.2.1 and II.2.2). The quantitative analysis of images acquired using the same parameters as for samples S1 to S3 (Table II.2.2), confirmed the good signal and the excellent contrast. However, tissue shrinkage was major (Figure II.2.2). Furthermore, this PTA-based staining protocol does not seem relevant in clinical practice because, to our knowledge, there is no procedure for rinsing it. Consequently, the contrast and deformation persist over time, and this does not seem compatible with a return of the fetus to the parents. Consequently, we excluded this staining protocol.

Figure II.2.1 – Evaluation grids of Micro-CT volume rendering and slice images for samples S1, S2 and S3 used for the qualitative comparison by experts (CRL = crown-rump length; WG = weeks of gestation).

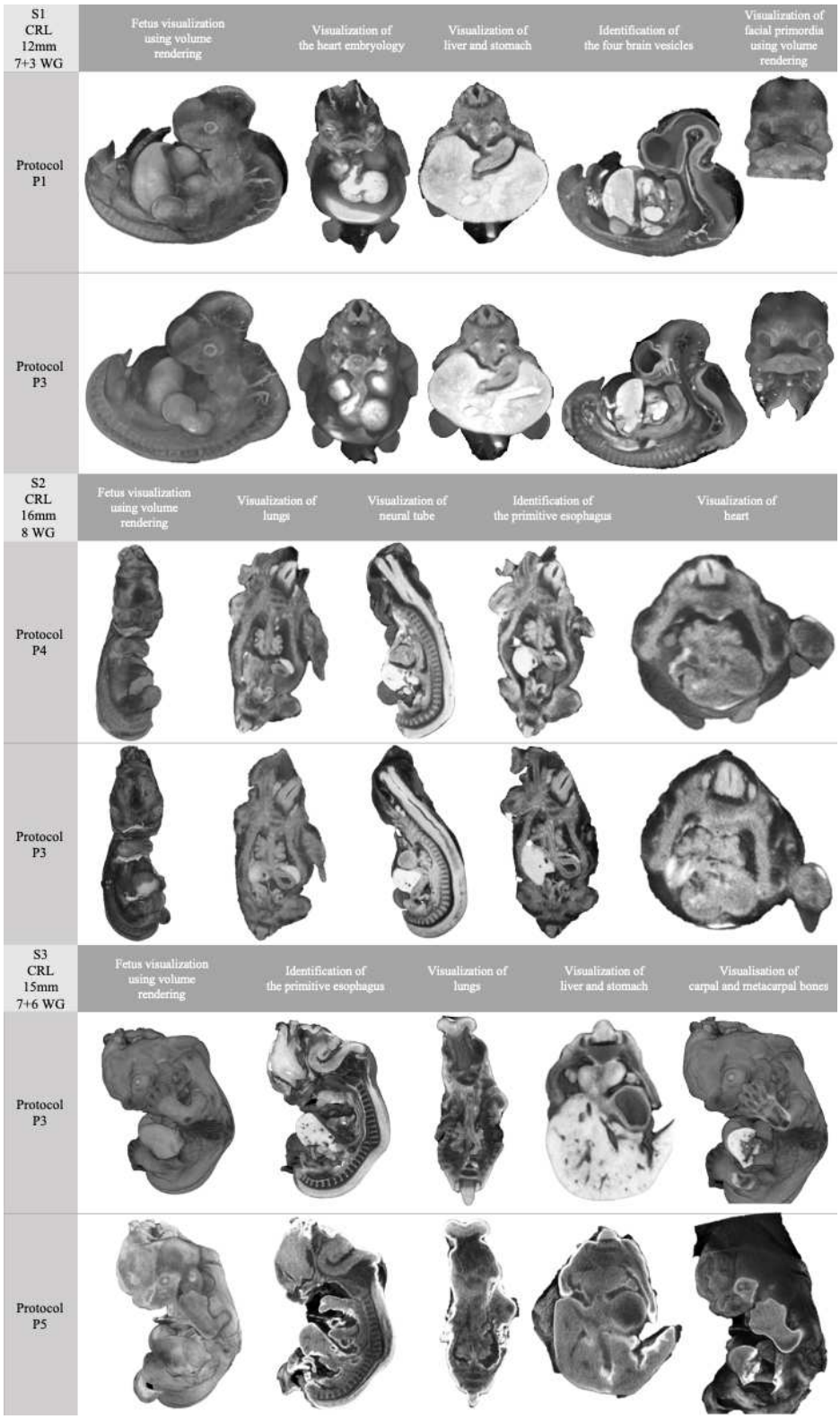

Figure II.2.2 – Micro-CT volume rendering and slice images of sample S4 highlight important soft tissue shrinkage after staining with protocol P2.

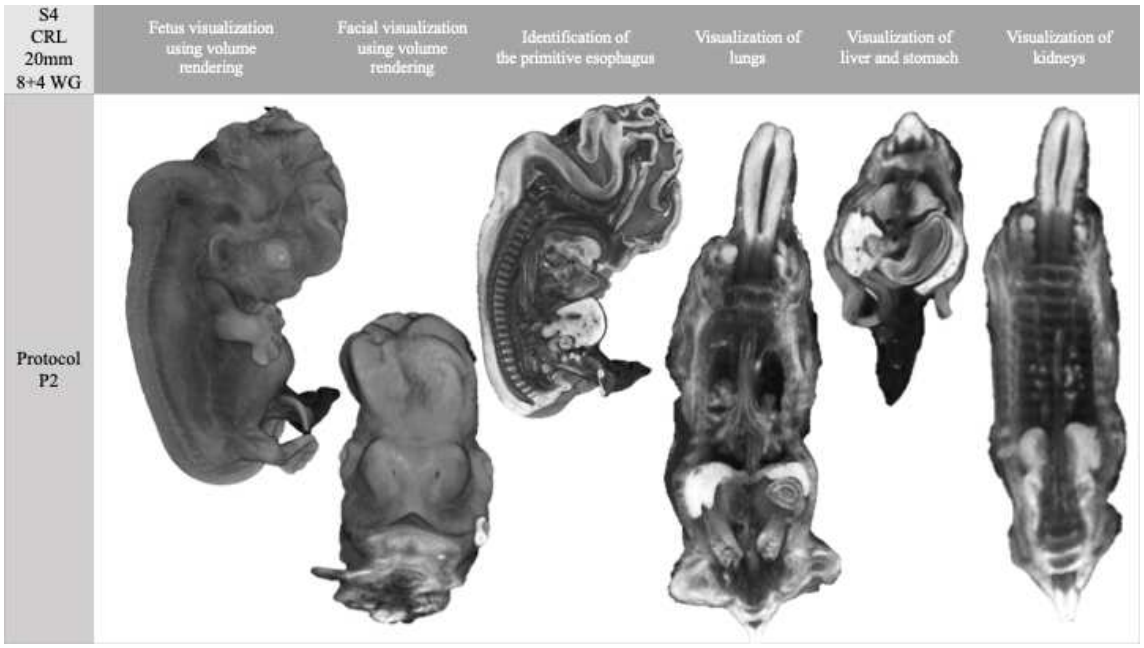

Therefore, the staining protocol P3 (4% PFA: Lugol' iodine, 1:1)[60,61,66,68,69,144,159] (Table 1) seemed a good compromise between contrast and tissue shrinkage in human fetuses based on the qualitative and quantitative assessments.

D) Discussion

To optimize organ visualization using PM-MCT of first-trimester human fetuses, the staining protocol described by Arthurs' group (4% PFA and I_2KI, with a total iodine content of 63.25mg/ml, 1:1 ratio; protocol P3) gave the highest contrast with acceptable tissue shrinkage.

This is concordant with literature, because this staining protocol become the world-wide used staining protocol. Tissue shrinkage could be reduced using buffered formalin, as proposed by Dawood et al.[142]. These authors showed the influence of the staining solution pH on tissue deformation. As tissue shrinkage leads to organ biometric changes, the previously published biometric references for *in vivo* US or for FPME cannot be used. The purpose of MCT must be clearly defined, and a distinction must be made between research use with minimal maceration to describe the embryo development, where measurements may be important, and clinical use with

potentially greater maceration, where measurements are less important compared with the detection of malformations.

Table II.2.1[60,145,173,175] highlights that protocol P3 was the only one that did not use ethanol (as solvent or for sample rinsing after staining). The use of formalin as solvent is relevant for maintaining the tissue trophicity and limiting decomposition.

One of the study limitations is the small sample size (n=4 fetuses). Therefore, we could compare only four staining protocols and eliminated the fifth without comparison due to major shrinkage. We did not test the buffered staining protocol[142] which is the same as the chosen staining protocol with the only exception that 4% PFA is replaced by buffered PFA. It was not possible to measure noise in the air, as usually made, because of the high signal variation between acquisitions probably linked to the post-treatment process. The staining protocol comparison was not randomized because the first staining solution had to be iodine-based to allow its elimination before staining with the second solution.

The main strengths of this study are the use of several methods to compare the staining protocols (qualitative analysis by experts blinded to the protocol, and quantitative analysis by calculating the signal and contrast).

E) Conclusion

To optimize contrast and organ visualization using PM-MCT, we recommend that first-trimester human fetuses should be stained using the staining protocol described by Arthurs' group (4% PFA and I_2KI, with a total iodine content of 63.25mg/ml, 1:1 ratio)[61,68,68,144] for a duration correlated to the fetal CRL.

3. Staining agent diffusion and staining bath duration.

Optimizing sample preparation prior to MCT imaging is crucial for advancing and expanding the applications of this technology[178]. A fundamental investigation into the fetal diffusion of contrast agents is essential for the design of optimized staining bath, particularly regarding the duration of staining[117].

Lamouroux A, Cardoso M, Bottero C, Fuchs F, Mousty E, Genevieve D, Subsol G, Goze-Bac C & Captier G.

Modelling of staining in post-mortem diffusible iodine-based contrast enhanced (Dice) micro-CT imaging of non-macerated first-trimester human fetuses.

Submitted in BMC Medical Imaging

(Annexe 2)

A) Background

A comprehensive approach is essential for clinical and scientific research into first trimester pregnancy loss[1]. Parents should be offered the option of investigating the circumstances of their pregnancy loss, which may include an autopsy[2]. However, some parents may be reluctant to pursue an autopsy because of its invasive nature[3–6]. Consequently, less invasive techniques, such as postmortem imaging, should be considered[7,8]. Postmortem microfocus computed tomography (MCT) is an imaging technology based on X-ray attenuation, typically offering an isotropic resolution of 10 µm[9,10]. It has been successfully used as an alternative to invasive autopsy of human fetuses in clinical practice[11,12] over 11 weeks of gestation (WG)[10], as well as earlier in research[13,14].

Staining by immersion of foetus in diffusible iodine-based contrast-enhanced (Dice) staining solution provides satisfactory contrast in MCTs[9–12,15], even in macerated fetuses[16]. However, several aspects of this staining contrast bath remain unclear. Simcock et al. conducted a pooled analysis of observed staining durations on the basis of theoretical age and weight[17], utilizing clinical cases with varying degrees of maceration[12,16,17] exhibiting MCT images consistent with prospective diagnoses[17].

The diffusion of iodine stains in biological tissues can be understood by combining general diffusion theory with tissue-specific compositions. The output parameters from these models, such as density, heterogeneity, and tortuosity of the tissue, can effectively be used to analyse and discuss the penetration of staining agents such as iodine into biological tissues[18–20].

Given these factors, this study investigated the diffusion of the Dice staining bath in non-macerated first-trimester fetuses and aimed to determine the optimal staining duration for fetuses of varying sizes via quantitative contrast and signal measurements.

B) Methods

a. Inclusion criteria and ethics

The present study was conducted as part of the Fetal Enhanced Three-dimensional and Translational Anatomical Landscape (FETTAL) project[14,21], which was approved by the French Biomedical Agency (PFS14--020 on January 29, 2015). The project involved the use of human fetuses obtained from elective abortions. Pregnant women seeking elective abortion were provided with an information document outlining the study's objectives and methodology. The non-inclusion criteria included being under 18 years of age or being unable to provide informed consent. Written informed consent was obtained from each participant prior to elective abortion, with the option to revoke consent at any time. The fetuses included were collected following medical expulsion. Consequently, this cohort consists solely of non-macerated and nonmalformed PM fetuses.

b. Dice-Micro-CT acquisition and post-treatment

Dice-MCT images were acquired via a SkyScan 1276 (Bruker) X-ray microtomograph. The acquisition settings, including spatial resolution, X-ray attenuation, power, and filter type, were carefully adjusted according to the manufacturer's recommendations : to avoid image saturation and ensure optimal contrast, X-ray absorption was maintained between 30% and 90% of saturation. Details acquisition parameters are collected for each acquisition. Serial radiographs,

native images, from the rotative acquisitions over 360° were converted into computed tomography images via N-RECON software (Skyscan, Brucker) in DICOM and TIFF formats. The reconstructed images were postprocessed with FIJI ImageJ software, where regions of interest (ROIs) were freehand manually delineated, and their characteristics were quantified and visualized.

c. Dynamical study of the staining agent diffusion and its quantification.

To study the dynamic diffusion of the staining agent, a foetus fixed in 4% paraformaldehyde (PFA)[18] was immersed in Dice staining solution composed of 4% PFA and I_2KI (with a total iodine content of 63.25 mg/ml) at a 1:1 ratio [9,11,12,16]. The foetus and its staining solution were placed in a hermetically sealed syringe, which was then loaded into the MCT device. Iterative acquisitions were performed using consistent settings, initially at one-hour intervals, followed by progressively longer intervals over the course of one week. The same postprocessing settings were applied throughout the study.

The objective was to obtain time series data on the diffusion of the staining agent within the fetus and visualize its progression over time. Iodine diffusion was monitored in three Dice MCT transverse sections: i) a cephalic section through the thalamic nuclei; ii) a thoracic section through the four cardiac chambers, including visualization of the pulmonary venous returns; and iii) an abdominal section encompassing the stomach, superior pole of the spleen, left adrenal gland and superior extremity of the right adrenal gland.

The three stacks of images were postprocessed via FIJI ImageJ software, with the ROIs manually selected from various organs. The evolution of the mean signal (MS) within each ROI was tracked and represented graphically. Its evolution was modelled via stretched exponential[19] [20] and double Weibull functions[22,23].

Contrast between two organs was displayed over time, with the distance between the lines indicating the contrast level. At the point where the lines intersect, the contrast between the two

organs is no longer observable. This visual representation allowed for the determination of the staining bath duration required to optimize contrast between the two organs of interest.

The results from this analysis will inform the next phase of the study, which will determine the optimal staining bath duration in relation to fetal size and weight. In the absence of direct fetal volume measurements, the size and weight of the fetus may be used as proxies for this parameter.

d. Modelling Signal Evolution Using Stretched Exponential and Double stretched exponential

The signal evolution was tested with several plots usually used to describe biological diffusion and choose the model best fit with our curve of diffusion. Consequently, we use a stretched exponential function $S(t) = A_0 + Amax\left(1 - exp\left(-\frac{t-t_0}{\lambda}\right)^{\beta}\right)$ where A_0 is the initial amplitude or baseline value of the signal, A_{max} is the maximum change, t_0 represents the starting time, λ is the characteristic time scale, and β is the stretching exponent[20]. Stretched exponential functions describe diffusion, where particle displacement probabilities deviate from the expected Gaussian distribution ($\beta = 1$). This type of diffusion is commonly observed in molecular transport within intracellular environments. In this context, the stretched exponential function exhibits slower decay compared to Gaussian diffusion, with the value of β reflecting this process ($\beta < 1$)[19]. When signal increases do not conform to a stretched exponential pattern, alternative models can be employed to provide a more accurate fit such as double stretched exponential $S(t) = A_0 + A_1\left(1 - exp\left(-\frac{t-t_1}{\lambda_1}\right)^{\beta_1}\right) + A_2\left(1 - exp\left(-\frac{t-t_2}{\lambda_2}\right)^{\beta_2}\right)$ with $t \geq t_1$ and $t_2 \geq t_1$. For instance, a double Weibull is a specific type of double stretched exponential[22,23].

e. Staining time according to fetal size

All the foetuses were fixed in 4% paraformaldehyde (PFA) for at least 72 hours, stored at +5 °C, and subsequently stained in Dice solution for various durations prior to MCT image

acquisition. The Dice staining durations for the fetuses, along with their specific characteristics, are detailed in Table II.3. MCT image acquisition and postprocessing were performed following previously described methods.

Table II.3 – Samples characteristics (crown-rump length CRL, weight et gestational age), Micro-CT preparation (staining duration) and acquisition details (filter, voltage and current) and contrast-to-noise ratio (CNR) between lung and liver (WG = weeks of gestation, SD = standard deviation).

Sample	Weight (g)	CRL (mm)	Gestational age according to Hadlock (WG)	Staining duration (hrs)	MCT resolution (µm)	Source voltage (kV)	Source current (µA)	Filter	CNR Liver to Lung
S1	0,29	16	8	72	18	94	155	Al 0,5	17,02
S2	0,51	17	8+1	48	21	95	200	Al+Cu	34,57
				72	21	95	200	Al+Cu	38,29
S3	0,68	20	8+4	48	21	67	156	Al 0,25	23,76
				72	10	80	200	Al 0,5	11,39
				96	10	80	200	Al 0,5	11,95
S4	0,67	20	8+4	72	14	95	200	Al 1	33,57
				96	14	95	200	Al 1	34,81
S5	1,05	22	8+5	72	10	98	200	Al 1	8,53
S6	3,55	40	10+5	72	42	70	200	Al 0,5	9,79
S7	7,95	51	11+4	96	21	100	200	Al+Cu	24,36
				120	21	100	200	Al+Cu	21,46
S8	15,13	52	12+3	56	21	100	200	Al+Cu	4,19
S9	20,45	54	11+6	56	21	66	200	Al 0,5	4,29
S10	14,10	58	12+1	120	42	95	200	Al+Cu	26,46
S11	16,00	59	12+2	72	42	97	200	Al+Cu	9,62
S12	17,14	63	12+4	96	21	100	200	Al+Cu	13,69
				120	21	100	200	Al+Cu	15,28
S13	17,80	63	12+4	120	42	95	200	Al+Cu	24,21
				144	42	95	200	Al+Cu	21,42
S14	19,60	68	12+4	48	21	100	200	Al+Cu	0,91
				72	21	100	200	Al+Cu	0,74
				96	21	100	200	Al+Cu	0,43
				120	21	100	200	Al+Cu	9,31
				144	21	100	200	Al+Cu	17,96
S15	30,40	72	13+1	144	21	100	200	Al+Cu	8,94
S16	28,00	77	13+3	72	42	97	200	Al+Cu	6,49
S17	34,00	78	13+4	72	42	97	200	Al+Cu	13,38
				96	42	95	200	Al+Cu	6,50
S18	46,24	89	14+2	123	42	100	200	Al+Cu	7,43
Mean (SD)	15,20 (13,33)	51,05 (23,33)		**Mediane (min;max)**	21 (10;42)	97 (66;100)	200 µA in 93% of the cases	Al+Cu used in 70% of acquisitions	

In the existing literature, noise and its standard deviation (SD) are often calculated using a ROI in the air as an external, stable reference point outside the sample[24]. However, due to the post-processing methods applied in this study, the air signal in our MCT images exhibited variability in both MS and SD, rendering it unsuitable as a reference. Instead, the cradle used during imaging was identified as a stable reference point. The MS and SD of the cradle were

determined across the entire acquisition volume and used as the reference for noise calculations. The signal-to-noise ratio (SNR) for a specific target organ was calculated by dividing the MS of the organ in question by the SD of the cradle. The contrast-to-noise ratio (CNR) for a specific region (such as the brain or abdomen) was calculated as the difference in MS between two neighbouring organs in the region, divided by the SD of the cradle.

To investigate factors influencing CNR variations, a Pearson correlation analysis was initially conducted to assess the relationships between the CNR and fetal characteristics. After normal distribution controlled, a linear regression analysis using ANOVA was subsequently performed with two explanatory variables: fetal characteristics, e.g., weight, crown–rump length (CRL), and staining protocol parameters, e.g., staining duration to highlight the relationship between variables. All the statistical analyses were performed via R++ software[25]. Additionally, the CNR values were plotted against fetal weight, the CRL, and the staining duration via R version 4.3.0 to visualize these relationships.

C) Results

A total of 19 fetuses, with gestational ages ranging from 8 to 14+2 WG on the basis of the Robinson formula[26], with CRL from 16 to 89 mm were collected for this study between January 2016 and July 2023.

a. Dynamical study of the staining agent diffusion and its quantification.

Foetus S0 (female sex, CRL = 80 mm, interparietal diameter = 14 mm, foot length = 14 mm, weight = 30.06 g, 13+4 WG) was used for a dynamic analysis of the diffusion of the staining agent. Time series images of the diffusion of the staining agent in the fetus were obtained via three MCT transverse sections of interest, as presented in figure II.3.1 and in videos of supplemental materials II.3.1, II.3.2 and II.3.3.

Figure II.3.1 – Dynamic representation of contrast agent diffusion in sample S0 (female sex; CRL = 80 mm, interparietal diameter = 14 mm, foot length = 14 mm, weight 30,06 g, 13+4 WG) as a function of the staining time using Micro-CT imaging. The upper, middle and lower panels depict cerebral, thoracic, and abdominal sections of the sample, respectively.

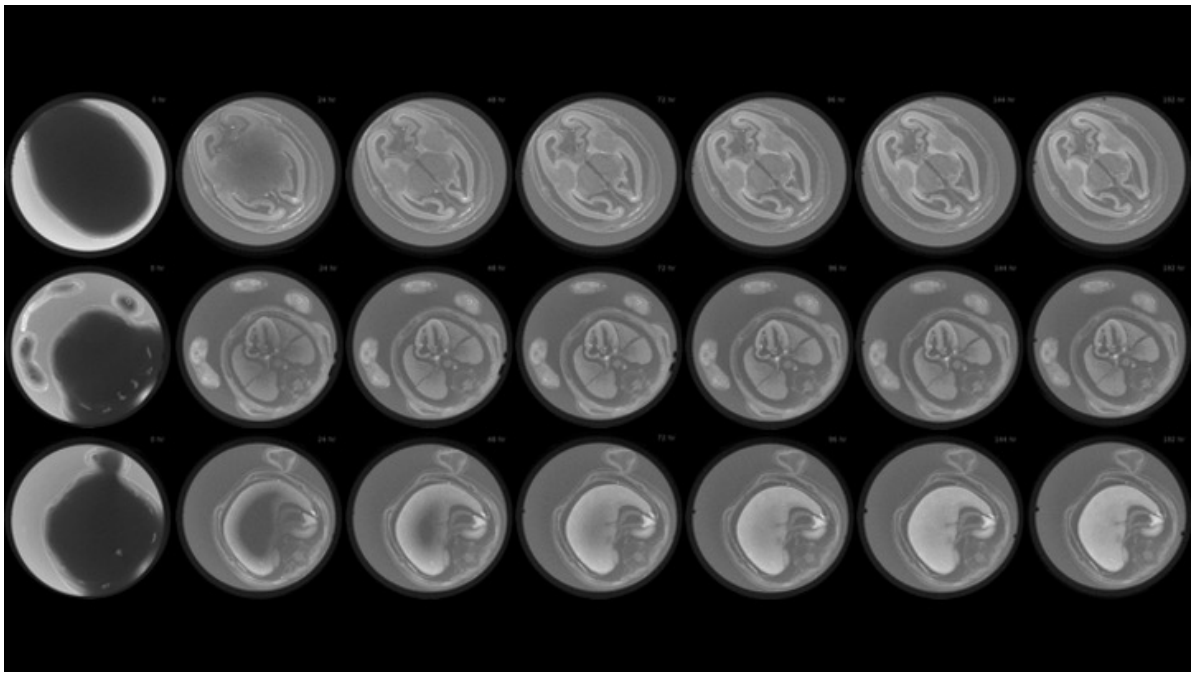

Supplemental material II.3.1 – Video - Time-lapse visualization of the contrast agent uptake in the Micro-CT cerebral section of sample S0 (female sex; CRL = 80 mm, interparietal diameter = 14 mm, foot length = 14 mm, weight 30,06 g, 13+4 WG). This video demonstrates the dynamic diffusion process within the brain structures over the staining duration.

Supplemental material II.3.2 – Video - Time-lapse visualization of the contrast agent uptake in the Micro-CT torso section of sample S0 (female sex; CRL = 80 mm, interparietal diameter = 14 mm, foot length = 14 mm, weight 30,06 g, 13+4 WG). The video highlights the staining progression in the thoracic region, including the cardiac chambers and major thoracic organs, as a function of time.

Supplemental material II.3.3 – Video - Time-lapse visualization of the contrast agent uptake in the Micro-CT abdominal section of sample S0 (female sex; CRL = 80 mm, interparietal diameter = 14 mm, foot length = 14 mm, weight 30,06 g, 13+4 WG). This video demonstrates the dynamic diffusion process over the staining duration focusing on abdominal organs such as the liver, spleen, stomach, and adrenal glands.

The iodine content in the staining solution was quantified as a CT signal, following a stretched exponential decay pattern (see Supplemental material II.3.4 – Figure). Diffusion dynamics were graphically represented over time, with MS values from ROI in different organs plotted in figure II.3.2. The data revealed that MS followed a stretched exponential model[183] in

all organs except the liver (Figure II.3.2 – upper graph). In the liver, staining diffusion was consistent with a double Weibull[185] distribution model (Figure II.3.2 – A, B and C and Table II.3.2). Fitted lines enabled the extraction of specific diffusion parameters for each organ (Table II.3.2).

As shown in Figure II.3.2, no contrast is evident between the posterior ventricle and the thalamic nuclei at 30 hours. However, a notable contrast between the posterior ventricle and the frontal cortex emerges over time. Figure II.3.2 A, B and C illustrates the contrast between the lung and liver showing a gradual transition from the periphery to the centre of the liver. At approximately 12 and 72 hours, the signal lines cross, and no contrast is observed between the lung and peripherical liver (Figure II.3.2A) or the hilum of the liver (Figure II.3.2C), respectively. Notably, sufficient contrast between the liver hilum and the lung was achieved only after a staining duration exceeding 120 hours. These diffusion characteristics guided the selection of specific staining bath durations to explore the correlation between contrast and fetal characteristics.

Supplemental material II.3.4 – Figure – Time-dependent decay of the contrast agent in various sections of the staining bath using Micro-CT imaging. The decay is expressed in arbitrary units (au) and plotted against the staining duration, illustrating the reduction in iodine concentration in the bath over time.

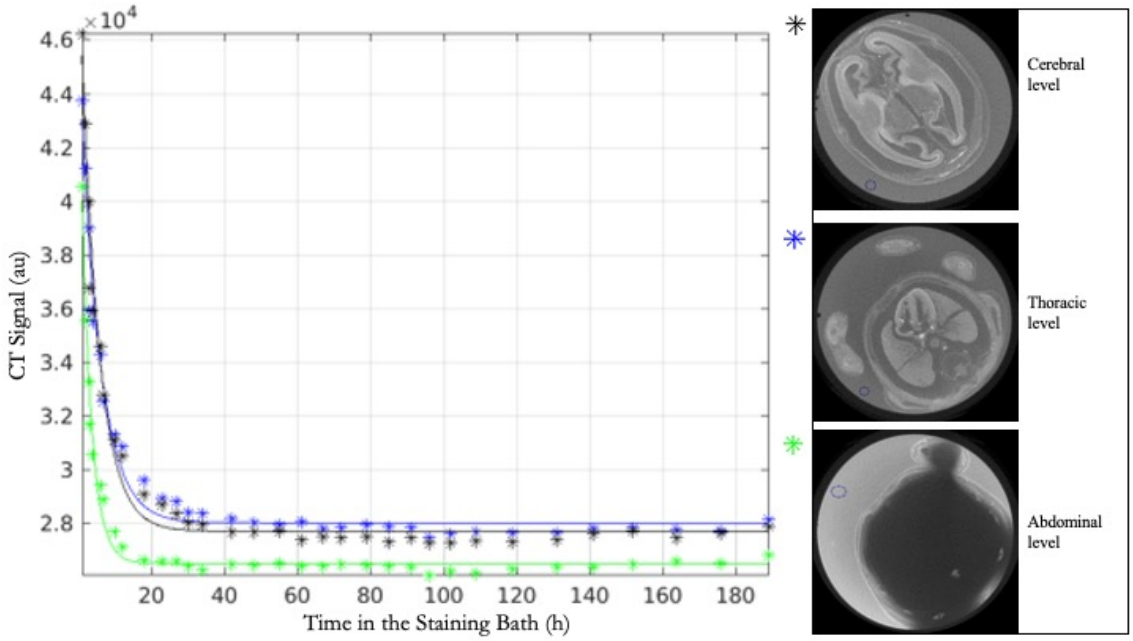

Figure II.3.2 – Time-dependent uptake of the contrast agent in various target fetal (top graph) and in the lung and liver (peripheral in **a**, central in **b** and hilum in **c**) using Micro-CT imaging. The uptake is measured in arbitrary units (au) over the staining duration.

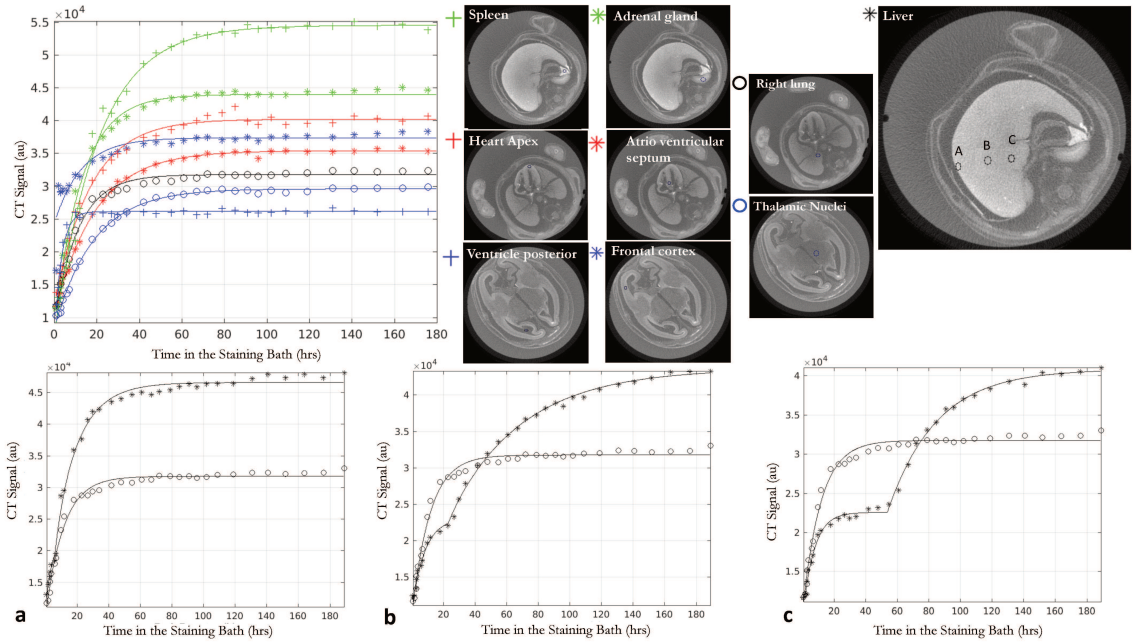

Table II.3.2 – Diffusion characteristics of the iodine solution in the target organs based on Weibull distribution and stretched exponential Models using Micro-CT imaging. The stretched exponential function $S(t) = A_0 + Amax\left(1 - exp\left(-\frac{t-t_0}{\lambda}\right)^{\beta}\right)$ where A_0 is the initial amplitude or baseline value of the signal, A_{max} is the maximum change, t_0 represents the starting time, λ is the characteristic time scale, and β is the stretching exponent[20].

Section	Targeted organs	Model fit	A_0 (au)	A_{max} (au)	t_0 (h)	λ (h)	β	Signal Growth rate (SNR/h)
Cerebral	Frontal cortex	stretched exp	125	12 919	0,13	7,30	0,57	507
	Thalamic nuclei	stretched exp	44	21 032	0,21	7,03	0,38	565
	Posterior ventricle	stretched exp	48	16 681	0,60	3,52	1,07	2 530
Thoracic	Atrioventricular septum	stretched exp	54	24 845	0,13	6,66	0,35	645
	Heart apex	stretched exp	60	28 477	0,04	6,64	0,40	850
	Right lung	stretched exp	49	22 096	0,22	6,10	0,54	975
Abdominal	Adrenal gland	stretched exp	44	35 275	0,12	6,41	0,50	1 370
	Spleen	stretched exp	43	45 990	0,68	7,30	0,35	1 114
	Liver - peripherical	Weibull	59	11 577	0,35	3,51	0,67	1 104
				23 389	6,00	62,56	3,91	731
	Liver - central			11 409	1,11	4,87	0,62	723
				20 585	23,00	71,66	1,54	221
	Liver - hilum			10 948	1,85	4,56	0,65	779
				18 237	53,87	70,23	2,27	295
Baths	on cerebral section	exp decay	141	18 584	0,77	3,32	0,69	1 938
	on thoracic section	exp decay	143	15 749	0,73	3,49	0,65	1 473
	on abdominal section	exp decay	135	15 494	0,63	3,38	1,25	2 857

b. Staining bath duration according to the fetal characteristics

After staining for varying durations, 18 fetuses were scanned via Dice MCT (Table II.3). The CNR from the liver to the lung was calculated via signal values from the ROIs in the liver (excluding the gallbladder and hepatic hilum) and in the lungs (avoiding pulmonary scissures where possible).

The Pearson correlation analysis revealed that the relationship between CNR Liver to Lung and biometric factors is negative, strong, and statistically significant for both CRL ($r = -0.56$, 95% CI [-0.77, -0.25], $p = 0.001$) and weight ($r = -0.54$, 95% CI [-0.75, -0.22], $p = 0.002$). Two linear regression models, fitted using Ordinary Least Squares (OLS), were used to predict CNR based on staining duration and either CRL or weight. Both models explain a substantial proportion of the variance in CNR (adjusted $R^2 = 0.71$ and 0.74, respectively, $p < 0.001$). In both models, staining duration showed a positive and significant effect ($\beta \approx 0.30$, $p < 0.001$), while CRL and weight exhibited negative significant effects (CRL: $\beta = -0.27$, $p = 0.004$; weight: $\beta = -0.58$, $p < 0.001$). Confidence intervals and p-values were calculated using the Wald t-distribution approximation.

As staining time increased relative to the CRL and weight, the CNR tended to increase, as represented by the green circles in Figure II.3.3. The dotted lines in the figures indicate the minimum staining duration required for a given CRL or weight to achieve a satisfactory contrast-to-noise ratio of 5 in accordance with the Rose criterion[187]. Thank to this line we were able to calculate the staining duration based on fetal weight and CRL: Staining duration = 2CRL - 12 and = 2weight + 12.5. For example, a fetus with a CRL of 50mm or a weight of 20g must be stained for a minimum of 96 hours to meet this threshold.

Figure II.3.3 – Scatter plot illustrating the correlation between fetal crown-rump length (CRL) in millimetres and fetal weight in grammes, respectively, and staining duration in hours to performed before micro-CT imaging. Data points are colour-coded based on the Contrast-to-Noise Ratio (CNR), with a gradient ranging from red (low CNR) to dark green (high CNR). The dotted line indicates the threshold where the CNR reaches 5, in accordance with the Rose criterion[187]. ***Staining duration = 2CRL - 12 = 2weight + 12.5***

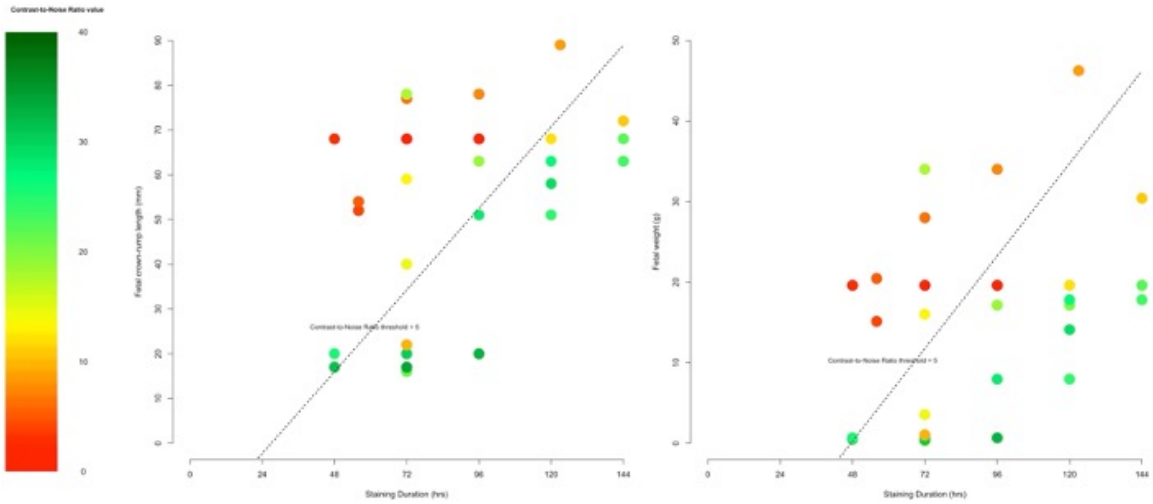

D) Discussion

The staining bath diffusion process is best described by a stretched exponential model in most organs. The duration required to achieve optimal contrast correlates with the fetal CRL and weight in non-macerated first-trimester fetuses. The use of an iodine staining bath significantly enhances contrast in Dice MCT imaging, with the duration tailored to the fetal CRL or weight ensuring optimal imaging quality.

Iodine staining is a common technique in histology and imaging. The preparation of the staining solution followed Arthurs' [9,11,12,16] methodology. Using a closed syringe limits iodine availability, ensuring reproducibility and clinical relevance. Over time, the iodine concentration correlated with the CT signal intensity and exhibited a stretched exponential decay (see Supplementary material II.3.2 – Figure).

Iodine staining in biological tissues results in intriguing interactions with stretched diffusion processes. While iodine transport typically follows classical diffusion in homogeneous media, its behaviour in tissues can deviate significantly because of factors such as tissue heterogeneity, molecular interactions, and environmental factors. This often leads to stretched exponential diffusion, characterized by a slower-than-expected iodine spread. In most organs, the staining bath diffusion process is effectively described by a stretched exponential model, reflecting the heterogeneous permeability of the tissue[20]. This model provides valuable insights into the rate of signal change and its maximal amplitude, both of which are directly influenced by the iodine concentration in the staining bath. Interestingly, liver staining revealed a unique absorption profile better characterized by a double Weibull distribution[23], resembling a double exponential distribution. This distinct pattern likely reflects the liver's dual vascular and duct systems.

To enhance clinical relevance, the study linked staining duration to the CRL and weight, both of which are widely used in clinical practice and are correlated with gestational age, and their relationship holds in cases with similar degrees of maceration. Maceration may confound the relationships among the CRL, weight, and staining duration. It is hypothesized that maceration alters tissue permeability, affecting iodine diffusion and contributing to variability in staining results[17]. Although higher maceration levels are associated with lower-quality MCT images, diagnostic accuracy is often still achievable[16]. Further studies should explore the impact of maceration levels and modes of death on staining protocols to refine techniques and improve imaging consistency in clinical scenarios.

The primary limitation of this study is its small sample size (n=18 fetuses), which may affect the generalizability of the findings. The hand free ROI delineation which may have a great variability intra and inter observatory. The several fetus size with organs size and density variability which may affect diffusion. However, its principal strength lies in its focus on a homogeneous population of non-macerated fetuses from abortions, minimizing variability. Given

the minimal maceration observed, these findings likely extend to cases of fresh miscarriage and termination of pregnancy.

E) Conclusion

The use of an iodine staining bath offers significant advantages in enhancing contrast in Dice MCT imaging of first-trimester human non-macerated fetuses. By tailoring the staining duration to fetal CRL or weight, optimal imaging outcomes can be achieved, facilitating more accurate and detailed analyses in both research and clinical settings.

PART III - MICRO-IMAGING FOR STUDYING FETAL ANATOMY

Facilitating the clinical application of micro-imaging requires the establishment of a detailed anatomical atlas of normal fetal development. Our research focused on two key gestational ages: 8 and 12 WG. At each gestational milestone, the study employed a multimodal imaging approach, combining MCT and HF-MRI to achieve a comprehensive characterization of early fetal anatomy. The study further incorporated quantitative contrast analyses at 8 WG and a biometric assessment at 12WG, enhancing our understanding of fetal development at these critical stages.

1. Micro-imaging at 8 weeks of gestation.

Lamouroux A, Cardoso M, Bottero C, Gallo M, Duraes M, Salerno J, Bertrand M, Rigau V, Fuchs F, Mousty E, Genevieve D, Subsol G, Goze-Bac C, & Captier G.

Micro-CT and high-field MRI for studying very early post-mortem human fetal anatomy at 8 weeks of gestation.

Prenat Diagn 2024; 44: 3–14.

(Annexe 3)

A) Introduction

The history of human embryology shows that 3D representations such as Da Vinci pictures of the *Fetus in the Womb*[188] and wax models[141,189] are important for studying, teaching and research. The concept of 3D reconstructions of serial histological sections of fetuses was first published in the 1980s [190]. A 3D atlas was published for practical implementation, and De Bakker's team made the atlas available to the scientific community in a dedicated website around 2015[191,192]. Despite computer assistance, these approaches remained tedious to design, gave uneven results, and are destructive to fetuses[173,193].

To explore fetal death, FPME, also called fetopathologic examination, is the gold standard for an accurate diagnosis and aims to allow for genetic counselling and to specify the recurrence risk[16]. FPME consists of a fetal and placental examination and includes standard radiographs;

photographs; external morphology examination with biometric data such as weight, size, cranial perimeter, and foot length; and internal examination (i.e., autopsy)[16]. FPME is summarized in Figure III.1.1. Systematic radiographs have a low diagnostic rate[124,128,194]. The rate of non-identifying causes of stillbirth is 30% to 60%[195]. In case of early ToP for FR from 11 to 16 WG, FPME with autopsy adds information in 55% of cases and modifies the genetics counselling in 21%[23,24]. Later in pregnancy, FPME may help in the grieving process[33], and couples refusing autopsy are more likely to regret their choices[105]. However, because of the invasive nature, CA and FPME are often declined by grieving couples[171].

Figure III.1.1 – Comparison between fetal pathological examination and very early virtual autopsy (HF-MRI: high-field MRI).

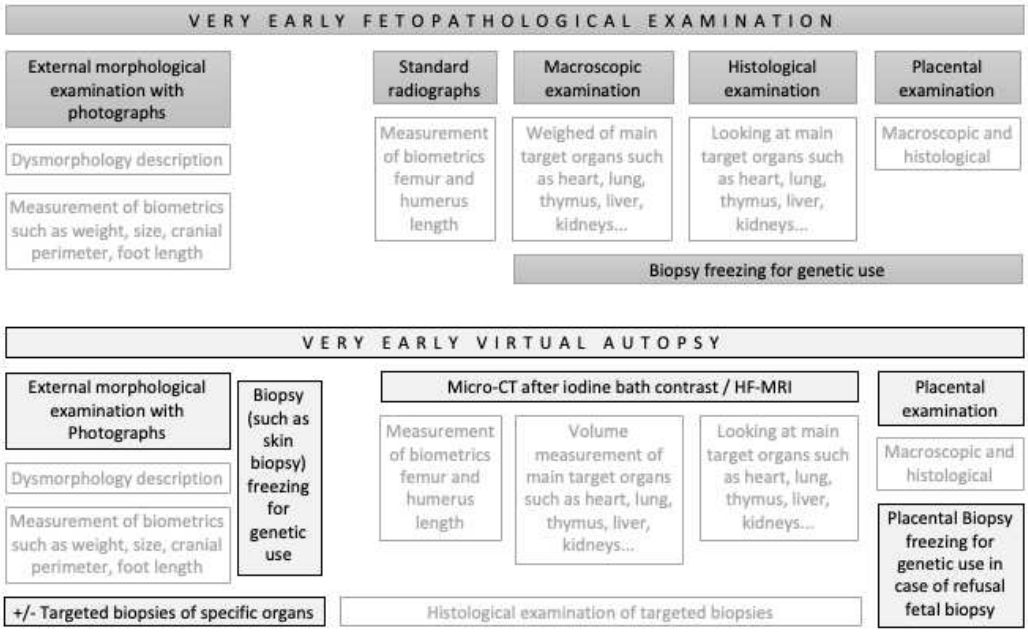

Consequently, virtual autopsy became possible with PM imaging such as MRI and CT, which have been used in clinical practice since 2010[36,37]. However, the fetal PM-MRI diagnostic yield depends on the anatomical area of interest[45–47] and is better than fetal PM-CT[39,130]. When results of prenatal ultrasonography and whole-body PM-MRI are concordant, there is limited benefit in performing a full autopsy[48]. Virtual autopsy also allows for better-quality brain imaging with fewer technical artefacts due to dissection[36–38]. Less invasive autopsy using MRI and CT has lower diagnostic accuracy when the fetus is < 24 WG[39,52]. However, virtual autopsy by imaging

has numerous advantages: it is non-invasive, data acquisition is fast and reproducible, it allows for less variability between operators and secondary reading of images by experts, and it improved the acceptance rate as compared with CA[35].

Micro-imaging such as MCT or HF-MRI provide high isotropic resolution of < 100 µm. Since 2001, these techniques have led to the development of non-destructive ways of visualizing small specimens such as animal embryos [173,196–199]. They have also allowed for performing human fetal non-invasive autopsy or virtual autopsy in fetuses < 24 WG by using PM micro-imaging such as HF-MRI since 2009[135] and MCT since 2017[43,144]. In comparison with HF-MRI, MCT is more common, costs less and requires Lugol's iodine solution (I2KI) contrast bath[52,69] before acquisition, which involves less time[171].

A recent review highlighted that current studies of MCT and HF-MRI mostly involved fetuses > 11 WG [52]. In comparing PM-MCT in early gestation to CA, Hutchinson et al. included fetuses from 11 to 21 WG[60]. In comparing HF-MRI versus MRI versus stereomicroscopic autopsy, Votino et al. included hearts at 11 to 20 WG [119]. Some case reports of MCT of fetuses at 6 WG[65], 7 WG[66] or 9 WG[117] have been published and two publications described fetuses < 11 WG: one involved MCT with 4 specimens from 7 to 11 WG [143] and one HF-MRI with 4 specimens at Carnegie stage 10 to 20 of about 3 to 9 WG [200]. Studies combining MCT and HF-MRI are few, and the most recent one focused on fetuses from 13 to 18 WG[62]. To our knowledge, no published study investigated multimodal micro-imaging in fetuses < 11 WG.

Early fetal loss is often downplayed. However, the psychological consequences of these losses should not be ignored. Indeed, miscarriage matters[26]. Miscarriage is common: 23 million miscarriages occur each year[26]. In the United Kingdom, Quenby et al. estimated the short-term national cost at 471 million pounds per year[26]. Psychological consequences are important and must be better diagnosed and treated[26]. The lack of interest and research on miscarriage was pointed out by a recent review in *The Lancet*[25,26]. So, PM explorations of fetuses < 11 WG are valuable for the medical community.

We studied very early PM human fetal anatomy at 8 WG by using whole-body multimodal micro-imaging such as MCT and HF-MRI and discuss its potential place in early first-trimester virtual autopsy.

B) Methods

We included pregnant women consulting for voluntary ToP, the majority, or early spontaneous miscarriage. Information sheets were given to the women during their consultation with the gynecologist or midwife. Written informed consent was obtained from each woman. All consents were revocable at any time. The exclusion criteria were age < 18 years or unable to give informed consent such as under guardianship or language barrier. The hospital's service for voluntary interruption of pregnancy collected the specimens after drug-induced expulsion and sometimes before surgical curettage in day hospitalization. Samples came from voluntary ToP and were externally examined by an expert in prenatal diagnosis to confirm malformation absence.

The protocol's workflow was 1) preparation with fixation, 2) imaging by MCT scan after staining protocols and by HF-MRI scan, which may be performed first or second, 3) imaging post-treatment and 4) obtaining several histologic sections obtained to control the procedure.

a. Micro-CT

We performed different preparation protocols before MCT acquisition with different fixation times and diffusive contrast baths (Table III.1.1) because preparation data at this early stage was limited. The 3 first sample preparation protocols[173 201] involved non-fixed (1) and late (2) and early (3) fixed specimens and was based on a contrast bath with a solution of 10% I2KI solution for 24 to 48 hr. This solution was obtained in the hospital pharmacy at the beginning of the study and was stored in a ventilated cabinet. This preparation was also not freshly made for each sample. From the preliminary results and in light of Gignac et al.[172,202] reviewing staining protocols for animal and human specimens, we derived protocol 4, which included early fixation with paraformaldehyde 4% (PFA 4%) after expulsion without any contrast bath. We finally set

up the protocol 5, diffusible iodine-based contrast-enhanced which consisted of immersing the early-fixed specimens with PFA 4% in a 1:1 ratio solution of PFA 4% and potassium triiodide (I2KI/Lugol's iodine solution, with total iodine content 63.25 mg/mL) for 72 hr as described by Hutchinson et al.[60]. Each preparation was freshly made in our laboratory.

Table III.1.1 – Detailed contrast bath protocols used before micro-CT imaging. (PFA 4%: paraformaldehyde 4%; I2KI: iodine potassium iodide 10% solution, dice: diffusible iodine-based contrast enhanced)

	Timing of the fixation in PFA 4%	Contrast Bath	I2KI 10% made in hospital pharmacy (contrast bath duration in hr)	PFA 4% and I2KI/Lugol's iodine, in a 1:1 ratio made freshly (contrast bath duration in hr)
Protocol 1	No	Done	48h	
Protocol 2	Late	Done	48h	
Protocol 3	Early	Done	48h	
Protocol 4	Early	No		
Protocol 5	Early	Done		72h

MCT acquisitions involved using the X-ray microtomographs SkyScan 1076 and SkyScan 1276 (Bruker) as detailed in Table III.1.2. In both cases, MCT settings such as spatial resolution, x-ray attenuation, power, and best filter were carefully determined and adjusted to the properties of the specimens to optimize the contrast between the tissues and the organs of interest (Table III.1.2).

b. HF-MRI

To enhance the contrast and safeness, the early-fixed specimens were immersed in fluorinert (PF40) in a hermetically sealed falcon tube during acquisition. HF-MRI acquisitions were performed on an Agilent 9.4 Tesla MRI scanner using 3D gradient echo multiple slices (Ge3D) with data matrix setting 512x256x256 isotropic voxels. HF-MRI settings such as

repetition time, echo time and accumulation were carefully determined and adjusted to the size and properties of the specimens to optimize the contrast (detailed in Table III.1.2).

c. *Image processing*

In MCT, the native images were first processed by using NRecon software (SkyScan, Bruker), which transforms serial views into CT. In some cases, DicomCT software was needed to convert TIFF files to DICOM (or dcm) files. Image processing and analysis of the HF-MRI acquisitions involved using homebuilt routines under the Matlab interface in DICOM format. The DICOM 3D reconstructions of the micro-imaging were post-processed and visualized by using Dataviewer v1.5.6.2 (SkyScan, Bruker); FIJI ImageJ v1.53q; Myrian v64 1.19.1 (Intrasense) and CT-Vox v3.3.0 r1383 (Bruker) software.

To highlight the potential clinical use of imaging, we aimed to match our imaging modalities with pictures illustrating ultrasound slices as recommended by the Conférence Nationale d'Echographie Obstétricale et Fœtale (CNEOF) group. These pictures are extracted from the French guidelines for good practice in obstetrical and fetal ultrasonography for second- and third-trimester ultrasound scans [203].

We performed a quantitative evaluation of signal-to-noise ratio (SNR) and contrast-to-noise ratio (CNR) for both imaging modalities. The different parameters were measured by using FIJI software with an evaluation of mean signal and its standard deviation of a specific region of interest. The noise was evaluated from the standard deviation of the cradle signal.

Table III.1.2 – Specimens included in the present study with their detailed characteristics, their preparation before micro-imaging, the type of micro-imaging performed and micro-imaging acquisition parameters. (WG: weeks of gestation).

Specimens	Specimen characteristics				Micro-CT acquisition							HF-MRI acquisition							Histology
	Gestational age according to the Robinson formula (WG)	Crown-rump length (mm)	Weight (mg)	Carnegie stage	Preparation before micro-CT	Micro-CT machine: SkyScan	Source voltage (kV) /current (µA)	Filter	Rotation step (degree)	Image pixel size (µm)	Scan duration (min)	Repetition time (ms)	Echo time (ms)	Flip angle (degree)	Average	Field of view (mm)	Voxel size (µm)	Scan Duration (hr)	
S1	7+3	12	300	17	Protocol 5	1276	87/175	Al 0.5mm	0.4	15	31	100	4.87	70	4	30x15x15	59	7h16	1
S2	7+5	14	243	18	Protocol 4	1276	44/100	No filter	0.4	15	34	100	5.30	70	6	24x12x12	47	10h55	
					Protocol 5	1276	95/166	Al 0.5mm	0.4	15	32								
S3	8	16	293	19	Protocol 5	1276	94/155	Al 0.5mm	0.4	18	31	100	5.30	70	6	24x12x12	47	10h55	
S4	8+1	17		19	Protocol 1	1076	59/167	No filter	0.1	9	134								
					Protocol 2	1076	59/167	Ti 0.025mm	0.34	36	22								
S5	8+3	19	678	20	Protocol 5	1276	80/200	Al 0.5mm	0.4	10	31	100	4.87	70	6	30x15x15	59	10h55	
S6	8+4	20	700	20	Protocol 4	1276	55/200	Al 0.25mm	0.4	20	32	100	4.76	70	6	32x16x16	62	10h55	
S7	8+4	20	690	20	Protocol 5	1276	95/200	Al 1 mm	0.4	14	10	100	4.87	70	6	30x15x15	59	10h55	
S8	8+5	21	1047	21	Protocol 4	1276	55/200	Al 0.25mm	0.4	21	28	100	4.76	70	6	32x16x16	62	10h55	
					Protocol 5	1276	98/200	Al 1mm	0.2	10	87								
S9	8+6	22	1000	21	Protocol 4	1076	59/167	Ti 0.025mm	0.2	36	38	60	4.87	70	4			4h28	1
					Protocol 3	1076	59/167	Ti 0.025mm	0.2	36	38								

d. Histology sections

Two specimens, S1 and S9 (Table III.1.2), underwent standard histology examination with hematoxylin and eosin staining and vascular immunostaining with CD34 to assess whether the specimen could be damaged, labelled or distorted by the contrast bath and MCT and HF-MRI acquisitions.

The French biomedicine agency (ABM) approved the FETTAL project (Fetal Enhanced Three-dimensional and Translational Anatomical Landscape project)[167,168]. This study is part of that project.

C) Results

Specimens were collected over 6 years, which resulted in a large sample of 75 fetuses. Twenty-three specimens were excluded because of incomplete miscarriage, partial fetus, or damaged specimens and 18 specimens were included in the genetics part of the FETTAL project. Among the 34 non-malformed fetuses included in the imaging part of the FETTAL project, the present study focused on the 9 specimens with crown-rump length (CRL) 10 to 24 mm and CRL-based gestational age from 7 to 9 WG according to the Robinson formula[177] (Figure III.1.2). Selected specimen characteristics such as CRL, gestational age, weight and Carnegie stage are summarized in Table III.1.2.

a. Micro-imaging

Table III.1.2 presents the MCT preparation protocols and acquisition parameters: machine, source voltage and current, filter use, image pixel size and scan duration; and HF-MRI acquisition parameters.

Protocols 1 to 4 gave no contrast, just natural contrast (left part of Figure III.1.3). However, MCT images with the protocol 5 were well contrasted and resulted in informative images. We also detail the anatomy of specimen S8 on the right part of Figure III.1.3: tongue [1],

oesophagus [2], trachea [3], and aorta (ascending [4] and descending [5]) can be clearly identified using MCT with protocol 5.

Figure III.1.2 – Flowchart with detailed cohort selection (CRL: crown–rump length; FETTAL: Fetal Enhanced Three-dimensional and Translational Anatomical Landscape project)

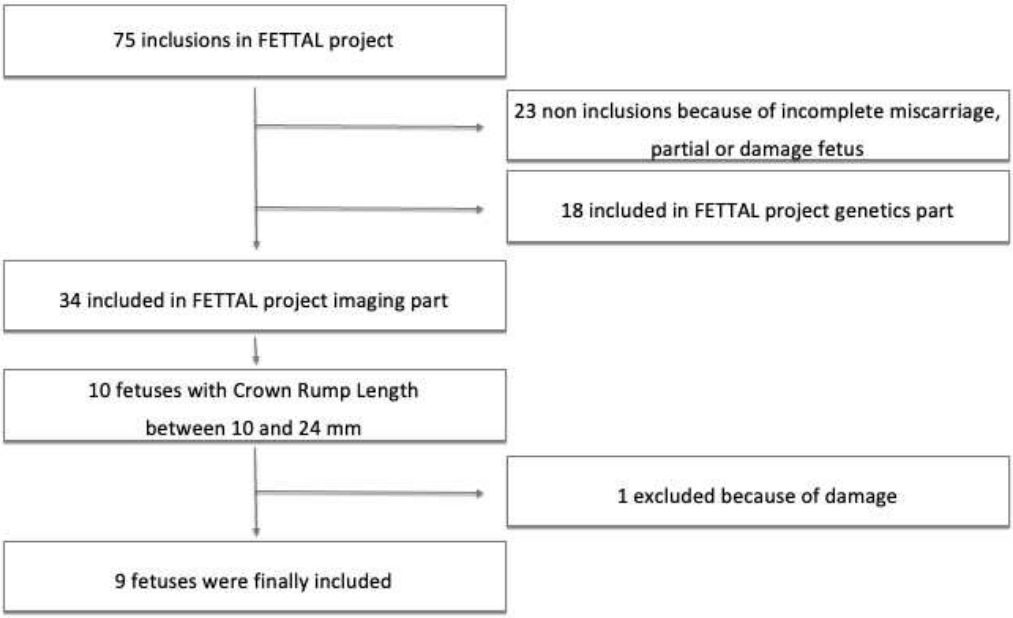

Figure III.1.3 – Micro-CT sagittal slice after protocol 4 (early fixation without any contrast bath) and protocol 5 (early fixation and 72hr immersion in contrast bath 1:1 ratio of PFA 4% and I2KI/Lugol's iodine made freshly) on specimen S9 (WG: weeks of gestation, CRL: crown–rump length). Using DataViewer (CT) software. (1: tongue; 2: oesophagus; 3: trachea; 4: ascending aorta arch; 5 descending aorta)

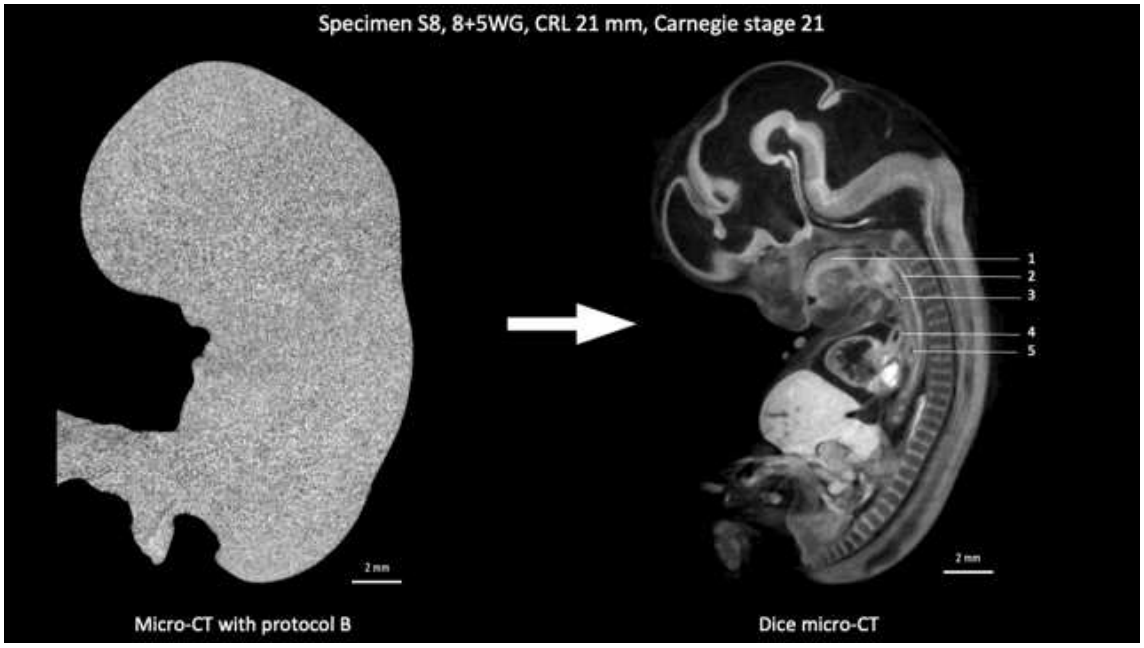

Figure III.1.4 shows the median sagittal view with MCT using protocol 5 and HF-MRI at different Carnegie stages in a fetus at about 8 WG. The detailed anatomy of these specimens is accessible clinically. Figure III.1.4 presents the thoracic-abdominal sagittal view of specimen S3. Unfortunately, this specimen had a rotation of the head, so the sagittal view of the head is in another plane.

Figure III.1.4 – Sagittal view of 6 specimens with both micro-CT after protocol 5 (early fixation and 72hr immersion in contrast bath 1:1 ratio of PFA 4% and I2KI/Lugol's iodine made freshly) and HF-MRI (high-field MRI) using DataViewer (CT) and Myrian (MRI) software (WG: weeks of gestation, CRL: crown–rump length).

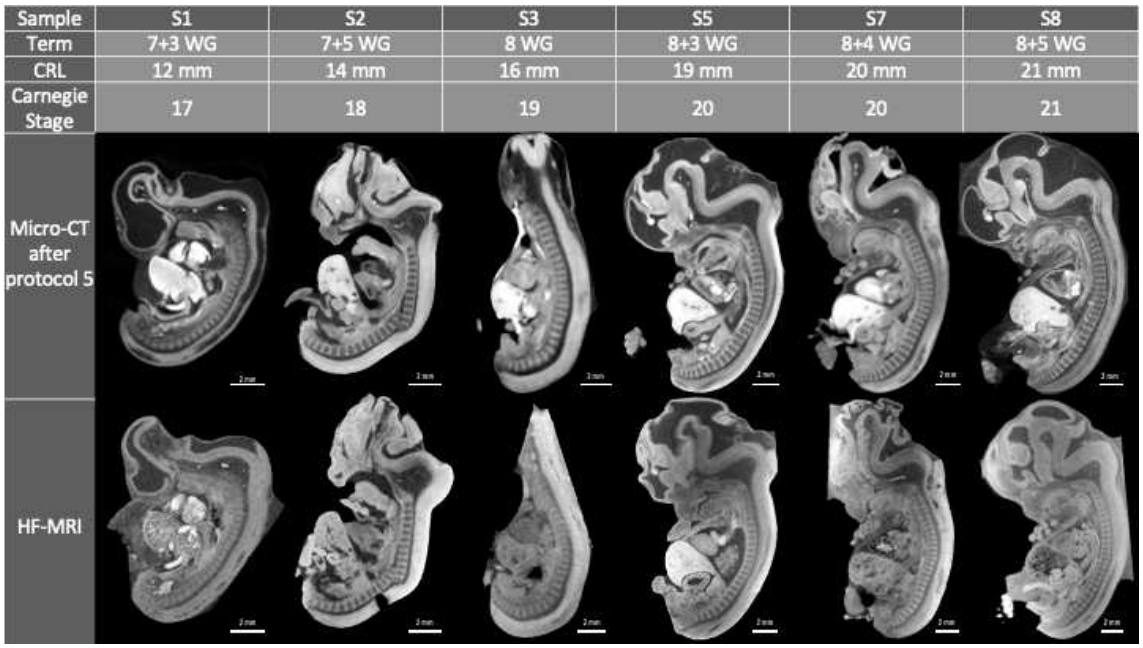

Three different pictures (inter-orbital distance, four-chamber view with pulmonary veins, transversal kidney view) are available from the CNEOF group French guidelines. These reference pictures aim to illustrate ultrasound images obtained during second- and third-trimester ultrasonography. We matched these pictures with slices of MCT using protocol 5 and HF-MRI for specimens S5 and S8 (Figure III.1.5). The thorax or abdominal transversal view is more circular during the second and third trimesters and more oval during the first trimester.

Figure III.1.5 – Specimens S5 and S8 with both micro-CT after protocol 5 (early fixation and 72hr immersion in contrast bath 1:1 ratio of PFA 4% and I2KI/Lugol's iodine made freshly) and HF-MRI (high-field MRI) in different slices matched with inter orbital distance view, four-chamber view with pulmonary veins, transversal-kidney view from the CNEOF French guidelines group[203] using DataViewer (CT) and Myrian (MRI) software.

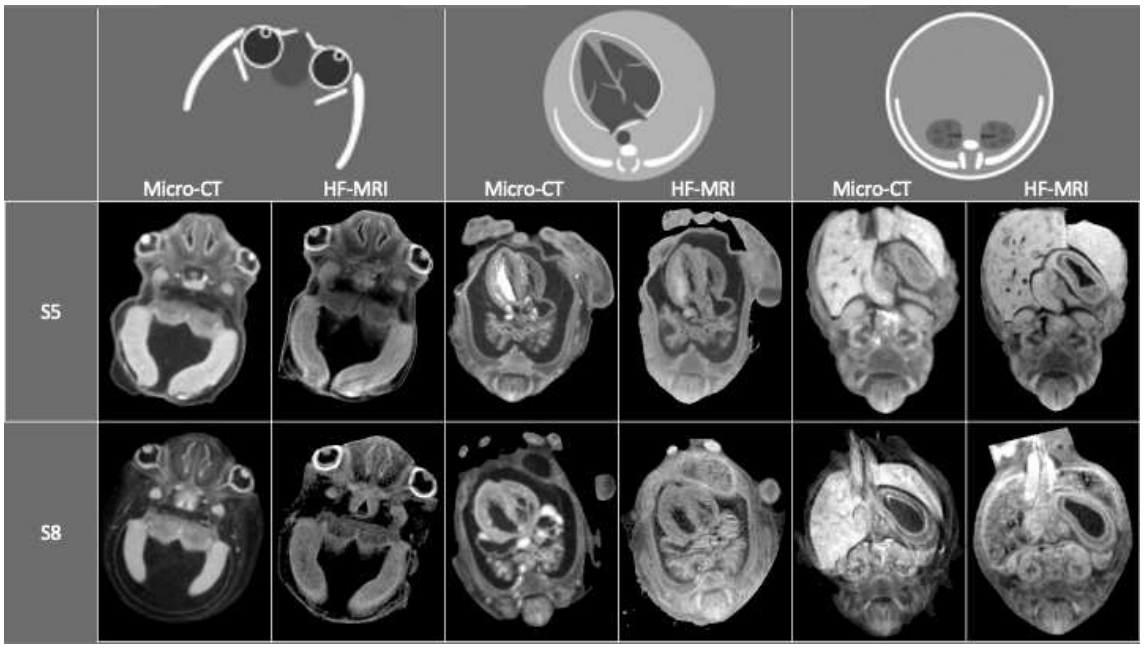

We performed quantitative signal evaluation using SNR and CNR. On inter-orbital distance view, the contrast is calculated between the crystalline lens and vitreous body; on four-chamber view, between the right ventricular wall and pericardium and on transversal kidney view, between the renal cortex and perinephric fat. The mean SNR with MCT and HF-MRI was 7.6 and 8.9, respectively and the mean CNR was 6.2 and 4.8, respectively (Figure III.1.6). So, our experimental conditions gave high SNR, > 5, according to the Rose criterion[187] and good CNR in most of the cases in both MCT using protocol 5 and HF-MRI.

Figure III.1.6 – Quantitative signal evaluation of specimens S5 and S8 using signal to noise (SNR) and contrast to noise (CNR) ratio. Arrowheads highlight crystalline lens (CL), right ventricular wall (RVW) and renal cortex (RC) and round tip arrows highlight vitreous body (VB), pericardium (PC) and perinephric fat (PNF).

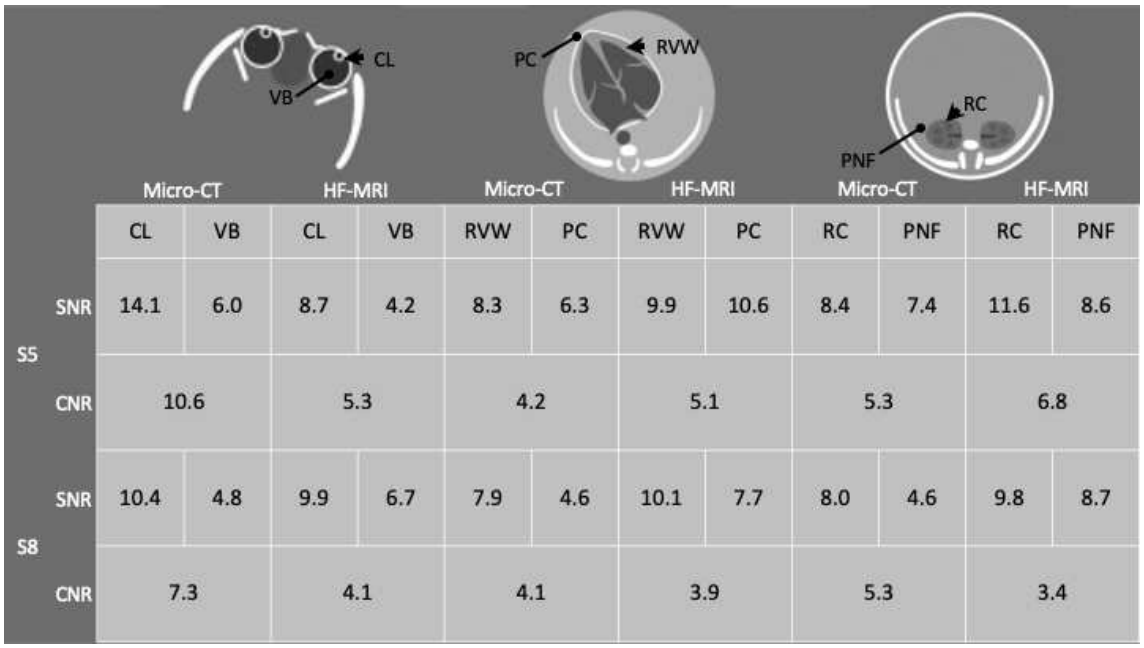

		CL	VB	CL	VB	RVW	PC	RVW	PC	RC	PNF	RC	PNF
S5	SNR	14.1	6.0	8.7	4.2	8.3	6.3	9.9	10.6	8.4	7.4	11.6	8.6
	CNR	10.6		5.3		4.2		5.1		5.3		6.8	
S8	SNR	10.4	4.8	9.9	6.7	7.9	4.6	10.1	7.7	8.0	4.6	9.8	8.7
	CNR	7.3		4.1		4.1		3.9		5.3		3.4	

b. Histology

Specimen S9 underwent both protocol 3 and 4 and specimen S1 protocol 5. Histology sections were submitted to a pathology specialist who did not find any damage or artifact or distortion. Coloration was homogenous, and quality was compatible with diagnosis. The histology sections were immunostained with CD34, which was positive (Figure III.1.7), despite the preparation protocols and micro-imaging acquisitions. Imaging did not alter the histology, allowing immunostaining and pathological examination.

Figure III.1.7 – Specimen S1 sagittal slice with micro-CT after protocol 5 (early fixation and 72hr immersion in contrast bath 1:1 ratio of PFA 4% and I2KI/Lugol's iodine made freshly), HF-MRI (high-field MRI) and histology in hematoxylin eosin and CD34 immunohistochemical staining using DataViewer (CT) and Myrian (MRI) software (WG: weeks of gestation, CRL: crown–rump length).

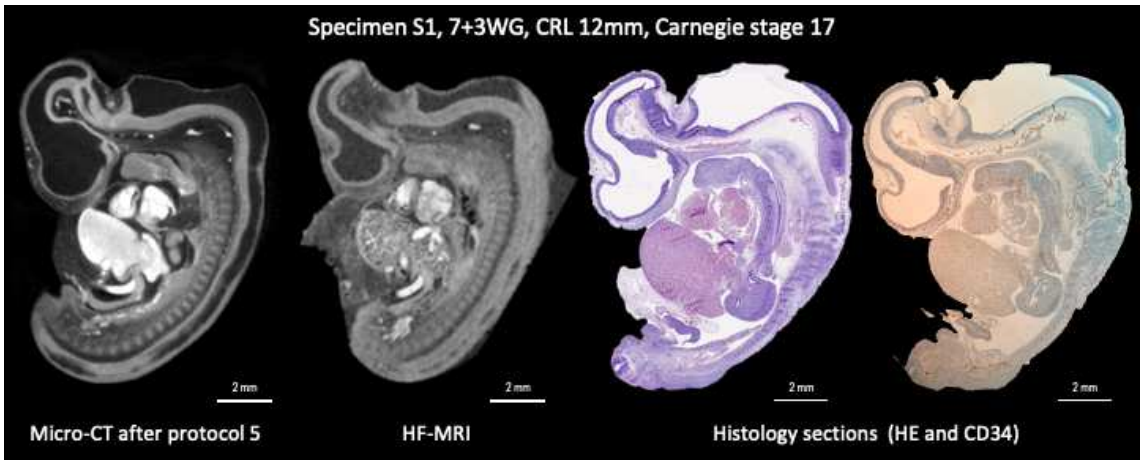

D) Discussion

This study shows the feasibility of investigating very early PM human fetal anatomy at 8 WG using whole-body multimodal micro-imaging such as MCT using protocol 5 and HF-MRI. The non-destructive morphological visualisation of the inner organs as early as 8 WG paves the way to virtual autopsy in the very early stage of the first trimester, which was limited until now.

As previously mentioned, a recent review highlighted the current limitations of imaging after 11 WG [52] except for some MCT case reports[65,66,117] and 2 small series of 4 cases [143,200]. We report for the first time the largest micro-imaging cohort of very young fetuses, around 8 WG. Several teams focused on a specific organ such as the heart[204], brain[145], and sacral artery[205]. As shown in our figures, the whole-body acquisitions can easily be used to focus on the desired organ. As shown in figure 5, PM micro-imaging allows an anatomical examination with better accuracy than second or third trimester prenatal ultrasonography as early as 8 WG. MCT and HF-MRI were found useful for virtual autopsy before 20 WG[52,128], and here we demonstrate that it can be reasonably extended to 8 WG.

Limitations of the present work are the small sample size for each of the modalities and the unicentric experience with only local expertise.

As compared with other protocols, iodinated MCT (using protocol 5) results in well-contrasted images, as shown in Figure 3. Our results are in favour of the need for early fixation before any contrast bath [172]. Therefore, the protocol 5 preparation should be freshly made just before use [69]. This protocol is specific because of its mixed character using a conservative solution (PFA 4%) and contrast solution (potassium triiodide I2KI/Lugol's iodine solution)[144]. A study comparing different previously published contrast baths might help support these observations.

Both iodinated MCT using protocol 5 and HF-MRI are valuable and result in great signal (SNR >5 according to the Rose criterion[187]) and comfortable CNR. The spatial resolution is better with MCT, 9 to 36 µm, as compared with HF-MRI, > 50 µm. The scan duration is variable, from about 30 min with MCT to 10 hr with HF-MRI (Table III.1.2), which favours the clinical use of MCT. However, a preparation protocol with contrast bath before MCT takes time, about 72 hr, whereas no preparation protocol is needed for HF-MRI. HF-MRI is the only technique used in preclinical imaging at present[128,171]. However, MCT is now used for virtual autopsy clinically [61,69,171]. HF-MRI machines are more expensive than MCT tomographs and are probably less available around the world. Because of the short learning curve for using MCT, this technology is probably more accessible to a wider range of practitioners. In contrast, HF-MRI needs specific expertise. In conclusion, each technique has its advantages and limitations, and the choice could probably be guided by the purpose: clinical use or research into embryology or a specific organ.

This study shows non-macerated fetuses without any malformation, which enables high-quality anatomical analysis. The use of these imaging techniques in clinical practice will need to consider and adapt to fetal maceration. Maceration may create artefacts even though anatomical examination remains possible [68].

Others considered that MCT has better diagnostic value and quality of imaging on quantitative and qualitative outcomes than HF-MRI [62]. Figure III.1.4 highlights the high liver absorption of the iodine contrast. This high absorption might be due to the sponge aspect of the

liver, which pooled systemic and portal vascularisation and the bile duct. This adds difficulty to the study of the liver using iodinated MCT with protocol 5. If we were to carry out a study focusing on the liver, we would probably use HF-MRI. We could also carry out a preliminary MCT study with a lower dilution of lugol or a shorter bath duration or rinsing techniques[142] more adapted for examining liver abnormalities. The cerebral cortex appears with different grey layers on HF-MRI, so HF-MRI seems better than MCT for examining the central nervous system. Future study should focus on the best imaging modalities to study each organ. When the prenatal diagnosis unit identifies an abnormality in a specific organ, the question is which imaging modality is the most pertinent for non-invasive FPME: HF-MRI, MCT, or PM-US.

Fetal pathology, FPME and CA described in Figure III.1.1 is currently the gold standard reference protocol. In fetuses < 11 weeks, invasive procedures are rarely performed because of microdissection difficulties and fast maceration. However, as previously mentioned, early fetal loss should not be downplayed because they are common, with 23 million occurring each year [26]. Miscarriage PM exploration is valuable both in the clinic and in research [25,26]. Consequently, we propose a feasible management circuit to perform early virtual autopsy in a fetus during the first trimester, before the fetus is released to the family (Figure III.1.1).

EE is needed and is of central relevance. The paucity of scientific literature on this subject, with only the good study by Abdalla et al. in 2015[19], is at odds with the clinical interest that experts in fetopathology see on a daily basis. Further scientific studies on EE are needed. Thus, EE occupies a central place before micro-imaging in the procedure we are proposing for virtual autopsy in the first trimester (Figure III.1.1).

A frozen sample such as a skin biopsy to explore genetics must be taken before iodinated MCT because the contrast bath contains paraformaldehyde and is also not compatible with genetics analysis on biopsy. In case of maceration or other causes of un-assessable genetics samples, a placental sample may be frozen and used for genetics exploration if needed. The coupling of MCT with biopsy should be able to perform genetic analysis in early pregnancy loss.

We suggest a double benefit of very early virtual autopsy: on the one hand, obtaining a precision phenotype allows a reverse phenotyping to select variants of interest in genome-wide analysis, offering potential genetic counselling for bereaved parents and on the other, medical follow-up and talking about the loss may both have great psychological benefit for the future of the couple.

Micro-imaging and autopsy might be combined if needed. Imaging did not alter the histology, allowing immunostaining and pathological examination. Finally, in most cases, virtual autopsy can be performed when the parents refuse an invasive procedure. A procedure with EE; biopsy, if possible; micro-imaging; and other alternative procedures (ultrasonography, minimally invasive procedures etc.) might be better than doing nothing.

Conclusion

PM non-destructive whole-body micro-imaging using iodinated MCT and HF-MRI allows for PM human fetal anatomy study as early as 8 WG. It paves the way to virtual autopsy in the very early first trimester. Obtaining a precision phenotype, even regarding miscarriage products, allows a reverse phenotyping to select variants of interest in genome-wide analysis, offering potential genetic counselling for bereaved parents.

2. Micro-imaging at 12 weeks of gestation.

The 12 WG mark represents a critical gestational age corresponding to the first-trimester ultrasound, measuring nuchal translucency (key marker of aneuploidy) and crown-rump length (reflecting gestational age), which also improves obstetrical outcomes. Recent advancements in first trimester US have significantly improved the early detection of congenital malformations. As the accuracy of these early assessments increases, the demand for more comprehensive knowledge of normal fetal anatomy at 12 WG using advanced imaging techniques like MCT will undoubtedly grow.

This study incorporates a biometric approach to establish normal reference ranges for fetal measurements at 12 weeks. While routine biometric measurements may not always be necessary for diagnosing malformations, they can provide valuable data for future research, particularly in cases with suspected pathologies. Careful selection of biometric parameters is crucial, as they can have significant implications for genetic counselling. For example, hypoplasia of the thymus, lungs, or kidneys are key indicators in certain genetic disorders, whereas adrenal hypoplasia may be less relevant in this context.

The objective was to explore PM-human fetal anatomy between 12 and 12+6 WG with crown-rump length (CRL) between 57 to 68 mm using Dice-MCT and HF-MRI.

A) Method

Non-macerated non-malformed fetuses obtained from abortion in the frame of the FETTAL Project were scanned with this objective of exploring the normal fetal development.

a. Micro-CT

The specimens preparation consist in an early fixation in paraformaldehyde 4% (PFA 4%) and a staining by immersion in a solution of PFA 4% and potassium triiodide (I2KI/Lugol's iodine solution, with a total iodine content of 63.25 mg/mL) in a 1:1 ratio as described by Arthurs team[60,69,178]. According to our previous study about samples preparation before MCT, the staining

duration was determined in link to the fetal size, CRL between 57 to 68 mm, corresponding to a staining duration about 120hrs. Each staining preparation was freshly prepared in our laboratory on the day of its use.

MCT acquisitions were performed using the X-ray microtomographs SkyScan 1276 (Bruker). The MCT settings such as spatial resolution, X-ray attenuation, power, and the optimal filter were carefully determined and adjusted according to the manufacturer recommendations to optimise the contrast (Table III.2.1).

MCT native images were initially processed using NRecon software (SkyScan, Bruker), which transforms serial views into CT in tiff or DICOM format. The DICOM 3D reconstructions were post-processed and visualised by using VG max software.

b. HF-MRI

To prevent tissue deterioration and preserve contrast integrity, early fixed specimens were immersed in fluorinert (PF40) within a hermetically sealed Falcon tube during acquisition. Fluorinert is well known for not producing an H+ signal in MRI. HF-MRI acquisitions were conducted on an Agilent 9.4 Tesla MRI scanner using 3D gradient echo multiple slices (Ge3D) with isotropic voxels. The HF-MRI settings, including repetition time, echo time and accumulation were carefully determined and adjusted to the dimensions and characteristics of the specimens to optimise contrast (Table III.2.1). The image processing and analysis of the HF-MRI acquisitions involved the use of custom-built routines under the Matlab interface in DICOM format.

Table III.2.1 – Specimen characteristics, micro-imaging preparation and acquisition settings (WG: weeks of gestation; CRL: crown-rump length; BPD: biparietal diameter; M: male ; F: female ; MCT: micro-CT; HF-MRI: high field MRI)

Fetus	**S1**	**S2**	**S3**	**S4**	**S5**
Term	12+2 WG	12+4 WG	12+4 WG	12+4 WG	12+6 WG
CRL (mm)	58	63	63	65	68
weight (g)	14,1	17,14	17,8	16,86	19,6
BPD (mm)	19	19	19	20	19
foot length (mm)	8,5	8	9	10	9
M/F	F	F	M	F	F
			Dice-MCT after staining during 120hr		
Source voltage (kV)	94	100	94	95	100
Source current (**µ**A)			200		
Filter			Al+Cu		
Rotation step	0,8°	0,4°	0,8°	0,8°	0,4°
Rotation			360°		
Image pixel size (**µ**m)	42	21	42	42	21
Scan duration (mn)	9	25	12	12	34
			HF-MRI		
Repetition time (ms)			100		
Echo time (ms)			4		
Flip angle (degree)			70		
Average	6	4	6	6	6
Field of view (mm)	80 X 40 X 40	70 X 35 X 35	80 X 40 X 40	80 X 40 X 40	80 X 40 X 40
Voxem size (**µ**m)	78	68	78	78	78
Scan duration (hr,mn)	10,55	7,16	10,55	10,55	10,55
Antenne diametre (mm)	63	43	63	63	63

c. Image processing

To highlight the potential clinical utility of imaging, we sought to match our imaging modalities with images illustrating ultrasound slices in accordance with the recommendations of the French national group for obstetric and fetal ultrasound, the *CNEOF (Conférence Nationale d'Echographie Obstétricale et Fœtale)*. These images were extracted from the French guidelines for good practice in obstetrical and fetal ultrasonography for second- and third-trimester ultrasound scans[203].

d. Statistical Analysis

The data was inputted into an independent database (Microsoft Excel, Seattle, WA). We performed descriptive statistical tests using R++ software[186]. Quantitative variables are expressed as the mean with the corresponding standard deviation.

B) Results

A total of 75 fetuses were included in FETTAL project, over a period of seven years. Twenty-three specimens were excluded due to incomplete miscarriage, partial fetus, or damaged specimens. Eighteen specimens were included in the genetics part of the FETTAL project. The present study focused on the five non-malformed fetuses with crown-rump length (CRL) between 57 to 68 mm and CRL-based gestational age from 12 to 12+6 WG according to the Robinson formula following the exclusion of one sample due to damage. This is illustrated in the flow chart on figure III.2.1. The selected specimen characteristics, including CRL, gestational age, weight, and sex, are presented in Table III.2.1.

Figure III.2.1 – Flowchart of the samples included in this study from the FETTAL project

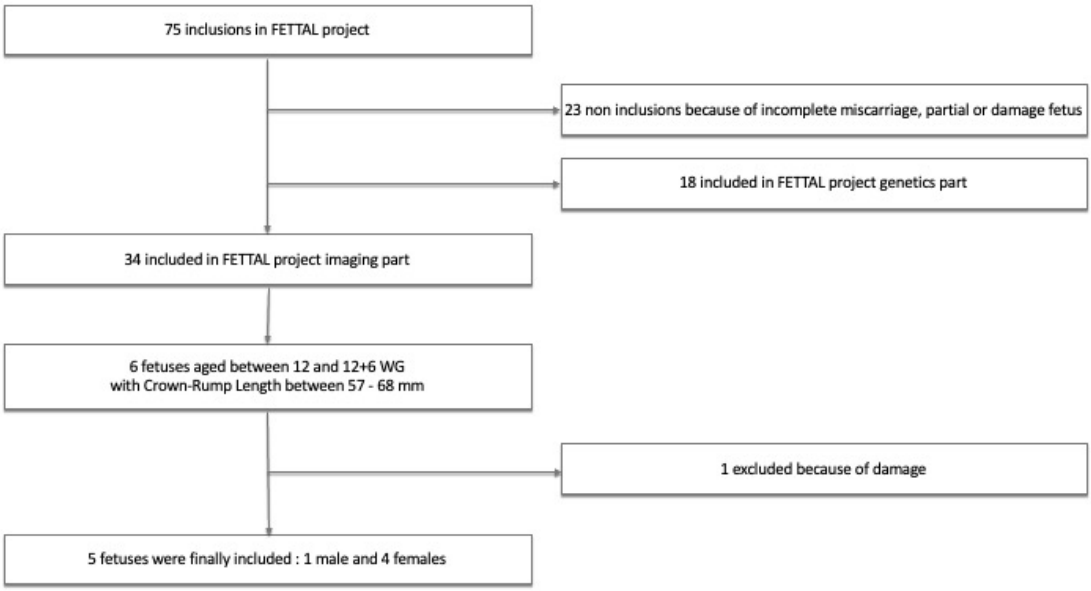

Figure III.2.2 depicts the median sagittal view of the cephalic extremity of fetuses using MCT and HF-MRI.

Figure III.2.2 – Cephalic sagittal sections using micro-CT (MCT) and high-field MRI (HF-MRI) of human fetuses aged of 12+3 to 12+6 weeks of gestation (WG) with a crown-rump length (CRL) of 61 to 68 mm.(M: male ; F: female)

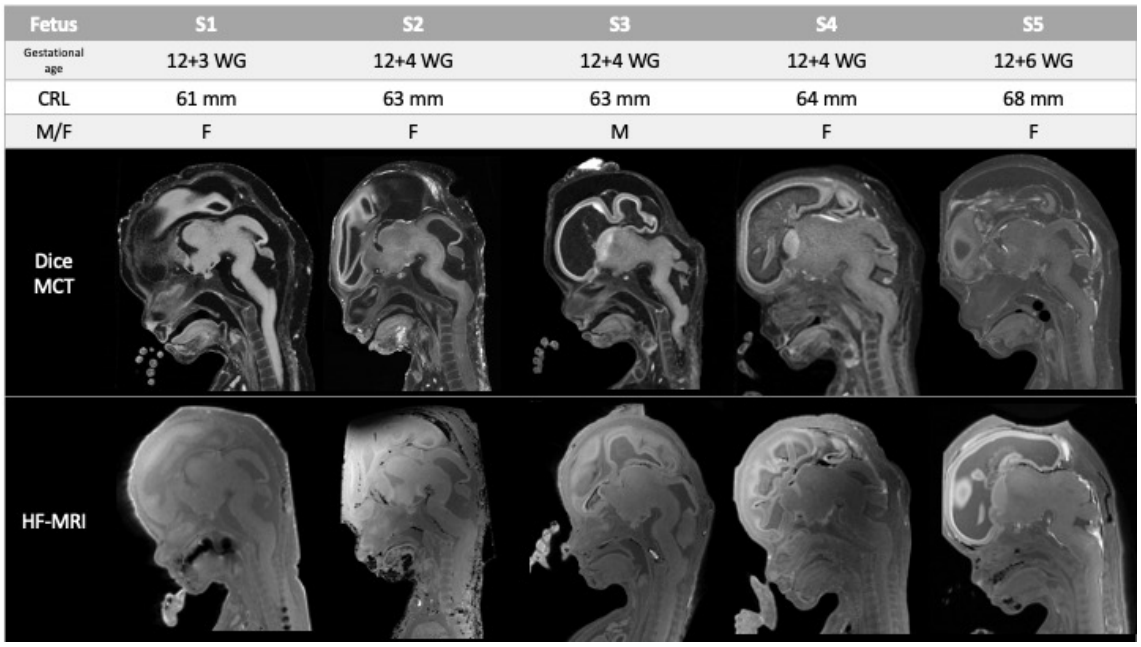

To gain a more detailed understanding of the anatomy, reference images from the CNEOF group[206] are matched with MCT and HF-MRI focusing on the head of sample S4 in Figure III.2.3, the torso and upper abdomen of sample S3 in Figure III.2.4, and sagittal view of the abdomen and skeletal system of sample S3 in Figure III.2.5.

Figure III.2.3 – Dice Micro-CT and high-field MRI imaging of female human fetus S4 at 12+4 weeks of gestation with a crown-rump length of 64 mm. Cephalic ultrasound referenced sections: biparietal (highlighting thalamic nucleus, septum pellucidum), posterior fossa, median sagittal and interorbital.

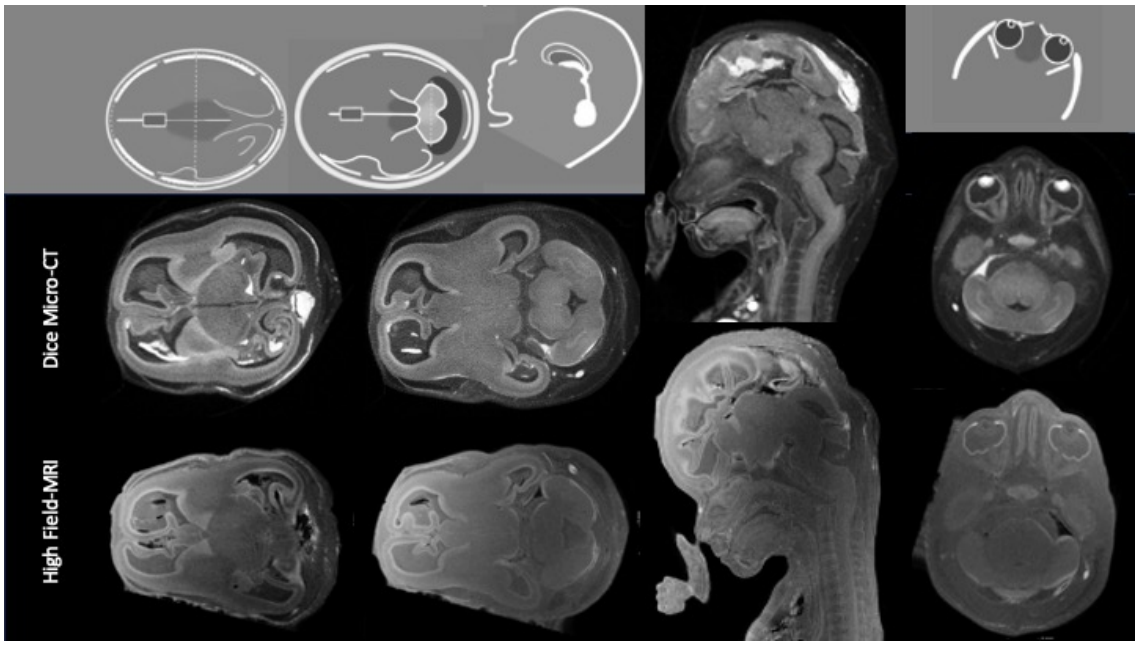

Figure III.2.4 – Dice Micro-CT and high-field MRI images of male human fetus S3 at 12+4 weeks of gestation with a crown-rump length of 63 mm. Ultrasound-referenced sections of the torso (four chamber view, three vessels view, pulmonary artery around aorta) and of the abdomen (abdominal circumference, transverse view of the kidneys).

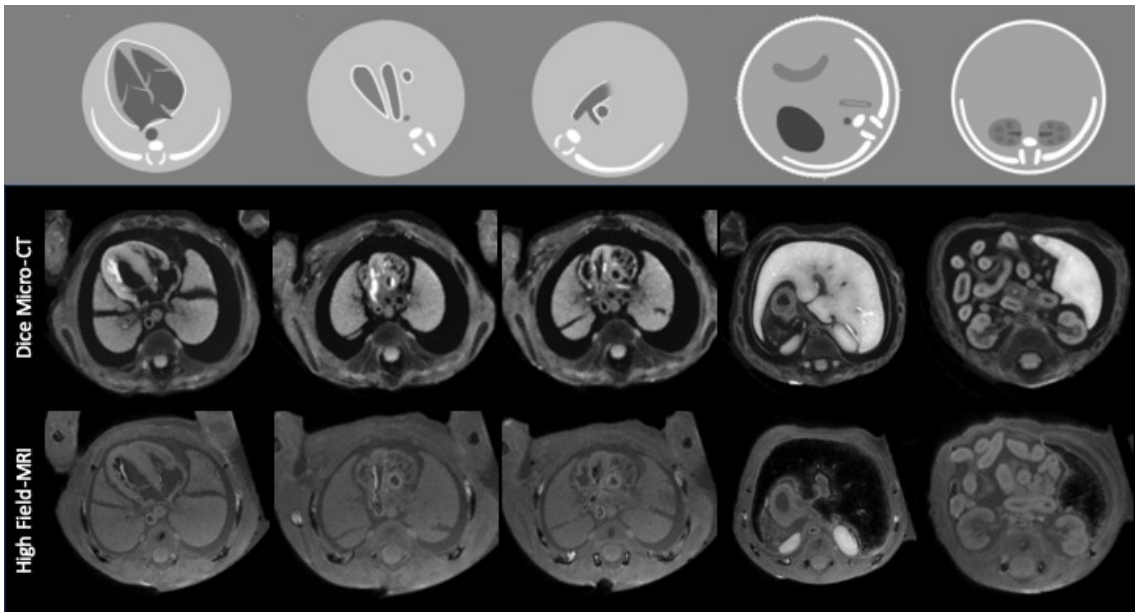

Figure III.2.5 – Dice Micro-CT and high-field MRI imaging of male human fetus S3 at 12+4 weeks of gestation with a crown-rump length of 63 mm. Ultrasound-referenced sections of the medullary canal in median sagittal view, of the parasagittal diaphragm with the stomach and transverse view of both femora.

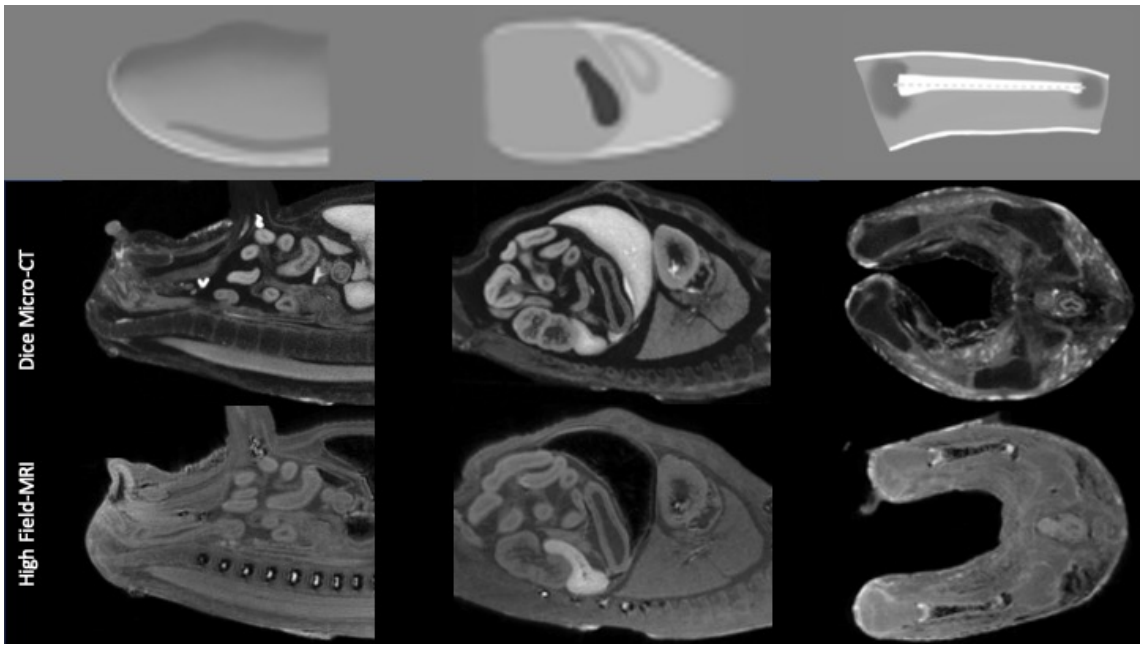

To provide a description of typical development, a series of biometric variables were measured. There was a notable discrepancy in the measurement of crown-rump length between EE conducted with a vernier calliper and those derived from imaging-based techniques using MCT and HF-MRI. This discrepancy is illustrated in Figure III.2.6, which presents the data in the form of a box plot. A summary of the mean and standard deviation of organ biometry obtained using MCT and HF-MRI is presented in Table III.2.2.

Figure III.2.6 – Discrepancy in the measurement of CRL between external examinations conducted with a Vernier calliper and those derived from imaging-based techniques using Micro-CT and HF-MRI.

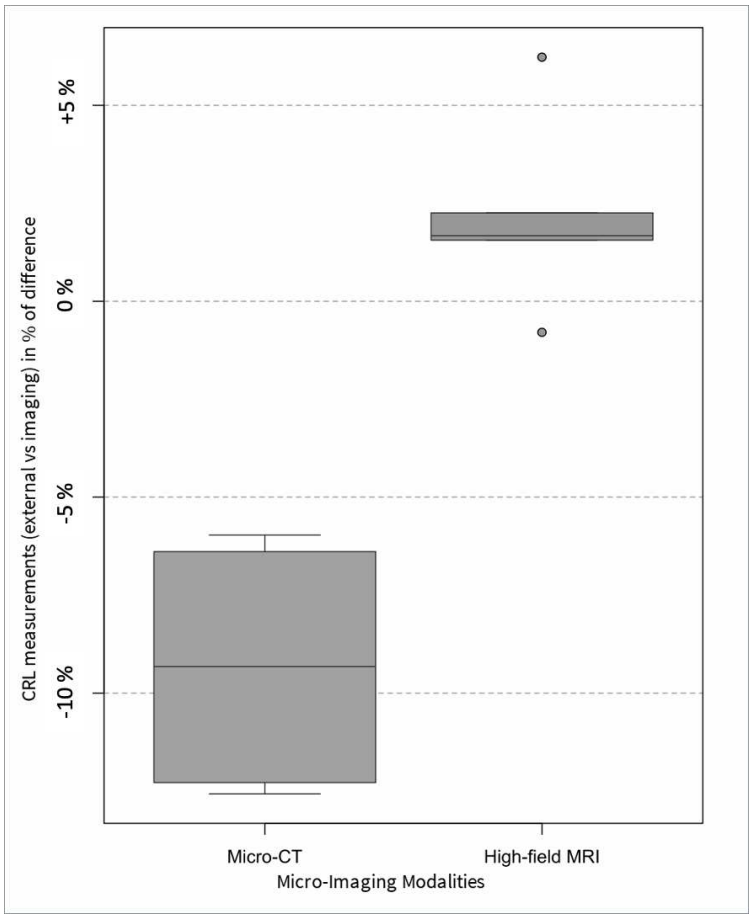

Table III.2.2 – Organ's biometry means, and standard deviation obtained using Micro-CT and HF-MRI to explore 12WG human fetus (TD = transversal diameter, AP = anteroposterior).

		Micro-imaging modality		Mean Shrinkage
		Micro-CT	High-field MRI	
		Mean (SD)	Mean (SD)	
Cervico cranial	Crown rump length using imaging	57.88 (3.46)	65.17 (2.4)	11%
	Cerebellum TD	10.29 (1.22)	12.56 (0.98)	18%
	Inter-orbital distance	4.85 (0.42)	5.28 (0.39)	8%
	Eye TD	3.78 (0.4)	4.37 (0.31)	14%
	Thyroid TD	2.96 (0.33)	3.55 (0.59)	15%
Thoracic	Thymus TD on 3 vessels view	2.44 (0.37)	3.03 (0.36)	20%
	Left lung height on frontal view	7.49 (0.69)	9.43 (0.57)	20%
	Right lung height on frontal view	7.44 (0.56)	8.87 (0.54)	16%
	Heart perimeter on 4 chamber view	18.65 (2.68)	21.1 (2.06)	12%
	Interventricular septum sickness	1.05 (0.04)	1.29 (0.35)	13%
Abdominal	Liver height on frontal view	11.15 (1.35)	12.94 (1.61)	13%
	Liver TD	12.73 (0.97)	14.35 (0.71)	11%
	Spleen great axis	2.12 (0.49)	2.64 (0.74)	19%
	Right kidney height on frontal view	4.47 (0.83)	5.29 (0.75)	16%
	Left kidney height on frontal view	4.49 (0.65)	5.68 (0.83)	21%
	Right kidney TD	2.56 (0.47)	3.47 (0.6)	26%
	Left kidney TD	2.7 (0.67)	3.79 (0.5)	28%
	Right adrenal height on frontal view	2.84 (0.68)	3.48 (1.01)	17%
	Left adrenal height on frontal view	2.67 (0.52)	3.62 (0.79)	25%
Extremities	Femoral length	12.97 (1.4)	13.96 (1.44)	4%
	Femoral shaft length	4.94 (0.69)	6.88 (1.57)	28%
	Tibial length	9.63 (0.85)	10.97 (0.96)	10%
	Fibular length	8.56 (0.93)	9.74 (1.69)	7%
	Humeral length	13.66 (0.64)	15.1 (0.94)	9%
	Humeral shaft length	5.96 (0.66)	7.32 (0.61)	18%
	Radial length	9.6 (0.35)	10.92 (0.75)	12%
	Ulnar length	10.17 (0.49)	11.43 (0.65)	11%

C) Discussion

Investigating PM human fetal anatomy at 12 WG using MCT and HF-MRI is both feasible and valuable for applying a biometric approach when necessary.

This study focusing on the normal development of non-macerated and non-malformed fetuses, as maceration significantly complicates the interpretation of PM imaging. Although MCT enables visualisation even in macerated fetuses[68]. Establishing a baseline of normal, non-macerated imaging features is crucial for advancing the clinical application of micro-imaging in FPME.

Our findings highlight that both micro-imaging techniques, MCT and HF-MRI, provide highly detailed visualisation of fetal anatomy, consistent with previous study[50,51,128,141,181]. Both techniques allow the detection of congenital malformations. We have illustrated their screening potential by referencing the CNEOF group's[206] recommendations on morphological ultrasound. These illustrations are intended to support colleagues specialising in prenatal diagnosis, serving as visual guides rather than enforcing a rigid imaging protocol. Micro-imaging generates 3D reconstructions from image stacks, which can be analysed in transverse, sagittal and coronal planes, facilitating accurate diagnosis of fetal congenital malformations.

We also explored several biometric measurements to describe normal development (Table 2). Despite a small sample size, the low standard deviation observed in these measurements suggests potential reproducibility, though further studies are needed to confirm this.

The choice of biometric data to be included is important due to their possible impact on genetic counselling. For example, thymic, pulmonary, or renal hypoplasia is a key phenotype in a genetic disorder diagnosis, whereas adrenal hypoplasia is less relevant. For instance, a thymic hypoplasia is a marker for 22q11.2 deletion syndrome[207]. However, the goal is not to systematically measure every organ, as this can be time-consuming without significantly enhancing diagnostic yield. Instead, targeted charts are used when organ abnormalities are suspected. Advancements in genetics and next-generation sequencing make it increasingly

relevant to integrate imaging with genetic findings of uncertain significance in a process known as reverse phenotyping.

Comparing the two micro-imaging modalities reveals differences: HF-MRI tends to expand measurements, while MCT retracts them (Figure III.2.6), likely due to tissue distortion caused by the contrast bath used in MCT. The true dimensions are probably in between closer to those observed with HF-MRI. Efforts to reduce MCT-related distortion, such as adjusting the pH of the contrast bath with buffered Lugol's solution, have been proposed[142].

The advantages of MCT include affordability, wide availability, and faster acquisition[50,51,128,141]. However, it requires a contrast bath, often over several days, followed by a rinsing step that can alter the external appearance of the fetus[50,51,128,141]. A recent study comparing MCT and HF MRI found that MCT offers superior resolution and contrast for organ recognition and assessment[62].

To maximize diagnostic accuracy, these micro-imaging techniques should be integrated into a broader diagnostic strategy. A detailed EE by specialists remains a cornerstone of PM fetal assessment[19], including biometric evaluations, dysmorphic facial features, and external malformations[15,16]. The French Society of Fetopathology has been training practitioners to perform FPME for several decades[15]. Practitioners come from a variety of backgrounds including pathology, clinical genetics, gynaecology/obstetrics and forensic medicine. Expertise in embryonic development and congenital malformations is essential for the appropriate management of FPME[15]. Combining prenatal history and EE help determine the most appropriate diagnostic approach, including PM imaging, CA and targeted biopsies.

In conclusion, MCT and HF-MRI are effective tools for studying PM human fetal anatomy at 12 WG, offering detailed visualization and enabling a biometric approach. Establishing micro-imaging baselines for non-macerated, non-malformed fetuses will expand the utility of micro-imaging in LIA FPME, ultimately improving access to genetic counselling for a broader population.

PART IV - POST-MORTEM MICRO-CT : CLINICAL APPLICATIONS AND INSIGHTS.

PM imaging is becoming a more acceptable part of perinatal autopsy, particularly for very early gestation or small fetuses where CA may be challenging and rejected by parents. MCT is a feasible tool for non-invasive diagnostic imaging in human fetuses below 24 WG. MCT provides good agreement with autopsy, particularly for brain, thoracic and abdominal pathologies, but the diagnostic yield in a large, unselected population which may contain macerated fetuses is unknown.

During my mobility program, I conducted a comprehensive extensive data collection on the first thousand MCT scans performed in Great Ormond Street hospital, performed the statistical analysis and wrote the draft. This second collaboration study shows the relative contribution of MCT to non-invasive autopsy in an unselected population of over 1000 fetuses in a real-world clinical setting.

Simcock IC, Lamouroux A, Shelmerdine SC, Sebire NJ, Hutchinson CJ & Arthurs OJ.
Fetal post-mortem imaging using microfocus computed tomography: single centre retrospective clinical experience.
Submitted in American Journal of Obstetrics and Gynecology
(Annexe 4)

1. Introduction

Perinatal invasive autopsy is the reference standard for the detection of congenital fetal abnormalities, which may contribute to the diagnosis of cause of pregnancy loss. For example, FPME as full fetal CA (EE, skeletal radiographs, internal macroscopic examination and histological examination of samples of target organs and macroscopic and microscopic examination of the placenta) can provide additional information in over 75% of cases compared to antenatal ultrasound, and can change genetic counselling in 32.5% of cases.[23]

Despite CA providing important information to parents and clinicians on recurrence risk or implications for future pregnancies, many parents now decline invasive autopsy and prefer non-invasive alternatives.[33] Often following an out-of-hospital miscarriage or pregnancy loss, parents are not aware of the range of options available and may avoid coming to medical attention unless there are complications. This population is largely ignored by medical practitioners and the true rate, and determinants of early pregnancy loss is largely unknown, as most studies are based on hospital data.

For those reasons, PM imaging has been developed to provide high resolution 3D imaging datasets which may be able to provide diagnostic information sufficient to avoid an invasive autopsy in most fetal cases. The use of conventional clinical techniques such as MRI is well established for PM imaging of older fetuses, but diagnostic accuracy rates fall with smaller fetal body weight, typically below 300 g,[50,113,116,128] with a lack of clinical alternatives for early gestation fetal loss.

Microfocus computed tomography (MCT) has been proposed as a clinical alternative, using iodine to generate high tissue contrast in small fetuses. Initial pilot studies using this technique were promising particularly for early gestation fetal cardiac anomalies[143,146] and tissue preparation protocols have now been developed.[69,142] We introduced MCT in our centre in 2016 and have seen a rapid increase in demand for this non-invasive tool, with an initial feasibility study demonstrating lack of additional benefit of progressing to invasive autopsy if MCT findings were normal or concordant with antenatal findings.[61]

The aim of this study was to establish the relative diagnostic yield of MCT compared to other non-invasive procedures (placental examination and EE) as part of LIAs in fetuses below 24 WG.

2. Methods

A) Study design

We completed a single centre, retrospective study of consecutive unselected whole-body iodinated PM-MCT performed as a part of FPME over a 7-year period at our tertiary referral centre (October 2016 - October 2023). We obtained ethical approval from the NHS Health Research Authority (HRA) Ethics Committee (IRAS ID: 131395).

MCT was offered to all centres and parents who referred fetuses to us below <300 g bodyweight, based on predicted maximum tissue preparation time of 14 days.[69,178] There were no exclusion criteria. Written parental consent was acquired for all PM imaging and subsequent autopsy, where performed. All parents gave fully informed written consent allowing for their "ceiling" autopsy type, i.e. maximum invasiveness FPME to be conducted, from a choice of a) full invasive autopsy, b) minimally invasive autopsy including detailed imaging, with keyhole or laparoscopic approaches permitted, or c) non-invasive autopsy including detailed imaging but no tissue sampling.[50,51,128] All parents were informed of the estimated time taken to iodinate and de-iodinate the baby together with possible skin colour changes.[61] All samples were handled in accordance with the Human Tissue Act 2004. Some demographic data was collected as part of routine clinical audit.

B) Procedures and definitions

All bodies were stored at 4°C in a mortuary following delivery and parental consent was obtained by the referring hospital prior to transfer to our centre.

Specialist paediatric pathologists first evaluated the clinical context with mode of death, estimated gestational age, maternal and familial medical history, consanguinity, ethnicity, first trimester explorations, ultrasound, fetal medicine unit and genetic data if available.

The mode of fetal death was collected and defined as

1. in utero death (IUD): any fetal death which occurred prior to delivery, ("missed miscarriage") irrespective of mode of delivery.

2. miscarriage (spontaneous or "fresh miscarriage") which correspond to spontaneous expulsion or onset of labour irrespective of the theoretical term.

3. termination of pregnancy (ToP), defined as induced labour with or without feticide. We further defined ToP for fetal reasons (FR) into categories including fetal malformation, chromosomal abnormality, twin pregnancy complications, or ToP for premature rupture of membrane (PROM), whether there was infection or anhydramnios.

C) Fetal Post-Mortem Examination contribution to the diagnosis

FPME was defined as contributory if a diagnosis (cause of fetal death or diagnosis of main abnormality) was reached overall, sub-categorised further by placental examination, EE, radiographs, MCT or invasive autopsy.

In all cases, an initial whole body skeletal radiograph (babygram or survey) was performed. Specialist paediatric pathologists then performed an PM EE with fetal size (i.e. crown – rump and crown – heel lengths, foot length, weight), maceration score (based on a severity scale of 0 (none) to 3 (severe)), gender, facial dysmorphism, external malformation included intrabuccal, choanal, genitalia and anal examination. Placental examination involved macroscopic and later microscopic and immunochemistry if necessary, according to national guidelines[17].

We divided overall diagnosis (cause of fetal death or diagnosis of main abnormality) into fetal and placental causes. We defined "imaging diagnostic performance" as MCT was contributory when the image quality was diagnostic, and non-contributory when severity of maceration rendered the imaging non-diagnostic. We divided MCT abnormalities by target organ and organ system, excluding traumatic lesions related to delivery, expulsion, maceration or obstetric complications, for example abdominal wall disruption in a severely macerated fetus was not termed a congenital abnormality.

D) Micro-CT Imaging protocol

The detailed study protocol has been published[69]. In brief, the fetus was immersed in a diluted I_2KI solution[178] for several days, and scanned using set parameters (100 - 130kV, 230-350uA, 250-350ms, 2 frames per projection) for a whole-body low-resolution scan at 21-113 microns, and separate high-resolution brain and body scans at typically 12-63 micron resolution[69]. Images were reported by one of two consultant radiologists (OJA or SCS), with 18- and 14-years' radiology experience, and 8- and 5-years MCT experience respectively. The fetus was then returned to the mortuary following imaging, placed in thiosulphate solution to remove the staining discolouration and then returned to the referring hospital and the parents.

We collected timing data include dates of delivery, receipt of the body, FPME, when placed into I_2KI solution ("dipped"), MCT performed, MCT reported, autopsy final report and body release from our hospital.

Some abnormalities were attributed to delivery, maceration or PM changes, which included brain abnormalities such as cracking of the cerebral hemispheres, or mid-brain disruption due to delivery, and body wall abnormalities such as herniation through an abdominal or thoracic wall defect when the abdominal wall was intact on antenatal imaging.

E) Conventional autopsy

The decision to perform an invasive autopsy was guided by PM EE including parental consent, medical history, antenatal context, PM EE, MCT imaging, placental examination, and the pathologist's opinion regarding potential additional benefit of further examination. We applied a clinical policy to do the minimum level of invasive autopsy required to reach a diagnosis (as per standard parental consent). For example, a markedly macerated fetus where the imaging was normal, placenta was normal and antenatal imaging was normal, would not proceed to invasive autopsy, even if the parents had consented.

However, if there was uncertainty regarding the diagnosis on MCT or findings that conflicted with the antenatal examination findings, then the pathologist would decide whether to proceed to autopsy on a case-by-case basis, assuming parental consent was provided, and a placental cause was not present. All autopsies were conducted in line with the standards set by the Royal College of Pathologists.[17] All perinatal autopsies were performed by one of 7 specialist paediatric pathologists with at least 6 years perinatal pathology experience.

F) Statistical Analysis

The data was inputted into an independent database (Microsoft Excel, Seattle, WA). We performed descriptive statistical tests using R++ software.[186] Qualitative variables are expressed as absolute number and percentage of the effective population. Quantitative variables are expressed as the mean with the corresponding standard deviation. Duration variables are expressed as median with the corresponding first and third quartile.

3. Results

We imaged 1007 fetuses over the study period (October 2016 - October 2023). Referrals to our centre increased rapidly following offering the service in 2016, with increase from 37 cases in 2017, to 215 in 2021 (Figure IV.1). We did not notice a significant effect of COVID disruption on being able to offer the service nor referral patterns (time affected March 2020 – March 2022). MCT numbers were lower for 2023 due to data collection ending in October 2023.

Figure IV.1 – Number of Micro-CT imaging cases performed per year according to the subgroup (Key – dark bars – In utero deaths (IUD); grey bars – miscarriage or ToP for SROM; white bars – ToP for fetal malformation or other reason).

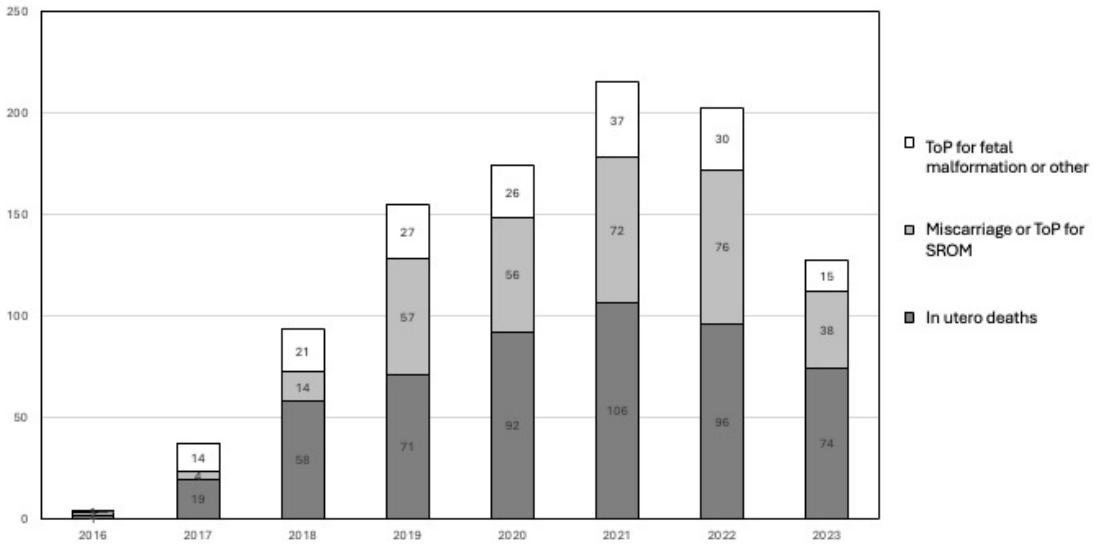

Demographics and referral data is provided in Table IV.1. We received referrals from 20 different referral hospitals, with no more than 15% of overall numbers from any individual centre. Most cases were born to Caucasian parents with no gender preponderance (Table IV.1). Mean theoretical term and mean real term (estimate using crown-rump length (CRL) and Robinson formula[177]) were 17.92 WG (SD 2.86) and 10.33 WG (SD 2.09), respectively. Mean CRL and mean body weight were 11.64 mm (SD 3.5) and 92.38g (SD 83.34), respectively. Over half of all fetuses were severely macerated by pathological evaluation (519 / 1007; 51.7%; Table IV.1).

Table IV.1 – Referral pattern and demographics, including gender, parental ethnicity, estimated gestation, fetal measurements and maceration score by subgroup (ToP termination of pregnancy, SROM spontaneous rupture of membranes)

		Overall	In Utero Deaths	Miscarriage or ToP for SROM	ToP for fetal malformations or other	Missing data
		1007 (100%)	**517 (51.34%)**	**319 (31.68%)**	**171 (16.98%)**	
GENDER	Male	497 (49. 35%)	266 (51.45%)	157 (49.22%)	74 (43.27%)	
	Female	439 (43.59%)	202 (39.07%)	156 (48.90%)	81 (47.37%)	0
	Undetermined	71 (7.05%)	49 (9.48%)	6 (1.88%)	16 (9.36%)	
MOTHER ETHNICITY	Caucasian	425 (66.10%)	240 (70.38%)	105 (55.85%)	80 (70.18%)	
	Black	97 (15.09%)	42 (12.32%)	45 (23.94%)	10 (8.77%)	364
	Indian	57 (8.86%)	26 (7.62%)	19 (10.11%)	12 (10.53%)	
	Other	64 (9.95%)	33 (9.68%)	19 (10.11%)	12 (10.53%)	
FATHER ETHNICITY	Caucasian	427 (66.41%)	246 (70.89%)	103 (56.91%)	78 (67.83%)	
	Black	84 (13.06%)	44 (12.68%)	30 (16.57%)	10 (8.70%)	364
	Indian	74 (11.51%)	32 (9.22%)	26 (14.36%)	16 (13.91%)	
	Other	58 (9.02%)	25 (7.20%)	22 (12.15%)	11 (9.57%)	
Theorical-term (weeks of gestation) : Mean (SD)		17.92 (2.86)	18.46 (2.9)	17.7 (2.3)	16.75 (3.19)	308
Term according to Crown-rump length according to Robinson formula (weeks of gestation) : Mean (SD)		10.33 (2.09)	9.83 (2.01)	11.16 (1.81)	10.32 (2.31)	3
Crown-Rump length (mm) : Mean (SD)		11.64 (3.5)	10.79 (3.37)	13.02 (3.04)	11.62 (3.88)	3
Crown to Heel Length (mm) : Mean (SD)		16.18 (5.18)	14.9 (4.93)	18.28 (4.61)	16.06 (5.67)	8
Foot Length (mm) : Mean (SD)		1.83 (0.84)	1.6 (0.79)	2.17 (0.79)	1.9 (0.85)	29
Post mortem weight (g) : Mean (SD)		92.38 (83.34)	61.72 (64.88)	131.77 (84.13)	111.59 (94.55)	0
MACERATION ACCORDING TO PATHOLOGICAL EXAMINATION	None	302 (30.11%)	7 (1.35%)	195 (61.32%)	100 (59.52%)	
	Mild	118 (11.76%)	27 (5.22%)	53 (16.67%)	38 (22.62%)	
	Moderate	64 (6.38%)	41 (7.93%)	13 (4.09%)	10 (5.95%)	4
	Severe	519 (51.74%)	442 (85.49%)	57 (17.92%)	20 (11.90%)	

A) Performance times

The median times taken for us to receive the baby from the referring hospital was 7 days (range 5 – 10 days), median time taken to scan and report the MCT was 9 days (range 6 – 14 days) and overall median time taken from receipt of the body to release from the mortuary was 18 days (range 13 – 23 days; Table IV.2).

Table IV.2 – Turnaround times: Birth to receipt of the baby reflects the time taken for the baby to arrive at our centre, with all other intervals referenced to the day of referral. (ToP termination of pregnancy, SROM spontaneous rupture of membranes, Q1 Q3 first and third quartile, Iodination means being placed in iodine)

Duration in days	Overall	In Utero Deaths	Miscarriage or ToP for SROM	ToP for fetal malformations or other
Median (Q1, Q3)	**1007 (100%)**	**517 (51.34%)**	**319 (31.68%)**	**171 (16.98%)**
Birth to Receipt	7 [5, 10]	7 [5, 10]	7 [5, 10]	6 [5, 10]
Receipt to Post mortem examination	1 [1, 3]	1 [1, 3]	1 [1, 2.75]	1 [1, 2]
Receipt to Iodination	1 [1, 2]	1 [1, 3]	1 [1, 2]	1 [1, 2]
Receipt to MicroCT	8 [6, 12]	7 [5, 11]	10 [6, 13]	8 [5.75, 13]
Receipt to MicroCT Report	9 [6, 14]	8 [6, 13]	10 [7, 14]	11 [6, 14]
Receipt to Final report	15 [12, 23]	15 [11, 22]	16 [13, 23]	16.5 [12, 25.25]
Receipt to Release	18 [13, 23]	15 [12, 22]	20 [15, 26]	19 [14, 23]

B) Fetal Post-Mortem Examination contribution

Although many parents consented to a full autopsy including MCT, our pathologists did not predict an additional yield from invasive autopsy in most cases (Figure IV.2). Only 43 fetuses proceeded to additional invasive autopsy to provide diagnostic clarification, implying an autopsy "avoidance rate" of 95.7% (964 / 1007).

Figure IV.2 – Post-mortem examination by parental consent vs type of post-mortem performed, categorised by subgroup (IUD, miscarriage, ToP). Key: dark squares = full autopsy; grey = minimally invasive autopsy MIA or less invasive autopsy approaches; white = external examination only

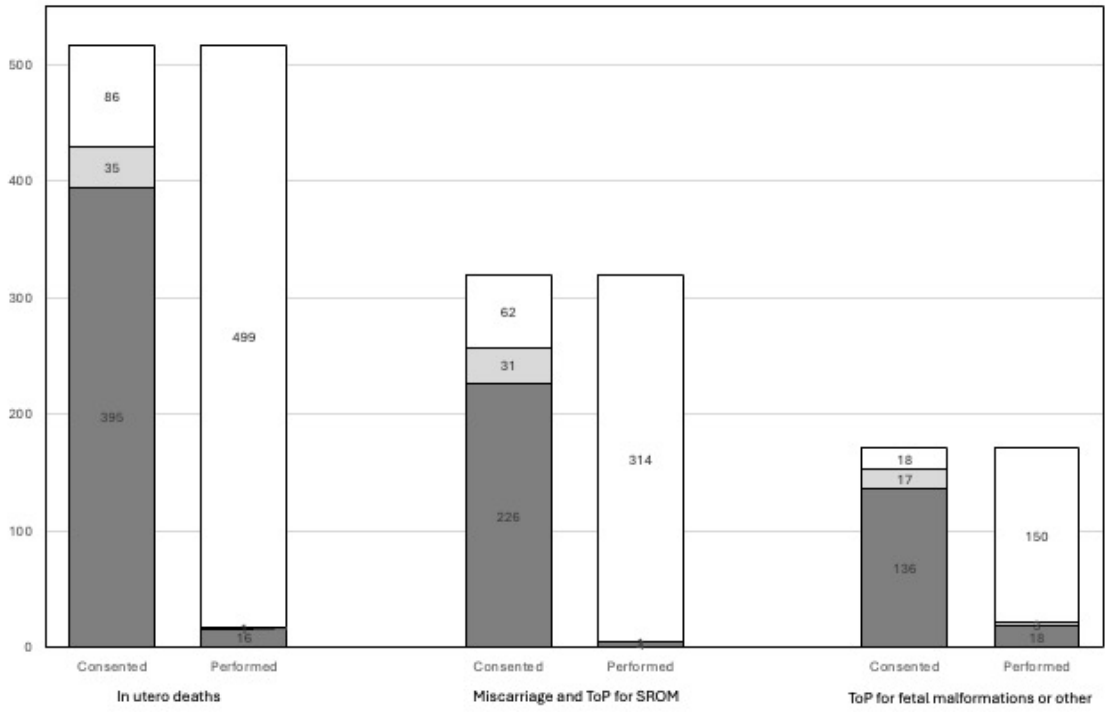

C) Micro-CT contribution

MCT was of acceptable quality in 598 / 1007 cases (59.4%), higher in miscarriage (80.3%) and ToP (74.9%) than in IUD (41.4%; Table IV.3). There was a gradual reduction in MCT image quality with increasing levels of maceration (Table IV.3).

MCT was abnormal in 312/1007 (31.0%), which were 223 / 1007 (22.1%) true abnormalities and 89 cases of delivery or maceration related trauma. Abnormality detection excluding trauma was unsurprisingly highest in ToP (80.7%) vs spontaneous miscarriage (6.9%) (Table IV.3). MCT detected the greatest number of abnormalities in the chest (140; 13.9%) such as ventricular septal defect (Figure IV.3), abdomen (127; 12.6%) as horseshoe kidney (Figure IV.4) or enlarged bladder with hydronephrosis (Figure IV.5) and skeletal systems (97; 9.6%). (Table IV.3)

Table IV.3 – Contribution of Micro-CT to the final diagnosis image quality and abnormalities identified, by subgroup (ToP termination of pregnancy, SROM spontaneous rupture of membranes).

		Overall	In Utero Deaths	Miscarriage or ToP for SROM	ToP for fetal malformations or other
		1007 (100%)	**517 (51.34%)**	**319 (31.68%)**	**171 (16.98%)**
MCT IMAGE QUALITY	**Missing data on MCT image quality**	**43 (4.27%)**	**6 (1.16%)**	**20 (6.27%)**	**17 (9.9%)**
	Diagnostic MCT image quality	**598 (59.38%)**	**214 (41.39%)**	**256 (80.25%)**	**128 (74.85%)**
	No maceration	249 (24.73%)	25 (4.84%)	148 (46.39%)	76 (44.44%)
	Mild maceration	134 (13.31%)	35 (6.77%)	70 (21.94%)	29 (16.96%)
	Moderate maceration	106 (10.53%)	70 (13.54%)	21 (6.58%)	15 (8.77%)
	Severe maceration	109 (10.82%)	84 (16.25%)	17 (5.33%)	8 (4.68%)
	Non-diagnostic MCT image quality	**366 (36.35%)**	**297 (57.45%)**	**43 (13.48%)**	**26 (15.2%)**
	Brain non-diagnostic	295 (29.29%)	240 (46.42%)	34 (10.66%)	21 (12.28%)
	Abdomen and brain non-diagnostic	61 (6.1%)	49 (9.48%)	8 (2.51%)	4 (2.34%)
	Whole body non-diagnostic	10 (1%)	8 (1.55%)	1 (0.31%)	1 (0.58%)
MCT FINDINGS	**MCT findings per organs system**				
	CNS	78 (7.75%)	13 (2.51%)	15 (4.92%)	50 (29.24%)
	Chest	140 (13.9%)	57 (11.03%)	14 (4.40%)	69 (40.35%)
	Abdominal	127 (12.61%)	60 (11.61%)	22 (6.92%)	45 (26.32%)
	Urinary tract	71 (7.10%)	20 (3.87%)	7 (2.20%)	44 (25.73%)
	Skeletal or Soft tissue	97 (9.63%)	22 (4.26%)	7 (2.20%)	68 (39.77%)
	MCT findings per case				
	Overall abnormal case number	312 (30.98%)	117 (22.63%)	57 (17.92%)	138 (80.70%)
	Overall abnormal cases excluding delivery trauma	223 (22.14%)	63 (12.19%)	22 (6.92%)	138 (80.70%)

Figure IV.3 – Axial Micro-CT image of a 13 weeks' gestation fetus demonstrating ventricular septal defect (arrow) in a moderately macerated fetus. Note reduced overall greyscale and loss of tissue boundaries caused by maceration.



Figure IV.4 – Axial and coronal Micro-CT of renal abnormalities: this case at 14 weeks gestation was diagnosed antenatally with malrotated kidneys (A, C), with the isthmus of a horseshoe kidney demonstrated on Micro-CT (B, D).

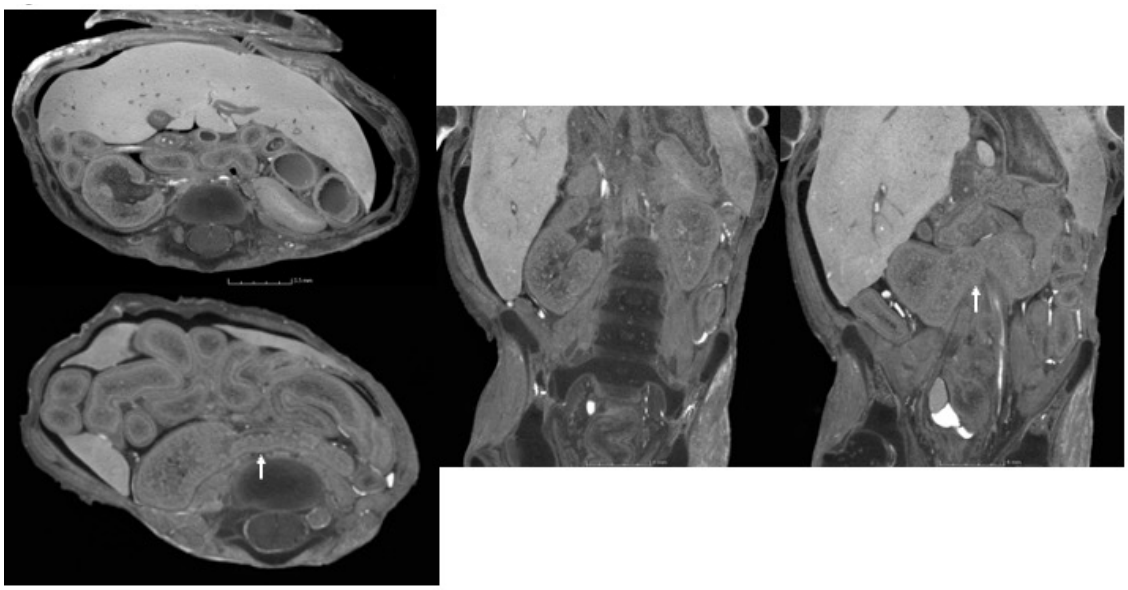

Figure IV.5 – Axial and coronal Micro-CT of renal abnormalities: this case at 13 weeks' gestation demonstrated grossly enlarged urinary bladder (closed white arrow; megacystis) with unilateral right kidney which showed hydronephrosis (open white arrows).

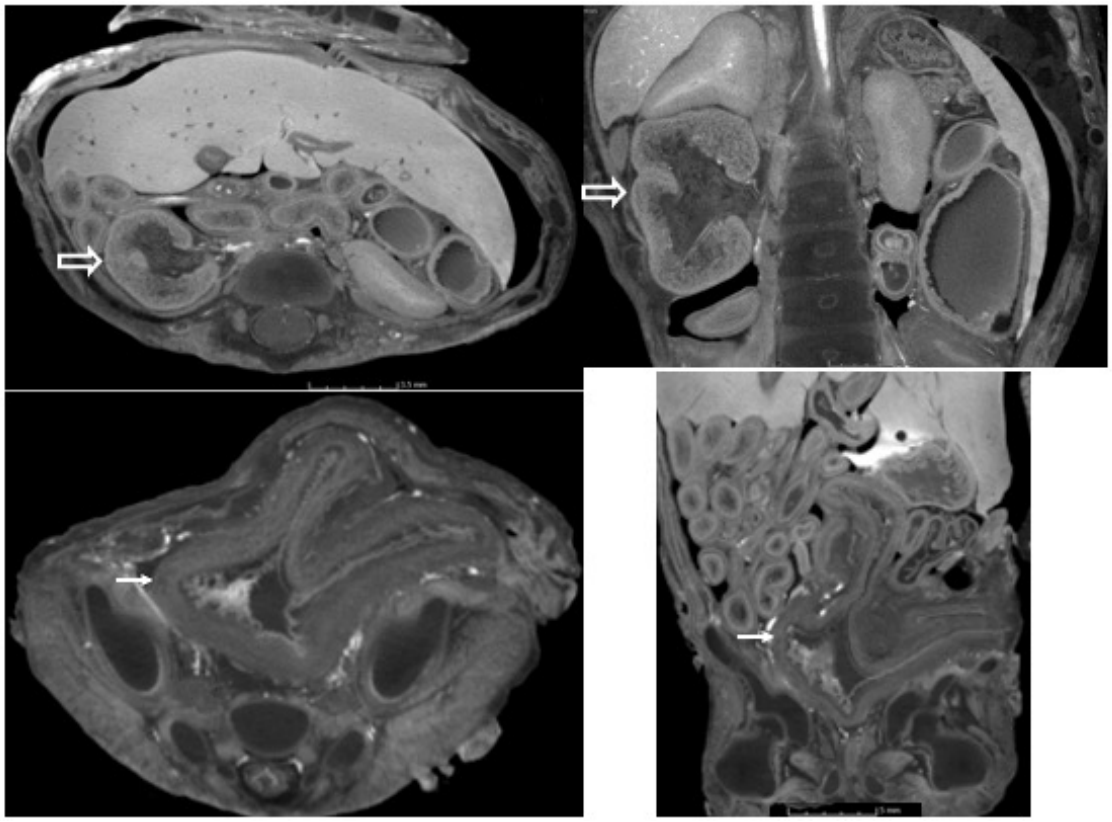

D) Overall contribution and cause of death

The single most important contributor to making a diagnosis in the 562 cases where this was possible (55.8%) was placental examination (284 cases; 28.2%; Figure IV.6). For example, EE contributed to final diagnosis in 171 cases (17.0%) but was the sole contributor in only 35 cases (3.5%), and whilst MCT contributed to the diagnosis in 148 cases (14.7%), it was the sole contributor in only 45 cases (4.5% of our cohort, or 8% of possible diagnoses) (Figure IV.6).

Figure IV.6 – Flow-chart presenting the relative contribution of each part of the PM examination, either sole contribution or contribution with other factors.

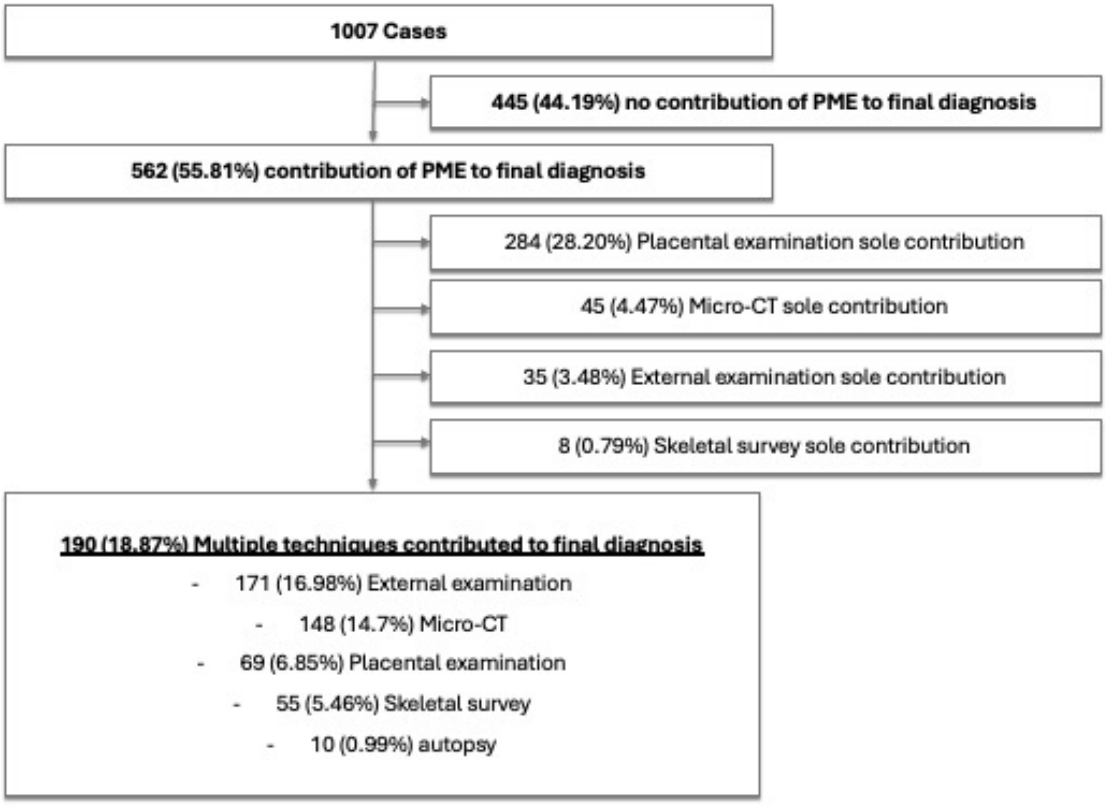

The cause of death was fetal in 212 / 1007 (21.1%), placental cause in 264 / 1007 (26.2%) and both fetal and placental in 39 / 1007 (3.9%); remained unexplained in 492/1007 (48.9%). There is more unexplained cause of death in IUD (69.4%; Table IV.4), and with increasing levels of maceration (85.5% severe).

Table IV.4 – Contribution from post-mortem examination (PME) to the final diagnosis and cause of death determination, by subgroup (ToP termination of pregnancy, SROM spontaneous rupture of membranes).

		Overall	In Utero Deaths	Miscarriage or ToP for SROM	TOP for fetal malformations or other
		1007 (100%)	**517 (51.34%)**	**319 (31.68%)**	**171 (16.98%)**
POST MORTEM EXAMINATION CONTRIBUTION TO THE FINAL DIAGNOSIS		No PME contribution	445 (44.23%)	317 (61.43%)	112 (35.11%)	16 (9.36%)
		Any PME contribution	562 (55.81%)	200 (38.68%)	207 (64.89%)	155 (90.64%)
	ANY CONTRIBUTION	Placenta examination	353 (35.05%)	137 (26.50%)	188 (58.93%)	28 (16.37%)
		External examination	206 (20.46%)	61 (11.80%)	31 (9.72%)	114 (66.67%)
		Skeletal survey	63 (6.26%)	7 (1.35%)	3 (0.94%)	53 (30.99%)
		MicroCT	193 (19.17%)	49 (9.48%)	21 (6.58%)	123 (71.93%)
		Autopsy	10 (0.99%)	1 (0.19%)	0 (0%)	9 (5.26%)
	SOLE CONTRIBUTION	Placenta examination alone	284 (28.20%)	112 (21.66%)	168 (52.66%)	4 (2.34%)
		External examination alone	35 (3.48%)	21 (4.06%)	4 (1.25%)	10 (5.85%)
		Skeletal survey alone	8 (0.79%)	2 (0.39%)	1 (0.31%)	5 (2.92%)
		MicroCT alone	45 (4.47%)	20 (3.87%)	4 (1.25%)	21 (12.28%)
		Autopsy alone	None	None	None	None
CAUSE OF DEATH		Unexplained	492 (48.86%)	359 (69.44%)	124 (38.87%)	9 (5.26%)
		Fetal	212 (21.05%)	53 (10.25%)	12 (3.76%)	147 (85.96%)
		Placenta	264 (26.22%)	83 (16.05%)	174 (54.55%)	7 (4.09%)
		Both fetal and placenta	39 (3.87%)	22 (4.26%)	9 (2.82%)	8 (4.68%)

4. Discussion

The main finding from our study was that less invasive fetal autopsy including MCT reached a diagnosis in 51% of fetal referrals, with 49% unexplained. The single most useful diagnostic contributor was placental examination, followed by EE and MCT examination, which compares favourably with a historic cohort of similar FPME carried out at the same centre.[20,99,208] We conclude that the introduction of MCT at our centre has avoided almost all invasive FPME but has a similar overall diagnostic yield.

The collaborative workflow between the perinatal pathologist and the paediatric radiologist now allows a variety of components of FPME to be performed that favour minimally invasive investigations. Whilst each part of a FPME can help identify a clinical diagnosis, we were able to contextualise the relative contributions of non-invasive components across this cohort of unselected fetuses. Unsurprisingly, placental examination contributed more commonly to the final diagnosis (cause of fetal death or diagnosis of main abnormality) than fetal imaging in our study. This is in keeping with previous findings, e.g. in individual studies of 512 early IUDs, 23.6% were attributed to placental disease,[22] and a systematic review of 9 studies totalling 1779 stillbirths found that placental pathology was present in 31.5 – 84.0%, with a range of placental diagnosis from 15.4 – 87.0% depending on criteria.[21] In a similar subgroup of early IUDs before 20 weeks already published, our own group identified a 53% abnormal placental examination rate.[195]

The EE is known to be an important part of the FPME, but published evidence is very limited. A Turkish paper found a diagnostic rate of 57.9% by experienced geneticists.[19] In early ToP before 16 weeks, a full autopsy (including EE and placental examination, skeletal survey, internal examination and histological examination of the placenta and tissues) provides additional information in 77.5% of cases compared with antenatal first trimester ultrasound and consequently changes genetic counselling in 32.5% of cases.[23]

MCT has previously been shown to have a high concordance with full autopsy of 97.5%,[60] with a high sensitivity of 92.3% and specificity of 98%[61] even in macerated fetuses.[68] Regarding individual organ systems, MCT was most accurate at detecting cardiothoracic, abdominal and skeletal abnormalities, but with a high non-diagnostic imaging rate for the brain, largely due to maceration following IUD. This is in keeping with other studies showing that PM imaging is affected by prolonged intra-uterine intervals and has a higher diagnostic yield in ToPs, where the pre-test probability of fetal anomalies is much higher.

Our parent's consent framework allows the perinatal pathologist to proceed with the least invasive components first, before considering invasive autopsy. The documented change in practice at our centre shows that increasingly non-invasive procedures are being performed, with MCT results becoming available within 10 days of receiving the body, turnaround times of less than 3 weeks,[209] which compares favourably to report turnaround times of up to 3 months nationally.

The strength of this study lies in presenting the use of MCT in clinical practice for human FPME in a large group of unselected cases from several referral hospitals. This reflects how imaging could be used within less invasive autopsy practice in other settings and demonstrates that a high-resolution PM imaging technique when used together with placental and other examinations can help avoid invasive autopsy in line with parental wishes.

The main limitations of this study are its single-centre nature, using expert specialist radiologists and pathologists which may not currently be reproducible in other centres. However, not all centres will wish to offer this level of service: given the dearth of perinatal pathologists in the UK at present, we have provided an example of how a "hub-and-spoke" model could work regarding referrals from a wide number of centres into a single specialist centre for autopsy provision.

A comparative study of MCT findings to invasive autopsy was not possible due to parental consent and pathologist ethical decision-making (although this has been done on a subset of earlier cases from our centre);[60] less than 50 autopsies were clinically justifiable in our cohort.

5. Conclusion

We have demonstrated the clinical utility of MCT imaging for early fetal death. In our study, the combination of routine EE, placental assessment and MCT imaging meant an autopsy avoidance rate of 96%, in line with parental consent. This has the potential to change clinical autopsy service delivery for early fetal death within the NHS.

GENERAL DISCUSSION

1. Summary of findings

In the first part entitled less invasive autopsy for early pregnancy loss, the overall framework of PM fetal imaging was reviewed highlighting its role in understanding fetal death to ease parental bereavement and guide future pregnancies. CA, though valuable as the gold standard, is often declined due to its invasiveness, less-invasive imaging-based approaches may be a more acceptable choice to parents. While conventional clinical imaging techniques like radiographs, CT, MRI and US have limited accuracy for fetuses before 20 WG, micro-imaging such as HF-MRI and MCT are more effective following early pregnancy losses. Expanding the use and availability of these innovative PM imaging techniques could offer parents more acceptable options, potentially increasing their uptake and improving diagnostic outcomes.

The methodological section presented in part 2 focuses on optimizing the sample preparation process, a critical step in achieving high-quality PM-MCT imaging of non-macerated first-trimester fetuses. A comparative analysis of staining baths confirmed the effectiveness of Dice staining, composed of 4% paraformaldehyde and Lugol's iodine (63.25 mg/ml total iodine content) in a 1:1 ratio. The study of staining in Dice PM-MCT imaging of non-macerated first trimester human fetuses highlighted that Dice solution diffuses following a stretched exponential model in most organs, except in the liver. The optimal staining duration, ensuring a contrast-to-noise ratio exceeding 5 (as per the Rose criterion), is directly correlated with fetal size, such as CRL or weight. For instance, a fetus with a CRL of 50 mm or a weight of 20 g requires a minimum of 96 hours of staining for optimal imaging contrast. By tailoring the staining duration to fetal CRL or weight, optimal imaging outcomes can be achieved, facilitating more accurate and detailed analysis in both research and clinical settings.

The current scientific literature on MCT and HF-MRI before 14 WG is weak. However, miscarriages are common and require further explorations and research. MCT and HF-MRI are

used in the third part to assess critical anatomical structures at 8 and 12 WG and pave the way for PM phenotyping before 14WG. We also established normal organs chart using MCT and HF-MRI on non-macerated and non-malformed fetuses at 12 WG. A biometric approach might be applied when necessary.

Dawood et al. performed a comparison between Dice MCT and HF-MRI with the objective to improve diagnostic yield. They conclude to superiority of MCT when compared to HF-MRI in qualitative and quantitative evaluation[62]. This conclusion is concordant with Ibarra Vilar's et al. recently Dice MCT has a better diagnostic yield than PM-US and HF MRI[210]. By its cost, speed of acquisition, MCT seems to impose world-wide as the best option for clinical applications of PM micro-imaging, as several teams bet before 2017[149]. MCT provides good agreement with autopsy, particularly for brain, thoracic and abdominal pathologies.

In addition, MCT has the advantage of being able to examine the fetal brain[145] when brain assessment is impossible or artefactual on CA due to extraction and maceration. MCT will not be conclusive in cases of extreme maceration, however, will allow brain assessment in several cases where CA is not possible.

MCT has demonstrated its value as part of a non-invasive autopsy approach in a real-world clinical setting using an unselected population involving over 1000 fetuses, with an average turnaround time of less than 21 days. Among cases when a diagnostic contributor was possibly identified (56%), placental examination was the most frequent (35.0%), followed by EE (20.5%) and MCT (19.2%). In this cohort, fetal and placental causes were identified in 21.1% and 26.2% of cases, respectively. Nevertheless, nearly half of the cases remained unexplained. These findings support the use of placental, external and MCT examinations as a feasible and acceptable FPME for early gestational age.

2. Future development

A) Research

MCT and HF-MRI can be used to assess critical anatomical structures during the first trimester, a period of key embryologic processes. This capability could be particularly valuable for investigating developmental anomalies. Here, we explore a potential application in the study of craniofacial development.

Craniofacial morphogenesis is a complex and dynamic field of research, particularly regarding palatal development and its associated anomalies. The palatal processes originate as bilateral extensions from the maxillary processes, growing and fusing along the anterior-posterior axis to form the secondary palate, which constitutes the roof of the oral cavity[211]. Disruptions in this process can lead to orofacial clefts, occurring either in isolation or as part of syndromic conditions[211].

Pierre Robin sequence is a congenital condition characterized by mandibular hypoplasia, glossoptosis, and often a U-shaped cleft palate. While its exact physiopathology remains unclear, several theories have been proposed. According to the developmental model, the primary defect in Pierre Robin sequence is insufficient mandibular growth around 9 WG, leaving the tongue high and retroposed. This abnormal positioning prevents palatal shelf fusion, resulting in a cleft. Additionally, glossoptosis contributes to respiratory and feeding difficulties. Genetic evidence highlights the role of ***SOX9***, a key regulator of Meckel's cartilage, which is essential for mandibular development. Disruptions in this pathway reinforce the hypothesis that mandibular deficiency is the initiating event in PRS, with secondary effects on palatal formation.

Micro-CT segmentation provides detailed insight into the development of the tongue, palate, and mandibles, allowing for precise visualization of their relative positioning and evolution over time (Figure GD.1). By visualizing these structures in their developmental context,

micro-CT segmentation enhances our understanding of normal craniofacial morphogenesis as well as congenital conditions like Pierre Robin sequence.

Figure GD – The development of the tongue, palate, and mandibles visualized through micro-CT segmentation (Myrian software)

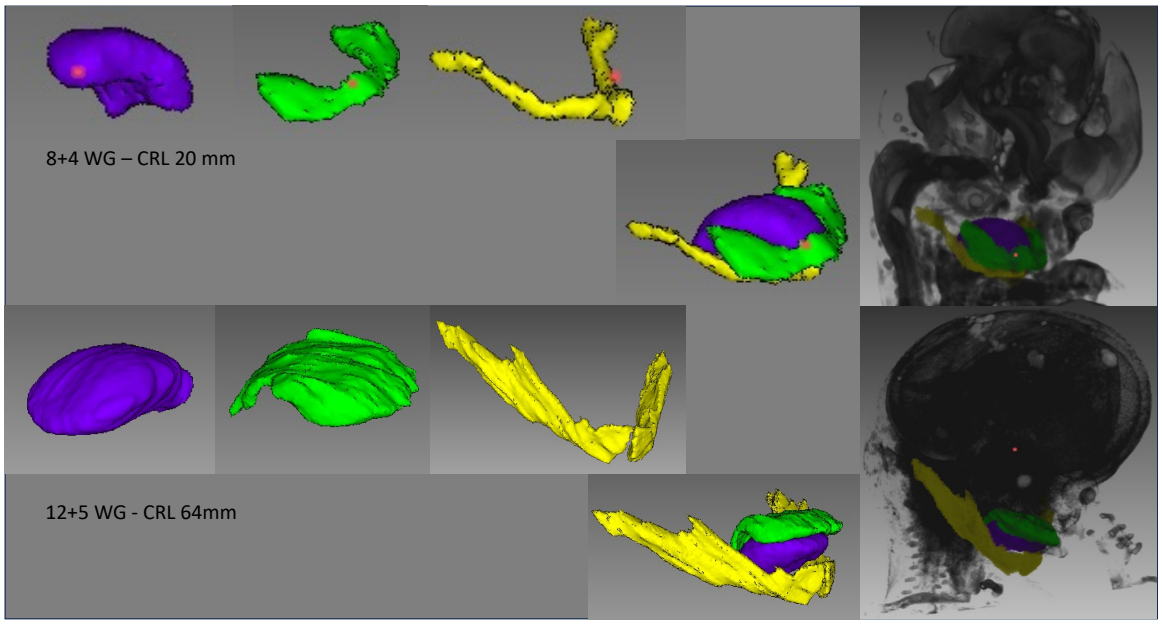

B) Clinical application in France

This thesis, combining fundamental research on non-macerated fetuses with the experience gained through my mobility program -where I learned to interpret MCT even in case of macerated fetuses – lays the foundation for a structured clinical research project. This project aims to evaluate the introduction of MCT into routine FPME of appropriate size and volume in clinical practice in France. While previous studies by highly specialized teams[60,117,209,210] have demonstrated the significant advancements MCT offers, its broader validation and adoption across different healthcare systems and teams remain essential.

The successful integration of MCT into FPME depends on the expertise of fetal pathologists, who must carefully select the most appropriate diagnostic approach for each fetus. This involves moving away from routine, low-yield examinations such as conventional PM-XR, which has diminished in diagnostic value with advances in prenatal US screening. In addition, the

diagnostic value of PM-XR in cases where an EE reveals no abnormalities can be considered. Pathologist must consider a range of factors, including prenatal history, organ of interest, gestational age and the death context. PM EE, often underestimated in its diagnostic potential[19], should account for the degree of maceration, dysmorphism, and external malformations to guide further exploration. Macroscopic placental analysis is also crucial, as is parental consent. Based on current scientific knowledge, PM-MCT imaging should be offered as an option to parents following miscarriage, IUD or ToP between 7 and 24 WG and incorporated into a comprehensive FPME. This multidisciplinary approach may include PM imaging (Dice PM-MCT or PM-MRI according to the gestational age, weight, length and maceration), targeted biopsies from placenta or organs for infection, chromosomal and genetic testing, tissue freezing for future analysis, histological examination for organs, and CA. This multidisciplinary approach ensures thorough evaluation and personalized medicine for each FPME.

The integration of MCT will require rethinking the allocation of resources, as EE and genetic testing are likely to increase, while reliance on CA may decrease. Experience from the UK shows that MCT reports are typically completed within 9 days (part IV). Given the limited number of specialists, ensuring optimal use of their expertise will be critical.

Parental acceptance of FPME is a crucial factor, offering minimally invasive alternatives such as MCT may increase acceptance rates[33,97]. Even parents who initially refused autopsies showed greater willingness to reconsider when initial conclusions were based on imaging findings. These preliminary observations highlight the need for formal studies in France to assess the impact of minimally invasive approaches on parental consent.

A dedicated clinical research project is essential to advance personalized FPME, foster the evolution of the fetal pathology specialty, and integrate innovative imaging techniques, ultimately providing grieving families with a more widely accepted and compassionate approach to investigating their loss.

3. Shifting paradigms in genetics.

The previous conclusion overlooks the ongoing revolution in genetics, which has dramatically transformed our approach to phenotypic exploration, particularly in assessing recurrence risk.

From a chromosomal perspective, the widespread adoption of chromosomal micro array (CMA) testing has significantly improved the detection of copy number variation (CNV)[212]. These advancements are poised to become standard in non-invasive diagnostic strategies, providing a powerful tool for the early identification of CNV[213,214]. In cases where CNVs of uncertain significance are detected, phenotypic data remain essential for accurate interpretation and precise diagnosis.

Genetics has undergone a paradigm shift, transitioning from a "phenotype-first" approach — where clinical presentation guided the selection of targeted genetic tests — to a “genotype first” strategy, where broad genetic screening is prioritized. Previously, establishing a phenotype dictated a sequential, hypothesis-driven series of genetic tests, often relying on Sanger sequencing. This process was slow and labour-intensive, requiring extensive clinical discussions, dysmorphology assessments, and lengthy diagnostic timelines that could span months or even years. In some cases, the initial hypothesis proved incorrect, delaying a definitive diagnosis.

With next-generation sequencing (NGS) and the advancement of bioinformatics, a "genotype-first" approach has become the new standard. This strategy prioritizes genotyping, using phenotypic data as a supplementary tool for variant interpretation. Variants of interest are filtered based on their frequency and molecular relevance, making genotype the primary driver of the diagnostic process while phenotype plays a supporting role. Recent studies analysing exome sequencing results—both prenatally and PM —have shown that reanalysing exomes in light of PM findings has only a marginal impact on molecular conclusions[11,12].

However, integrating clinical terminology into the Human Phenotype Ontology (HPO) within bioinformatics pipelines has been proven to enhance diagnostic yield of NGS, whether

performed on an exome or genome level[215,216]. When molecular analysis identifies a variant of uncertain significance, class 3 according to American College of Medical Genetics classification[217], phenotypic data play a crucial role in guiding "reverse phenotyping," refining the diagnosis process, and resolving uncertainty.

Prenatal diagnostic have also undergone a revolution with the use of exome sequencing and, more recently, genome sequencing[12,218–220]. When a precise molecular diagnosis is established prenatally, particularly in cases leading to a medical ToP, FPME becomes less critical, as recurrence risk is already determined.

Consequently, we are tasked with envisioning the future of FPME to build an effective process that achieves a precise diagnosis as quickly as possible. This involves using chromosomal microarray, exome, and genome sequencing, as well as prenatal diagnostic elements such as ultrasound scan results and prenatal MRI. Based on these elements, FPME specialist performed EE and placental examination, and choose the appropriate FPME explorations to perform, including CA, PM-MRI, or PM-MCT. We aim for effective, minimally invasive explorations to provide genetic counselling for many couples within a month after their loss. To achieve this objective, a French practical study should be conducted with a medico-economic evaluation.

CONCLUSION

While CA remains the gold standard for detailing phenotypic elements and translating them into HPO terms for bioinformatic interpretation, its invasive nature often leads to parental refusal. As an alternative, LIA using PM imaging techniques, such as Dice micro-CT and high-field MRI, provide high-resolution insights into fetal anatomy, even in early gestation. By optimizing sample preparation based on fetal size, Dice PM-MCT enables highly detailed phenotypic assessments.

Current evidence supports the routine offering of PM-MCT imaging to parents following miscarriage, IUD or ToP between 7 and 24 WG. A comprehensive FPME, combining EE, placental analysis, and MCT imaging has been shown to significantly reduce the need for CA while maintaining high parental consent rates. The integration of MCT into clinical practice for FPME in France represents a critical step toward accurate, less-invasive diagnostic procedures. However, broader adoption will require structured research, standardised clinical workflows, and a multidisciplinary approach to implementation.

The advancements in NGS and bioinformatics have solidified the "genotype-first" approach as the cornerstone of modern clinical genetics. However, FPME remains crucial for providing detailed phenotypic data in HPO terms, increasing the diagnostic yield of NGS and facilitating the reinterpretation of variants of uncertain significant through “reverse phenotyping”. Ongoing collaboration between fetal pathology and clinical and genetics is crucial to fully integrate these advancements into routine clinical practice, ultimately offering families more effective, less-invasive diagnostic options.

THESE EN FRANÇAIS : MICRO-IMAGERIE PAR MICRO-TDM ET IRM A HAUT CHAMP POUR L'ETUDE ANATOMIQUE POST-MORTEM DU FŒTUS HUMAIN AU PREMIER TRIMESTRE VERS UNE UTILISATION EN FŒTOPATHOLOGIE.

RESUME DE THESE VULGARISE POUR LE GRAND PUBLIC

En cas de décès fœtal spontané ou induit pour une pathologie grave, les explorations post-mortem permettent d'aborder avec les couples le risque de récidive. Les autopsies moins invasives utilisant des imageries post-mortem sont mieux acceptées que l'autopsie conventionnelle jugée trop invasive. Contrairement aux imageries post-mortem conventionnelles, le micro-scanner et l'IRM à haut champ (>3 Tesla) permettent d'obtenir une résolution isotropique <100 µm compatible avec l'exploration de l'anatomie fœtale dès le premier trimestre. Après une préparation par immersion du fœtus dans un bain d'iode pendant une durée adaptée à sa taille, le micro-scanner permet d'obtenir des images plus contrastées que l'IRM, mais au prix d'un rétrécissement tissulaire nécessitant des normes biométriques adaptées. L'utilisation clinique du micro-scanner, dans le cadre d'un examen post-mortem global, permet d'établir un diagnostic dans 51% des cas et d'éviter 96 % des autopsies conventionnelles.

RESUME DE LA THESE

En cas de décès fœtal, qu'il soit spontané (fausse couche ou mort in utero) ou provoqué (interruption médicale de grossesse) en raison de malformations congénitales (3,2 % des grossesses), l'autopsie conventionnelle est la référence pour déterminer la cause du décès. Cependant, son caractère invasif peut conduire à un refus parental. Cette thèse explore l'utilisation du micro-TDM (micro-CT, MCT) et de l'IRM à champ élevé (IRM-HF) dans l'imagerie post-mortem du fœtus humain au premier trimestre permettant d'accéder à une anatomie détaillée vers une utilisation en fœtopathologie.

Cette thèse débute par une revue des connaissances sur l'autopsie moins invasives utilisant de l'imagerie post-mortem (PM) **(*Simcock IC, Lamouroux A, et al. Less-invasive autopsy for early pregnancy loss. Prenat Diagn. 2023*)**. Les techniques conventionnelles d'imagerie PM (radiographie, scanner, IRM et échographie) offrent une précision limitée avant 20 semaines d'aménorrhée (SA). En revanche, les techniques de micro-imagerie, telles que MCT et IRM-HF (> 3 Tesla), offrent une résolution isotrope < 100 µm, permettant une visualisation détaillée dès le premier trimestre.

La partie méthodologique vise à l'optimisation de la préparation des échantillons par l'utilisation de bain de contraste iodé composé d'un rapport équimolaire de paraformaldéhyde à 4 % et de Lugol (avec un contenu total en iode de 63,25 mg/ml) **(*A. Lamouroux et al. Modelling of staining in post-mortem diffusible iodine-based contrast-enhanced (Dice) micro-CT imaging of non-macerated first-trimester human fetuses*, soumis à *BMC Medical Imaging*)**. Ce bain iodé diffuse dans la plupart des organes selon un modèle d'exponentielle étirée, hormis dans le foie. La durée optimale de coloration, permettant d'obtenir un ratio contraste sur bruit supérieur à 5 (selon les critères de Rose), dépend de la longueur cranio-caudale (LCC) ou du poids (par exemple, 96h pour un fœtus non macéré avec une LCC de 50 mm ou un poids de 20 g).

Dice MCT et l'IRM-HF permettent dans la troisième partie une visualisation précise de l'anatomie fœtale PM dès 8 SA. (***Lamouroux A et al. Micro-CT and high-field MRI for studying***

very early post-mortem human fetal anatomy at 8 weeks of gestation. Prenat Diagn. 2024). Le Dice MCT offre un contraste supérieur à celui de l'IRM-HF pour les fœtus à 8 SA, mais au prix de rétrécissements tissulaires, nécessitant des normes biométriques spécifiques ajustées telles que fournies pour les fœtus à 12 SA. Dice MCT semble plus adaptée aux applications cliniques que l'IRM-HF.

La quatrième partie ouvre sur des perspectives d'utilisation du PM-MCT en pratique clinique dans le cadre d'un examen PM moins invasifs. Une large étude clinique portant sur plus de 1000 fœtus non sélectionnés réalisant une autopsie moins invasive utilisant le MCT avec une prise en charge moyenne inférieure à 21 jours **(*Simcock IC, Lamouroux A et al. Fetal post-mortem imaging using microfocus computed tomography: single centre retrospective clinical experience*, *soumis à American Journal of Obstetrics and Gynecology*).** Une cause au décès a été identifiée dans 47 % des cas—21 % étant liés au fœtus et 26 % au placenta—tandis que 49 % sont restés inexpliqués, notamment en cas de décès in utero (69 %) et de macération sévère (86 %). La combinaison de l'examen externe (21% de contribution au diagnostic), de l'évaluation placentaire (35%) et de l'imagerie MCT (19%) a conduit à un taux d'évitement d'autopsie de 96 %.

En conclusion, bien que l'autopsie conventionnelle reste la référence, son caractère invasif limite son acceptabilité. La Dice MCT avec une préparation optimisée des échantillons et l'IRM-HF permettent une imagerie fœtale haute résolution dès le premier trimestre. L'autopsie moins invasive, combinant de la MCT avec l'examen externe et l'analyse placentaire réduit le recours à l'autopsie en maintenant un taux élevé de consentement parental.

RESUME SUBSTANTIEL

INTRODUCTION GENERALE

La médecine fœtale s'entend des pratiques médicales, ayant pour but le diagnostic, via l'échographie et l'évaluation pronostique, d'une affection d'une particulière gravité ou susceptible d'avoir un impact sur le devenir du fœtus ou de l'enfant à naître[1]. Le dépistage des malformations congénitales est un enjeu de santé publique. Ces malformations représentent 3,2 % des naissance en France[2] et contribuent à 10 % des décès néonataux selon l'OMS[3]. En France, trois échographies de dépistage autour de 12, 22 et 32 SA sont recommandées en population à bas risque (Figure GI.1 et GI.2)[8]. Une interruption médicale de grossesse pour motif fœtal (IMG) peut, à la demande de la femme, quel que soit l'âge gestationnel, être pratiquée si deux médecins membres du centre pluridisciplinaire de diagnostic prénatal (CPDPN) attestent qu'il existe une forte probabilité que l'enfant à naître soit atteint d'une affection d'une particulière gravité reconnue comme incurable au moment du diagnostic[13]. Le CPDPN indique la réalisation d'un examen fœtopathologique (EFP)[13].

Les micro-imageries, telle que le micro-TDM (Micro-CT ou MCT) et l'IRM à haut champ (HF-IRM) sont des imageries 3D avec une résolution isotropique < 100 µm[41,51,52,60–63]. Le MCT est une technique d'imagerie basée sur l'atténuation des rayons X, utilisant un émetteur et un récepteur avec l'objet positionnés entre les deux. L'image sera obtenue par les projections successives avec des angles multiples qui seront reconstruit en images tomographiques grâce un algorithme informatique[63,69]. Permettant ainsi une visualisation tridimensionnelle de haute qualité et en haute résolution, avec un temps d'acquisition et un coût faible par rapport à l'HF-IRM [52,69–71]. Cette dernière utilise un champ magnétique élevé au-delà de 3 Tesla, permettant une acquisition avec une résolution isotropique inframillimétrique[52,62].

L'EFP[15–17] comporte la réalisation de radiographies standards et si besoin d'imageries complémentaires (échographie [18], TDM et IRM [15]). L'examen externe[19] associé à la réalisation de

photographies comportent l'évaluation de la dysmorphie, des biométries (poids, distance vertex coccyx, vertex talon, périmètre crânien et pied...) et les malformations externes (Figure GI.3). L'examen interne ou autopsie conventionnelle comporte un examen macroscopique, précisant le situs, des malformations et le poids des organes cibles, fixés en vue d'un examen histologique. L'examen placentaire macroscopique et microscopique a un rendement diagnostic important[20–22]. L'EFP est l'examen de référence pour aboutir à un diagnostic de précision et à un conseil génétique[23,24] (Figure GI.3)[15–17,23]. Les difficultés techniques de l'EFP à un terme précoce, le taux de refus d'autopsie et l'évolution des techniques d'imagerie ont fait émerger la possibilité d'examen PM moins invasif[25–27]. L'IRM en PM ayant un rendement diagnostic limité pour les termes inférieurs à 24 SA, la micro-imagerie est une option pertinente.

Objectifs de la thèse

Cette thèse explore l'utilisation de la micro-imagerie fœtale post-mortem au premier trimestre par MCT et IRM à haut champ, en visualisant l'anatomie détaillée ouvrant la voie à une application clinique.

Elle commence par une revue des connaissances concernant l'autopsie fœtale moins invasive, en mettant l'accent sur les techniques d'imagerie post-mortem conventionnelles et haute résolution (***Simcock IC, Lamouroux A, Sebire NJ, Shelmerdine SC, Arthurs OJ. Less-invasive autopsy for early pregnancy loss. Prenat Diagn. 2023 Jun 1;43(7):937–49***).

La deuxième partie décrit une méthodologie visant à améliorer la qualité d'image en MCT en modélisant le processus de diffusion du contraste et en déterminant la durée optimale des bains de contraste en fonction de la taille fœtale (***A. Lamouroux, et al. Modelling of staining in post-mortem diffusible iodine-based contrast enhanced (Dice) micro-CT imaging of non-macerated first-trimester human fetuses, soumis à BMC Medical Imaging***).

Dans la troisième partie, la MCT et l'IRM à haut champ sont utilisées pour évaluer précisément les structures anatomiques à 8 et 12 SA, en analysant leur visualisation et leur précision de mesure (***Lamouroux A, Cardoso M, Bottero C, et al. Micro-CT and high-field MRI***

for studying very early post-mortem human fetal anatomy at 8 weeks of gestation. Prenat Diagn. 2024 Jan;44(1):3–14).

La quatrième partie offre des perspectives sur l'intégration future de la MCT post-mortem dans la pratique clinique de l'autopsie moins invasive, en s'appuyant sur une étude clinique de grande envergure portant sur l'utilisation du MCT sur plus de 1 000 fœtus (***Simcock IC, Lamouroux A, et al. Fetal post-mortem imaging using microfocus computed tomography: single centre retrospective clinical experience, soumis à American Journal of Obstetrics and Gynecology***).

Enfin, la discussion intègre ces résultats aux avancées de la génétique, projetant leur impact combiné sur l'évolution des pratiques cliniques futures.

PARTIE I - ÉTAT DES CONNAISSANCES DE L'IMAGERIE FŒTALE POST-MORTEM.

J'ai effectué ma mobilité entre novembre 2022 et novembre 2023, au Great Ormond Street Hospital for Children NHS Foundation Trust à Londres dans le service de radio pédiatrie dirigé par Pr Owen Arthurs. J'ai participé à la rédaction de ce papier et à sa relecture.

Simcock IC, Lamouroux A, Sebire NJ, Shelmerdine SC & Arthurs OJ.
Less-invasive autopsy for early pregnancy loss.
Prenatal Diagnosis 2023. Jun 1;43(7):937–49. (Annexe 1)

Les examens post-mortem (PM) plus ou moins invasif vont de l'autopsie conventionnelle jusqu'à l'autopsie non invasive (Tableau I.1).

1. Les techniques d'imagerie conventionnelle

Les radiographies fœtales PM, peu chères et très disponibles[51], ont un rendement diagnostic pertinent < 1 % des cas en routine[124]. Le TDM PM, très disponible, peu cher et rapide, a un rendement faible pour les petits termes[39,129,130]. L'IRM PM est assez disponible mais l'acquisition assez longue[121,133] en limite l'accès pour les examens PM. Les IRM cliniques utilisent un champ de 3 Tesla ce qui semble peu pertinent pour des fœtus de moins de 20 SA[119,122,135]. L'échographie PM est une alternative disponible, peu coûteuse mais dont le rendement diagnostique reste limité avant 20 SA[54,56–58,126].

2. Les techniques d'imagerie à haute résolution

Le MCT est adapté au terme précoce (figures I.1 et I.2)[60,61,66,67,69,113,122,141,143–147]. Il nécessite la réalisation de bains de contraste à base d'iode[69,117,141] sur plusieurs semaines en fonction de la taille du fœtus (figure I.3)[69,141,147,150,151]. Cette iodination n'est que partiellement réversible par l'utilisation de thiosulfate de sodium, les parents devront en être prévenus de la modification de la coloration cutanée du fœtus (figure I.4)[69,117]. L'IRM-HF nécessite des

acquisitions plus longues[51,52,69,135] et plus chères[62], mais ne nécessite pas d'agent de contraste exogène (Figure I.5)[52,135,141,162–164].

Les techniques de micro-imageries semblent plus adaptées aux fœtus les plus jeunes (Figure I.6) et devront être intégrées dans une prise en charge globale d'imagerie PM (Figure I.7) en ayant recours à des prélèvements invasifs ciblés si nécessaires.

PARTIE II - METHODOLOGIE – PREPARATION DES ECHANTILLONS AVANT MICRO-TDM

1. Le projet FETTAL

Depuis 2016, 28 fœtus non macérés et non malformés avec un terme entre 6+3 et 14 +6 SA, âge gestationnel calculé sur la longueur cranio caudal mesurée et la formule de Robinson[177] ont été inclus dans le projet FETTAL[167,168] (tableau II.1). Ils sont issus d'interruptions volontaires de grossesse avec consentement éclairé signé conformément au protocole de recherche approuvé par l'Agence française de la biomédecine en avril 2015.

2. Comparaison des bains de contraste

Cinq bains de contraste, préalablement publiés[60,61,66,68,69,143–145,159,173–175] (tableau II.2.1), ont été comparés (tableau II.2.2). La comparaison qualitative en aveugle (figure II.2.1 et II.2.2) et quantitative (ratio signal sur bruit et contraste sur bruit) a retrouvé une supériorité du bain composé de paraformaldéhyde à 4% and lugol I_2KI, avec un contenu en iode de 63.25mg/ml (ratio 1:1).

3. Diffusion du contraste et durée des bains de contraste.

Lamouroux A, Cardoso M, Bottero C, Fuchs F, Mousty E, Geneviève D, Subsol G, Goze-Bac C & Captier G.

Modelling of staining in post-mortem diffusible iodine-based contrast enhanced (Dice) micro-CT imaging of non-macerated first-trimester human fetuses.

Soumis à BMC Medical Imaging (Annexe 2)

Pour étudier la diffusion en dynamique, nous avons immergé un fœtus de sexe féminin, de 80mm de longueur cranio-caudale (LCC) et pesant 30,06 g à 13 + 4 SA dans un bain de contraste à base d'iode composé de paraformaldéhyde à 4% and lugol (I_2KI), avec un contenu en iode de 63.25mg/ml (ratio 1:1). Nous avons obtenu des séries d'images en fonction du temps

témoignant de la prise de contraste de l'échantillon (figure II.3.1 et matériel supplémentaire II.3.1, II.3.2 et II.3.3- vidéo) et de la diminution de la quantité d'iode dans le bain de contraste (matériel supplémentaire II.3.4- figure). Cette diffusion dynamique a été modélisée par l'évolution du signal moyen d'une segmentation de régions d'intérêt dans différents organes en fonction du temps (figure II.3.2). Cette évolution suit un modèle d'exponentielle étirée[183] dans tous les organes (Figure II.3.2 – graphique du dessus) sauf dans le foie qui suit un modèle de distribution de Weibull[185] (Figure II.3.2 – A, B and C, matériel supplémentaire II.3.5 – Tableau).

Pour l'analyse concernant la durée des bains de contraste, 18 fœtus ont été placés dans des bains pendant des durées variables, allant de 48 à 144 heures (tableau II.3). Le temps de coloration augmente en fonction de la LCC et du poids. Le ratio contraste sur bruit est une quantification chiffrée du contraste, son augmentation est représentée par une couleur des cercles de plus en plus verts dans la figure II.3.3. Les lignes en pointillé indiquent la durée de coloration minimale requise pour une LCC ou un poids donné afin d'obtenir un ratio contraste sur bruit satisfaisant > 5 conformément au critère de Rose[187]. Par exemple, un fœtus avec une LCC de 50 mm ou un poids de 20 g doit être coloré pendant au moins 96 heures pour atteindre ce seuil (Figure II.3.3).

L'utilisation d'un bain de contraste à base d'iode permet d'améliorer le contraste en MCT chez des fœtus humains non macérés du premier trimestre ce qui est concordant avec la littérature[69,141,147,150,178]. En adaptant la durée du bain de contraste à la LCC ou au poids du fœtus, il est possible d'obtenir des résultats d'imagerie optimaux, ce qui facilite des analyses, aussi bien dans le cadre de la recherche que de la pratique clinique.

PARTIE III - MICRO-IMAGERIE POUR ETUDE DE L'ANATOMIE FŒTALE

Pour faciliter l'application clinique de la micro-imagerie, il est essentiel d'établir un atlas anatomique détaillé du développement fœtal normal. Notre recherche s'est concentrée sur deux termes cibles à 8 et 12 SA.

1. Micro-imagerie à 8 SA

Lamouroux A, Cardoso M, Bottero C, Gallo M, Duraes M, Salerno J, Bertrand M, Rigau V, Fuchs F, Mousty E, Geneviève D, Subsol G, Goze-Bac C, & Captier G.

Micro-CT and high-field MRI for studying very early post-mortem human fetal anatomy at 8 weeks of gestation.

Prenat Diagn 2024; 44: 3–14. (Annexe 3)

L'examen fœtopathologique conventionnel a été mis en parallèle de l'autopsie virtuelle par micro-imageries PM dans la figure III.1.1. Les fœtus inclus âgés entre 7+3 et 8 +5 SA dans cette étude ainsi que leurs modalités d'imagerie et de préparation sont détaillés dans le tableau III.1.2 et dans la figure III.1.2. L'anatomie détaillée de ces fœtus est illustrée par une comparaison entre le MCT avec et sans préparation et l'IRM-HF dans la figure III.1.3 et une comparaison entre le MCT après iodination et l'IRM-HF. Afin d'étayer la visualisation anatomique la figure III.1.5 s'est attaché à représenter des coupes de référence échographique en parallèle de coupes en micro-imagerie. Une évaluation quantitative du ratio contraste sur bruit retrouvait une tendance pour des résultats meilleurs en MCT en comparaison à l'IRM-HF (Figure III.1.6). Une comparaison des résultats obtenus par MCT, IRM-HF et histologie a été illustrée dans la figure III.1.7.

La micro-imagerie PM non destructive du corps entier utilisant le MCT après iodination et l'IRM-HF permet l'étude PM de l'anatomie du fœtus humain dès 8SA. L'autopsie virtuelle devient possible au début du premier trimestre. L'obtention d'un phénotype précis ouvre la voie à un conseil génétique potentiel aux parents dans des contextes de Fausses couches précoces.

2. Micro-imagerie à 12 SA

Le terme de 12 SA représente un âge gestationnel important correspondant à l'échographie du premier trimestre. L'exploration des techniques de micro-imagerie, en particulier le MCT après iodination et l'IRM-HF, à ce terme clef, a été réalisée et étoffée pour inclure des analyses descriptives et quantitatives, en incorporant une approche biométrique.

Cinq fœtus non macérés et non malformés dont la LCC était comprise entre 57 et 68 mm et dont l'âge gestationnel basé sur la LCC était compris entre 12 et 12+6 WG selon la formule de Robinson[177], après l'exclusion d'un échantillon en raison de dommages ont été inclus (figure III.2.1), leurs caractéristiques sont détaillées dans le tableau III.2.1.

La visualisation anatomique utilisant la micro-imagerie par MCT après iodination et IRM-HF s'est concentrée sur des coupes sagittales du pôle céphalique (figure III.2.2), une corrélation avec des coupes de référence échographique du pôle céphalique (figure III.2.3), du thorax, de l'abdomen, du pelvis en sagittal et du fémur (figure III.2.4 et III.2.5).

L'analyse biométrique des fœtus a retrouvé des différences dans les mesures entre le MCT après iodination et l'IRM-HF concernant aussi bien la LCC (figure III.2.6) que les mesures des organes (tableau III.2.2). Le pourcentage de rétraction tissulaire a donc également été quantifiée (tableau III.2.2).

En conclusion, la micro-imagerie par MCT après iodination et IRM-HF sont des outils efficaces pour étudier l'anatomie fœtale humaine PM à 12 SA, offrant une visualisation détaillée et permettant une approche biométrique.

PARTIE IV - MICRO-TDM POST-MORTEM : APPLICATION CLINIQUE.

Pendant ma mobilité à Londres, j'ai effectué le recueil de donnée, les analyses statistiques et participé à la rédaction du manuscrit.

Simcock IC, Lamouroux A, Shelmerdine SC, Sebire NJ, Hutchinson CJ & Arthurs OJ.

Fetal post-mortem imaging using microfocus computed tomography: single centre retrospective clinical experience.

Soumis à American Journal of Obstetrics and Gynecology (Annexe 4)

Cette étude avait pour objectif d'établir le rendement diagnostique du MCT après iodination comparativement à d'autres modalités non invasives (l'examen externe et placentaire) comme autant de parties de l'autopsie moins invasive du fœtus avant 24 SA.

Cette étude monocentrique rétrospective portant sur des M-TDM corps entier après iodination réalisés de manière consécutive et non sélectionné sur une période de sept ans entre octobre 2016 et octobre 2023 a inclus 1007 fœtus. Le nombre de fœtus adressé a rapidement augmenté passant de 37 en 2017 à 215 en 2021 (figure IV.1). La majorité des fœtus étaient issus de parents caucasiens (tableau IV.1). Les termes théoriques et réels estimées sur la LCC selon la formule de Robinson[177] étaient respectivement de 17.92 et 10.33 SA avec une LCC de 11.64 mm et un poids de 92.38 g (tableau IV.1). La macération était jugée sévère sur l'examen externe chez 51.7 % des fœtus (tableau IV.1). Le temps passé par les fœtus dans le centre était en moyenne de 18 jours (tableau IV.2). Même si beaucoup de parents ont consenti à une autopsie complète, l'évaluation par un examen externe par un pathologiste spécialisé n'a pas retenu d'indication à une autopsie conventionnelle au vu du faible rendement attendu (Figure IV.2). Au total, seulement 43 fœtus ont eu une autopsie conventionnelle réalisant un taux d'évitement de l'autopsie de 95.7 %.

La qualité des images en MCT était acceptable pour réaliser un diagnostic dans 80.3 % des fausses couches, 74.9 % des IMG et 41.4 % des morts *in utero* et elle diminue proportionnellement à l'augmentation du niveau de macération (tableau IV.3). Le MCT était anormal dans 223 / 1007 fœtus à l'exclusion de 89 traumatismes en lien avec la macération ou

l'accouchement. La détection d'anomalies était plus importante en cas d'IMG (80.7 %) par rapport au fausse couche spontanée (6.9 %) (tableau IV.3). Le MCT a détecté un grand nombre d'anomalies dans le thorax (140 ; 13,9 %) telle qu'une communication interventriculaire (figure IV.3), dans l'abdomen (127 ; 12,6 %) comme un rein en fer à cheval (figure IV.4) ou une vessie hypertrophiée avec hydronéphrose (Figure IV.5) et le système squelettique (97 ; 9,6 %) (tableau IV.3).

Lorsqu'on intègre le MCT dans une démarche globale d'examen PM, il est possible de détailler la contribution relative de chaque élément (figure IV.6). La cause du décès restait inexpliquée dans 48. 9 % des cas, d'autant plus en cas de décès *in utero* 69.4 % et de macération sévère 85.5 % (tableau IV.4). Lorsque la cause du décès était retrouvée, elle était d'origine fœtale et placentaire dans 21,1 % et 26.2 % des cas respectivement.

L'autopsie fœtale moins invasive, incluant le MCT a permis d'établir un diagnostic dans 51 % des cas et d'éviter 96% d'autopsie. L'examen du placenta est l'élément diagnostique le plus utile (35%), suivi de l'examen externe (20.5%) et de la micro-imagerie par MCT (19.2%). Ceci a une implication pour la prise en charge des décès fœtaux précoces.

CONCLUSION

L'autopsie conventionnelle reste la référence pour détailler le phénotype, mais son caractère invasif en limite l'accès. Les techniques d'autopsie moins invasives utilisent l'imagerie post-mortem. Les techniques d'imageries post-mortem conventionnelles ont une résolution inadaptée au fœtus les plus jeunes. La micro-imagerie permet une résolution isotropique inférieure à 100µm. Le MCT après une préparation par un bain d'iode pendant une durée suffisante adaptée à la taille fœtale et l'IRM-HF permettent une analyse détaillée de l'anatomie fœtale dès 8SA. L'imagerie PM par MCT doit s'intégrer dans un examen PM global, combinant un examen externe, une analyse placentaire. L'utilisation combinée de ces éléments a démontré une réduction de 96% du recours à l'autopsie conventionnelle tout en maintenant un consentement parental élevé. La possibilité d'explorer une fausse couche, une mort in utero (IUD) ou une interruption médicale de grossesse (ToP) entre 7 et 24 SA par de l'imagerie PM MCT en pratique clinique dans le cadre d'un examen PM structuré en France constitue une avancée essentielle qui nécessite la poursuite des recherches, l'établissement de protocoles cliniques standardisés et une approche multidisciplinaire pour sa mise en œuvre.

Le phénotype ainsi établi peut être traduit en terme HPO (human phenotype ontology). Il pourra être pris en compte dans le traitement bio-informatique de variant d'intérêt retrouvé lors de séquençage pangénomique tel que l'exome ou le génome. Cette approche « génotype first » dès le diagnostic prénatal réduira probablement le nombre d'examen PM mais qui restera central pour interpréter des variants de signification incertaine, on parle de « reverse phenotyping ». La collaboration multidisciplinaire entre diagnostic prénatal, examen post-mortem, génétique clinique et biologie moléculaire est essentielle pour intégrer pleinement ces avancées dans la pratique clinique et proposer aux familles des options diagnostiques efficaces et moins invasives.

ABBREVIATIONS

CT = computed tomography

CA = Conventional autopsy

CNR = contrast to noise ratio

CRL = crown-rump length

Dice = diffusible iodine-based contrast enhanced

FPME = Fetal post-mortem examination

FR = fetal reasons

HF-MRI = high field MRI or ultra-high-field MRI

I_2KI = Lugol's iodine

IUD = *in utero* death

LIA = less-invasive autopsy

MCT = Microfocus computed tomography

MRI = magnetic resonance imaging

PROM = premature rupture of membrane

ToP = termination of pregnancy

PFA = paraformaldehyde

PTA = phosphotungstic acid

PM = post-mortem

PM-CT = post-mortem computed-tomography

PM-HF-MRI = post-mortem high-field MRI

PM-MCT = post-mortem Microfocus computed-tomography

PM-MRI = post-mortem magnetic resonance imaging

PM-XR = post-mortem radiographs

PM-US = post-mortem ultrasound scan

ROI = region of interest

SNR = signal to noise ratio

US = ultrasound scan

WG = weeks of gestation

REFERENCES

1 Légifrance. Article 2 - Arrêté du 18 juin 2024. Gouvernement Français, 2025https://www.legifrance.gouv.fr/jorf/article_jo/JORFARTI000049765088 (accessed 29 Jan2025).

2 Khoshnood B, Lelong N, Lecourbe A, Ballon M, Goffinet F. REGISTRE DES MALFORMATIONS CONGENITALES DE PARIS Surveillance épidémiologique et diagnostic prénatal des malformations : Evolution sur trente-cinq ans (1981-2014). 2016.

3 OMS | Anomalies congénitales. WHO. http://www.who.int/mediacentre/factsheets/fs370/fr/ (accessed 1 Jun2016).

4 Donald I, Macvicar J, Brown TG. Investigation of abdominal masses by pulsed ultrasound. *Lancet Lond Engl* 1958; **1**: 1188–1195.

5 Campbell S. A Short History of Sonography in Obstetrics and Gynaecology. *Facts Views Vis ObGyn* 2013; **5**: 213–229.

6 Recker F, Gembruch U, Strizek B. Clinical Ultrasound Applications in Obstetrics and Gynecology in the Year 2024. *J Clin Med* 2024; **13**: 1244.

7 Robinson I. Fetal magnetic resonance imaging: a valuable diagnostic tool. 2009https://www.semanticscholar.org/paper/Fetal-magnetic-resonance-imaging%3A-a-valuable-tool-Robinson/7a16f2739b30e0e3e5dc6976950e43d109c54125 (accessed 9 Jan2025).

8 HAS. Haute Autorité de Santé - Suivi et orientation des femmes enceintes en fonction des situations à risque identifiées. Has-Santefr. 2016.https://www.has-sante.fr/portail/jcms/c_547976/fr/suivi-et-orientation-des-femmes-enceintes-en-fonction-des-situations-a-risque-identifiees (accessed 29 Mar2018).

9 Karim J. N., Roberts N. W., Salomon L. J., Papageorghiou A. T. Systematic review of first-trimester ultrasound screening for detection of fetal structural anomalies and factors that affect screening performance. *Ultrasound Obstet Gynecol* 2017; **50**: 429–441.

10 Rossi AC, Prefumo F. Accuracy of Ultrasonography at 11–14 Weeks of Gestation for Detection of Fetal Structural Anomalies: A Systematic Review. *Obstet Gynecol* 2013; **122**: 1160–1167.

11 Bourgon N, Garde A, Bruel A-L, Lefebvre M, Mau-Them FT, Moutton S *et al.* Same performance of exome sequencing before and after fetal autopsy for congenital abnormalities: toward a paradigm shift in prenatal diagnosis? *Eur J Hum Genet EJHG* 2022; **30**: 967–975.

12 Thauvin-Robinet C, Garde A, Delanne J, Racine C, Rousseau T, Simon E *et al.* Prenatal exome sequencing, a powerful tool for improving the description of prenatal features associated with genetic disorders. *Prenat Diagn* 2024; **44**: 1179–1197.

13 Article L2213-1 - Code de la santé publique - Légifrance. https://www.legifrance.gouv.fr/codes/article_lc/LEGIARTI000043896164 (accessed 29 Jan2025).

14 Agence de la biomédecine - rapport médical et scientifique. https://www.agence-biomedecine.fr/annexes/bilan2017/donnees/diag-prenat/02-centres/synthese.htm#tCPDPN1 (accessed 29 Jan2025).

15 Société française de foetopathologie. *Pathologie foetale & placentaire pratique*. Sauramps médical: Montpellier, 2008.

16 Haute Autorité de santé. [Standard protocol for fetal or perinatal autopsy. Haute Autorité de santé]. *Ann Pathol* 2014; **34**: 415–433.

17 The Royal College of Pathologists. Autopsy guidelines series. 2024.https://www.rcpath.org/profession/guidelines/autopsy-guidelines-series.html (accessed 26 Jun2024).

18 Tuchtan L, Lessieur E, Bartoli C. Diagnosis of congenital abnormalities with post-mortem ultrasound in perinatal death. *Diagn Interv Imaging* 2018; **99**: 143–149.

19 Abdalla EM, El Desouky LM, Hassanein NM. Postmortem clinical examination by experienced clinical geneticists as an alternative to conventional autopsy for assessment of fetal and perinatal deaths in countries with limited resources. *Turk J Pediatr* 2015; **57**: 146–153.

20 Man J, Hutchinson JC, Heazell AE, Ashworth M, Jeffrey I, Sebire NJ. Stillbirth and intrauterine fetal death: role of routine histopathological placental findings to determine cause of death. *Ultrasound Obstet Gynecol Off J Int Soc Ultrasound Obstet Gynecol* 2016; **48**: 579–584.

21 Graham N, Heazell AEP. When the Fetus Goes Still and the Birth Is Tragic: The Role of the Placenta in Stillbirths. *Obstet Gynecol Clin North Am* 2020; **47**: 183–196.

22 Gibbins KJ, Pinar H, Reddy UM, Saade GR, Goldenberg RL, Dudley DJ *et al.* Findings in Stillbirths Associated With Placental Disease. *Am J Perinatol* 2020; **37**: 708–715.

23 Peyronnet V, Anselem O, Loeuillet L, Roux N, Tsatsaris V. Diagnostic value of fetal autopsy after early termination of pregnancy for fetal anomalies. *PLoS ONE* 2022; **17**: e0275674.

24 Gitz L, Khung-Savatovsky S, Viot G, Tantau J, Grangé G, Lewin F *et al.* Fetopathologic examination for early termination of pregnancy: dogma or necessity? *Am J Obstet Gynecol* 2011; **205**: 467.e1–9.

25 The Lancet. Miscarriage: worldwide reform of care is needed. *The Lancet* 2021; **397**: 1597.

26 Quenby S, Gallos ID, Dhillon-Smith RK, Podesek M, Stephenson MD, Fisher J *et al.* Miscarriage matters: the epidemiological, physical, psychological, and economic costs of early pregnancy loss. *The Lancet* 2021; **397**: 1658–1667.

27 Coomarasamy A, Gallos ID, Papadopoulou A, Dhillon-Smith RK, Al-Memar M, Brewin J *et al.* Sporadic miscarriage: evidence to provide effective care. *The Lancet* 2021; **397**: 1668–1674.

28 Meaney S, Gallagher S, Lutomski JE, O'Donoghue K. Parental decision making around perinatal autopsy: a qualitative investigation. *Health Expect Int J Public Particip Health Care Health Policy* 2015; **18**: 3160–3171.

29 Lewis C, Latif Z, Hill M, Riddington M, Lakhanpaul M, Arthurs OJ *et al.* "We might get a lot more families who will agree": Muslim and Jewish perspectives on less invasive perinatal and paediatric autopsy. *PLoS ONE* 2018; **13**: e0202023.

30 Stock SJ, Goldsmith L, Evans MJ, Laing IA. Interventions to improve rates of post-mortem examination after stillbirth. *Eur J Obstet Gynecol Reprod Biol* 2010; **153**: 148–150.

31 Lewis C, Hill M, Arthurs OJ, Hutchinson C, Chitty LS, Sebire NJ. Factors affecting uptake of postmortem examination in the prenatal, perinatal and paediatric setting. *BJOG Int J Obstet Gynaecol* 2018; **125**: 172–181.

32 Khong T, Tanner AR. Foetal and neonatal autopsy rates and use of tissue for research: The influence of 'organ retention' controversy and new consent process. *J Paediatr Child Health* 2006; **42**: 366–369.

33 Lewis C, Simcock IC, Arthurs OJ. Improving uptake of perinatal autopsy. *Curr Opin Obstet Gynecol* 2021; **33**: 129–134.

34 Heazell A, McLaughlin M-J, Schmidt E, Cox P, Flenady V, Khong T *et al.* A difficult conversation? The views and experiences of parents and professionals on the consent process for perinatal postmortem after stillbirth. *BJOG Int J Obstet Gynaecol* 2012; **119**: 987–997.

35 Kang X, Cos T, Guizani M, Cannie MM, Segers V, Jani JC. Parental acceptance of minimally invasive fetal and neonatal autopsy compared with conventional autopsy. *Prenat Diagn* 2014; **34**: 1106–1110.

36 Thayyil S, Chitty LS, Robertson NJ, Taylor AM, Sebire NJ. Minimally invasive fetal postmortem examination using magnetic resonance imaging and computerised tomography: current evidence and practical issues. *Prenat Diagn* 2010; **30**: 713–718.

37 Thayyil S. Less invasive autopsy: an evidenced based approach. *Arch Dis Child* 2011; **96**: 681–687.

38 Dirnhofer R, Jackowski C, Vock P, Potter K, Thali MJ. VIRTOPSY: Minimally Invasive, Imaging-guided Virtual Autopsy. *RadioGraphics* 2006; **26**: 1305–1333.

39 Arthurs OJ, Guy A, Thayyil S, Wade A, Jones R, Norman W *et al.* Comparison of diagnostic performance for perinatal and paediatric post-mortem imaging: CT versus MRI. *Eur Radiol* 2015; : 1–10.

40 Goergen SK, Alibrahim E, Govender N, Stanislavsky A, Abel C, Prystupa S *et al.* Diagnostic assessment of foetal brain malformations with intra-uterine MRI versus perinatal post-mortem MRI. *Neuroradiology* 2019; **61**: 921–934.

41 McDowell AR, Shelmerdine SC, Carmichael DW, Arthurs OJ. High resolution isotropic diffusion imaging in post-mortem neonates: a feasibility study. *Br J Radiol* 2018; **91**: 20180319.

42 Barber JL, Sebire NJ, Chitty LS, Taylor AM, Arthurs OJ. Lung aeration on post-mortem magnetic resonance imaging is a useful marker of live birth versus stillbirth. *Int J Legal Med* 2015; **129**: 531–536.

43 Arthurs OJ, Hutchinson JC, Sebire NJ. Current issues in postmortem imaging of perinatal and forensic childhood deaths. *Forensic Sci Med Pathol* 2017; **13**: 58–66.

44 Thayyil S, Sebire NJ, Chitty LS, Wade A, Chong W, Olsen O *et al.* Post-mortem MRI versus conventional autopsy in fetuses and children: a prospective validation study. *The Lancet* 2013; **382**: 223–233.

45 Arthurs OJ, Thayyil S, Olsen OE, Addison S, Wade A, Jones R *et al.* Diagnostic accuracy of post-mortem MRI for thoracic abnormalities in fetuses and children. *Eur Radiol* 2014; **24**: 2876–2884.

46 Arthurs OJ, Thayyil S, Owens CM, Olsen OE, Wade A, Addison S *et al.* Diagnostic accuracy of post mortem MRI for abdominal abnormalities in foetuses and children. *Eur J Radiol* 2015; **84**: 474–481.

47 Ashwin C, Hutchinson JC, Kang X, Langan D, Jones R, Norman W *et al.* Learning effect on perinatal post-mortem magnetic resonance imaging reporting: single reporter diagnostic accuracy of 200 cases. *Prenat Diagn* 2017; **37**: 566–574.

48 Shelmerdine SC, Arthurs OJ, Gilpin I, Norman W, Jones R, Taylor AM *et al.* Is traditional perinatal autopsy needed after detailed fetal ultrasound and post-mortem MRI? *Prenat Diagn* 2019; **39**: 818–829.

49 Shelmerdine SC, Chung KL, Hutchinson JC, Elliott C, Sebire NJ, Arthurs OJ. Feasibility of Postmortem Imaging Assessment of Brain: Liver Volume Ratios with Pathological Validation. *Fetal Diagn Ther* 2019; **46**: 360–367.

50 Simcock IC, Lamouroux A, Sebire NJ, Shelmerdine SC, Arthurs OJ. Less-invasive autopsy for early pregnancy loss. *Prenat Diagn* 2023; **43**: 937–949.

51 Shelmerdine SC, Arthurs OJ. Post-mortem perinatal imaging: what is the evidence? *Br J Radiol* 2022; : 20211078.

52 Dawood Y, Strijkers GJ, Limpens J, Oostra RJ, de Bakker BS. Novel imaging techniques to study postmortem human fetal anatomy: a systematic review on microfocus-CT and ultra-high-field MRI. *Eur Radiol* 2019. doi:10.1007/s00330-019-06543-8.

53 Shelmerdine SC, Sebire NJ, Arthurs OJ. Perinatal post-mortem ultrasound (PMUS): radiological-pathological correlation. *Insights Imaging* 2019; **10**: 81.

54 Shelmerdine S, Langan D, Sebire NJ, Arthurs O. Diagnostic accuracy of perinatal post-mortem ultrasound (PMUS): a systematic review. *BMJ Paediatr Open* 2019; **3**: e000566.

55 Shelmerdine SC, Sebire NJ, Arthurs OJ. Perinatal post mortem ultrasound (PMUS): a practical approach. *Insights Imaging* 2019; **10**: 35.

56 Kang X, Shelmerdine SC, Hurtado I, Bevilacqua E, Hutchinson C, Mandalia U *et al.* Postmortem examination of human fetuses: comparison of two-dimensional ultrasound with invasive autopsy. *Ultrasound Obstet Gynecol Off J Int Soc Ultrasound Obstet Gynecol* 2019; **53**: 229–238.

57 Kang X, Sanchez TC, Arthurs OJ, Bevilacqua E, Cannie MM, Segers V *et al.* Postmortem fetal imaging: prospective blinded comparison of two-dimensional ultrasound with

magnetic resonance imaging. *Ultrasound Obstet Gynecol* 2019; **54**: 791–799.

58 Shelmerdine SC, Sebire NJ, Arthurs OJ. Diagnostic accuracy of postmortem ultrasound vs postmortem 1.5-T MRI for non-invasive perinatal autopsy. *Ultrasound Obstet Gynecol Off J Int Soc Ultrasound Obstet Gynecol* 2021; **57**: 449–458.

59 Shelmerdine SC, Langan D, Mandalia U, Sebire NJ, Arthurs OJ. Maceration determines diagnostic yield of fetal and neonatal whole body post-mortem ultrasound. *Prenat Diagn* 2020; **40**: 232–243.

60 Hutchinson JC, Kang X, Shelmerdine SC, Segers V, Lombardi CM, Cannie MM *et al.* Postmortem microfocus computed tomography for early gestation fetuses: a validation study against conventional autopsy. *Am J Obstet Gynecol* 2018; **218**: 445.e1-445.e12.

61 Shelmerdine SC, Simcock IC, Hutchinson JC, Guy A, Ashworth MT, Sebire NJ *et al.* Postmortem microfocus computed tomography for noninvasive autopsies: experience in >250 human fetuses. *Am J Obstet Gynecol* 2021; **224**: 103.e1-103.e15.

62 Dawood Y, Honhoff C, van der Post A-S, Roosendaal SD, Coolen BF, Strijkers GJ *et al.* Comparison of postmortem whole-body contrast-enhanced microfocus computed tomography and high-field magnetic resonance imaging of human fetuses. *Ultrasound Obstet Gynecol Off J Int Soc Ultrasound Obstet Gynecol* 2022; **60**: 109–117.

63 Docter D, Dawood Y, Jacobs K, Hagoort J, Oostra R-J, van den Hoff MJB *et al.* Microfocus computed tomography for fetal postmortem imaging: an overview. *Pediatr Radiol* 2022. doi:10.1007/s00247-022-05517-1.

64 Feldkamp LA, Goldstein SA, Parfitt MA, Jesion G, Kleerekoper M. The direct examination of three-dimensional bone architecture in vitro by computed tomography. *J Bone Miner Res* 1989; **4**: 3–11.

65 Dawood Y, de Bakker BS. Micro-CT of Early Human Development. *Radiology* 2020; **297**: 32–32.

66 Shelmerdine SC, Hutchinson JC, Kang X, Suich JD, Ashworth M, Cannie MM *et al.* Novel usage of microfocus computed tomography (micro-CT) for visualisation of human embryonic development-Implications for future non-invasive post-mortem investigation. *Prenat Diagn* 2018; **38**: 538–542.

67 Shelmerdine SC, Simcock IC, Hutchinson JC, Aughwane R, Melbourne A, Nikitichev DI *et al.* 3D printing from microfocus computed tomography (micro-CT) in human specimens: education and future implications. *Br J Radiol* 2018; **91**: 20180306.

68 Simcock IC, Shelmerdine SC, Langan D, Anna G, Sebire NJ, Arthurs OJ. Micro-CT yields high image quality in human fetal post-mortem imaging despite maceration. *BMC Med Imaging* 2021; **21**: 128.

69 Simcock IC, Shelmerdine SC, Hutchinson JC, Sebire NJ, Arthurs OJ. Human fetal whole-body postmortem microfocus computed tomographic imaging. *Nat Protoc* 2021. doi:10.1038/s41596-021-00512-6.

70 Ashton JR, West JL, Badea CT. In vivo small animal micro-CT using nanoparticle contrast agents. *Front Pharmacol* 2015; **6**: 256.

71 Clark DP, Badea CT. Advances in micro-CT imaging of small animals. *Phys Medica PM Int J Devoted Appl Phys Med Biol Off J Ital Assoc Biomed Phys AIFB* 2021; **88**: 175–192.

72 Albers J, Svetlove A, Duke E. Synchrotron X-ray imaging of soft biological tissues - principles, applications and future prospects. *J Cell Sci* 2024; **137**: jcs261953.

73 Reichmann J, Schnurpfeil A, Mittelstädt S, Jensen PM, Dahl VA, Dahl AB *et al.* 3D multiscale characterization of the human placenta: Bridging anatomy and histology by X-ray phase-contrast tomography. *PNAS Nexus* 2025; **4**: pgae583.

74 Kaneko Y, Shinohara G, Hoshino M, Morishita H, Morita K, Oshima Y *et al.* Intact Imaging of Human Heart Structure Using X-ray Phase-Contrast Tomography. *Pediatr Cardiol* 2017; **38**: 390–393.

75 Rougé-Labriet H, Berujon S, Mathieu H, Bohic S, Fayard B, Ravey J-N *et al.* X-ray Phase Contrast osteo-articular imaging: a pilot study on cadaveric human hands. *Sci Rep* 2020;

10: 1911.

76 Wan Y, McDole K, Keller PJ. Light-Sheet Microscopy and Its Potential for Understanding Developmental Processes. *Annu Rev Cell Dev Biol* 2019; **35**: 655–681.

77 Keller PJ. In vivo imaging of zebrafish embryogenesis. *Methods San Diego Calif* 2013; **62**: 268–278.

78 Nagarajan S, Bardhan S, Naganathan SR. Light Sheet Microscopy Imaging and Mounting Strategies for Early Zebrafish Embryos. *J Vis Exp JoVE* 2024. doi:10.3791/66735.

79 Maes A, Pestiaux C, Marino A, Balcaen T, Leyssens L, Vangrunderbeeck S *et al.* Cryogenic contrast-enhanced microCT enables nondestructive 3D quantitative histopathology of soft biological tissues. *Nat Commun* 2022; **13**: 6207.

80 Maes A, Borgel O, Braconnier C, Balcaen T, Wevers M, Halbgebauer R *et al.* X-Ray-Based 3D Histopathology of the Kidney Using Cryogenic Contrast-Enhanced MicroCT. *Int J Biomed Imaging* 2024; **2024**: 3924036.

81 Stillbirths and stillbirth rates. UNICEF DATA. https://data.unicef.org/topic/child-survival/stillbirths/ (accessed 12 Nov2024).

82 MacWilliams K, Hughes J, Aston M, Field S, Moffatt FW. Understanding the Experience of Miscarriage in the Emergency Department. *J Emerg Nurs* 2016; **42**: 504–512.

83 Rossen LM, Ahrens KA, Branum AM. Trends in Risk of Pregnancy Loss Among US Women, 1990–2011. *Paediatr Perinat Epidemiol* 2018; **32**: 19–29.

84 Blackmore ER, Côté-Arsenault D, Tang W, Glover V, Evans J, Golding J *et al.* Previous prenatal loss as a predictor of perinatal depression and anxiety. *Br J Psychiatry* 2011; **198**: 373–378.

85 Engelhard IM, van den Hout MA, Arntz A. Posttraumatic stress disorder after pregnancy loss. *Gen Hosp Psychiatry* 2001; **23**: 62–66.

86 Lok IH, Yip AS-K, Lee DT-S, Sahota D, Chung TK-H. A 1-year longitudinal study of psychological morbidity after miscarriage. *Fertil Steril* 2010; **93**: 1966–1975.

87 Horey D, Flenady V, Conway L, McLeod E, Yee Khong T. Decision influences and aftermath: parents, stillbirth and autopsy. *Health Expect* 2014; **17**: 534–544.

88 Banno C, Sugiura-Ogasawara M, Ebara T, Ide S, Kitaori T, Sato T *et al.* Attitude and perceptions toward miscarriage: a survey of a general population in Japan. *J Hum Genet* 2020; **65**: 155–164.

89 Brier N. Understanding and managing the emotional reactions to a miscarriage. *Obstet Gynecol* 1999; **93**: 151–155.

90 Availability of less invasive prenatal, perinatal and paediatric autopsy will improve uptake rates: a mixed-methods study with bereaved parents - Lewis - 2019 - BJOG: An International Journal of Obstetrics & Gynaecology - Wiley Online Library. https://obgyn-onlinelibrary-wiley-com.ezpum.scdi-montpellier.fr/doi/10.1111/1471-0528.15591 (accessed 12 Nov2024).

91 Ernst LM. A pathologist′s perspective on the perinatal autopsy. *Semin Perinatol* 2015; **39**: 55–63.

92 Rahman HA, Khong TY. Perinatal and infant postmortem examination. Survey of women's reactions to perinatal necropsy. *BMJ* 1995; **310**: 870–871.

93 Ellis A, Chebsey C, Storey C, Bradley S, Jackson S, Flenady V *et al.* Systematic review to understand and improve care after stillbirth: a review of parents' and healthcare professionals' experiences. *BMC Pregnancy Childbirth* 2016; **16**: 16.

94 Nese Nalan, Yesim Bulbul. Diagnostic value of perinatal autopsies: analysis of 486 cases - PubMed. 2018.https://pubmed-ncbi-nlm-nih-gov.ezpum.scdi-montpellier.fr/28841576/ (accessed 12 Nov2024).

95 Gordijn SJ, Erwich JJHM, Khong TY. Value of the perinatal autopsy: critique. *Pediatr Dev Pathol Off J Soc Pediatr Pathol Paediatr Pathol Soc* 2002; **5**: 480–488.

96 Boyd PA, Tondi F, Hicks NR, Chamberlain PF. Autopsy after termination of pregnancy for fetal anomaly: retrospective cohort study. *BMJ* 2004; **328**: 137.

97 Lewis C, Riddington M, Hill M, Arthurs OJ, Hutchinson JC, Chitty LS *et al.*

Availability of less invasive prenatal, perinatal and paediatric autopsy will improve uptake rates: a mixed-methods study with bereaved parents. *BJOG Int J Obstet Gynaecol* 2019; **126**: 745–753.

98 Lewis C, Hill M, Arthurs OJ, Hutchinson JC, Chitty LS, Sebire N. Health professionals' and coroners' views on less invasive perinatal and paediatric autopsy: a qualitative study. *Arch Dis Child* 2018; **103**: 572–578.

99 Man J, Hutchinson JC, Heazell AE, Ashworth M, Levine S, Sebire NJ. Stillbirth and intrauterine fetal death: factors affecting determination of cause of death at autopsy. *Ultrasound Obstet Gynecol Off J Int Soc Ultrasound Obstet Gynecol* 2016; **48**: 566–573.

100 Basu MN, Johnsen IBG, Wehberg S, Sørensen RG, Barington T, Nørgård BM. Causes of death among full term stillbirths and early neonatal deaths in the Region of Southern Denmark. *J Perinat Med* 2018; **46**: 197–202.

101 Lewis C, Riddington M, Hill M, Bevan C, Fisher J, Lyas L *et al.* 'The communication and support from the health professional is incredibly important': A qualitative study exploring the processes and practices that support parental decision-making about postmortem examination. *Prenat Diagn* 2019; **39**: 1242–1253.

102 Wiener L, Sweeney C, Baird K, Merchant MS, Warren KE, Corner GW *et al.* What Do Parents Want to Know When Considering Autopsy for Their Child With Cancer? *J Pediatr Hematol Oncol* 2014; **36**: 464.

103 Breeze ACG, Statham H, Hackett GA, Jessop FA, Lees CC. Perinatal Postmortems: What Is Important to Parents and How Do They Decide? *Birth* 2012; **39**: 57–64.

104 Baker JN, Windham JA, Hinds PS, Gattuso JS, Mandrell B, Gajjar P *et al.* Bereaved parents' intentions and suggestions about research autopsies in children with lethal brain tumors. *J Pediatr* 2013; **163**: 581–586.

105 Rankin J, Wright C, Lind T. Cross sectional survey of parents' experience and views of the postmortem examination. *BMJ* 2002; **324**: 816–818.

106 Sieswerda-Hoogendoorn T, van Rijn RR. Current techniques in postmortem imaging with specific attention to paediatric applications. *Pediatr Radiol* 2010; **40**: 141–152.

107 Kock KF, Vestergaard V, Hardt-Madsen M, Garne E. Declining autopsy rates in stillbirths and infant deaths: results from Funen County, Denmark, 1986-96. *J Matern-Fetal Neonatal Med Off J Eur Assoc Perinat Med Fed Asia Ocean Perinat Soc Int Soc Perinat Obstet* 2003; **13**: 403–407.

108 Newton D, Coffin CM, Clark EB, Lowichik A. How the Pediatric Autopsy Yields Valuable Information in a Vertically Integrated Health Care System. *Arch Pathol Lab Med* 2004; **128**: 1239–1246.

109 Lewis JA. Jewish Perspectives on Pregnancy and Childbearing. *MCN Am J Matern Nurs* 2003; **28**: 306.

110 Cullen S, Mooney E, Casey B, Downey P. An audit of healthcare professionals' knowledge regarding perinatal autopsy. *Ir J Med Sci 1971 -* 2019; **188**: 583–585.

111 Lewis C, Hutchinson JC, Riddington M, Hill M, Arthurs OJ, Fisher J *et al.* Minimally invasive autopsy for fetuses and children based on a combination of post-mortem MRI and endoscopic examination: a feasibility study. *Health Technol Assess Winch Engl* 2019; **23**: 1–104.

112 BBC Radio 4 - File on 4, How did my child die? The crisis in paediatric pathology. BBC. https://www.bbc.co.uk/programmes/m001gkwd (accessed 12 Nov2024).

113 Kang X, Carlin A, Cannie MM, Sanchez TC, Jani JC. Fetal postmortem imaging: an overview of current techniques and future perspectives. *Am J Obstet Gynecol* 2020; **223**: 493–515.

114 Sebire NJ. Towards the minimally invasive autopsy? *Ultrasound Obstet Gynecol* 2006; **28**: 865–867.

115 Nayak SS, Shukla A, Lewis L, Kadavigere R, Mathew M, Adiga PK *et al.* Clinical utility of fetal autopsy and its impact on genetic counseling. *Prenat Diagn* 2015; **35**: 685–691.

116 Jawad N, Sebire NJ, Wade A, Taylor AM, Chitty LS, Arthurs OJ. Body weight

lower limits of fetal postmortem MRI at 1.5 T. *Ultrasound Obstet Gynecol Off J Int Soc Ultrasound Obstet Gynecol* 2016; **48**: 92–97.

117 Docter D, Dawood Y, Jacobs K, Hagoort J, Oostra R-J, van den Hoff MJB *et al.* Microfocus computed tomography for fetal postmortem imaging: an overview. *Pediatr Radiol* 2022. doi:10.1007/s00247-022-05517-1.

118 Shelmerdine SC, Hutchinson JC, Arthurs OJ, Sebire NJ. Latest developments in post-mortem foetal imaging. *Prenat Diagn* 2020; **40**: 28–37.

119 Votino C, Jani J, Verhoye M, Bessieres B, Fierens Y, Segers V *et al.* Postmortem examination of human fetal hearts at or below 20 weeks' gestation: a comparison of high-field MRI at 9.4 T with lower-field MRI magnets and stereomicroscopic autopsy. *Ultrasound Obstet Gynecol Off J Int Soc Ultrasound Obstet Gynecol* 2012; **40**: 437–444.

120 Kang X, Cannie M, Jani JC. Effect of staining using gadolinium and formaldehyde on fetal whole-body postmortem 3-Tesla magnetic resonance imaging. *Ultrasound Obstet Gynecol* 2020; **55**: 277–278.

121 Kang X, Cannie MM, Arthurs OJ, Segers V, Fourneau C, Bevilacqua E *et al.* Post-mortem whole-body magnetic resonance imaging of human fetuses: a comparison of 3-T vs. 1.5-T MR imaging with classical autopsy. *Eur Radiol* 2017; **27**: 3542–3553.

122 Sandaite I, Lombardi C, Cook AC, Fabietti I, Deprest J, Boito S. Micro-computed tomography of isolated fetal hearts following termination of pregnancy: A feasibility study at 8 to 12 weeks' gestation. *Prenat Diagn* 2020; **40**: 984–990.

123 Nijkamp JW, Sebire NJ, Bouman K, Korteweg FJ, Erwich JJHM, Gordijn SJ. Perinatal death investigations: What is current practice? *Semin Fetal Neonatal Med* 2017; **22**: 167–175.

124 Arthurs OJ, Calder AD, Kiho L, Taylor AM, Sebire NJ. Routine perinatal and paediatric post-mortem radiography: detection rates and implications for practice. *Pediatr Radiol* 2014; **44**: 252–257.

125 Kamphuis-van Ulzen K, Koopmanschap DHJLM, Marcelis CLM, van Vugt JMG, Klein WM. When is a post-mortem skeletal survey of the fetus indicated, and when not? *J Matern-Fetal Neonatal Med Off J Eur Assoc Perinat Med Fed Asia Ocean Perinat Soc Int Soc Perinat Obstet* 2016; **29**: 991–997.

126 Votino C, Cos Sanchez T, Bessieres B, Segers V, Kadhim H, Razavi F *et al.* Minimally invasive fetal autopsy using ultrasound: a feasibility study. *Ultrasound Obstet Gynecol Off J Int Soc Ultrasound Obstet Gynecol* 2018; **52**: 776–783.

127 Calder AD, Offiah AC. Foetal radiography for suspected skeletal dysplasia: technique, normal appearances, diagnostic approach. *Pediatr Radiol* 2015; **45**: 536–548.

128 Shelmerdine SC, Hutchinson JC, Lewis C, Simcock IC, Sekar T, Sebire NJ *et al.* A pragmatic evidence-based approach to post-mortem perinatal imaging. *Insights Imaging* 2021; **12**: 101.

129 Addison S, Arthurs OJ, Thayyil S. Post-mortem MRI as an alternative to non-forensic autopsy in foetuses and children: from research into clinical practice. *Br J Radiol* 2014; **87**: 20130621.

130 Arthurs OJ, Taylor AM, Sebire NJ. Indications, advantages and limitations of perinatal postmortem imaging in clinical practice. *Pediatr Radiol* 2015; **45**: 491–500.

131 Votino C, Cannie M, Segers V, Dobrescu O, Dessy H, Gallo V *et al.* Virtual autopsy by computed tomographic angiography of the fetal heart: a feasibility study. *Ultrasound Obstet Gynecol* 2012; **39**: 679–684.

132 Sarda-Quarello L, Bartoli C, Laurent P-E, Torrents J, Piercecchi-Marti M-D, Sigaudy S *et al.* Whole body perinatal postmortem CT angiography. *Diagn Interv Imaging* 2016; **97**: 121–124.

133 Norman W, Jawad N, Jones R, Taylor AM, Arthurs OJ. Perinatal and paediatric post-mortem magnetic resonance imaging (PMMR): sequences and technique. *Br J Radiol* 2016; **89**: 20151028.

134 Arthurs OJ, Thayyil S, Pauliah SS, Jacques TS, Chong WK, Gunny R *et al.*

Diagnostic accuracy and limitations of post-mortem MRI for neurological abnormalities in fetuses and children. *Clin Radiol* 2015; **70**: 872–880.

135 Thayyil S, Cleary JO, Sebire NJ, Scott RJ, Chong K, Gunny R *et al.* Post-mortem examination of human fetuses: a comparison of whole-body high-field MRI at 9.4 T with conventional MRI and invasive autopsy. *Lancet Lond Engl* 2009; **374**: 467–475.

136 Rodriguez MA, Prats P, Rodríguez I, Cusí V, Comas C. Concordance between prenatal ultrasound and autopsy findings in a tertiary center. *Prenat Diagn* 2014; **34**: 784–789.

137 Kang X, Resta S, Cos Sanchez T, Carlin A, Bevilacqua E, Jani JC. Impact of the delay between fetal death and delivery on the success of postmortem ultrasound following termination of pregnancy. *J Matern-Fetal Neonatal Med Off J Eur Assoc Perinat Med Fed Asia Ocean Perinat Soc Int Soc Perinat Obstet* 2021; **34**: 1613–1618.

138 Shelmerdine SC, Hutchinson JC, Ward L, Sekar T, Ashworth MT, Levine S *et al.* Feasibility of INTACT (INcisionless TArgeted Core Tissue) biopsy procedure for perinatal autopsy. *Ultrasound Obstet Gynecol Off J Int Soc Ultrasound Obstet Gynecol* 2020; **55**: 667–675.

139 Hutchinson JC, Shelmerdine SC, Lewis C, Parmenter J, Simcock IC, Ward L *et al.* Minimally invasive perinatal and pediatric autopsy with laparoscopically assisted tissue sampling: feasibility and experience of the MinImAL procedure. *Ultrasound Obstet Gynecol Off J Int Soc Ultrasound Obstet Gynecol* 2019; **54**: 661–669.

140 Chambers G, Shelmerdine SC, Aertsen M, Dohna M, Goergen SK, Johnson K *et al.* Current and future funding streams for paediatric postmortem imaging: European Society of Paediatric Radiology survey results. *Pediatr Radiol* 2023; **53**: 273–281.

141 Dawood Y, Buijtendijk MFJ, Shah H, Smit JA, Jacobs K, Hagoort J *et al.* Imaging fetal anatomy. *Semin Cell Dev Biol* 2022. doi:10.1016/j.semcdb.2022.02.023.

142 Dawood Y, Hagoort J, Siadari BA, Ruijter JM, Gunst QD, Lobe NHJ *et al.* Reducing soft-tissue shrinkage artefacts caused by staining with Lugol's solution. *Sci Rep* 2021; **11**: 19781.

143 Lombardi CM, Zambelli V, Botta G, Moltrasio F, Cattoretti G, Lucchini V *et al.* Postmortem microcomputed tomography (micro-CT) of small fetuses and hearts. *Ultrasound Obstet Gynecol* 2014; **44**: 600–609.

144 Hutchinson JC, Shelmerdine SC, Simcock IC, Sebire NJ, Arthurs OJ. Early clinical applications for imaging at microscopic detail: microfocus computed tomography (micro-CT). *Br J Radiol* 2017; **90**: 20170113.

145 Lombardi S, Scola E, Ippolito D, Zambelli V, Botta G, Cuttin S *et al.* Micro-computed tomography: a new diagnostic tool in postmortem assessment of brain anatomy in small fetuses. *Neuroradiology* 2019; **61**: 737–746.

146 Hutchinson JC, Arthurs OJ, Ashworth MT, Ramsey AT, Mifsud W, Lombardi CM *et al.* Clinical utility of postmortem microcomputed tomography of the fetal heart: diagnostic imaging vs macroscopic dissection. *Ultrasound Obstet Gynecol Off J Int Soc Ultrasound Obstet Gynecol* 2016; **47**: 58–64.

147 Simcock IC, Shelmerdine SC, Langan D, Sebire NJ, Arthurs OJ. Predictors of image quality at human foetal post-mortem micro CT. Insights into Imaging.: RPS 314-6, 2021 doi:2021;12(2):291.

148 Shelmerdine SC, Simcock IC, Hutchinson JC, Aughwane R, Melbourne A, Nikitichev DI *et al.* 3D printing from microfocus computed tomography (micro-CT) in human specimens: education and future implications. *Br J Radiol* 2018; **91**: 20180306.

149 Hutchinson JC, Shelmerdine SC, Simcock IC, Sebire NJ, Arthurs OJ. Early clinical applications for imaging at microscopic detail: microfocus computed tomography (micro-CT). *Br J Radiol*; **90**. doi:10.1259/bjr.20170113.

150 Pauwels E, Van Loo D, Cornillie P, Brabant L, Van Hoorebeke L. An exploratory study of contrast agents for soft tissue visualization by means of high resolution X-ray computed tomography imaging. *J Microsc* 2013; **250**: 21–31.

151 Stephenson RS, Boyett MR, Hart G, Nikolaidou T, Cai X, Corno AF *et al.* Contrast Enhanced Micro-Computed Tomography Resolves the 3-Dimensional Morphology of

the Cardiac Conduction System in Mammalian Hearts. *PLoS ONE* 2012; **7**. doi:10.1371/journal.pone.0035299.

152 Vickerton P, Jarvis J, Jeffery N. Concentration-dependent specimen shrinkage in iodine-enhanced microCT. *J Anat* 2013; **223**: 185–193.

153 Dunmore-Buyze PJ, Tate E, Xiang F, Detombe SA, Nong Z, Pickering JG *et al.* Three-dimensional imaging of the mouse heart and vasculature using micro-CT and whole-body perfusion of iodine or phosphotungstic acid. *Contrast Media Mol Imaging* 2014; **9**: 383–390.

154 Zhou Y-Q, Davidson L, Henkelman RM, Nieman BJ, Foster FS, Yu LX *et al.* Ultrasound-guided left-ventricular catheterization: a novel method of whole mouse perfusion for microimaging. *Lab Invest* 2004; **84**: 385–389.

155 Aydin E, Levy B, Oria M, Nachabe H, Lim F-Y, Peiro JL. Optimization of Pulmonary Vasculature Tridimensional Phenotyping in The Rat Fetus. *Sci Rep* 2019; **9**: 1244.

156 Montaldo P, Addison S, Oliveira V, Lally PJ, Taylor AM, Sebire NJ *et al.* Quantification of maceration changes using post mortem MRI in fetuses. *BMC Med Imaging* 2016; **16**: 34.

157 Cain MA, Guidi CB, Steffensen T, Whiteman VE, Gilbert-Barness E, Johnson DR. Postmortem Ultrasonography of the Macerated Fetus Complements Autopsy following in Utero Fetal Demise. *Pediatr Dev Pathol* 2014; **17**: 217–220.

158 Piercecchi-Marti MD, Liprandi A, Sigaudy S, Fredouille C, Adalian P, Figarella-Branger D *et al.* Value of fetal autopsy after medical termination of pregnancy. *Forensic Sci Int* 2004; **144**: 7–10.

159 Hutchinson JC, Barrett H, Ramsey AT, Haig IG, Guy A, Sebire NJ *et al.* Virtual pathological examination of the human fetal kidney using micro-CT. *Ultrasound Obstet Gynecol Off J Int Soc Ultrasound Obstet Gynecol* 2016; **48**: 663–665.

160 Sandrini C, Rossetti L, Zambelli V, Zanarotti R, Bettinazzi F, Soldá R *et al.* Accuracy of Micro-Computed Tomography in Post-mortem Evaluation of Fetal Congenital Heart Disease. Comparison Between Post-mortem Micro-CT and Conventional Autopsy. *Front Pediatr* 2019; **7**: 92.

161 Sandrini C, Lombardi C, Shearn AIU, Ordonez MV, Caputo M, Presti F *et al.* Three-Dimensional Printing of Fetal Models of Congenital Heart Disease Derived From Microfocus Computed Tomography: A Case Series. *Front Pediatr* 2020; **7**: 567.

162 Umutlu L, Ladd ME, Forsting M, Lauenstein T. 7 Tesla MR Imaging: Opportunities and Challenges. *RöFo - Fortschritte Auf Dem Geb Röntgenstrahlen Bildgeb Verfahr* 2014; **186**: 121–129.

163 Kraff O, Quick HH. 7T: Physics, safety, and potential clinical applications. *J Magn Reson Imaging* 2017; **46**: 1573–1589.

164 Staicu A, Albu C, Popa-Stanila R, Chiriac L, Boitor-Borza D, Bondor C *et al.* Potential clinical benefits and limitations of fetal virtopsy using high-field MRI at 7 Tesla versus stereomicroscopic autopsy to assess first trimester fetuses. *Prenat Diagn* 2019; **39**: 505–518.

165 Castillo P, Ussene E, Ismail MR, Jordao D, Lovane L, Carrilho C *et al.* Pathological Methods Applied to the Investigation of Causes of Death in Developing Countries: Minimally Invasive Autopsy Approach. *PLOS ONE* 2015; **10**: e0132057.

166 Nuzum D, Meaney S, O'Donoghue K. The impact of stillbirth on bereaved parents: A qualitative study. *PLOS ONE* 2018; **13**: e0191635.

167 Lamouroux A, Captier G, Genevieve D. Projet FETTAL, Fetal Enhanced Tridimentional and Translationel Anatomical Landscape. *Morphologie* 2017. doi:10.1016/j.morpho.2017.07.062.

168 Lamouroux A, Genevieve D, Fuchs F, Letouzey V, Subsol G, Captier G. OC18. 01: Fetal enhanced tridimensional and translational anatomical landscape: FETTAL Project. *Ultrasound Obstet Gynecol* 2017; : 37.

169 Université de Montpellier. https://www.umontpellier.fr. https://www.umontpellier.fr (accessed 19 Jan2025).

170 BioNanoImaging Foundry. https://bnif.umontpellier.fr/ (accessed 19 Jan2025).

171 Shelmerdine SC, Arthurs OJ. Post-mortem perinatal imaging: what is the evidence? *Br J Radiol* 2022; : 20211078.

172 Gignac PM, Kley NJ, Clarke JA, Colbert MW, Morhardt AC, Cerio D *et al.* Diffusible iodine-based contrast-enhanced computed tomography (diceCT): an emerging tool for rapid, high-resolution, 3-D imaging of metazoan soft tissues. *J Anat* 2016; **228**: 889–909.

173 Metscher BD. MicroCT for developmental biology: A versatile tool for high-contrast 3D imaging at histological resolutions. *Dev Dyn* 2009; **238**: 632–640.

174 Metscher BD. MicroCT for comparative morphology: simple staining methods allow high-contrast 3D imaging of diverse non-mineralized animal tissues. *BMC Physiol* 2009; **9**: 11.

175 Vymazalová K, Vargová L, Zikmund T, Kaiser J. The possibilities of studying human embryos and foetuses using micro-CT: a technical note. *Anat Sci Int* 2017; **92**: 299–303.

176 Germann M, Shim S, Angst F, Saltybaeva N, Boss A. Spiral breast computed tomography (CT): signal-to-noise and dose optimization using 3D-printed phantoms. *Eur Radiol* 2021; **31**: 3693–3702.

177 Robinson HP. Sonar Measurement of Fetal Crown-Rump Length as Means of Assessing Maturity in First Trimester of Pregnancy. *Br Med J* 1973; **4**: 28–31.

178 Simcock IC, Shelmerdine SC, Hutchinson JC, Sebire NJ, Arthurs OJ. Body weight-based iodinated contrast immersion timing for human fetal postmortem microfocus computed tomography. *BJR Open* 2023; **6**: tzad006.

179 Légifrance - Droit national en vigueur - Circulaires et instructions - CIRCULAIRE N° DGOS/R1/2015/140 du 22 avril 2015 relative à la campagne tarifaire et budgétaire 2015 des établissements de santé. https://www.legifrance.gouv.fr/download/pdf/circ?id=39565 (accessed 8 Nov2024).

180 Cannie M, Votino C, Moerman Ph, Vanheste R, Segers V, Van Berkel K *et al.* Acceptance, reliability and confidence of diagnosis of fetal and neonatal virtuopsy compared with conventional autopsy: a prospective study. *Ultrasound Obstet Gynecol* 2012; **39**: 659–665.

181 Lamouroux A, Cardoso M, Bottero C, Gallo M, Duraes M, Salerno J *et al.* Micro-CT and high-field MRI for studying very early post-mortem human fetal anatomy at 8 weeks of gestation. *Prenat Diagn* 2024; **44**: 3–14.

182 Stauffer D, Aharony A. *Introduction To Percolation Theory: Second Edition*. 2nd ed. Taylor & Francis: London, 2018 doi:10.1201/9781315274386.

183 Lee KC, Siegel J, Webb SE, Lévêque-Fort S, Cole MJ, Jones R *et al.* Application of the stretched exponential function to fluorescence lifetime imaging. *Biophys J* 2001; **81**: 1265–1274.

184 Jayakumar K, Babu MG. Some Generalizations of Weibull Distribution and Related Processes. *J Stat Theory Appl* 2015; **14**: 425–434.

185 Weibull W. A Statistical Distribution Function of Wide Applicability. *J Appl Mech* 1951; **18**: 293–297, hal-03112318.

186 Genolini Christophe, Evain Andeol, Lopez Julien, Heinrich Marc. 'R++, l'essentiel', version 1.6.15, for Windows, released 2024-03-25. 2024.

187 Hsieh SS, Leng S, Yu L, Huber NR, McCollough CH. A minimum SNR criterion for computed tomography object detection in the projection domain. *Med Phys* 2022; **49**: 4988–4998.

188 Gilson H. Leonardo da Vinci's Embryological Drawings of the Fetus. *Embryo Proj Encycl* 2008.http://embryo.asu.edu/handle/10776/1929 (accessed 29 Nov2022).

189 Buklijas T, Hopwood N. Remodelling: Publishing in wax and print. Mak. Visible Embryos. 2008.http://www.hps.cam.ac.uk/visibleembryos/s5_3.html (accessed 27 Feb2020).

190 Ameil M, Delattre JF, Cordobes B, Flament JB. Computerized reconstruction of an anatomical structure based on digitized sections. Preliminary study. *Anat Clin* 1984; **5**: 261–264.

191 de Bakker BS, de Jong KH, Hagoort J, Oostra R-J, Moorman AFM. Towards a 3-dimensional atlas of the developing human embryo: The Amsterdam experience. *Reprod*

Toxicol 2012; **34**: 225–236.

192 de Bakker BS, de Jong KH, Hagoort J, de Bree K, Besselink CT, de Kanter FEC *et al.* An interactive three-dimensional digital atlas and quantitative database of human development. *Science* 2016; **354**: aag0053.

193 Labrousse M, Micard E, Tonnelet R, Cendre R, Delmas V, Naidich T *et al.* Embryo Form Project: An original technique for the three-dimensional reconstruction of human embryo morphology. *Reprod Toxicol Elmsford N* 2015; **58**: 1–7.

194 Kamphuis-van Ulzen K, Koopmanschap DHJLM, Marcelis CLM, van Vugt JMG, Klein WM. When is a post-mortem skeletal survey of the fetus indicated, and when not? *J Matern-Fetal Neonatal Med Off J Eur Assoc Perinat Med Fed Asia Ocean Perinat Soc Int Soc Perinat Obstet* 2016; **29**: 991–997.

195 Man J, Hutchinson JC, Heazell AE, Ashworth M, Levine S, Sebire NJ. Stillbirth and intrauterine fetal death: factors affecting determination of cause of death at autopsy. *Ultrasound Obstet Gynecol Off J Int Soc Ultrasound Obstet Gynecol* 2016; **48**: 566–573.

196 Johnson JT, Hansen MS, Wu I, Healy LJ, Johnson CR, Jones GM *et al.* Virtual Histology of Transgenic Mouse Embryos for High-Throughput Phenotyping. *PLoS Genet* 2006; **2**. doi:10.1371/journal.pgen.0020061.

197 Wong MD, Maezawa Y, Lerch JP, Henkelman RM. Automated pipeline for anatomical phenotyping of mouse embryos using micro-CT. *Dev Camb Engl* 2014; **141**: 2533–2541.

198 Dhenain M, Ruffins SW, Jacobs RE. Three-Dimensional Digital Mouse Atlas Using High-Resolution MRI. *Dev Biol* 2001; **232**: 458–470.

199 Ruffins SW, Martin M, Keough L, Truong S, Fraser SE, Jacobs RE *et al.* Digital Three-Dimensional Atlas of Quail Development Using High-Resolution MRI. *Sci World J* 2007; **7**: 592–604.

200 Lhuaire M, Martinez A, Kaplan H, Nuzillard J-M, Renard Y, Tonnelet R *et al.* Human developmental anatomy: Microscopic magnetic resonance imaging (μMRI) of four human embryos (from Carnegie Stage 10 to 20). *Ann Anat - Anat Anz* 2014; **196**: 402–409.

201 Wong MD, Dorr AE, Walls JR, Lerch JP, Henkelman RM. A novel 3D mouse embryo atlas based on micro-CT. *Development* 2012; **139**: 3248–3256.

202 Gignac PM, Kley NJ. Iodine-enhanced micro-CT imaging: Methodological refinements for the study of the soft-tissue anatomy of post-embryonic vertebrates. *J Exp Zoolog B Mol Dev Evol* 2014; **322**: 166–176.

203 Benoist G, Bessis R, Truong Canh MB, Bohl I, Bouhanna P, Boukobza P *et al.* Recommandations de la CNEOF 2022 – synthèse. *Gynécologie Obstétrique Fertil Sénologie* 2023. doi:10.1016/j.gofs.2023.01.006.

204 Sandrini C, Boito S, Lombardi CM, Lombardi S. Postmortem Micro-CT of Human Fetal Heart—A Systematic Literature Review. *J Clin Med* 2021; **10**: 4726.

205 Meignan P, Binet A, Cook AR, Lardy H, Captier G. Fetal median sacral artery anatomy study by micro-CT imaging. *Surg Radiol Anat* 2018; **40**: 735–741.

206 Benoist G, Bessis R, Truong Canh MB, Bohl I, Bouhanna P, Boukobza P *et al.* Recommandations de la CNEOF 2022 – synthèse. *Gynécologie Obstétrique Fertil Sénologie* 2023; **51**: 221–226.

207 Lamouroux A, Mousty E, Prodhomme O, Bigi N, Le Gac M-P, Letouzey V *et al.* [Absent or hypoplastic thymus: A marker for 22q11.2 microdeletion syndrome in case of polyhydramnios]. *J Gynecol Obstet Biol Reprod (Paris)* 2015. doi:10.1016/j.jgyn.2015.04.015.

208 Man J, Hutchinson JC, Ashworth M, Judge-Kronis L, Levine S, Sebire NJ. Stillbirth and intrauterine fetal death: role of routine histological organ sampling to determine cause of death. *Ultrasound Obstet Gynecol Off J Int Soc Ultrasound Obstet Gynecol* 2016; **48**: 596–601.

209 Simcock IC, Arthurs OJ, Hutchinson JC, Sebire NJ, Jacques TS, Sekar T *et al.* Impact of non-invasive post-mortem micro-CT imaging on a fetal autopsy service: a single centre retrospective study. *Clin Radiol* 2024; **79**: 791–798.

210 Ibarra Vilar P, Jani JC, Cannie MM, Shelmerdine SC, Lecomte S, Verhoye M *et al.* Postmortem imaging of fetuses at early gestations: A comparison of microfocus computed tomography with postmortem magnetic resonance at 9.4 T and postmortem ultrasound. *Prenat Diagn* 2024; **44**: 572–579.

211 Greene RM, Pisano MM. Palate Morphogenesis: Current Understanding and Future Directions. *Birth Defects Res Part C Embryo Today Rev* 2010; **90**: 133–154.

212 Olayiwola JO, Marhabaie M, Koboldt D, Matthews T, Siemon A, Mouhlas D *et al.* Clinically significant findings in a decade-long retrospective study of prenatal chromosomal microarray testing. *Mol Genet Genomic Med* 2024; **12**: e2349.

213 Rafalko J, Soster E, Caldwell S, Almasri E, Westover T, Weinblatt V *et al.* Genome-wide cell-free DNA screening: a focus on copy-number variants. *Genet Med Off J Am Coll Med Genet* 2021; **23**: 1847–1853.

214 Familiari A, Boito S, Rembouskos G, Ischia B, Accurti V, Fabietti I *et al.* Cell-free DNA analysis of maternal blood in prenatal screening for chromosomal microdeletions and microduplications: a systematic review. *Prenat Diagn* 2021; **41**: 1324–1331.

215 Thompson R, Papakonstantinou Ntalis A, Beltran S, Töpf A, de Paula Estephan E, Polavarapu K *et al.* Increasing phenotypic annotation improves the diagnostic rate of exome sequencing in a rare neuromuscular disorder. *Hum Mutat* 2019; **40**: 1797–1812.

216 The 100,000 Genomes Project Pilot Investigator. 100,000 Genomes Pilot on Rare-Disease Diagnosis in Health Care — Preliminary Report. *N Engl J Med* 2021; **385**: 1868–1880.

217 Richards S, Aziz N, Bale S, Bick D, Das S, Gastier-Foster J *et al.* Standards and Guidelines for the Interpretation of Sequence Variants: A Joint Consensus Recommendation of the American College of Medical Genetics and Genomics and the Association for Molecular Pathology. *Genet Med Off J Am Coll Med Genet* 2015; **17**: 405–424.

218 Westenius E, Conner P, Pettersson M, Sahlin E, Papadogiannakis N, Lindstrand A *et al.* Whole-genome sequencing in prenatally detected congenital malformations: prospective cohort study in clinical setting. *Ultrasound Obstet Gynecol Off J Int Soc Ultrasound Obstet Gynecol* 2024; **63**: 658–663.

219 Lord J, McMullan DJ, Eberhardt RY, Rinck G, Hamilton SJ, Quinlan-Jones E *et al.* Prenatal exome sequencing analysis in fetal structural anomalies detected by ultrasonography (PAGE): a cohort study. *The Lancet* 2019; **393**: 747–757.

220 Tran Mau-Them F, Delanne J, Denommé-Pichon A-S, Safraou H, Bruel A-L, Vitobello A *et al.* Prenatal diagnosis by trio exome sequencing in fetuses with ultrasound anomalies: A powerful diagnostic tool. *Front Genet* 2023; **14**: 1099995.

TABLES AND FIGURES

Figure GI.1 – Ultrasound scan at 12+1 weeks of gestation (WG) highlighting crown-rump length (CRL) and nuchal translucency measurement as well as morphological evaluation of cephalic pole with plexus choroids, heart using colour doppler, femoral length and foot (Dr Lamouroux) 12

Figure GI.2 – Ultrasound scan using 3D imaging at 12+6 weeks of gestation (Dr Lamouroux) 12

Figure GI.3 – Illustrative clinical case of a fetal post-mortem examination A- Prenatal ultrasound imaging (2D and 3D) at 25+5 weeks of gestation (WG) highlighting suspected arthrogryposis with reduced fetal movements and bilateral club feet. Further assessment at 27+1 WG highlighted severe camptodactyly (Dr Frédéric Richard) B- External examination confirming arthrogryposis. (Dr Audrey Lamouroux) C- Macroscopic neuropathological examination revealing porencephaly (black arrow) and unilateral ventriculomegaly (white arrowhead) (Dr Constance Wells) This phenotype prompted whole-exome sequencing, which identified a probably pathogenic variant (ACMG class 4) in the *HECW2* gene, known to cause neurodevelopmental disorder with hypotonia, seizures, and absent language..... 15

Table I.1 – Four terms used to describe the different post-mortem investigational approaches. 23

Figure I.1 – Coronal post-mortem iodinated Micro-CT image of 15-weeks' gestation fetus, resolution 60μm (A), axial images at the level of the ventricles of the brain (B), and heart (C) and the liver (D) demonstrating the high-resolution imaging Micro-CT provides for early gestation pregnancy losses. Figure adapted from Shelmerdine et al. 2020 with permission[60,61,66,69,113,118,122,141,143–146,148,149] 26

Figure I.2 – (A) Volume rendered a 3-dimensional image of a 7-weeks' gestation embryo demonstrating early eyelid and external ear development along with individual digits of the hand and toe notches. (B) A sagittal post-mortem Micro-CT of the same embryo at 9.7 μm with (C) corresponding histopathological section stained with haematoxylin and eosin staining demonstrating the equivalent internal detail attainable with both Micro-CT and histopathology. Figure adapted from Shelmerdine et al.2018 with permission[66]..... 27

Figure I.3 – Iodination of the fetus occurs as iodine solution diffuses towards the interior of the fetus over time as demonstrated by (a) pre-iodination, (b-d) progressive iodination seen with iodination from the external surface of the fetus towards the centre, until (e) full iodination occurs. Figure adapted from Docter et al. 2022 with permission [117]..... 28

Figure I.4 – A 14- weeks' gestation fetus (a) having been refrigerated post-delivery, (b) following immersion in a mixture of potassium tri-iodide solution and 10% formalin to achieve fixation and full iodination where the skin is stained a darker shade, and (c) following immersion in thiosulphate solution prior to being returned to the parents, where the skin colour is returned to close to its original colour. 29

Figure I.5 – Coronal slices demonstrating the high-resolution imaging possible of internal anatomy including liver and stomach (a and c) and primary bronchi and lungs (b and

d) for both Micro-CT (a and b) and high-field MRI 7T (c) and 3T (d). Figure adapted from Dawood et al. 2021 with permission[62]. 31

Figure I.6 – A demonstration of when Micro-CT and high-field MRI can provide superior imaging for early gestation fetuses relative to other imaging modalities. Figure adapted from Shelmerdine et al. 2021 with permission[128]. 34

Figure I.7 – A stepwise flowchart for non-invasive investigation of perinatal loss including options for Micro-CT and high-field MRI. Figure adapted from Shelmerdine et al. 2021 with permission[128]. 34

Table II.1 – Inclusions in the FETTAL Project since 2016 with their characteristics and their corresponding numbers in the different studies 38

Table II.2.1 – Staining protocols analysed in this study published by Metscher[173,174], by Owen Arthurs' teams [60,61,66,68,69,144], by Lombardi et al.[143,145], and by Vymazalovà et al.[175] (E = ethanol; FA = formaldehyde; I2 = iodine; PFA = paraformaldehyde; PTA = phosphotungstic acid; stage = Carnegie stage; WG = weeks of gestation). 40

Table II.2.2 – Qualitative and quantitative comparisons of the studied staining protocols (CRL = crown-rump length; SNR = signal to noise ratio; CNR = contrast to noise ratio). 40

Figure II.2.1 – Evaluation grids of Micro-CT volume rendering and slice images for samples S1, S2 and S3 used for the qualitative comparison by experts (CRL = crown-rump length; WG = weeks of gestation). 43

Figure II.2.2 – Micro-CT volume rendering and slice images of sample S4 highlight important soft tissue shrinkage after staining with protocol P2. 44

Table II.3 – Samples characteristics (crown-rump length CRL, weight et gestational age), Micro-CT preparation (staining duration) and acquisition details (filter, voltage and current) and contrast-to-noise ratio (CNR) between lung and liver (WG = weeks of gestation, SD = standard deviation). 50

Figure II.3.1 – Dynamic representation of contrast agent diffusion in sample S0 (female sex; CRL = 80 mm, interparietal diameter = 14 mm, foot length = 14 mm, weight 30,06 g, 13+4 WG) as a function of the staining time using Micro-CT imaging. The upper, middle and lower panels depict cerebral, thoracic, and abdominal sections of the sample, respectively. 52

Supplemental material II.3.1 – Video - Time-lapse visualization of the contrast agent uptake in the Micro-CT cerebral section of sample S0 (female sex; CRL = 80 mm, interparietal diameter = 14 mm, foot length = 14 mm, weight 30,06 g, 13+4 WG). This video demonstrates the dynamic diffusion process within the brain structures over the staining duration. 52

Supplemental material II.3.2 – Video - Time-lapse visualization of the contrast agent uptake in the Micro-CT torso section of sample S0 (female sex; CRL = 80 mm, interparietal diameter = 14 mm, foot length = 14 mm, weight 30,06 g, 13+4 WG). The video highlights the staining progression in the thoracic region, including the cardiac chambers and major thoracic organs, as a function of time. 52

Supplemental material II.3.3 – Video - Time-lapse visualization of the contrast agent uptake in the Micro-CT abdominal section of sample S0 (female sex; CRL = 80 mm, interparietal diameter = 14 mm, foot length = 14 mm, weight 30,06 g, 13+4 WG).

This video demonstrates the dynamic diffusion process over the staining duration focusing on abdominal organs such as the liver, spleen, stomach, and adrenal glands. 52

Supplemental material II.3.4 – Figure – Time-dependent decay of the contrast agent in various sections of the staining bath using Micro-CT imaging. The decay is expressed in arbitrary units (au) and plotted against the staining duration, illustrating the reduction in iodine concentration in the bath over time. 53

Figure II.3.2 – Time-dependent uptake of the contrast agent in various target fetal (top graph) and in the lung and liver (peripheral in **a**, central in **b** and hilum in **c**) using Micro-CT imaging. The uptake is measured in arbitrary units (au) over the staining duration. 54

Table II.3.2 – Diffusion characteristics of the iodine solution in the target organs based on Weibull distribution and stretched exponential Models using Micro-CT imaging. The stretched exponential function $S(t) = A0 + Amax1 - exp - t - t0\lambda\beta$ where A_0 is the initial amplitude or baseline value of the signal, A_{max} is the maximum change, t_0 represents the starting time, λ is the characteristic time scale, and β is the stretching exponent[20]. 54

Figure II.3.3 – Scatter plot illustrating the correlation between fetal crown-rump length (CRL) in millimetres and fetal weight in grammes, respectively, and staining duration in hours to performed before micro-CT imaging. Data points are colour-coded based on the Contrast-to-Noise Ratio (CNR), with a gradient ranging from red (low CNR) to dark green (high CNR). The dotted line indicates the threshold where the CNR reaches 5, in accordance with the Rose criterion[187]. ***Staining duration = 2CRL - 12 = 2weight + 12.5*** 56

Figure III.1.1 – Comparison between fetal pathological examination and very early virtual autopsy (HF-MRI: high-field MRI). 60

Table III.1.1 – Detailed contrast bath protocols used before micro-CT imaging. (PFA 4%: paraformaldehyde 4%; I2KI: iodine potassium iodide 10% solution, dice: diffusible iodine-based contrast enhanced) 63

Table III.1.2 – Specimens included in the present study with their detailed characteristics, their preparation before micro-imaging, the type of micro-imaging performed and micro-imaging acquisition parameters. (WG: weeks of gestation). 65

Figure III.1.2 – Flowchart with detailed cohort selection (CRL: crown–rump length; FETTAL: Fetal Enhanced Three-dimensional and Translational Anatomical Landscape project) 67

Figure III.1.3 – Micro-CT sagittal slice after protocol 4 (early fixation without any contrast bath) and protocol 5 (early fixation and 72hr immersion in contrast bath 1:1 ratio of PFA 4% and I2KI/Lugol's iodine made freshly) on specimen S9 (WG: weeks of gestation, CRL: crown–rump length). Using DataViewer (CT) software. (1: tongue; 2: oesophagus; 3: trachea; 4: ascending aorta arch; 5 descending aorta) 67

Figure III.1.4 – Sagittal view of 6 specimens with both micro-CT after protocol 5 (early fixation and 72hr immersion in contrast bath 1:1 ratio of PFA 4% and I2KI/Lugol's iodine made freshly) and HF-MRI (high-field MRI) using DataViewer (CT) and Myrian (MRI) software (WG: weeks of gestation, CRL: crown–rump length). 68

Figure III.1.5 – Specimens S5 and S8 with both micro-CT after protocol 5 (early fixation and 72hr immersion in contrast bath 1:1 ratio of PFA 4% and I2KI/Lugol's iodine made freshly) and HF-MRI (high-field MRI) in different slices matched with inter orbital distance view, four-chamber view with pulmonary veins, transversal-kidney view from the CNEOF French guidelines group[203] using DataViewer (CT) and Myrian (MRI) software. 69

Figure III.1.6 – Quantitative signal evaluation of specimens S5 and S8 using signal to noise (SNR) and contrast to noise (CNR) ratio. Arrowheads highlight crystalline lens (CL), right ventricular wall (RVW) and renal cortex (RC) and round tip arrows highlight vitreous body (VB), pericardium (PC) and perinephric fat (PNF). 70

Figure III.1.7 – Specimen S1 sagittal slice with micro-CT after protocol 5 (early fixation and 72hr immersion in contrast bath 1:1 ratio of PFA 4% and I2KI/Lugol's iodine made freshly), HF-MRI (high-field MRI) and histology in hematoxylin eosin and CD34 immunohistochemical staining using DataViewer (CT) and Myrian (MRI) software (WG: weeks of gestation, CRL: crown–rump length). 71

Table III.2.1 – Specimen characteristics, micro-imaging preparation and acquisition settings (WG: weeks of gestation; CRL: crown-rump length; BPD: biparietal diameter; M: male ; F: female ; MCT: micro-CT; HF-MRI: high field MRI)..... 77

Figure III.2.1 – Flowchart of the samples included in this study from the FETTAL project 78

Figure III.2.2 – Cephalic sagittal sections using micro-CT (MCT) and high-field MRI (HF-MRI) of human fetuses aged of 12+3 to 12+6 weeks of gestation (WG) with a crown-rump length (CRL) of 61 to 68 mm.(M: male ; F: female) 79

Figure III.2.3 – Dice Micro-CT and high-field MRI imaging of female human fetus S4 at 12+4 weeks of gestation with a crown-rump length of 64 mm. Cephalic ultrasound referenced sections: biparietal (highlighting thalamic nucleus, septum pellucidum), posterior fossa, median sagittal and interorbital. 80

Figure III.2.4 – Dice Micro-CT and high-field MRI images of male human fetus S3 at 12+4 weeks of gestation with a crown-rump length of 63 mm. Ultrasound-referenced sections of the torso (four chamber view, three vessels view, pulmonary artery around aorta) and of the abdomen (abdominal circumference, transverse view of the kidneys). 80

Figure III.2.5 – Dice Micro-CT and high-field MRI imaging of male human fetus S3 at 12+4 weeks of gestation with a crown-rump length of 63 mm. Ultrasound-referenced sections of the medullary canal in median sagittal view, of the parasagittal diaphragm with the stomach and transverse view of both femora..... 81

Figure III.2.6 – Discrepancy in the measurement of CRL between external examinations conducted with a Vernier calliper and those derived from imaging-based techniques using Micro-CT and HF-MRI. 82

Table III.2.2 – Organ's biometry means, and standard deviation obtained using Micro-CT and HF-MRI to explore 12WG human fetus (TD = transversal diameter, AP = anteroposterior). 83

Figure IV.1 – Number of Micro-CT imaging cases performed per year according to the subgroup (Key – dark bars – In utero deaths (IUD); grey bars – miscarriage or ToP for SROM; white bars – ToP for fetal malformation or other reason). 92

Table IV.1 – Referral pattern and demographics, including gender, parental ethnicity, estimated gestation, fetal measurements and maceration score by subgroup (ToP termination of pregnancy, SROM spontaneous rupture of membranes) 93

Table IV.2 – Turnaround times: Birth to receipt of the baby reflects the time taken for the baby to arrive at our centre, with all other intervals referenced to the day of referral. (ToP termination of pregnancy, SROM spontaneous rupture of membranes, Q1 Q3 first and third quartile, Iodination means being placed in iodine) 94

Figure IV.2 – Post-mortem examination by parental consent vs type of post-mortem performed, categorised by subgroup (IUD, miscarriage, ToP). Key: dark squares = full autopsy; grey = minimally invasive autopsy MIA or less invasive autopsy approaches; white = external examination only 95

Table IV.3 – Contribution of Micro-CT to the final diagnosis image quality and abnormalities identified, by subgroup (ToP termination of pregnancy, SROM spontaneous rupture of membranes). 96

Figure IV.3 – Axial Micro-CT image of a 13 weeks' gestation fetus demonstrating ventricular septal defect (arrow) in a moderately macerated fetus. Note reduced overall greyscale and loss of tissue boundaries caused by maceration. 97

Figure IV.4 – Axial and coronal Micro-CT of renal abnormalities: this case at 14 weeks gestation was diagnosed antenatally with malrotated kidneys (A, C), with the isthmus of a horseshoe kidney demonstrated on Micro-CT (B, D). 97

Figure IV.5 – Axial and coronal Micro-CT of renal abnormalities: this case at 13 weeks' gestation demonstrated grossly enlarged urinary bladder (closed white arrow; megacystis) with unilateral right kidney which showed hydronephrosis (open white arrows). 98

Figure IV.6 – Flow-chart presenting the relative contribution of each part of the PM examination, either sole contribution or contribution with other factors. 99

Table IV.4 – Contribution from post-mortem examination (PME) to the final diagnosis and cause of death determination, by subgroup (ToP termination of pregnancy, SROM spontaneous rupture of membranes) 100

Figure GD – The development of the tongue, palate, and mandibles visualized through micro-CT segmentation (Myrian software) 107

ANNEXE 1

Simcock IC, Lamouroux A, Sebire NJ, Shelmerdine SC & Arthurs OJ.

Less-invasive autopsy for early pregnancy loss.

Prenatal Diagnosis 2023. Jun 1;43(7):937–49.

Check for updates

Received: 22 February 2023 | Revised: 20 April 2023 | Accepted: 21 April 2023

DOI: 10.1002/pd.6361

REVIEW

PRENATAL DIAGNOSIS WILEY

Less-invasive autopsy for early pregnancy loss

Ian C. Simcock[1,2,3] | Audrey Lamouroux[1,4,5,6] | Neil J. Sebire[2,3,7] | Susan C. Shelmerdine[1,2,3] | Owen J. Arthurs[1,2,3]

[1]Department of Clinical Radiology, Great Ormond Street Hospital for Children, London, UK

[2]UCL Great Ormond Street Institute of Child Health, Great Ormond Street Hospital for Children, London, UK

[3]NIHR Great Ormond Street Hospital Biomedical Research Centre, London, UK

[4]Obstetrical Gynaecology Department, Nîmes University Hospital, Nîmes, France

[5]Clinical Genetics Department, Montpellier University Hospital, Montpellier, France

[6]ICAR Research Team, LIRMM, CNRS and Charles Coulomb Laboratory, UMR 5221 CNRS-UM, BNIF User Facility Imaging, University of Montpellier, Nîmes and Montpellier, Montpellier, France

[7]Department of Histopathology, Great Ormond Street Hospital for Children, London, UK

Correspondence

Ian C. Simcock, Department of Clinical Radiology, Paediatric Clinical Academic Radiographer, Great Ormond Street Hospital for Children, London, UK.
Email: ian.simcock@gosh.nhs.uk

Funding information

Nimes and Montpellier University Hospital Mobility Grant; Programme Grants for Applied Research, Grant/Award Numbers: ICA-CDRF-2017-03-53, NIHR-301322, NIHR-CDF-2017-10-037, NIHR302390

Abstract

Autopsy investigations provide valuable information regarding fetal death that can assist in the parental bereavement process, and influence future pregnancies, but conventional autopsy is often declined by parents because of its invasive approach. This has led to the development of less-invasive autopsy investigations based on imaging technology to provide a more accessible and acceptable choice for parents when investigating their loss. Whilst the development and use of more conventional clinical imaging techniques (radiographs, CT, MRI, US) are well described in the literature for fetuses over 20 weeks of gestational age, these investigations have limited diagnostic accuracy in imaging smaller fetuses. Techniques such as ultra-high-field MRI (>3T) and micro-focus computed tomography have been shown to have higher diagnostic accuracy whilst still being acceptable to parents. By further developing and increasing the availability of these more innovative imaging techniques, parents will be provided with a greater choice of acceptable options to investigate their loss, which may in turn increase their uptake. We provide a narrative review focussing on the development of high-resolution, non-invasive imaging techniques to evaluate early gestational pregnancy loss.

Key points

What's already known about this topic?

- Autopsy investigations provide valuable information regarding fetal death that can help parental bereavement and influence future pregnancies.
- Conventional invasive autopsy is often declined by parents.
- Less-invasive autopsy investigations provide a wider and more acceptable choice for parents.

What does this review add?

- Conventional clinical imaging techniques (radiographs, CT, MRI, US) have limited accuracy in imaging smaller fetuses below 20 weeks of gestational age.
- High-field MRI and micro-CT are the most useful post-mortem imaging techniques following early pregnancy fetal loss.

This review has not been published at any conferences.

This is an open access article under the terms of the Creative Commons Attribution License, which permits use, distribution and reproduction in any medium, provided the original work is properly cited.

© 2023 The Authors. Prenatal Diagnosis published by John Wiley & Sons Ltd.

- More widespread availability of these techniques will help parents access the most appropriate and acceptable investigations following pregnancy loss.

1 | INTRODUCTION

Pregnancy loss is a common event with an estimated 23 million miscarriages (<24 weeks gestation) and nearly 2 million stillbirths (>24 weeks gestation) occurring worldwide every year.[1,2] These numbers are increasing and could be far higher as many women may not present to the health services and data is therefore often based on approximate estimates.[3–5]

Any pregnancy loss can be traumatic for the family and can lead to prolonged grief, depression, anxiety, and post-traumatic stress, with effects possibly lasting for several years.[6–10] Alongside this, miscarriage is little understood by both the general public and healthcare professionals and has been recognised as an under investigated area of medicine.[1,11] Compounding these issues around awareness, parents often believe that they are somehow at fault, which can stop them seeking help and support from healthcare professionals, preventing the true number of miscarriages in the community to be identified.[4,12] In this traumatic context, the delivery of information and its reception by the couple is particularly challenging. Therefore, providing support and a supportive environment where families can make an informed and appropriate choice for themselves is key.

Investigating the possible causes of pregnancy loss has multiple advantages including guiding future pregnancies and advancing medical knowledge,[13–15] but helping bereaved parents understand the implications of their choices at this difficult time can be extremely challenging.[16] Staff training is key to imparting complex information at this difficult time, and experience and guidance in this area for the staff is important to clearly convey key complex information.[14,17] This training should come in differing formats including formal courses, case discussions, and involvement in multidisciplinary meetings to raise awareness of the impact autopsy, and alternative less invasive investigations can make.[17,18]

2 | HISTORICAL BACKGROUND

Conventional autopsy (CA) is the traditional reference standard investigation into pregnancy loss and consists of multiple investigations also called feto-placental examination including a review of the clinical history, an external examination with photography, internal macroscopic examination and histological analysis, tissue sampling for genetic testing and macroscopic/microscopic examination of the placenta.[15,19] Together these investigations provide new clinical information in 40%–70% of cases, depending on the clinical question to be answered.[15,20–22]

Most perinatal and fetal autopsies are carried out with parental consent for diagnostic purposes, rather than being directed by the coroner/medical examiner for forensic purposes. Involving parents in the decision-making process is essential to increase uptake rates and provide care for the families.[13,23] Some parents choose conventional autopsy as the "reference standard" or maximum level of investigation possible as they wish to be sure they have excluded all possible causes for their loss,[15,24] but this may not be appropriate for all cases: there remains a significant proportion of pregnancy losses where the cause is still 'undetermined' despite full investigation.[15,25,26] Others decline all autopsy investigations as they wish to avoid 'further harm' to their child and are not prepared to undergo a more mental turmoil at this challenging time but can later regret this decision.[14,16,24,27,28]

Parents choose to investigate their loss for multiple reasons, including to understand their child's death more fully,[29] the recurrence risk of future pregnancies,[30] to advance scientific knowledge,[31] for a degree of 'closure' after their loss[32] and to rule out self-blame[15,24]

However, autopsy uptake has been declining for many years[10,17,22,33–37] with parental reasons for declining including wishing to protect the baby, practical aspects over transfer to a specialist hospital, misconceptions regarding the benefits of autopsy, poor communication between families and healthcare professionals, uncertainty about the value of the procedure, a mistrust of the hospital system, religious and personal beliefs, and the invasiveness of the procedure.[10,14,38,39] Added to this, there is now a relatively small number of specialist paediatric pathologists (relative to the number of deaths to be investigated[40]), meaning that access to specialist paediatric pathology services in the UK is becoming less accessible.

To challenge the declining consent rate, less-invasive autopsy (LIA) techniques, such as laparoscopic examination of the internal organs through smaller incisions or imaging techniques alone, have been developed in recent years, providing a greater and more acceptable choice to parents.[10,13,14,27,28,37,39,41–44] Significant challenges remain in identifying the cause of fetal demise <20 weeks gestational age (GA) or <500 g, as routine imaging techniques (magnetic resonance imaging (MRI), computed tomography (CT), ultrasound, radiographs) cannot provide sufficient resolution, tissue contrast, or soft tissue detail.[41,45–49] It should also be noted that identifying abnormalities in early gestation through CA also remains challenging.[47,48,50–57] Several terms are commonly used to describe the different post-mortem approaches towards diagnosis, and it is important to understand the investigations each term refers to and what can be achieved (Table 1).

In this narrative review article, we aim to focus on the development of high-resolution, non-invasive imaging techniques to identify the possible causes of early pregnancy loss in this challenging area. We defined up to 20 weeks as "early" gestation but clarified it according to the published literature. Articles published in the last

10970223, 0, Downloaded from https://obgyn.onlinelibrary.wiley.com/doi/10.1002/pd.6361 by Bib Montpellier, Wiley Online Library on [10/05/2023]. See the Terms and Conditions (https://onlinelibrary.wiley.com/terms-and-conditions) on Wiley Online Library for rules of use; OA articles are governed by the applicable Creative Commons License

10970223, 0, Downloaded from https://obgyn.onlinelibrary.wiley.com/doi/10.1002/pd.6361 by Bib Montpellier, Wiley Online Library on [10/05/2023]. See the Terms and Conditions (https://onlinelibrary.wiley.com/terms-and-conditions) on Wiley Online Library for rules of use; OA articles are governed by the applicable Creative Commons License

TABLE 1 Four terms used to describe the different post-mortem investigational approaches.

Key terminology				
Term	**Explanation**	**Includes**	**Histology**	**Genetics**
Conventional autopsy	Collection of investigations and gold standard for identifying the cause of fetal demise	Review of the clinical history, external examination with photographs, internal macroscopic examination and placental examination	Yes, all target organs as recommended in guidelines of the Royal College of Pathologists	Tissue samples from target organs for genetic testing
Less-invasive autopsy	Umbrella term including any autopsy procedure (CA or imaging) that is performed with smaller, less or no incisions than CA	Minimally invasive autopsy, non-invasive autopsy and placental examination	Yes, most organs with focal biopsy via minimally invasive autopsy approach	Tissue samples from target organs for genetic testing
Minimally invasive autopsy	Combination of imaging investigations, utilizes smaller incisions than for CA	Laparoscopic or image-guided needle-biopsy approach and placental examination	Yes, most organs with focal biopsy	Tissue samples from target organs for genetic testing
Non-invasive autopsy	Imaging only, no incisions required	External examination, placental examination and all non-invasive imaging investigations	No histology available	No genetic testing available

15 years were identified in December 2022. As there is no definitive gestation related to many of the investigations described, we aim to include 20 weeks, but will identify specific gestations where the literature allows. Articles were identified in December 2022 through a search of MEDLINE and PubMed using a Boolean search strategy with word variations relating to 'autopsy', 'conventional', less-invasive', minimally invasive', 'non-invasive', 'imaging', 'early gestation', and 'fetus'.

3 | CONVENTIONAL CLINICAL IMAGING TECHNIQUES

3.1 | Post-mortem radiographs

Fetal post mortem radiographs (PMXR) are cheap, quick, widely available, easy to perform, and largely used to estimate gestational age and assess the developing skeleton.[47] As most skeletal dysplasias and abnormalities are now typically identified through ante-natal ultrasound,[58] PMXR of all fetuses has been shown to add diagnostically useful information in less than 1% of routine cases.[59] Whilst PMXR is diagnostic in suspected skeletal dysplasia, improvements in antenatal diagnosis mean that these abnormalities are being detected earlier at earlier gestations, when the bones are less ossified, and therefore PMXR are less discriminatory.[60–62]

3.2 | Post-mortem computed tomography

Post-mortem computed tomography (PMCT) is also widely available, cheap, and quick to perform[47,63] but the combination of small size and poor soft-tissue contrast limits its diagnostic ability in small fetuses.[56,64,65] Although PMCT angiography can increase the soft tissue contrast, large validation studies are still required.[56,66,67] PMCT can also provide information on dysplasia imaging through 3D reconstructions, but with limited additional diagnostic utility due to limited ossification at early gestation negating this advantage in early pregnancy.[56]

3.3 | Post-mortem magnetic resonance imaging (1.5 and 3T)

Post-mortem magnetic resonance imaging (PMMRI) is widely available and provides excellent soft-tissue information. However, due to the increasing clinical pressures combined with the time required to perform detailed PMMRI (approx. 60 min),[52,68] there is often difficulty in accessing these scanners for post-mortem imaging.

The main challenge for PMMRI at field strengths below 3T is the low spatial resolution and subsequent difficulty in visualising structures in <20 weeks GA due to poor tissue contrast and low signal-to-noise.[41,45,52–54,69] PMMRI at 3T field strength provides fewer non-diagnostic scans than 1.5T for fetuses <20 weeks GA through better image contrast, with higher sensitivity (34.6% vs. 17.3%)), specificity (65.1% vs. 45.3%), and concordance (55.1% vs. 36.1%) with CA.[52] Field strengths above 3T have reported further improvement for fetuses <20 weeks gestation.[49,57,70] Soft tissue contrast and signal-to-noise ratio (SNR) can be improved through immersion of smaller fetuses in a Gadolinium/formaldehyde solution prior to scanning at 3T, but this technique has not been optimised for clinical use.[50] Overall, conventional PMMRI has limited diagnostic accuracy below 20 weeks gestation.[41,52,71,72]

3.4 | Post-mortem ultrasound

Post-mortem ultrasound (PMUS) may be a suitable alternative when cross-sectional imaging techniques are less available. It can provide information on a wide array of body systems including the head, neck, spine, cardiac and vascular imaging, thorax and abdomen, musculoskeletal and soft tissue malformations.[73]

It may also be better understood by parents when consenting for post-mortem imaging having already undergone ante-natal ultrasound scanning and is also unaffected by tissue fixation.[61,72,74–77] PMUS also has the advantage of being able to direct needle biopsies for tissue sampling.[47,73,78–81] However, PMUS is operator-dependent, requiring specialist training to develop the skills and experience to accurately identify possible causes of pregnancy loss in these smaller fetuses.[47,51,61,74]

A high-resolution linear or curvilinear probe is advised given the small fetal size. The loss of normal live tissue rigidity can lead to slumping and difficulty maintaining contact with the ultrasound probe, and so a 'water bath' technique has been described, where the whole fetus is fully immersed within a cold, still water bath with a gel stabilising pad.[74] Alternatively, ultrasound transmission gel can be used to generate a stand-off, although cleaning the body afterwards is more challenging and may lead to fungal growth in residual gel.[61]

Although relatively high sensitivities and specificities have been reported from multiple studies (ranging from 73% to 97%, similar to 1.5T PMMR), most studies have found lower diagnostic rates and higher yield of non-diagnostic imaging in fetuses below 20 weeks gestation.[51,61,72,75,76]

4 | HIGHER RESOLUTION IMAGING

More advanced post-mortem imaging techniques including High-field (HF) PMMRI and Micro-focus Computed Tomography (micro-CT) imaging[50,71,82,83] have been developed for early fetal loss, primarily to address the combined issues of poor resolution, and low signal and contrast-to-noise ratios.[41,46,49,55,57,61,71,72,82,84–88]

4.1 | Micro-focus computed tomography

Micro-CT provides non-invasive micron-level resolution imaging (Figure 1), with increased spatial resolution as fetal size decreases (Figure 2), making it ideal for early GA pregnancy loss and providing isotropic datasets which can be reconstructed for visualisation in different planes.[41,57,83–85,88–95]

To provide adequate soft tissue contrast, however, an exogenous contrast agent is required, typically potassium tri-iodide (I_2KI), which stains the soft tissue through cellular diffusion.[46,83,85] Sufficient time must be allowed for complete diffusion, which can take several days or weeks and is dependent on the size of the fetus (Figure 3).[83,85,89,96,97]

One downside is that concentrated I_2KI may result in tissue distortion, although this can be minimised by using a buffered solution.[46,71,85,86,98] Endovascular staining using various contrast agents has also been investigated[99–101] and may offer opportunities to iodinate larger fetuses in a reduced timeframe in the future.[46]

Iodination can cause visible darkening of the fetus, which should be discussed with parents during the consent process and may be initially undesirable but can be partially reversed by sodium thiosulphate solution (Figure 4).[46,83] This does not necessarily remove the iodine from all body tissues; however, in many cases, it is sufficient to just de-stain the skin for cosmetic purposes prior to returning the body to the parents.

Micro-CT has shown a high level of agreement with CA across multiple organ systems for 11 and 21 weeks GA of 21 fetuses, with overall sensitivities and specificities of 93.8% and 100%. Although non-diagnostic rates were higher for <14 weeks GA than above (12% vs. 4.7%), there were fewer non-diagnostic indices <14 weeks GA, with higher positive predictive values, 97.3% versus 85.7%.[88]

A large study analysing 268 micro-CT scans (GA 11–24 weeks) demonstrated that sensitivity and specificity were 92.3% and 98%, respectively, for fetuses up to 24 weeks GA, and pathologists deemed invasive autopsy unnecessary in 86.9% of cases.[84]

Maceration, the breakdown of tissue structure due to immersion within a fluid filled cavity (amniotic fluid) combined with autolysis following fetal demise, is a major challenge in identifying the cause of early pregnancy loss both through imaging and CA.[25,70,79,103] Through the late diagnosis of a miscarriage and a delay between fetal demise, identifying pregnancy loss and delivery of the fetus, it is exposed to an often unknown intra-uterine retention time. Maceration affects many early pregnancy losses and can affect the accuracy of PMUS even within 48 h, with between 25% and 40% of scans becoming non-diagnostic due to severe maceration.[51,72,78,79,104–106] Equally, in-utero maceration deteriorates image quality for micro-CT, yet high quality is still possible in over 95% of cases despite the presence of a range of maceration states.[102]

Micro-CT can also be used as an adjunct to CA providing high resolution imaging of excised organs, for example, of the kidney,[107] brain[92] and heart.[57,93,94,108] Diagnostic accuracy of ex-vivo imaging is also high, for example, for congenital heart disease equal to CA and superior for smaller specimens[108] and has been used to assess cardiac anatomy between 8−13 weeks GA to validate prenatal diagnosis following TOP for cardiac anomalies.[57]

One practical limitation of micro-CT is that due to the high-resolution of the technique, the data files are large (approximately 50 GB per clinical patient) requiring large provision of storage for clinical use relative to other suitable techniques (ultra-high-field PMMRI <1GB per patient).[83,85]

Overall, due to the relative higher-resolution, low cost, and quick scan times, micro-CT has clear advantages[71] and is an excellent alternative to CA.[48,57,84] It can be used to create detailed scale 3D models or augmented virtual reality to aid parental counselling and

10970223, 0, Downloaded from https://obgyn.onlinelibrary.wiley.com/doi/10.1002/pd.6361 by Bib Montpellier, Wiley Online Library on [10/05/2023]. See the Terms and Conditions (https://onlinelibrary.wiley.com/terms-and-conditions) on Wiley Online Library for rules of use; OA articles are governed by the applicable Creative Commons License

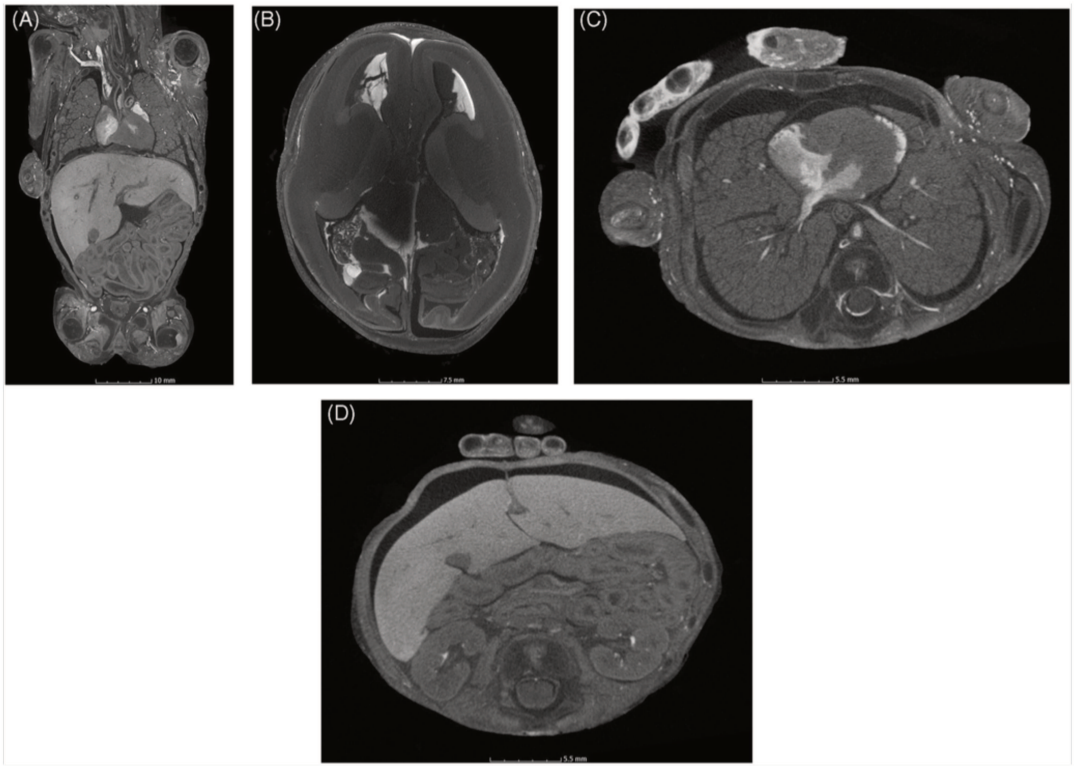

FIGURE 1 Coronal post-mortem iodinated micro-CT image of a 15-week gestation fetus, resolution 60 μm (A), axial images at the level of the ventricles of the brain (B), and heart (C) and the liver (D) demonstrating the high-resolution imaging micro-CT provides for early gestation pregnancy losses. Figure adapted from Shelmerdine et al. 2020 with permission.[48]

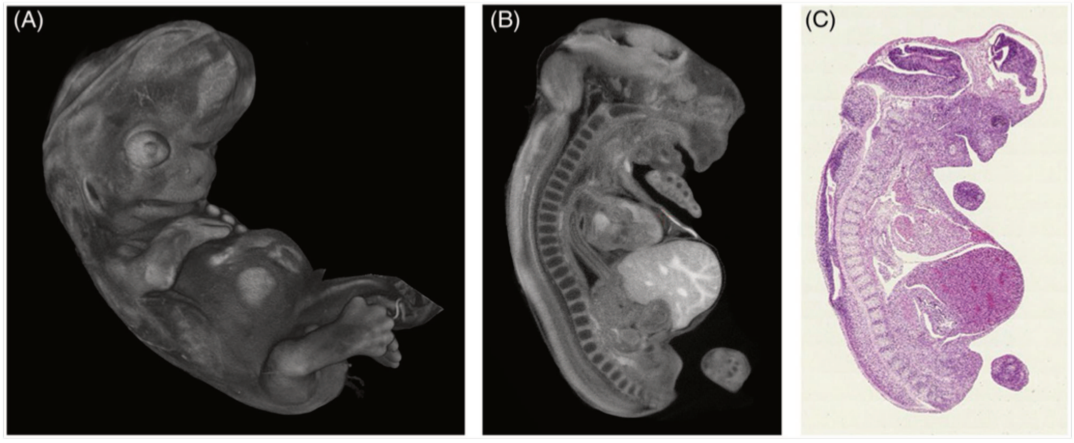

FIGURE 2 (A) Volume rendered a 3-dimensional image of a 7-week gestation embryo demonstrating early eyelid and external ear development along with individual digits of the hand and toe notches. (B) A sagittal post-mortem micro-CT of the same embryo at 9.7 μm with (C) corresponding histopathological section stained with haematoxylin and eosin staining demonstrating the equivalent internal detail attainable with both micro-CT and histopathology. Figure adapted from Shelmerdine et al. 2018 with permission.[91]

10970223, 0, Downloaded from https://obgyn.onlinelibrary.wiley.com/doi/10.1002/pd.6361 by Biu Montpellier, Wiley Online Library on [10/05/2023]. See the Terms and Conditions (https://onlinelibrary.wiley.com/terms-and-conditions) on Wiley Online Library for rules of use; OA articles are governed by the applicable Creative Commons License

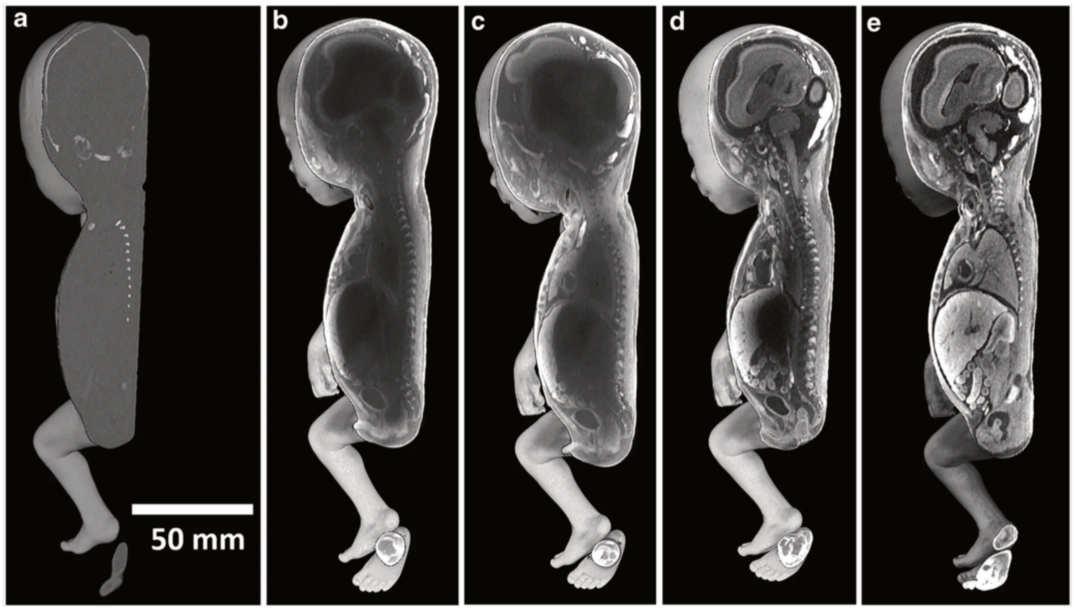

FIGURE 3 Iodination of the fetus occurs as an iodine solution diffuses towards the interior of the fetus over time as demonstrated by (A) pre-iodination, (B-D) progressive iodination seen with iodination from the external surface of the fetus towards the centre, until (E) full iodination occurs. Figure adapted from Docter et al. 2022 with permission.[46]

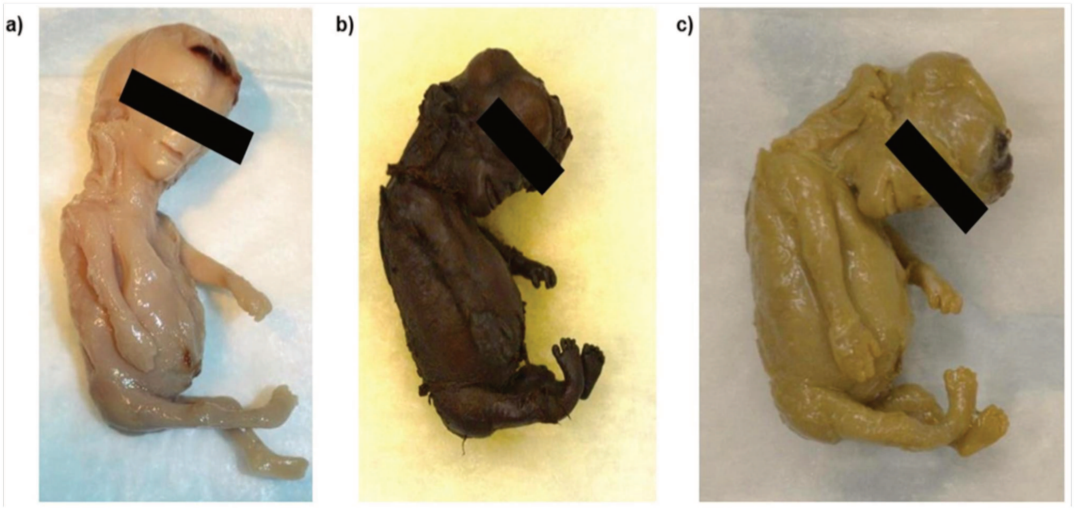

FIGURE 4 A 14- week gestation fetus (A) having been refrigerated post-delivery, (B) following immersion in a mixture of potassium tri-iodide solution and 10% formalin to achieve fixation and full iodination where the skin is stained a darker shade, and (C) following immersion in thiosulphate solution prior to being returned to the parents, where the skin colour is returned to close to its original colour.

10970223, 0, Downloaded from https://obgyn.onlinelibrary.wiley.com/doi/10.1002/pd.6361 by Biu Montpellier, Wiley Online Library on [10/05/2023]. See the Terms and Conditions (https://onlinelibrary.wiley.com/terms-and-conditions) on Wiley Online Library for rules of use; OA articles are governed by the applicable Creative Commons License

education of congenital anomalies/fetal development,[41,57,83–85,88–95,109] with a range of fetal gestations scanning from 6 weeks[87] to 24 weeks[84] with relatively short scanning times.[83]

4.2 | Ultra-high-field post-mortem magnetic resonance imaging

Despite the numerous studies and multiple technical advances in recent years, the main disadvantage for PMMRI is the low image quality below <20 weeks GA or 300 g.[49,70,110] To overcome this, HF-MRI (7T and above) offers a significant increase in the SNR which can either improve the resolution or decrease the scan time, whilst also offering superior soft tissue contrast, whilst reducing the complexity of introducing an exogenous contrast agent.[55,70,85,110–112]

HF-MRI images are able to accurately identify anatomical structures, particularly of the heart, below 20 weeks GA[49] albeit with a lower resolution than seen with micro-CT (137 μm in HF-MRI vs. 22 μm in micro-CT),[71] whilst a high concordance between HF-MRI and CA is seen for a range of anatomical structures with sensitivity (94.6%), specificity (97.6%) and positive and negative predictive values respectively (93% and 98.2%).[112] One study comparing CA with 9.4 and 1.5T PMMRI of the brain demonstrated that CA provided no additional information to that of HF-MRI and where CA was non-diagnostic, HF-MRI could provide diagnostic information in 69% of cases.[70] HF-MRI provided greater spatial resolution, higher tissue contrast and better diagnostic information than 1.5T and was equivalent to CA when there was minimal maceration.[70]

Micro-CT can also provide increased SNR and CNR than HF-PMMRI (7T) for human fetal scanning (4 fetuses, 13–18 weeks GA, 17–137 g) with a greater ability to identify anatomical structures in micro-CT (Figure 5).[7,1]

HF-MRI typically takes longer scanning times (>18 h), making it difficult to implement in a clinical setting,[47,55,70,83] and may be more expensive than Micro-CT (400 Euros per patient in comparison to 200 Euros for micro-CT).[71] Most HF-MRI scanners have a small-bore size (16–30 cm diameter), thus limiting the field-of-view, to smaller fetuses.[55] The smaller the fetus, the more likely micro-CT would be a better imaging modality, as even higher spatial resolution should be possible by positioning the fetus closer to the X-ray source,[71,83] whilst also maintaining shorter scanning times.[55]

Overall, as with micro-CT, most HF-MRI scanners are research based with limited clinical availability[41,55,61,70]; Relative to HF-MRI, micro-CT provides greater cost efficiencies and higher resolution.[71]

5 | AUTOPSY IN ADDITION TO LIA

Whilst LIA techniques are proven to provide answers to parents, it is important to identify whether any additional yield would be possible from completing an invasive autopsy.[113] Shelmerdine et al., demonstrated that when there was concordance between PMMRI and prenatal ultrasound, additional clinically significant information was found at autopsy in only 4.5% (2/44) of cases, where autopsy found additional brain abnormalities after prenatal ultrasound and PMMRI reported only ventriculomegaly.[113]

6 | TISSUE SAMPLING FOLLOWING EARLY PREGNANCY LOSS

Laparoscopic autopsy allows evaluation and tissue sampling of all internal organs via a smaller incision than that employed in CA; thus, it is more cosmetically acceptable to parents.[13,28,39] It has been shown to be useful in fetuses as early 15 weeks of GA but is more difficult with smaller fetuses.[47,81] It also provides similar tissue sampling success (>80%) when compared with more invasive approaches and comparable results to CA in identifying a cause of death.[81] Ultrasound-guided needle biopsy of organs is also a feasible method of tissue sampling, providing biopsy rates of around 85% organ success, and improved accuracy compared to 'blind' tissue sampling (76% vs. <52%),.[80] The INTACT approach, tissue biopsy through the umbilicus, is particularly appealing as it combines tissue sampling without making an incision, leaving the fetus cosmetically intact, although not all organs (brain, thyroid, thymus) could be sampled by this approach.[80] Ultrasound guided tissue sampling at post-mortem has obvious implications for the developing world, for example, for microbiological assessment in infectious outbreaks in children.[114]

7 | CHALLENGES FOR IMPLEMENTATION

Although post-mortem imaging guidance can be used to optimise perinatal investigation and pregnancy loss,[82] and has been embedded within specific autopsy protocols from the UK Royal College of Pathologists for infants and second/third trimester pregnancies, there is currently no specific guidance available for the first trimester loss. A stepwise approach has been suggested for fetal post-mortem examination with imaging used to triage further investigations,[41] whilst further advice is offered for fetuses <500 g when more specialised investigations are available (HF-MRI and micro-CT) (Figures 6 and 7).[47] The developing role of imaging means that new guidelines and referral pathways would be welcome and are likely to support investment and raise awareness for post-mortem investigations following early pregnancy loss.[82]

8 | FUTURE DIRECTIONS/OTHER DEVELOPMENTS

Major challenges for the implementation of both micro-CT and HF-MRI for investigating early pregnancy loss are the lack of availability for both scanning techniques within a clinical setting, along with

10970223, 0, Downloaded from https://obgyn.onlinelibrary.wiley.com/doi/10.1002/pd.6361 by Biu Montpellier, Wiley Online Library on [10/05/2023]. See the Terms and Conditions (https://onlinelibrary.wiley.com/terms-and-conditions) on Wiley Online Library for rules of use; OA articles are governed by the applicable Creative Commons License

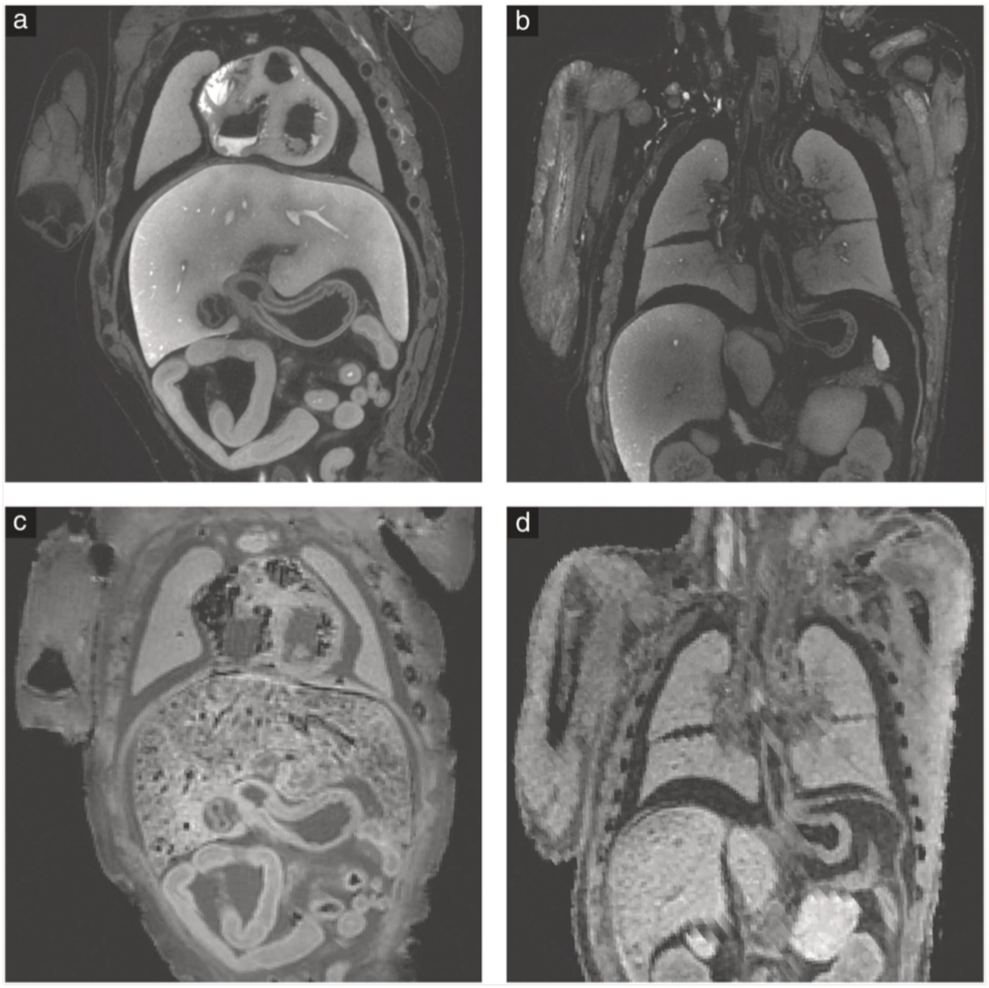

FIGURE 5 Coronal slices demonstrating the high-resolution imaging possible of internal anatomy including liver and stomach (A, C) and primary bronchi and lungs (B, D) for both micro-CT (A, B) and high-field magnetic resonance imaging (MRI) 7T (C) and 3T (D). Figure adapted from Dawood et al. 2021 with permission.[71]

staff training in image acquisition and interpretation. Limited funding for these types of services in specific jurisdictions will further limit clinical experience and patient access. Alongside this, referrers and parents should be educated on the benefits of post-mortem investigations and what these innovative techniques can yield. Similarly, national guidance is required to determine their economic role in the wider service provision at a time of acute shortage of paediatric pathologists.

A detailed health economic assessment is needed, weighing up the costs of scanning against the benefit of helping the grieving process, and a potential reduction in the future burden of mental health issues and ongoing pregnancy losses.[82] Important features of this process include providing the information in sensitive, easily understood terms according to the families personal situation, with time spent answering questions to ensure parents can make decisions that they do not later regret, whilst providing unbiased support in the decision-making process.[14,18,30,115]

9 | CONCLUSIONS

LIA investigations are preferred by parents for a variety of reasons, and through greater provision and choice there will be uptake in parental consent. Micro-CT and HF-MRI offer superior post-mortem image quality for early pregnancy loss through increased resolution and CNR when compared to more established NIA techniques.

10970223, 0, Downloaded from https://obgyn.onlinelibrary.wiley.com/doi/10.1002/pd.6361 by Bib Montpellier, Wiley Online Library on [10/05/2023]. See the Terms and Conditions (https://onlinelibrary.wiley.com/terms-and-conditions) on Wiley Online Library for rules of use; OA articles are governed by the applicable Creative Commons License

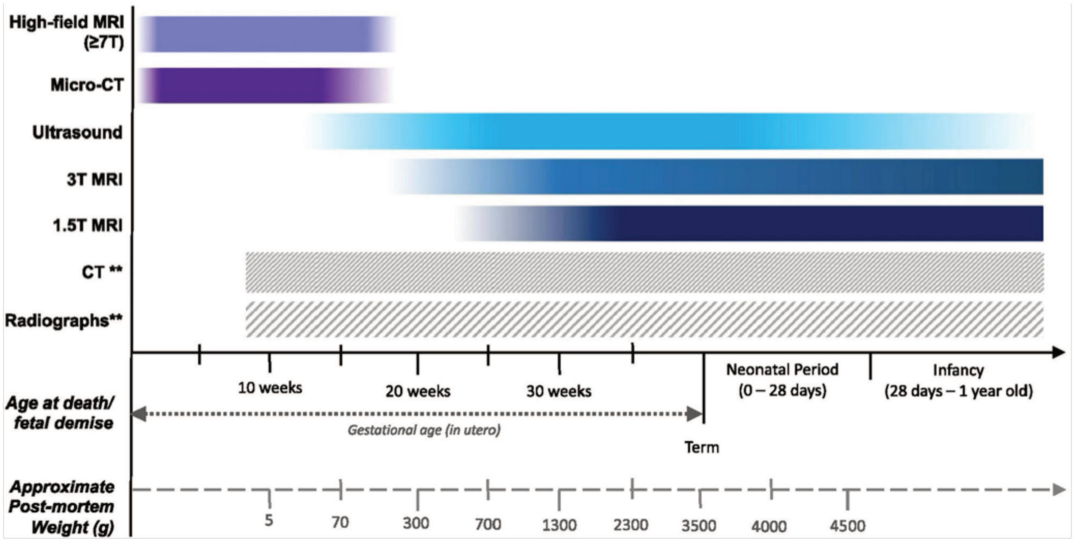

FIGURE 6 Demonstration of when micro-CT and high-field magnetic resonance imaging (MRI) can provide superior imaging for early gestation fetuses relative to other imaging modalities. Figure adapted from Shelmerdine et al. 2021 with permission.[63]

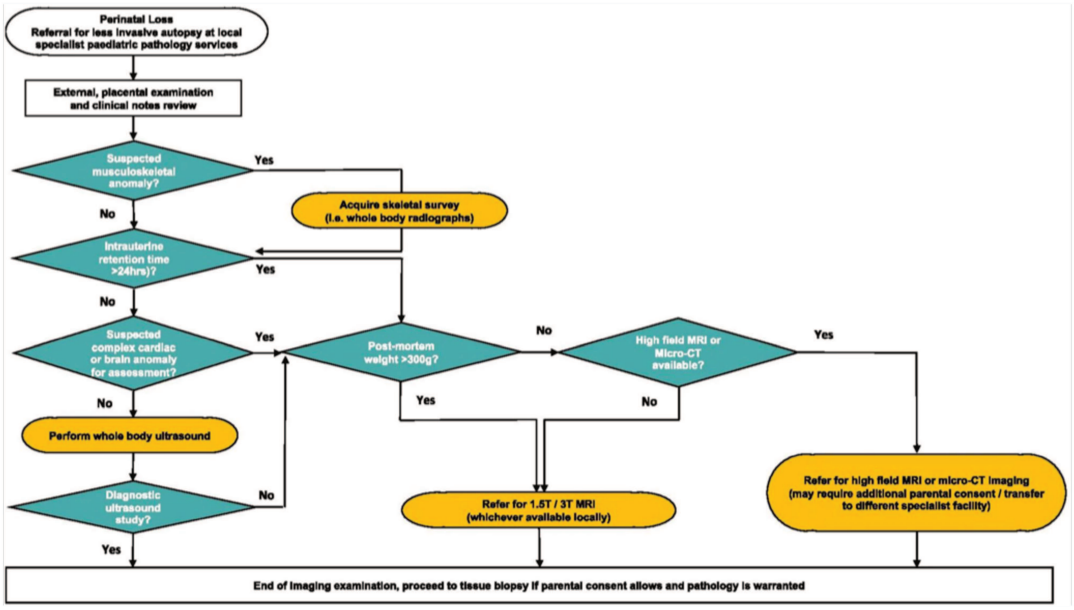

FIGURE 7 Step-wise flowchart for non-invasive investigation of perinatal loss including options for micro-CT and high-field magnetic resonance imaging (MRI). Figure adapted from Shelmerdine et al. 2021 with permission.[63]

Wider adoption of these investigations will increase the societal awareness surrounding miscarriage and reduce the emotional cost for parents by investigating their loss in a more acceptable personalised manner.

ACKNOWLEDGMENTS

Ian C. Simcock is funded by a National Institute for Health Research (NIHR) (ICA-CDRF-2017-03-53 and NIHR302390), Owen J Arthurs is funded by an NIHR Career Development Fellowship (NIHR-CDF-

10970223, 0, Downloaded from https://obgyn.onlinelibrary.wiley.com/doi/10.1002/pd.6361 by Bib Montpellier, Wiley Online Library on [10/05/2023]. See the Terms and Conditions (https://onlinelibrary.wiley.com/terms-and-conditions) on Wiley Online Library for rules of use; OA articles are governed by the applicable Creative Commons License

2017-10-037). Susan C. Shelmerdine is funded by an NIHR Advanced Fellowship Award (NIHR-301322). Audrey Lamouroux is funded by Nîmes and Montpellier University Hospital mobility grant. This article presents independent research funded by the NIHR and Nimes and Montpellier University Hospital and the views expressed are those of the author(s) and not necessarily those of the NHS, the NIHR or the Department of Health and Social Care. The funder of the study played no role in the study design, data collection, data analysis, data interpretation, or writing of the report. The authors and chief investigator (Ian C. Simcock, Audrey Lamouroux, Neil J. Sebire, Susan C. Shelmerdine, Owen J. Arthurs) had full access to the paper and final responsibility for the decision to submit for publication.

CONFLICT OF INTEREST STATEMENT

The authors report no conflicts of interest.

DATA AVAILABILITY STATEMENT

Data sharing is not applicable to this article as no datasets were generated or analysed during the current study.

ETHICS STATEMENT

No ethical consent was required for this review article.

ORCID

Ian C. Simcock https://orcid.org/0000-0002-5619-0785
Audrey Lamouroux https://orcid.org/0000-0001-7108-9581
Susan C. Shelmerdine https://orcid.org/0000-0001-6642-9967
Owen J. Arthurs https://orcid.org/0000-0003-1213-3516

REFERENCES

1. The Lancet. Miscarriage: worldwide reform of care is needed. *Lancet*. 2021(10285):397.
2. UNICEF. Stillbirths; 2022. https://data.unicef.org/topic/child-survival/stillbirths/
3. Quenby S, Gallos ID, Dhillon-Smith RK, et al. Miscarriage matters: the epidemiological, physical, psychological, and economic costs of early pregnancy loss. *Lancet*. 2021;397(10285):1658-1667. https://doi.org/10.1016/s0140-6736(21)00682-6
4. MacWilliams K, Hughes J, Aston M, Field S, Moffatt FW. Understanding the experience of miscarriage in the emergency department. *J Emerg Nurs*. 2016;42(6):504-512. https://doi.org/10.1016/j.jen.2016.05.011
5. Rossen LM, Ahrens KA, Branum AM. Trends in risk of pregnancy loss among US Women, 1990-2011. *Paediatr Perinat Epidemiol*. 2018;32(1):19-29. https://doi.org/10.1111/ppe.12417
6. Blackmore ER, Côté-Arsenault D, Tang W, et al. Previous prenatal loss as a predictor of perinatal depression and anxiety. *Br J Psychiatry*. 2018;198(5):373-378. https://doi.org/10.1192/bjp.bp.110.083105
7. Engelhard IM, van den Hout MA, Arntz A. Posttraumatic stress disorder after pregnancy loss. *Gen Hosp Psychiatr*. 2001;23(2):62-66. https://doi.org/10.1016/s0163-8343(01)00124-4
8. Lok IH, Yip ASK, Lee DTS, Sahota D, Chung TKH. A 1-year longitudinal study of psychological morbidity after miscarriage. *Fertil Steril*. 2010;93(6):1966-1975. https://doi.org/10.1016/j.fertnstert.2008.12.048
9. Horey D, Flenady V, Conway L, McLeod E, Yee Khong T. Decision influences and aftermath: parents, stillbirth and autopsy. *Health Expect*. 2014;17(4):534-544. https://doi.org/10.1111/j.1369-7625.2012.00782.x
10. Lewis C, Hill M, Arthurs O, Hutchinson C, Chitty L, Sebire N. Factors affecting uptake of postmortem examination in the prenatal, perinatal and paediatric setting. *BJOG*. 2018;125(2):172-181. https://doi.org/10.1111/1471-0528.14600
11. Banno C, Sugiura-Ogasawara M, Ebara T, et al. Attitude and perceptions toward miscarriage: a survey of a general population in Japan. *J Hum Genet*. 2020;65(2):155-164. https://doi.org/10.1038/s10038-019-0694-1
12. Brier N. Understanding and managing the emotional reactions to a miscarriage. *Obstetrics Gynecol*. 1999;93(1):151-155. https://doi.org/10.1016/s0029-7844(98)00294-4
13. Lewis C, Riddington M, Hill M, et al. Availability of less invasive prenatal, perinatal and paediatric autopsy will improve uptake rates: a mixed -methods study with bereaved parents. *BJOG*. 2019;126(6):754-753. https://doi.org/10.1111/1471-0528.15591
14. Lewis C, Simcock IC, Arthurs OJ. Improving uptake of perinatal autopsy. *Prenat Diagn*. 2021;33(2):129-134. https://doi.org/10.1097/gco.0000000000000691
15. Ernst LM. A pathologist's perspective on the perinatal autopsy. *Semin Perinatol*. 2015;39(1):55-63. https://doi.org/10.1053/j.semperi.2014.10.008
16. Rahman H, Khong TY. Perinatal and infant postmortem examination. Survey of women's reactions to perinatal necropsy. *Br Med J*. 1995;310(1):870-871. https://doi.org/10.1136/bmj.310.6983.870e
17. Stock SJ, Goldsmith L, Evans MJ, Laing IA. Interventions to improve rates of post-mortem examination after stillbirth. *Eur J Obstet Gynecol Reprod Biol*. 2010;153(2):148-150. https://doi.org/10.1016/j.ejogrb.2010.07.022
18. Ellis A, Chebsey C, Storey C, et al. Systematic review to understand and improve care after stillbirth: a review of parents' and healthcare professionals' experiences. *BMC Pregnancy Childbirth*. 2016;16(1):16. https://doi.org/10.1186/s12884-016-0806-2
19. Peyronnet V, Anselem O, Loeuillet L, Roux N, Tsatsaris V. Diagnostic value of fetal autopsy after early termination of pregnancy for fetal anomalies. *PLoS One*. 2022;17(10):e0275674. https://doi.org/10.1371/journal.pone.0275674
20. Nese N, Bulbul Y. Diagnostic value of perinatal autopsies: analysis of 486 cases. *J Perinat Med*. 2018;46(2):175-181. https://doi.org/10.1515/jpm-2016-0396
21. Gordijn SJ, Erwich JJ, Khong TY. Value of the perinatal autopsy: critique. *Pediatr Dev Pathol*. 2002;5(5):480-488. https://doi.org/10.1007/s10024-002-0008-y
22. Boyd PA, et al. Autopsy after termination of pregnancy for fetal anomaly: retrospective cohort study. *BMJ*. 2004;328(7432):137-140. https://doi.org/10.1136/bmj.37939.570104.ee
23. Lewis C, Hill M, Arthurs OJ, Hutchinson JC, Chitty LS, Sebire N. Health professionals' and coroners' views on less invasive perinatal and paediatric autopsy: a qualitative study. *Arch Dis Child*. 2018;103(6):572-578. https://doi.org/10.1136/archdischild-2017-314424
24. Meaney S, Gallagher S, Lutomski JE, O'Donoghue K. Parental decision making around perinatal autopsy: a qualitative investigation. *Health Expect*. 2015;18(6):3160-3171. https://doi.org/10.1111/hex.12305
25. Man J, Hutchinson JC, Heazell AE, Ashworth M, Levine S, Sebire NJ. Stillbirth and intrauterine fetal death: factors affecting determination of cause of death at autopsy. *Ultrasound Obstet Gynecol*. 2016;48(5):566-573. https://doi.org/10.1002/uog.16016
26. Basu MN, Johnsen IBG, Wehberg S, Sørensen RG, Barington T, Nørgård BM. Causes of death among full term stillbirths and early neonatal deaths in the Region of Southern Denmark. *J Perinat Med*. 2018;46(2):197-202. https://doi.org/10.1515/jpm-2017-0171

10970223, 0, Downloaded from https://obgyn.onlinelibrary.wiley.com/doi/10.1002/pd.6361 by Bib Montpellier, Wiley Online Library on [10/05/2023]. See the Terms and Conditions (https://onlinelibrary.wiley.com/terms-and-conditions) on Wiley Online Library for rules of use; OA articles are governed by the applicable Creative Commons License

27. Lewis C, Riddington M, Hill M, et al. The communication and support from the health professional is incredibly important: a qualitative study exploring the processes and practices that support parental decision-making about postmortem examination. *Prenat Diagn*. 2019;39(13):1242-1253. https://doi.org/10.1002/pd.5575
28. Lewis C, Latif Z, Hill M, et al. We might get a lot more families who will agree: Muslim and Jewish perspectives on less invasive perinatal and paediatric autopsy. *PLoS One*. 2018;13(8):e0202023. https://doi.org/10.1371/journal.pone.0202023
29. Wiener L, Sweeney C, Baird K, et al. What do parents want to know when considering autopsy for their child with cancer? *J Pediatr Hematol Oncol*. 2014;36(6):464-470. https://doi.org/10.1097/mph.0000000000000078
30. Breeze CG, Statham H, Hackett GA, Jessop FA, Lees CC. Perinatal postmortems What is important to parents and How do they decide? *Birth Issues Perinat Care*. 2012;39(1):57-64. https://doi.org/10.1111/j.1523-536x.2011.00513.x
31. Baker JN, Windham JA, Hinds PS, et al. Bereaved parents' intentions and suggestions about research autopsies in children with lethal brain tumors. *J Pediatr*. 2013;163(2):581-586. https://doi.org/10.1016/j.jpeds.2013.01.015
32. Rankin J, Wright C, Lind T. Cross sectional survey of parents' experience and views of the postmortem examination. *Br Med J*. 2002;324(7341):816-818. https://doi.org/10.1136/bmj.324.7341.816
33. Heazell AE, McLaughlin MJ, Schmidt E, et al. A difficult conversation? The views and experiences of parents and professionals on the consent process for perinatal postmortem after stillbirth. *BJOG*. 2012;119(8):987-997. https://doi.org/10.1111/j.1471-0528.2012.03357.x
34. Sieswerda-Hoogendoorn T, van Rijn RR. Current techniques in postmortem imaging with specific attention to paediatric applications. *Pediatr Radiol*. 2010;40(2):141-152. https://doi.org/10.1007/s00247-009-1486-0
35. Kock KF, Vestergaard V, Hardt-Madsen M, Garne E. Declining autopsy rates in stillbirths and infant deaths: results from Funen County, Denmark, 1986-96. *J Matern Fetal Neonatal Med*. 2003;13(6):403-407. https://doi.org/10.1080/713605929
36. Newton D, Coffin CM, Clark EB, Lowichik A. How the Pediatric Autopsy Yields valuable information in a vertically integrated health care system. *Arch Pathology Laboratory Med*. 2004;128(11):1239-1246. https://doi.org/10.5858/2004-128-1239-htpayv
37. Lewis J. Jewish perspectives on pregnancy and childbearing. *Am J Matern/Child Nurs*. 2003;28(5):306-312. https://doi.org/10.1097/00005721-200309000-00008
38. Cullen S, Mooney E, Casey B, Downey P. An audit of healthcare professionals' knowledge regarding perinatal autopsy. *Ir J Med Sci*. 2019;188(2):583-585. https://doi.org/10.1007/s11845-018-1907-x
39. Lewis C, Hutchinson JC, Riddington M, et al. Minimally invasive autopsy for fetuses and children based on a combination of postmortem MRI and endoscopic examination: a feasibility study. *Health Technol Assess*. 2019;23(46):1-104. https://doi.org/10.3310/hta23460
40. Coporation BB. File on 4, in How did my child die? The crisis in paediatric pathology. In: Goldberg A, ed. *British Broadcasting Coporation: BBC iplayer*; 2023.
41. Kang X, et al. Fetal postmortem imaging: an overview of current techniques and future perspectives. *Am J Obstet Gynecol*. 2020;223(4):493-515. https://doi.org/10.1016/j.ajog.2020.04.034
42. Kang X, Cos T, Guizani M, Cannie MM, Segers V, Jani JC. Parental acceptance of minimally invasive fetal and neonatal autopsy compared with conventional autopsy. *Prenat Diagn*. 2014;34(11):1106-1110. https://doi.org/10.1002/pd.4435
43. Sebire NJ. Towards the minimally invasive autopsy? *Ultrasound Obstet Gynecol*. 2006;28(7):865-867. https://doi.org/10.1002/uog.3869
44. Nayak SS, Shukla A, Lewis L, et al. Clinical utility of fetal autopsy and its impact on genetic counseling. *Prenat Diagn*. 2015;35(7):685-691. https://doi.org/10.1002/pd.4592
45. Jawad N, Sebire NJ, Wade A, Taylor AM, Chitty LS, Arthurs OJ. Body weight lower limits of fetal postmortem MRI at 1.5 T. *Ultrasound Obstet Gynecol*. 2016;48(1):92-97. https://doi.org/10.1002/uog.14948
46. Docter D, Dawood Y, Jacobs K, et al. Microfocus computed tomography for fetal postmortem imaging: an overview. *Pediatr Radiol*. 2022;53(4):632-639. https://doi.org/10.1007/s00247-022-05517-1
47. Shelmerdine SC, Arthurs OJ. Post-mortem perinatal imaging: what is the evidence? *Br J Radiol*. 2022:20211078. https://doi.org/10.1259/bjr.20211078
48. Shelmerdine SC, Hutchinson JC, Arthurs OJ, Sebire NJ. Latest developments in post-mortem foetal imaging. *Prenat Diagn*. 2020;40(1):28-37. https://doi.org/10.1002/pd.5562
49. Votino C, Jani J, Verhoye M, et al. Postmortem examination of human fetal hearts at or below 20 weeks' gestation: a comparison of high-field MRI at 9.4 T with lower-field MRI magnets and stereomicroscopic autopsy. *Ultrasound Obstet Gynecol*. 2012;40(4):437-444. https://doi.org/10.1002/uog.11191
50. Kang X, Cannie M, Jani JC. Effect of staining using gadolinium and formaldehyde on fetal whole-body postmortem 3-Tesla magnetic resonance imaging. *Ultrasound Obstet Gynecol*. 2020;55(2):277-278. https://doi.org/10.1002/uog.20356
51. Shelmerdine SC, Sebire NJ, Arthurs OJ. Diagnostic accuracy of postmortem ultrasound vs postmortem 1.5-T MRI for non-invasive perinatal autopsy. *Ultrasound Obstet Gynecol*. 2021;57(3):449-458. https://doi.org/10.1002/uog.22012
52. Kang X, Cannie MM, Arthurs OJ, et al. Post-mortem whole-body magnetic resonance imaging of human fetuses: a comparison of 3-T vs. 1.5-T MR imaging with classical autopsy. *Eur Radiol*. 2017;27(8):3542-3553. https://doi.org/10.1007/s00330-016-4725-4
53. Arthurs OJ, Thayyil S, Owens CM, et al. Diagnostic accuracy of post mortem MRI for abdominal abnormalities in foetuses and children. *Eur J Radiol*. 2015;84(3):474-481. https://doi.org/10.1016/j.ejrad.2014.11.030
54. Arthurs OJ, Thayyil S, Olsen OE, et al. Diagnostic accuracy of postmortem MRI for thoracic abnormalities in fetuses and children. *Eur Radiol*. 2014;24(11):2876-2884. https://doi.org/10.1007/s00330-014-3313-8
55. Dawood Y, et al. Novel imaging techniques to study postmortem human fetal anatomy: a systematic review on microfocus-CT and ultra-high-field MRI. *Eur Radiol*. 2020;30(4):2280-2292. https://doi.org/10.1007/s00330-019-06543-8
56. Arthurs OJ, Guy A, Thayyil S, et al. Comparison of diagnostic performance for perinatal and paediatric post-mortem imaging: CT versus MRI. *Eur Radiol*. 2016;26(7):2327-2336. https://doi.org/10.1007/s00330-015-4057-9
57. Sandaite I, et al. Micro-computed tomography of isolated fetal hearts following termination of pregnancy: a feasibility study at 8 - 12 week's gestation. *Prenat Diagn*. 2020;40(8):984-990. https://doi.org/10.1002/pd.5719
58. Nijkamp JW, Sebire N, Bouman K, Korteweg F, Erwich J, Gordijn S. Perinatal death investigations: What is current practice? *Semin Fetal Neonatal Med*. 2017;22(3):167-175. https://doi.org/10.1016/j.siny.2017.02.005
59. Arthurs OJ, Calder AD, Kiho L, Taylor AM, Sebire NJ. Routine perinatal and paediatric post-mortem radiography: detection rates and implications for practice. *Pediatr Radiol*. 2014;44(3):252-257. https://doi.org/10.1007/s00247-013-2804-0

10970223, 0, Downloaded from https://obgyn.onlinelibrary.wiley.com/doi/10.1002/pd.6361 by Bu Montpellier, Wiley Online Library on [10/05/2023]. See the Terms and Conditions (https://onlinelibrary.wiley.com/terms-and-conditions) on Wiley Online Library for rules of use; OA articles are governed by the applicable Creative Commons License

60. Kamphuis-van Ulzen K, Koopmanschap DH, Marcelis CL, van Vugt JMG, Klein WM. When is a post-mortem skeletal survey of the fetus indicated, and when not? *J Matern Fetal Neonatal Med*. 2016;29(6):991-997. https://doi.org/10.3109/14767058.2015.1029913
61. Votino C, Cos Sanchez T, Bessieres B, et al. Minimally invasive fetal autopsy using ultrasound: a feasibility study. *Ultrasound Obstet Gynecol*. 2018;52(6):776-783. https://doi.org/10.1002/uog.14642
62. Calder AD, Offiah AC. Foetal radiography for suspected skeletal dysplasia: technique, normal appearances, diagnostic approach. *Pediatr Radiol*. 2015;45(4):536-548. https://doi.org/10.1007/s00247-014-3130-x
63. Shelmerdine SC, Hutchinson JC, Lewis C, et al. A pragmatic evidence-based approach to post-mortem perinatal imaging. *Insights Imaging*. 2021;12(101):101. https://doi.org/10.1186/s13244-021-01042-1
64. Addison S, Arthurs OJ, Thayyil S. Post-mortem MRI as an alternative to non-forensic autopsy in foetuses and children: from research into clinical practice. *Br J Radiol*. 2014;87(1036):20130621. https://doi.org/10.1259/bjr.20130621
65. Arthurs OJ, Taylor AM, Sebire NJ. Indications, advantages and limitations of perinatal postmortem imaging in clinical practice. *Pediatr Radiol*. 2015;45(4):491-500. https://doi.org/10.1007/s00247-014-3165-z
66. Votino C, Cannie M, Segers V, et al. Virtual autopsy by computed tomographic angiography of the fetal heart: a feasibility study. *Ultrasound Obstet Gynecol*. 2012;39(6):679-684. https://doi.org/10.1002/uog.11150
67. Sarda-Quarello L, Bartoli C, Laurent PE, et al. Whole body perinatal postmortem CT angiography. *Diagn Interv Imaging*. 2016;97(1):121-124. https://doi.org/10.1016/j.diii.2014.11.002
68. Norman W, Jawad N, Jones R, Taylor AM, Arthurs OJ. Perinatal and paediatric post-mortem magnetic resonance imaging (PMMR): sequences and technique. *Br J Radiol*. 2016;89(1062):20151028. https://doi.org/10.1259/bjr.20151028
69. Arthurs O, Thayyil S, Pauliah S, et al. Diagnostic accuracy and limitations of post-mortem MRI for neurological abnormalities in fetuses and children. *Clin Radiol*. 2015;70(8):872-880. https://doi.org/10.1016/j.crad.2015.04.008
70. Thayyil S, Cleary JO, Sebire NJ, et al. Post-mortem examination of human fetuses: a comparison of whole-body high-field MRI at 9·4 T with conventional MRI and invasive autopsy. *Lancet*. 2009;374(9688):467-475. https://doi.org/10.1016/s0140-6736(09)60913-2
71. Dawood Y, et al. Comparison of postmortem whole-body contrast-enhanced microfocus computed tomography and high field magnetic resonance imaging of human fetuses. *Ultrasound Obstet Gynecol*. 2021;60(1):109-117. https://doi.org/10.1002/uog.24827
72. Kang X, Sanchez TC, Arthurs OJ, et al. Postmortem fetal imaging: prospective blinded comparison of two-dimensional ultrasound with magnetic resonance imaging. *Ultrasound Obstet Gynecol*. 2019;54(6):791-799. https://doi.org/10.1002/uog.20217
73. Shelmerdine SC, Sebire NJ, Arthurs OJ. Perinatal post-mortem ultrasound (PMUS): radiological-pathological correlation. *Insights Imaging*. 2019;10(1):81. https://doi.org/10.1186/s13244-019-0762-2
74. Shelmerdine SC, Sebire NJ, Arthurs OJ. Perinatal post mortem ultrasound (PMUS): a practical approach. *Insights Imaging*. 2019;10(1):35. https://doi.org/10.1186/s13244-019-0723-9
75. Shelmerdine S, Langan D, Sebire NJ, Arthurs O. Diagnostic accuracy of perinatal post-mortem ultrasound (PMUS): a systematic review. *BMJ Paediatr Open*. 2019;3(1):e000566. https://doi.org/10.1136/bmjpo-2019-000566
76. Kang X, Shelmerdine SC, Hurtado I, et al. Postmortem examination of human fetuses: comparison of two-dimensional ultrasound with invasive autopsy. *Ultrasound Obstet Gynecol*. 2019;53(2):229-238. https://doi.org/10.1002/uog.18828
77. Rodriguez MA, Prats P, Rodríguez I, Cusí V, Comas C. Concordance between prenatal ultrasound and autopsy findings in a tertiary center. *Prenat Diagn*. 2014;34(8):784-789. https://doi.org/10.1002/pd.4368
78. Kang X, Resta S, Cos Sanchez T, Carlin A, Bevilacqua E, Jani JC. Impact of the delay between fetal death and delivery on the success of postmortem ultrasound following termination of pregnancy. *J Matern Fetal Neonatal Med*. 2021;34(10):1613-1618. https://doi.org/10.1080/14767058.2019.1642868
79. Shelmerdine SC, Langan D, Mandalia U, Sebire NJ, Arthurs OJ. Maceration determines diagnostic yield of fetal and neonatal whole body post-mortem ultrasound. *Prenat Diagn*. 2020;40(2):232-243. https://doi.org/10.1002/pd.5615
80. Shelmerdine SC, Hutchinson JC, Ward L, et al. INTACT (INcision-less TArgeted Core Tissue) biopsy procedure for perinatal autopsy: initial feasibility. *Ultrasound Obstet Gynecol*. 2019;55(5):667-675. https://doi.org/10.1002/uog.20387
81. Hutchinson JC, Shelmerdine SC, Lewis C, et al. Minimally invasive perinatal and pediatric autopsy with laparoscopically assisted tissue sampling: feasibility and experience of the MinImAL procedure. *Ultrasound Obstet Gynecol*. 2019;54(5):661-669. https://doi.org/10.1002/uog.20211
82. Chambers G, et al. Current and future funding streams for paediatric postmortem imaging: European society of paediatric radiology survey results. *Pediatr Radiol*. 2023;53(2):273-281. https://doi.org/10.1007/s00247-022-05485-6
83. Simcock IC, Shelmerdine SC, Hutchinson JC, Sebire NJ, Arthurs OJ. Human fetal whole-body postmortem microfocus computed tomographic imaging. *Nat Protoc*. 2021;16(5):2594-2614. https://doi.org/10.1038/s41596-021-00512-6
84. Shelmerdine SC, et al. Post-mortem micro-CT for non-invasive autopsies: experience in > 250 human fetuses. *Am J Obstet Gynecol*. 2021;224(1):103. https://doi.org/10.1016/j.ajog.2020.07.019
85. Dawood Y, Buijtendijk MF, Shah H, et al. Imaging fetal anatomy. *Semin Cell Dev Biol*. 2022;131:78-92. https://doi.org/10.1016/j.semcdb.2022.02.023
86. Dawood Y, Hagoort J, Siadari BA, et al. Reducing soft-tissue shrinkage artefacts caused by staining with Lugol's solution. *Sci Rep*. 2021;11(1):19781. https://doi.org/10.1038/s41598-021-99202-2
87. Dawood Y, de Bakker BS. Micro-CT of early human development. *Radiology*. 2020;297(1):32. https://doi.org/10.1148/radiol.2020201660
88. Hutchinson JC, Kang X, Shelmerdine SC, et al. Postmortem microfocus computed tomography for early gestation fetuses: a validation study against conventional autopsy. *Am J Obstet Gynecol*. 2018;218(4):445.e1-445.e12. https://doi.org/10.1016/j.ajog.2018.01.040
89. Simcock IC, et al. Predictors of image quality at human foetal post-mortem micro CT. *Insights Into Imaging*. 2021;12(2):291.
90. Hutchinson JC, Shelmerdine SC, Simcock IC, Sebire NJ, Arthurs OJ. Early clinical applications for imaging at microscopic detail: microfocus computed tomography (micro-CT). *Br J Radiol*. 2017;90(1075):20170113. https://doi.org/10.1259/bjr.20170113
91. Shelmerdine SC, Hutchinson JC, Kang X, et al. Novel usage of microfocus computed tomography (micro-CT) for visualisation of human embryonic development-Implications for future non-invasive post-mortem investigation. *Prenat Diagn*. 2018;38(7):538-542. https://doi.org/10.1002/pd.5281
92. Lombardi S, Scola E, Ippolito D, et al. Micro-computed tomography: a new diagnostic tool in postmortem assessment of brain anatomy

10970223, 0, Downloaded from https://obgyn.onlinelibrary.wiley.com/doi/10.1002/pd.6361 by Bib Montpellier, Wiley Online Library on [10/05/2023]. See the Terms and Conditions (https://onlinelibrary.wiley.com/terms-and-conditions) on Wiley Online Library for rules of use; OA articles are governed by the applicable Creative Commons License

in small fetuses. *Neuroradiology*. 2019;61(7):737-746. https://doi.org/10.1007/s00234-019-02168-2
93. Hutchinson JC, Arthurs OJ, Ashworth MT, et al. Clinical utility of postmortem microcomputed tomography of the fetal heart: diagnostic imaging vs macroscopic dissection. *Ultrasound Obstet Gynecol*. 2016;47(1):58-64. https://doi.org/10.1002/uog.15764
94. Lombardi CM, Zambelli V, Botta G, et al. Postmortem microcomputed tomography (micro-CT) of small fetuses and hearts. *Ultrasound Obstet Gynecol*. 2014;44(5):600-609. https://doi.org/10.1002/uog.13330
95. Shelmerdine SC, Simcock IC, Hutchinson JC, et al. 3D printing from microfocus computed tomography (micro-CT) in human specimens: education and future implications. *Br J Radiol*. 2018:20180306. https://doi.org/10.1259/bjr.20180306
96. Pauwels E, Van Loo D, Cornillie P, Brabant L, Van Hoorebeke L. An exploratory study of contrast agents for soft tissue visualization by means of high resolution X-ray computed tomography imaging. *J Microsc*. 2013;250(1):21-31. https://doi.org/10.1111/jmi.12013
97. Stephenson RS, Boyett MR, Hart G, et al. Contrast enhanced micro-computed tomography resolves the 3-dimensional morphology of the cardiac conduction system in mammalian hearts. *PLoS One*. 2012;7(4):e35299. https://doi.org/10.1371/journal.pone.0035299
98. Vickerton P, Jarvis J, Jeffery N. Concentration-dependent specimen shrinkage in iodine-enhanced microCT. *J Anat*. 2013;223(2):185-193. https://doi.org/10.1111/joa.12068
99. Dunmore-Buyze PJ, Tate E, Xiang F, et al. Three-dimensional imaging of the mouse heart and vasculature using micro-CT and whole-body perfusion of iodine or phosphotungstic acid. *Contrast Media Mol Imaging*. 2014;9(5):383-390. https://doi.org/10.1002/cmmi.1588
100. Zhou YQ, Davidson L, Henkelman RM, et al. Ultrasound-guided left-ventricular catheterization: a novel method of whole mouse perfusion for microimaging. *Lab Invest*. 2004;84(3):385-389. https://doi.org/10.1038/sj.labinvest.3700038
101. Aydin E, Levy B, Oria M, Nachabe H, Lim FY, Peiro JL. Optimization of pulmonary vasculature tridimensional phenotyping in the rat fetus. *Sci Rep*. 2019;9(1):1244. https://doi.org/10.1038/s41598-018-37906-8
102. Simcock IC, Shelmerdine SC, Langan D, Anna G, Sebire NJ, Arthurs OJ. Micro-CT yields high image quality in human fetal post-mortem imaging despite maceration. *BMC Med Imag*. 2021;21(1):128. https://doi.org/10.1186/s12880-021-00658-5
103. Montaldo P, Addison S, Oliveira V, et al. Quantification of maceration changes using post mortem MRI in fetuses. *BMC Med Imag*. 2016;16(1):34. https://doi.org/10.1186/s12880-016-0137-9
104. Cain MA, Guidi CB, Steffensen T, Whiteman VE, Gilbert-Barness E, Johnson DR. Postmortem ultrasonography of the macerated fetus complements autopsy following in utero fetal demise. *Pediatr Dev Pathol*. 2014;17(3):217-220. https://doi.org/10.2350/14-02-1439-cr.1
105. Piercecchi-Marti MD, Liprandi A, Sigaudy S, et al. Value of fetal autopsy after medical termination of pregnancy. *Forensic Sci Int*. 2004;144(1):7-10. https://doi.org/10.1016/j.forsciint.2004.01.022
106. Tuchtan L, Lesieur E, Bartoli C, et al. Diagnosis of congenital abnormalities with post-mortem ultrasound in perinatal death. *Diagn Interv Imaging*. 2018;99(3):143-149. https://doi.org/10.1016/j.diii.2017.11.005
107. Hutchinson JC, Barrett H, Ramsey AT, et al. Virtual pathological examination of the human fetal kidney using micro-CT. *Ultrasound Obstet Gynecol*. 2016;48(5):663-665. https://doi.org/10.1002/uog.15859
108. Sandrini C, Rossetti L, Zambelli V, et al. Accuracy of micro-computed tomography in post-mortem evaluation of fetal congenital heart disease. Comparison between post-mortem micro-CT and conventional autopsy. *Front Pediatr*. 2019;7:92. https://doi.org/10.3389/fped.2019.00092
109. Sandrini C, Lombardi C, Shearn AIU, et al. Three-dimensional printing of fetal models of congenital heart disease derived from microfocus computed tomography: a case series. *Front Pediatr*. 2019;7:567. https://doi.org/10.3389/fped.2019.00567
110. Umutlu L, Ladd M, Forsting M, Lauenstein T. 7 Tesla MR imaging: opportunities and challenges. *Röfo*. 2014;186(2):121-129. https://doi.org/10.1055/s-0033-1350406
111. Kraff O, Quick HH, 7T. Physics, safety, and potential clinical applications. *J Magn Reson Imag*. 2017;46(6):1573-1589. https://doi.org/10.1002/jmri.25723
112. Staicu A, Albu C, Popa-Stanila R, et al. Potential clinical benefits and limitations of fetal virtopsy using high-field MRI at 7 Tesla versus stereomicroscopic autopsy to assess first trimester fetuses. *Prenat Diagn*. 2019;39(7):505-518. https://doi.org/10.1002/pd.5457
113. Shelmerdine SC, Arthurs OJ, Gilpin I, et al. Is traditional perinatal autopsy needed after detailed fetal ultrasound and post-mortem MRI? *Prenat Diagn*. 2019;39(9):818-829. https://doi.org/10.1002/pd.5448
114. Castillo P, Ussene E, Ismail MR, et al. Pathological methods applied to the investigation of causes of death in developing countries: minimally invasive autopsy approach. *PLoS One*. 2015;10(6):e0132057. https://doi.org/10.1371/journal.pone.0132057
115. Warland J, Meaney S, O'Donoghue K. The impact of stillbirth on bereaved parents: a qualitative study. *Plos One*. 2018;13(1):e0191635. https://doi.org/10.1371/journal.pone.0191635

How to cite this article: Simcock IC, Lamouroux A, Sebire NJ, Shelmerdine SC, Arthurs OJ. Less-invasive autopsy for early pregnancy loss. *Prenat Diagn*. 2023;1-13. https://doi.org/10.1002/pd.6361

10970223, 0, Downloaded from https://obgyn.onlinelibrary.wiley.com/doi/10.1002/pd.6361 by Bib Montpellier, Wiley Online Library on [10/05/2023]. See the Terms and Conditions (https://onlinelibrary.wiley.com/terms-and-conditions) on Wiley Online Library for rules of use; OA articles are governed by the applicable Creative Commons License

ANNEXE 2

Lamouroux A, Cardoso M, Bottero C, Fuchs F, Mousty E, Genevieve D, Subsol G, Goze-Bac C & Captier G.

Modelling of staining in post-mortem diffusible iodine-based contrast enhanced (Dice) micro-CT imaging of non-macerated first-trimester human fetuses

submitted in BMC Medical Imaging

ARTICLE TITLE

Modelling of staining in postmortem Dice micro-CT imaging of nonmacerated first-trimester human fetuses.

Authors list:

Audrey Lamouroux[1 2 3 4 5], Maïda Cardoso[4 5] (orcid 0000-0001-6149-3695), Célia Bottero[1 4], Florent Fuchs[4 6 7 8] (orcid 0000-0003-3530-6328), Eve Mousty[1 4] (orcid 0000 0002 3648 0304) , David Genevieve[2 4 9] (orcid 0000-0001-6928-6287), Gérard Subsol[3 4] (orcid 0000-0002-7461-4932), Christophe Goze-Bac[4 5 10] (orcid 0000-0002-9063-4140), Guillaume Captier[3 4 11 12] (orcid 0000-0002-1705-2339)

[1] Obstetrical Gynaecology Department, Centre Hospitalier Universitaire de Nîmes, Univ. Montpellier, Nîmes, France

[2] Clinical Genetics Department, Centre Hospitalier Universitaire de Montpellier, Univ. Montpellier, Montpellier, France

[3] ICAR research team, LIRMM, Laboratoire d'Informatique de Robotique et de Microelectronique de Montpellier, Univ. Montpellier, UM, CNRS, Montpellier, France

[4] Montpellier Université d'Excellence, Univ. Montpellier, UM, Montpellier, France

[5] BNIF user facility imaging, Montpellier Université d'Excellence, UM, Montpellier, France

[6] Obstetrical Gynaecology Department, Centre Hospitalier Universitaire de Montpellier, Univ. Montpellier, Montpellier, France

[7] Inserm, CESP Center for research in Epidemiology and Population Health, U1018, Reproduction and child development, Gustave Roussy, Villejuif.

[8] Desbrest Institute of Epidemiology and Public Health (IDESP), Univ. Montpellier, UM, INSERM delegation regional Occitanie Méditerranée, Montpellier, France

[9] Center for rare disease development anomaly and malformative syndromes, Centre Hospitalier Universitaire de Montpellier, Univ. Montpellier, Montpellier, France

[10] Charles Coulomb Laboratory, UMR 5221 CNRS-UM, CNRS delegation Languedoc-Roussillon, Montpellier, France

[11] Anatomy Laboratory of Montpellier, Université de Montpellier, Faculté de Médecine Montpellier-Nimes, UM, Montpellier, France

[12] Orthopedic and Plastic Pediatric surgery Department, Centre Hospitalier Universitaire de Montpellier, Univ. Montpellier, Montpellier, France

Corresponding author:

Audrey Lamouroux, https://orcid.org/0000-0001-7108-9581

Service de gynécologie obstétrique, Place du Pr Robert Debré, CHU Carémeau, 30000 Nimes, France.

email: audrey.lamouroux@chu-nimes.fr

Telephone number: +33 (0)4 66 68 43 67

ABSTRACT

Background

To optimize organ visualization via postmortem micro-CT imaging, this study investigated staining in nonmacerated first-trimester fetuses by examining the dynamic diffusion of a diffusible iodine-based contrast-enhanced (Dice) staining agent and determining the optimal staining duration for fetuses of varying sizes through quantitative signal and contrast measurements.

Methods

After obtaining consent from protocol approved by the French Biomedicine Agency, fetuses from elective abortions were collected, stained with Dice solution composed of 4% paraformaldehyde and Lugol's iodine (total iodine content of 63.25 mg/ml) at a 1:1 ratio for varying durations, and then scanned via micro-CT.

Results

A total of 19 fetuses, with gestational ages ranging from 8 to 14+2 WG on the basis of the Robinson formula, with crown–rump length from 16 to 89 mm were collected for this study between January 2016 and July 2023.

The initial phase of the study focused on examining the dynamic diffusion of the Dice staining agent in a foetus with a crown–rump length of 80 mm and weight of 30.06 g. The data suggest that the staining bath diffusion process is best described by a stretched exponential model in most organs.

Furthermore, the staining duration required to achieve optimal contrast was found to be correlated with fetal crown–rump length and weight in nonmacerated first trimester fetuses. For example, a foetus with a crown–rump length of 50 mm or a weight of 20 g

must be stained for at least 96 hours to achieve a contrast-to-noise ratio greater than 5, in accordance with the Rose criterion.

Conclusions

The use of an iodine staining bath offers significant advantages in enhancing contrast in Dice micro-CT imaging of first-trimester human nonmacerated fetuses. By tailoring the staining duration to fetal crown–rump length or weight, optimal imaging outcomes can be achieved, facilitating more accurate and detailed analyses in both research and clinical settings.

Keywords

Microtomography, postmortem imaging, virtual autopsy, iodine, staining

BACKGROUND

A comprehensive approach is essential for clinical and scientific research into first trimester pregnancy loss[1]. Parents should be offered the option of investigating the circumstances of their pregnancy loss, which may include an autopsy[2]. However, some parents may be reluctant to pursue an autopsy because of its invasive nature[3–6]. Consequently, less invasive techniques, such as postmortem imaging, should be considered[7,8]. Postmortem microfocus computed tomography (MCT) is an imaging technology based on X-ray attenuation, typically offering an isotropic resolution of 10 μm[9,10]. It has been successfully used as an alternative to invasive autopsy of human fetuses in clinical practice[11,12] over 11 weeks of gestation (WG)[10], as well as earlier in research[13,14].

89 Staining by immersion of foetus in diffusible iodine-based contrast-enhanced
90 (Dice) staining solution provides satisfactory contrast in MCTs[9–12,15], even in macerated
91 fetuses[16]. However, several aspects of this staining contrast bath remain unclear. Simcock
92 et al. conducted a pooled analysis of observed staining durations on the basis of
93 theoretical age and weight[17], utilizing clinical cases with varying degrees of
94 maceration[12,16,17] exhibiting MCT images consistent with prospective diagnoses[17].
95 The diffusion of iodine stains in biological tissues can be understood by
96 combining general diffusion theory with tissue-specific compositions. The output
97 parameters from these models, such as density, heterogeneity, and tortuosity of the tissue,
98 can effectively be used to analyse and discuss the penetration of staining agents such as
99 iodine into biological tissues[18–20].
100 Given these factors, this study investigated the diffusion of the Dice staining bath
101 in nonmacerated first-trimester fetuses and aimed to determine the optimal staining
102 duration for fetuses of varying sizes via quantitative contrast and signal measurements.

103 # METHODS

104 ## Inclusion criteria and ethics

105 The present study was conducted as part of the Fetal Enhanced Three-dimensional
106 and Translational Anatomical Landscape (FETTAL) project[14,21], which was approved by
107 the French Biomedical Agency (PFS14--020 on January 29, 2015). The project involved
108 the use of human fetuses obtained from elective abortions. Pregnant women seeking
109 elective abortion were provided with an information document outlining the study's
110 objectives and methodology. The noninclusion criteria included being under 18 years of
111 age or being unable to provide informed consent. Written informed consent was obtained

112 from each participant prior to elective abortion, with the option to revoke consent at any
113 time. The fetuses included were collected following medical expulsion. Consequently,
114 this cohort consists solely of nonmacerated and nonmalformed PM fetuses.

115 Dice MCT acquisition and posttreatment

116 Dice-MCT images were acquired via a SkyScan 1276 (Bruker) X-ray
117 microtomograph. The acquisition settings, including spatial resolution, X-ray attenuation,
118 power, and filter type, were carefully adjusted according to the manufacturer's
119 recommendations : to avoid image saturation and ensure optimal contrast, X-ray
120 absorption was maintained between 30% and 90% of saturation. Details acquisition
121 parameters are collected for each acquisition. Serial radiographs, native images, from the
122 rotative acquisitions over 360° were converted into computed tomography images via N-
123 RECON software (Skyscan, Brucker) in DICOM and TIFF formats. The reconstructed
124 images were postprocessed with FIJI ImageJ software, where regions of interest (ROIs)
125 were freehand manually delineated, and their characteristics were quantified and
126 visualized.

127 Dynamic study of the diffusion of the staining agent and its quantification.

128 To study the dynamic diffusion of the staining agent, a foetus fixed in 4%
129 paraformaldehyde (PFA)[18] was immersed in Dice staining solution composed of 4% PFA
130 and I_2KI (with a total iodine content of 63.25 mg/ml) at a 1:1 ratio [9,11,12,16]. The foetus
131 and its staining solution were placed in a hermetically sealed syringe, which was then
132 loaded into the MCT device. Iterative acquisitions were performed using consistent
133 settings, initially at one-hour intervals, followed by progressively longer intervals over
134 the course of one week. The same postprocessing settings were applied throughout the
135 study.

136 The objective was to obtain time series data on the diffusion of the staining agent
137 within the fetus and visualize its progression over time. Iodine diffusion was monitored
138 in three Dice MCT transverse sections: i) a cephalic section through the thalamic nuclei;
139 ii) a thoracic section through the four cardiac chambers, including visualization of the
140 pulmonary venous returns; and iii) an abdominal section encompassing the stomach,
141 superior pole of the spleen, left adrenal gland and superior extremity of the right adrenal
142 gland.

143 The three stacks of images were postprocessed via FIJI ImageJ software, with the
144 ROIs manually selected from various organs. The evolution of the mean signal (MS)
145 within each ROI was tracked and represented graphically. Its evolution was modelled via
146 stretched exponential[19 20] and double Weibull functions[22,23].

147 Contrast between two organs was displayed over time, with the distance between
148 the lines indicating the contrast level. At the point where the lines intersect, the contrast
149 between the two organs is no longer observable. This visual representation allowed for
150 the determination of the staining bath duration required to optimize contrast between the
151 two organs of interest.
152 The results from this analysis will inform the next phase of the study, which will
153 determine the optimal staining bath duration in relation to fetal size and weight. In the
154 absence of direct fetal volume measurements, the size and weight of the fetus may be
155 used as proxies for this parameter.

156 Modelling Signal Evolution Using Stretched Exponential and Double Weibull Functions

The signal evolution was tested with several plots usually used to describe biological diffusion and choose the model best fit with our curve of diffusion. Consequently, we use a stretched exponential function $S = A_0 + A_{max}(1 - \exp^{-(\frac{t-t_0}{\lambda})^{-\beta}})$ where A_0 is the initial amplitude or baseline value of the signal, A_{max} is the maximum change, t_0 represents the starting time, λ is the characteristic time scale, and β is the stretching exponent[20]. Stretched exponential functions describe diffusion, where particle displacement probabilities deviate from the expected Gaussian distribution ($\beta = 1$). This type of diffusion is commonly observed in molecular transport within intracellular environments. In this context, the stretched exponential function exhibits slower decay compared to Gaussian diffusion, with the value of β reflecting this process ($\beta < 1$)[19]. When signal increases do not conform to a stretched exponential pattern, alternative models, such as the double Weibull distribution, can be employed to provide a more accurate fit. For a random variable *x*, the cumulative distribution function (CDF) of the double Weibull distribution is given by: *F(x; α, β, τ) = { (1/2) * exp(-((τ - x) / α) ** β) for x < τ 1 - (1/2) * exp(-((x - τ) / α) ** β) for x >= τ }* where: *α* is the scale parameter ; *β* is the shape parameter and *τ* is the threshold parameter[22,23].

Staining time according to fetal size

All the foetuses were fixed in 4% paraformaldehyde (PFA) for at least 72 hours, stored at +5 °C, and subsequently stained in Dice solution for various durations prior to MCT image acquisition. The Dice staining durations for the fetuses, along with their specific characteristics, are detailed in Table 1. MCT image acquisition and postprocessing were performed following previously described methods.

179 In the existing literature, noise and its standard deviation (SD) are often calculated
180 using a ROI in the air as an external, stable reference point outside the sample[24]. However,
181 due to the post-processing methods applied in this study, the air signal in our MCT images
182 exhibited variability in both MS and SD, rendering it unsuitable as a reference. Instead,
183 the cradle used during imaging was identified as a stable reference point. The MS and SD
184 of the cradle were determined across the entire acquisition volume and used as the
185 reference for noise calculations. The signal-to-noise ratio (SNR) for a specific target
186 organ was calculated by dividing the MS of the organ in question by the SD of the cradle.
187 The contrast-to-noise ratio (CNR) for a specific region (such as the brain or abdomen)
188 was calculated as the difference in MS between two neighbouring organs in the region,
189 divided by the SD of the cradle.

190 To investigate factors influencing CNR variations, a Pearson correlation analysis
191 was initially conducted to assess the relationships between the CNR and fetal
192 characteristics. After normal distribution controlled, a linear regression analysis using
193 ANOVA was subsequently performed with two explanatory variables: fetal
194 characteristics, e.g., weight, crown–rump length (CRL), and staining protocol parameters,
195 e.g., staining duration to highlight the relationship between variables. All the statistical
196 analyses were performed via R++ software[25]. Additionally, the CNR values were plotted
197 against fetal weight, the CRL, and the staining duration via R version 4.3.0 to visualize
198 these relationships.

RESULTS

A total of 19 fetuses, with gestational ages ranging from 8 to 14+2 WG on the basis of the Robinson formula[26], with CRL from 16 to 89 mm were collected for this study between January 2016 and July 2023.

Dynamic study of the diffusion of the staining agent and its quantification.

Foetus S0 (female sex, CRL = 80 mm, interparietal diameter = 14 mm, foot length = 14 mm, weight = 30.06 g, 13+4 WG) was used for a dynamic analysis of the diffusion of the staining agent. Time series images of the diffusion of the staining agent in the fetus were obtained via three MCT transverse sections of interest, as presented in Figure 1 and in videos of supplemental materials 1, 2 and 3.

The iodine content in the staining solution was quantified as a CT signal, following a stretched exponential decay pattern (see Supplemental material 4 – Figure). Diffusion dynamics were graphically represented over time, with MS values from ROIs in different organs plotted in Figure 2. The data revealed that MS followed a stretched exponential model[20] in all organs except the liver (Figure 2 – upper graph). In the liver, staining diffusion was consistent with a double Weibull[23] distribution model (Figure 2 – A, B and C; Table 2). The fitted lines enabled the extraction of specific diffusion parameters for each organ (Table 2).

As shown in Figure 2, no contrast was evident between the posterior ventricle and the thalamic nuclei at 30 hours. However, a notable contrast between the posterior ventricle and the frontal cortex emerges over time. Figure 2 A, B and C illustrates the contrast between the lung and liver, showing a gradual transition from the periphery to the center of the liver. At approximately 12 and 72 hours, the signal lines cross, and no contrast is observed between the lung and peripherical liver (Figure 2A) or the hilum of

223 the liver (Figure 2C). Notably, sufficient contrast between the liver hilum and the lung
224 was achieved only after the duration of staining exceeded 120 hours. These diffusion
225 characteristics guided the selection of specific staining bath durations to explore the
226 correlation between contrast and fetal characteristics.

227 Staining bath duration according to fetal characteristics

228 After staining for varying durations, 18 fetuses were scanned via Dice MCT
229 (Table 1). The CNR from the liver to the lung was calculated via signal values from the
230 ROIs in the liver (excluding the gallbladder and hepatic hilum) and in the lungs (avoiding
231 pulmonary scissures where possible).

232 The Pearson correlation analysis revealed that the relationship between CNR
233 Liver to Lung and biometric factors is negative, strong, and statistically significant for
234 both CRL ($r = -0.56$, 95% CI [-0.77, -0.25], $p = 0.001$) and weight ($r = -0.54$, 95% CI [-
235 0.75, -0.22], $p = 0.002$). Two linear regression models, fitted using Ordinary Least
236 Squares (OLS), were used to predict CNR based on staining duration and either CRL or
237 weight. Both models explain a substantial proportion of the variance in CNR (adjusted
238 $R^2 = 0.71$ and 0.74, respectively, $p < 0.001$). In both models, staining duration showed a
239 positive and significant effect ($\beta \approx 0.30$, $p < 0.001$), while CRL and weight exhibited
240 negative significant effects (CRL: $\beta = -0.27$, $p = 0.004$; weight: $\beta = -0.58$, $p < 0.001$).
241 Confidence intervals and p-values were calculated using the Wald t-distribution
242 approximation.

243 As the staining time increased relative to the CRL and weight, the CNR tended to
244 increase, as represented by the green circles in Figure 3. The dotted lines in the figures
245 indicate the minimum staining duration required for a given CRL or weight to achieve a
246 satisfactory CNR of 5 in accordance with the Rose criterion[27]. Thank to this line we were

able to calculate the staining duration based on fetal weight and CRL: Staining duration = 2CRL - 12 and = 2weight + 12.5. For example, a foetus with a CRL of 50 mm or a weight of 20 g must be stained for a minimum of 96 hours to meet this threshold.

DISCUSSION

The staining bath diffusion process is best described by a stretched exponential model in most organs. The duration required to achieve optimal contrast correlates with the fetal CRL and weight in nonmacerated first-trimester fetuses. The use of an iodine staining bath significantly enhances contrast in Dice MCT imaging, with the duration tailored to the fetal CRL or weight ensuring optimal imaging quality.

Iodine staining is a common technique in histology and imaging. The preparation of the staining solution followed Arthurs' [9,11,12,16] methodology. Using a closed syringe limits iodine availability, ensuring reproducibility and clinical relevance. Over time, the iodine concentration correlated with the CT signal intensity and exhibited a stretched exponential decay (see Supplementary material 2 – Figure).

Iodine staining in biological tissues results in intriguing interactions with stretched diffusion processes. While iodine transport typically follows classical diffusion in homogeneous media, its behaviour in tissues can deviate significantly because of factors such as tissue heterogeneity, molecular interactions, and environmental factors. This often leads to stretched exponential diffusion, characterized by a slower-than-expected iodine spread. In most organs, the staining bath diffusion process is effectively described by a stretched exponential model, reflecting the heterogeneous permeability of the tissue[20]. This model provides valuable insights into the rate of signal change and its maximal amplitude, both of which are directly influenced by the iodine concentration in

the staining bath. Interestingly, liver staining revealed a unique absorption profile better characterized by a double Weibull distribution[23], resembling a double exponential distribution. This distinct pattern likely reflects the liver's dual vascular and duct systems.

To enhance clinical relevance, the study linked staining duration to the CRL and weight, both of which are widely used in clinical practice and are correlated with gestational age, and their relationship holds in cases with similar degrees of maceration. Maceration may confound the relationships among the CRL, weight, and staining duration. It is hypothesized that maceration alters tissue permeability, affecting iodine diffusion and contributing to variability in staining results[17]. Although higher maceration levels are associated with lower-quality MCT images, diagnostic accuracy is often still achievable[16]. Further studies should explore the impact of maceration levels and modes of death on staining protocols to refine techniques and improve imaging consistency in clinical scenarios.

The primary limitation of this study is its small sample size (n=18 fetuses), which may affect the generalizability of the findings. The handfree ROI delineation which may have a great variability intra and inter observatory. The several fetus size with organs size and density variability which may affect diffusion. However, its principal strength lies in its focus on a homogeneous population of nonmacerated fetuses from abortions, minimizing variability. Given the minimal maceration observed, these findings likely extend to cases of fresh miscarriage and termination of pregnancy.

CONCLUSIONS

In conclusion, the use of an iodine staining bath offers significant advantages in enhancing contrast in Dice MCT imaging of first-trimester human nonmacerated fetuses.

By tailoring the staining duration to fetal CRL or weight, optimal imaging outcomes can be achieved, facilitating more accurate and detailed analyses in both research and clinical settings.

List of abbreviations

- contrast-to-noise ratio (CNR)
- crown-rump length (CRL)
- diffusible iodine-based contrast enhanced (Dice)
- Fetal Enhanced Three-dimensional and Translational Anatomical Landscape (FETTAL)
- mean signal (MS)
- microfocus computed tomography (MCT)
- paraformaldehyde (PFA)
- Region of interest (ROI)
- signal-to-noise ratio (SNR)
- standard deviation (SD)
- weeks of gestation (WG)

Declarations

- Ethics approval and consent to participate

Institutional Review Board approval was obtained. This study was authorized by the French Biomedicine Agency (PFS14-020 on January 29, 2015)

- Consent for publication

Not applicable

- Availability of data and materials

The datasets used and/or analysed during the current study are available from the corresponding author on reasonable request.

- Competing interests

The authors declare that they have no competing interests

- Funding

The authors state that this work has not received any funding.

- Authors' contributions

Conceptualization and methodology were performed by AL, GS, CGB, DG and GC. The Project administration by AL and GC. Acquisitions via microCT were performed by AL, MC and CB. Post processing and software were used by AL, MC, CB, GS et CGB. Plot and statistical analysis were performed by AL, MC and CGB. AL was a major contributor in writing the manuscript. CB participate to write the manuscript. All authors read and approved the final manuscript.

- Acknowledgements

We are grateful to all the women who participated in this research project, making this work possible. We thank the Montpellier university hospital obstetrics team, particularly Pierre Boulot (MD, PhD) for his support. We thank Elisabetta Andermarcher for her careful English language proofreading.

- Authors' information (optional)

REFERENCES

1. Quenby S, Gallos ID, Dhillon-Smith RK, Podesek M, Stephenson MD, Fisher J, et al. Miscarriage matters: the epidemiological, physical, psychological, and

341 economic costs of early pregnancy loss. *The Lancet* 2021; 397: 1658–1667.
342 2. Légifrance - Droit national en vigueur - Circulaires et instructions -
343 CIRCULAIRE N° DGOS/R1/2015/140 du 22 avril 2015 relative à la campagne tarifaire
344 et budgétaire 2015 des établissements de santé.,
345 https://www.legifrance.gouv.fr/download/pdf/circ?id=39565 (accessed 8 November
346 2024).
347 3. Lewis C, Riddington M, Hill M, Arthurs OJ, Hutchinson JC, Chitty LS, et
348 al. Availability of less invasive prenatal, perinatal and paediatric autopsy will improve
349 uptake rates: a mixed-methods study with bereaved parents. *BJOG* 2019; 126: 745–753.
350 4. Kang X, Cos T, Guizani M, Cannie MM, Segers V, Jani JC. Parental
351 acceptance of minimally invasive fetal and neonatal autopsy compared with conventional
352 autopsy. *Prenatal Diagnosis* 2014; 34: 1106–1110.
353 5. Cannie M, Votino C, Moerman Ph, Vanheste R, Segers V, Van Berkel K,
354 et al. Acceptance, reliability and confidence of diagnosis of fetal and neonatal virtuopsy
355 compared with conventional autopsy: a prospective study. *Ultrasound in Obstetrics &*
356 *Gynecology* 2012; 39: 659–665.
357 6. Lewis C, Hill M, Arthurs OJ, Hutchinson C, Chitty LS, Sebire NJ. Factors
358 affecting uptake of postmortem examination in the prenatal, perinatal and paediatric
359 setting. *BJOG* 2018; 125: 172–181.
360 7. Shelmerdine SC, Arthurs OJ. Postmortem perinatal imaging: what is the
361 evidence? *BJR* 2022; 20211078.
362 8. Simcock IC, Lamouroux A, Sebire NJ, Shelmerdine SC, Arthurs OJ. Less-
363 invasive autopsy for early pregnancy loss. *Prenat Diagn* 2023; 43: 937–949.
364 9. Simcock IC, Shelmerdine SC, Hutchinson JC, Sebire NJ, Arthurs OJ.

365 Human fetal whole-body postmortem microfocus computed tomographic imaging. *Nat*
366 *Protoc*. Epub ahead of print 14 April 2021. DOI: 10.1038/s41596-021-00512-6.
367 10. Dawood Y, Strijkers GJ, Limpens J, Oostra RJ, de Bakker BS. Novel
368 imaging techniques to study postmortem human fetal anatomy: a systematic review on
369 microfocus-CT and ultrahigh-field MRI. *Eur Radiol*. Epub ahead of print 13 December
370 2019. DOI: 10.1007/s00330-019-06543-8.
371 11. Hutchinson JC, Kang X, Shelmerdine SC, Segers V, Lombardi CM,
372 Cannie MM, et al. Postmortem microfocus computed tomography for early gestation
373 fetuses: a validation study against conventional autopsy. *American Journal of Obstetrics*
374 *and Gynecology* 2018; 218: 445.e1-445.e12.
375 12. Shelmerdine SC, Simcock IC, Hutchinson JC, Guy A, Ashworth MT,
376 Sebire NJ, et al. Postmortem microfocus computed tomography for noninvasive
377 autopsies: experience in >250 human fetuses. *Am J Obstet Gynecol* 2021; 224: 103.e1-
378 103.e15.
379 13. Lombardi CM, Zambelli V, Botta G, Moltrasio F, Cattoretti G, Lucchini
380 V, et al. Postmortem microcomputed tomography (micro-CT) of small fetuses and hearts.
381 *Ultrasound Obstet Gynecol* 2014; 44: 600–609.
382 14. Lamouroux A, Cardoso M, Bottero C, Gallo M, Duraes M, Salerno J, et
383 al. Micro-CT and high-field MRI for studying very early postmortem human fetal
384 anatomy at 8 weeks of gestation. *Prenat Diagn* 2024; 44: 3–14.
385 15. Dawood Y, Honhoff C, van der Post A-S, Roosendaal SD, Coolen BF,
386 Strijkers GJ, et al. Comparison of postmortem whole-body contrast-enhanced microfocus
387 computed tomography and high-field magnetic resonance imaging of human fetuses.
388 *Ultrasound Obstet Gynecol* 2022; 60: 109–117.

16. Simcock IC, Shelmerdine SC, Langan D, Anna G, Sebire NJ, Arthurs OJ. Micro-CT yields high image quality in human fetal postmortem imaging despite maceration. *BMC Med Imaging* 2021; 21: 128.

17. Simcock IC, Shelmerdine SC, Hutchinson JC, Sebire NJ, Arthurs OJ. Body weight-based iodinated contrast immersion timing for human fetal postmortem microfocus computed tomography. *BJR Open* 2023; 6: tzad006.

18. Gignac PM, Kley NJ, Clarke JA, Colbert MW, Morhardt AC, Cerio D, et al. Diffusible iodine-based contrast-enhanced computed tomography (diceCT): an emerging tool for rapid, high-resolution, 3-D imaging of metazoan soft tissues. *J Anat* 2016; 228: 889–909.

19. Stauffer D, Aharony A. *Introduction To Percolation Theory: Second Edition*. 2nd ed. London: Taylor & Francis. Epub ahead of print 10 December 2018. DOI: 10.1201/9781315274386.

20. Lee KC, Siegel J, Webb SE, Lévêque-Fort S, Cole MJ, Jones R, et al. Application of the stretched exponential function to fluorescence lifetime imaging. *Biophys J* 2001; 81: 1265–1274.

21. Lamouroux A, Genevieve D, Fuchs F, Letouzey V, Subsol G, Captier G. OC18. 01: Fetal enhanced tridimensional and translational anatomical landscape: FETTAL Project. *UOG* 2017; 37.

22. Jayakumar K, Babu MG. Some Generalizations of Weibull Distribution and Related Processes. *J Stat Theory Appl* 2015; 14: 425–434.

23. Weibull W. A Statistical Distribution Function of Wide Applicability. *Journal of Applied Mechanics* 1951; 18: 293–297, hal-03112318.

24. Germann M, Shim S, Angst F, Saltybaeva N, Boss A. Spiral breast

computed tomography (CT): signal-to-noise and dose optimization using 3D-printed phantoms. *Eur Radiol* 2021; 31: 3693–3702.

25. Genolini Christophe, Evain Andeol, Lopez Julien, Heinrich Marc. 'R++, l'essentiel', version 1.6.15, for Windows, released 2024-03-25.

26. Robinson HP. Sonar Measurement of Fetal Crown-Rump Length as Means of Assessing Maturity in First Trimester of Pregnancy. *Br Med J* 1973; 4: 28–31.

27. Hsieh SS, Leng S, Yu L, Huber NR, McCollough CH. A minimum SNR criterion for computed tomography object detection in the projection domain. *Med Phys* 2022; 49: 4988–4998.

FIGURES

Figure 1 - Dynamic representation of contrast agent diffusion in foetus S0 (female sex; CRL = 80 mm, interparietal diameter = 14 mm, foot length = 14 mm, weight = 30,06 g, 13+4 WG) as a function of the staining time. The upper, middle and lower panels depict cerebral, thoracic, and abdominal sections of the foetus, respectively.

Figure 2 – Time-dependent uptake of the contrast agent in various target fetuses (top graph) and in the lung and liver, focusing on different regions: peripheral (A), central (B) and hilum (C). The uptake was measured in arbitrary units (au) over the duration of staining.

Figure 3 – Scatter plot illustrating the correlation between fetal crown–rump length (CRL) in millimeters and fetal weight in grams and staining duration in hours. The data points are color-coded on the basis of the contrast-to-noise ratio (CNR), with a gradient ranging from red (low CNR) to dark green (high CNR). The dotted line indicates

436 the threshold where the CNR reaches 5, in accordance with the Rose criterion[27].
437 *Staining duration = 2CRL - 12 = 2weight + 12.5*

438 # TABLES

439 Table 1 – Fetal characteristics (crown-rump length (CRL), weight and gestational
440 age), micro-CT preparation (staining duration), acquisition details (filter, voltage and
441 current) and contrast–to–noise ratio (CNR) between the lung and liver (WG = weeks of
442 gestation, SD = standard deviation).

443 Table 2 – Diffusion characteristics of the iodine solution in the target organs on
444 the basis of the Weibull distribution and stretched exponential models. The stretched
445 exponential function is $S = A_0 + A_{max}(1 - \exp^{-(\frac{t-t_0}{\lambda})^{-\beta}})$, where A_0 is the initial
446 amplitude or baseline value of the signal, A_{max} is the maximum change, t_0 represents the
447 starting time, λ is the characteristic time scale, and β is the stretching exponent. (SNR =
448 signal-to-noise ratio)

449 # SUPPLEMENTAL MATERIAL

450 Supplemental material 1 – Video - Time-lapse visualization of contrast agent
451 uptake in cerebral sections of foetus S0 (female sex; CRL = 80 mm, interparietal diameter
452 = 14 mm, foot length = 14 mm, weight = 30,06 g, 13+4 WG) via micro-CT imaging. This
453 video demonstrates the dynamic diffusion process within the brain structures over the
454 duration of staining.

455 Supplemental material 2 – Video - Time-lapse visualization of contrast agent
456 uptake in the torso section of foetus S0 (female sex; CRL = 80 mm, interparietal diameter
457 = 14 mm, foot length = 14 mm, weight = 30,06 g, 13+4 WG) via micro-CT imaging. The

458 video highlights the progression of staining in the thoracic region, including the cardiac
459 chambers and major thoracic organs, as a function of time.
460 Supplemental material 3 – Video - Time-lapse visualization of contrast agent
461 uptake in the abdominal section of foetus S0 (female sex; CRL = 80 mm, interparietal
462 diameter = 14 mm, foot length = 14 mm, weight = 30,06 g, 13+4 WG) via micro-CT
463 imaging. This video shows the dynamic diffusion process over the duration of staining,
464 with a focus on abdominal organs such as the liver, spleen, stomach, and adrenal glands.
465 Supplemental material 4 - Figure – Time-dependent decay of the contrast agent in
466 various sections of the staining bath via micro-CT imaging. The decay is expressed in
467 arbitrary units (au) and plotted against the staining duration, illustrating the reduction in
468 iodine concentration in the bath over time.
469
470

ANNEXE 3

Lamouroux A, Cardoso M, Bottero C, Gallo M, Duraes M, Salerno J, Bertrand M, Rigau V, Fuchs F, Mousty E, Genevieve D, Subsol G, Goze-Bac C, & Captier G.

Micro-CT and high-field MRI for studying very early post-mortem human fetal anatomy at 8 weeks of gestation.

Prenat Diagn 2024; 44: 3–14.

Received: 7 June 2023 | Revised: 19 October 2023 | Accepted: 2 December 2023

DOI: 10.1002/pd.6489

ORIGINAL ARTICLE

PRENATAL DIAGNOSIS WILEY

Micro-CT and high-field MRI for studying very early post-mortem human fetal anatomy at 8 weeks of gestation

Audrey Lamouroux[1,2,3,4,5] | Maïda Cardoso[3,5] | Célia Bottero[2,5] | Mathieu Gallo[5,6] | Martha Duraes[4,5,7,8] | Jennifer Salerno[2,5,9] | Martin Bertrand[5,10,11] | Valérie Rigau[5,6] | Florent Fuchs[5,8,12,13] | Eve Mousty[2,5] | David Genevieve[1,5,14] | Gérard Subsol[4,5] | Christophe Goze-Bac[3,5] | Guillaume Captier[4,5,7,15]

[1]Clinical Genetics Department, Montpellier University Hospital, University of Montpellier, Montpellier, France

[2]Obstetrical Gynaecology Department, Nîmes University Hospital, University of Montpellier, Nîmes, France

[3]Charles Coulomb Laboratory, UMR 5221 CNRS-UM, BNIF User Facility Imaging, University of Montpellier, CNRS, Montpellier, France

[4]ICAR Research Team, LIRMM, University of Montpellier, CNRS, Montpellier, France

[5]Univ. Montpellier, Montpellier, France

[6]Pathology Department, Montpellier University Hospital, University of Montpellier, Montpellier, France

[7]Anatomy Laboratory, Faculty of Medicine Montpellier-Nimes, University of Montpellier, Montpellier, France

[8]Obstetrical Gynaecology Department, Montpellier University Hospital, University of Montpellier, Montpellier, France

[9]Gynaecology and Gynaecology Surgery Department, Clinique Beau Soleil, Montpellier, France

[10]Experimental Anatomy Department, Faculty of Medicine Montpellier-Nimes, University Montpellier, Nîmes, France

[11]Digestive Surgery Department, Nimes University Hospital, Nîmes, France

[12]Inserm, CESP Center for Research in Epidemiology and Population Health, U1018, Reproduction and Child Development, Villejuif, France

[13]Desbrest Institute of Epidemiology and Public Health (IDESP), University of Montpellier, INSERM, Montpellier, France

[14]Center for Rare Disease Development Anomaly and Malformative Syndromes, Montpellier University Hospital, Montpellier, France

[15]Paediatric Surgery Department, Montpellier University Hospital, University of Montpellier, Montpellier, France

Correspondence
Audrey Lamouroux, Fetopathology Unit, Clinical Genetics Department, Montpellier University Hospital, 371, Av du Doyen Gaston Giraud, Montpellier 34090, France.
Email: a-lamouroux@chu-montpellier.fr

Funding information
Montpellier University Hospital: MobilityGrant; Nîmes University Hospital: MobilityGrant; Agence Nationale de la Recherche, Grant/Award Number: ANR-10-INBS-04; Labex CEMEB, Grant/Award Number: ANR-10-LABX-0004; NUMEV, Grant/Award Number: ANR-10-LABX-0020; Nîmes

Abstract

Objective: This study involved very early post-mortem (PM) examination of human fetal anatomy at 8 weeks of gestation (WG) using whole-body multimodal micro-imaging: micro-CT and high-field MRI (HF-MRI). We discuss the potential place of this imaging in early first-trimester virtual autopsy.

Methods: We performed micro-CT after different contrast-bath protocols including diffusible iodine-based contrast-enhanced (dice) and HF-MRI with a 9.4 T machine with qualitative and quantitative evaluation and obtained histological sections.

Results: Nine fetuses were included: the crown–rump length was 10–24 mm and corresponded to 7 and 9 WG according to the Robinson formula. The Carnegie stages were 17–21. Dice micro-CT and HF-MRI presented high signal to noise ratio, >5, according to the Rose criterion, and for allowed anatomical phenotyping in these

Some images from micro-imaging of these specimens were previously presented at the International Society of Ultrasound in Obstetrics & Gynaecology World Congress and at the "Association Française des Morphologistes" meeting in 2017.

 © 2024 John Wiley & Sons Ltd.

specimens. Imaging did not alter the histology, allowing immunostaining and pathological examination.

Conclusion: PM non-destructive whole-body multimodal micro-imaging: dice micro-CT and HF-MRI allows for PM human fetal anatomy study as early as 8 WG. It paves the way to virtual autopsy in the very early first trimester. Obtaining a precision phenotype, even regarding miscarriage products, allows a reverse phenotyping to select variants of interest in genome-wide analysis, offering potential genetic counseling for bereaved parents.

Key points

What's already known about this topic?

- Autopsies considered too invasive are often refused by grieving couples after fetal loss.
- Fetal virtual autopsy has developed with standard imaging (MRI and CT) used after 24 weeks of gestation (WG) and micro-CT and high-field MRI (HF-MRI) used from 11 to 24 WG.
- The current scientific literature on micro-CT and HF-MRI before 11 WG is weak.
- Miscarriages are common and require further explorations and research.

What does this study add?

- Iodine-contrast micro-CT and HF-MRI allow for post-mortem human fetal anatomy visualization as early as 8 WG and pave the way for virtual autopsy at very early first trimester and thus precise phenotyping of miscarriage products.
- The choice of either technique will be based on cost, availability, ease of use, target organ of interest, preparation and acquisition duration.
- Micro-imaging does not appear to exclude subsequent histological examination.

1 | INTRODUCTION

The history of human embryology shows that 3D representations such as Da Vinci pictures of the *Fetus in the Womb*[1] and wax models[2,3] are important for studying, teaching and research. The concept of 3D reconstructions of serial histological sections of fetuses was first published in the 1980s.[4] A 3D atlas was published for practical implementation, and De Bakker's team made the atlas available to the scientific community in a dedicated website around 2015.[5,6] Despite computer assistance, these approaches remained tedious to design, gave uneven results, and are destructive to fetuses.[7,8]

To explore fetal death, post-mortem (PM) examination, also called fetopathologic examination, is the gold standard for an accurate diagnosis and aims to allow for genetic counseling and to specify the recurrence risk.[9] PM examination consists of a fetal and placental examination and includes standard radiographs; photographs; external morphology examination with biometric data such as weight, size, cranial perimeter, and foot length; and internal examination (i.e., autopsy).[9] PM examination is summarized in Figure 1. Systematic radiographs have a low diagnostic rate.[10–12] The rate of non-identifying causes of stillbirth is 30%–60%.[13] In case of early termination of pregnancy for medical reasons from 11 to 16 weeks of gestation (WG), PM examination with autopsy adds information in 55% of cases and modifies the genetics counseling in 21%.[14,15] Later in pregnancy, PM explorations may help in the grieving process,[16] and couples refusing autopsy are more likely to regret their choices.[17] However, because of the invasive nature, autopsy and PM examination are often declined by grieving couples.[18]

Consequently, virtual autopsy became possible with PM imaging such as MRI and CT, which have been used in clinical practice since 2010.[19,20] However, the fetal PM MRI diagnostic yield depends on the anatomical area of interest[21–23] and is better than fetal PM CT.[24,25] When results of prenatal ultrasonography and PM whole-body MRI are concordant, there is limited benefit in performing a full autopsy.[26] Virtual autopsy also allows for better-quality brain imaging with fewer technical artefacts due to dissection.[19,20,27] Less invasive autopsy using MRI and CT has lower diagnostic accuracy when the fetus is <24 WG.[24,28] However, virtual autopsy by imaging has numerous advantages: it is non-invasive, data acquisition is fast and reproducible, it allows for less variability between operators and secondary reading of images by experts, and it improved the acceptance rate as compared with conventional autopsy.[29]

Micro-imaging such as micro-CT or high-field MRI (HF-MRI) provide high isotropic resolution of <100 μm. Since 2001, these techniques have led to the development of non-destructive ways of visualizing small specimens such as animal embryos.[7,30–33] They have

RIGHTSLINK

10970223, 2024, 1, Downloaded from https://obgyn.onlinelibrary.wiley.com/doi/10.1002/pd.6489 by Bu Montpellier, Wiley Online Library on [24/10/2024]. See the Terms and Conditions (https://onlinelibrary.wiley.com/terms-and-conditions) on Wiley Online Library for rules of use; OA articles are governed by the applicable Creative Commons License

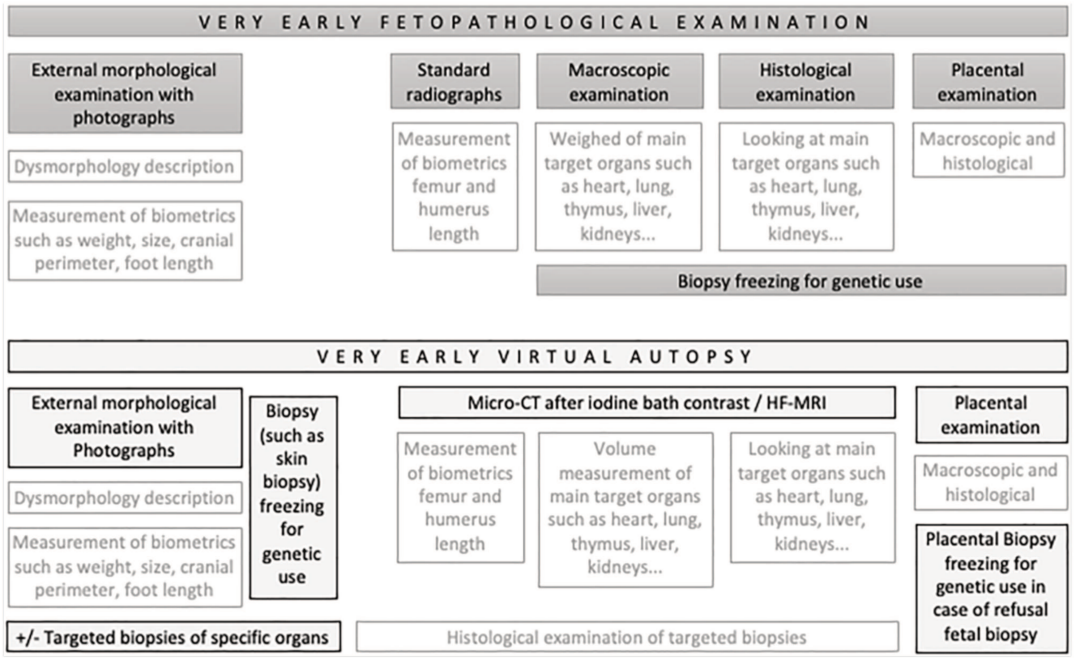

FIGURE 1 Comparison between fetal pathological examination and very early virtual autopsy. HF-MRI, high-field MRI.

also allowed for performing human fetal non-invasive autopsy or virtual autopsy in fetuses <24 WG by using PM micro-imaging such as HF-MRI since 2009[34] and micro-CT since 2017.[35,36] In comparison with HF-MRI, micro-CT is more common, costs less and requires Lugol's iodine solution (I2KI) contrast bath[28,37] before acquisition, which involves less time.[18]

A recent review highlighted that current studies of micro-CT and HF-MRI mostly involved fetuses >11 WG.[28] In comparing PM micro-CT in early gestation to conventional autopsy, Hutchinson et al. included fetuses from 11 to 21 WG.[38] In comparing ultra-HF-MRI versus MRI versus stereomicroscopic autopsy, Votino et al. included hearts at 11–20 WG.[39] Some case reports of micro-CT of fetuses at 6 WG,[40] 7 WG[41] or 9 WG[42] have been published and two publications described fetuses <11 WG: one involved micro-CT with four specimens from 7 to 11 WG[43] and one HF-MRI with four specimens at Carnegie stage 10–20 of about 3–9 WG.[44] Studies combining micro-CT and HF-MRI are few, and the most recent one focused on fetuses from 13 to 18 WG.[45] To our knowledge, no published study investigated multimodal micro-imaging in fetuses <11 WG.

Early fetal loss is often downplayed. However, the psychological consequences of these losses should not be ignored. Indeed, miscarriage matters.[46] Miscarriage is common: 23 million miscarriages occur each year.[46] In the United Kingdom, Quenby et al. estimated the short-term national cost at 471 million pounds per year.[46] Psychological consequences are important and must be better diagnosed and treated.[46] The lack of interest and research on miscarriage was pointed out by a recent review in *The Lancet*.[46,47] So, PM explorations of fetuses <11 WG are valuable for the medical community.

We studied very early PM human fetal anatomy at 8 WG by using whole-body multimodal micro-imaging such as micro-CT and HF-MRI and discuss its potential place in early first-trimester virtual autopsy.

2 | METHODS

We included pregnant women consulting for voluntary termination of pregnancy, the majority, or early spontaneous miscarriage. Information sheets were given to the women during their consultation with the gynecologist or midwife. Written informed consent was obtained from each woman. All consents were revocable at any time. The exclusion criteria were age <18 years or unable to give informed consent such as under guardianship or language barrier. The hospital's service for voluntary interruption of pregnancy collected the specimens after drug-induced expulsion and sometimes before surgical curettage in day hospitalization. Samples came from voluntary terminations of pregnancy and were externally examined by an expert in prenatal diagnosis to confirm malformation absence.

The protocol's workflow was (1) preparation with fixation, (2) imaging by micro-CT scan after staining protocols and by HF-MRI scan, which may be performed first or second, (3) imaging post-

RIGHTSLINK

10970223, 2024, 1, Downloaded from https://obgyn.onlinelibrary.wiley.com/doi/10.1002/pd.6489 by Bu Montpellier, Wiley Online Library on [24/10/2024]. See the Terms and Conditions (https://onlinelibrary.wiley.com/terms-and-conditions) on Wiley Online Library for rules of use; OA articles are governed by the applicable Creative Commons License

treatment, and (4) obtaining several histologic sections obtained to control the procedure.

2.1 | Micro-CT

We performed different preparation protocols before micro-CT acquisition with different fixation times and diffusive contrast baths (Table 1) because preparation data at this early stage was limited. The three first sample preparation protocols[7,48] involved non-fixed (1) and late (2) and early (3) fixed specimens and was based on a contrast bath with a solution of 10% I2KI solution for 24–48 h. This solution was obtained in the hospital pharmacy at the beginning of the study and was stored in a ventilated cabinet. This preparation was also not freshly made for each sample. From the preliminary results and in light of Gignac et al.[49,50] reviewing staining protocols for animal and human specimens, we derived protocol, which included early fixation with paraformaldehyde 4% (PFA 4%) after expulsion without any contrast bath. We finally set up the protocol 5, diffusible iodine-based contrast-enhanced which consisted of immersing the early-fixed specimens with PFA 4% in a 1:1 ratio solution of PFA 4% and potassium triiodide (I2KI/Lugol's iodine solution, with total iodine content 63.25 mg/mL) for 72 h as described by Hutchinson et al.[38] Each preparation was freshly made in our laboratory.

Micro-CT acquisitions involved using the X-ray microtomographs SkyScan 1076 and SkyScan 1276 (Bruker) as detailed in Table 2. In both cases, micro-CT settings such as spatial resolution, x-ray attenuation, power, and best filter were carefully determined and adjusted to the properties of the specimens to optimize the contrast between the tissues and the organs of interest (Table 2).

2.2 | High-field MRI

To enhance the contrast and safeness, the early-fixed specimens were immersed in fluorinert (PF40) in a hermetically sealed falcon tube during acquisition. HF-MRI acquisitions were performed on an Agilent 9.4 T MRI scanner using 3D gradient echo multiple slices with data matrix setting 512 × 256 × 256 isotropic voxels. HF-MRI settings such as repetition time, echo time and accumulation were carefully determined and adjusted to the size and properties of the specimens for optimizing the contrast (detailed in Table 2).

2.3 | Image processing

In micro-CT, the native images were first processed by using NRecon software (SkyScan, Bruker), which transforms serial views into CT. In some cases, DicomCT software was needed to convert TIFF files to DICOM (or dcm) files. Image processing and analysis of the HF-MRI acquisitions involved using homebuilt routines under the Matlab interface in DICOM format. The DICOM 3D reconstructions of the micro-imaging were post-processed and visualized by using Dataviewer v1.5.6.2 (SkyScan, Bruker); FIJI ImageJ v1.53q; Myrian v64 1.19.1 (Intrasense) and CT-Vox v3.3.0 r1383 (Bruker microCT) software.

To highlight the potential clinical use of imaging, we aimed to match our imaging modalities with pictures illustrating ultrasound slices as recommended by the Conférence Nationale d'Echographie Obstétricale et Fœtale (CNEOF) group. These pictures are extracted from the French guidelines for good practice in obstetrical and fetal ultrasonography for second- and third-trimester ultrasound scans.[51]

We performed a quantitative evaluation of signal-to-noise ratio (SNR) and contrast-to-noise ratio (CNR) for both imaging modalities. The different parameters were measured by using FIJI software with an evaluation of mean signal and its standard deviation of a specific region of interest. The noise was evaluated from the standard deviation of the cradle signal.

2.4 | Histology sections

Two specimens, S1 and S9 (Table 2), underwent standard histology examination with hematoxylin and eosin staining and vascular immunostaining with CD34 to assess whether the specimen could be damaged, labeled or distorted by the contrast bath and micro-CT and HF-MRI acquisitions.

TABLE 1 Detailed contrast bath protocols used.

	Timing of the fixation in PFA 4%	Contrast bath	I2KI 10% made in hospital pharmacy (contrast bath duration in h)	PFA 4% and I2KI/Lugol's iodine, in a 1:1 ratio made freshly (contrast bath duration in h)
Protocol 1	No	Done	48	
Protocol 2	Late	Done	48	
Protocol 3	Early	Done	48	
Protocol 4	Early	No		
Protocol 5	Early	Done		72

Abbreviations: I2KI, iodine potassium iodide 10% solution; PFA 4%, paraformaldehyde 4%.

RIGHTSLINK

10970223, 2024, 1, Downloaded from https://obgyn.onlinelibrary.wiley.com/doi/10.1002/pd.6489 by Bu Montpellier, Wiley Online Library on [24/10/2024]. See the Terms and Conditions (https://onlinelibrary.wiley.com/terms-and-conditions) on Wiley Online Library for rules of use; OA articles are governed by the applicable Creative Commons License

TABLE 2 Specimens included in the present study with their detailed characteristics, their preparation before micro-imaging, the type of micro-imaging performed and micro-imaging acquisition parameters.

	Specimen characteristics				Micro-CT acquisition							HF-MRI acquisition						
Specimens	Gestational age according to the Robinson formula (WG)	Crown–rump length (mm)	Weight (mg)	Carnegie stage	Preparation before micro-CT	Micro-CT machine: SkyScan	Source voltage (kV)/current (μA)	Filter	Rotation step (degree)	Image pixel size (μm)	Scan duration (min)	Repetition time (ms)	Echo time (ms)	Flip angle (degree)	Average	Field of view (mm)	Voxel size (μm)	Scan duration (h)	Histology
S1	7 + 3	12	300	17	Protocol 5	1276	87/175	Al 0.5 mm	0.4	15	31	100	4.87	70	4	30 × 15 × 15	59	7 h16	1
S2	7 + 5	14	243	18	Protocol 4	1276	44/100	No filter	0.4	15	34	100	5.30	70	6	24 × 12 × 12	47	10 h 55	
					Protocol 5	1276	95/166	Al 0.5 mm	0.4	15	32								
S3	8	16	293	19	Protocol 5	1276	94/155	Al 0.5 mm	0.4	18	31	100	5.30	70	6	24 × 12 × 12	47	10 h 55	
S4	8 + 1	17		19	Protocol 1	1076	59/167	No filter	0.1	9	134								
					Protocol 2	1076	59/167	Ti 0.025 mm	0.34	36	22								
S5	8 + 3	19	678	20	Protocol 5	1276	80/200	Al 0.5 mm	0.4	10	31	100	4.87	70	6	30 × 15 × 15	59	10 h 55	
S6	8 + 4	20	700	20	Protocol 4	1276	55/200	Al 0.25 mm	0.4	20	32	100	4.76	70	6	32 × 16 × 16	62	10 h 55	
S7	8 + 4	20	690	20	Protocol 5	1276	95/200	Al 1 mm	0.4	14	10	100	4.87	70	6	30 × 15 × 15	59	10 h 55	
S8	8 + 5	21	1047	21	Protocol 4	1276	55/200	Al 0.25 mm	0.4	21	28	100	4.76	70	6	32 × 16 × 16	62	10 h 55	
					Protocol 5	1276	98/200	Al 1 mm	0.2	10	87								
S9	8 + 6	22	1000	21	Protocol 4	1076	59/167	Ti 0.025 mm	0.2	36	38	60	4.87	70	4			4 h 28	1
					Protocol 3	1076	59/167	Ti 0.025 mm	0.2	36	38								

Abbreviation: WG, weeks of gestation.

RIGHTSLINK

10970223, 2024, 1, Downloaded from https://obgyn.onlinelibrary.wiley.com/doi/10.1002/pd.6489 by Bu Montpellier, Wiley Online Library on [24/10/2024]. See the Terms and Conditions (https://onlinelibrary.wiley.com/terms-and-conditions) on Wiley Online Library for rules of use; OA articles are governed by the applicable Creative Commons License

The French biomedicine agency (ABM) approved the FETTAL project (fetal enhanced three-dimensional and translational anatomical landscape project).[52,53] This study is part of that project.

3 | RESULTS

Specimens were collected over 6 years, which resulted in a large sample of 75 fetuses. Twenty-three specimens were excluded because of incomplete miscarriage, partial fetus, or damaged specimens and 18 specimens were included in the genetics part of the FETTAL project. Among the 34 non-malformed fetuses included in the imaging part of the FETTAL project, the present study focused on the nine specimens with crown–rump length (CRL) 10–24 mm and CRL-based gestational age from 7 to 9 WG according to the Robinson formula (Figure 2). Selected specimen characteristics such as CRL, gestational age, weight and Carnegie stage are summarized in Table 2.

3.1 | Micro-imaging

Table 2 presents the micro-CT preparation protocols and acquisition parameters: machine, source voltage and current, filter use, image pixel size and scan duration; and HF-MRI acquisition parameters.

Protocols 1–4 gave no contrast, just natural contrast (left part of Figure 3). However, micro-CT images with the protocol 5 were well contrasted and resulted in informative images. We also detail the anatomy of specimen S8 on the right part of Figure 3: tongue (1), esophagus (2), trachea (3), and aorta (ascending [4] and descending

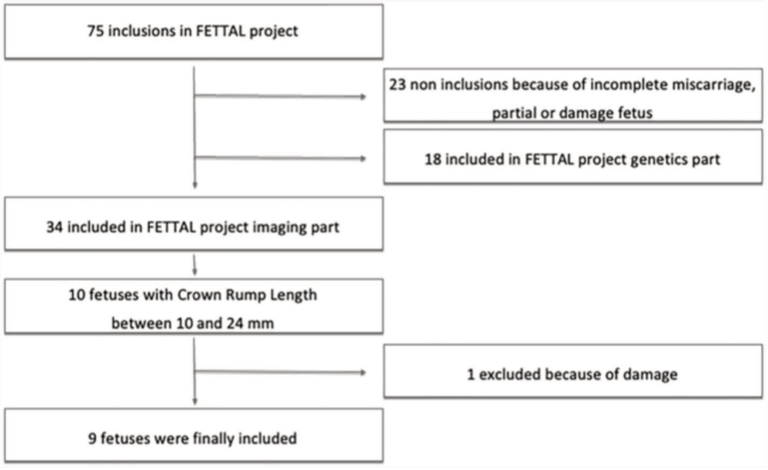

FIGURE 2 Flowchart with detailed cohort selection. CRL, crown–rump length; FETTAL, fetal enhanced three-dimensional and translational anatomical landscape project.

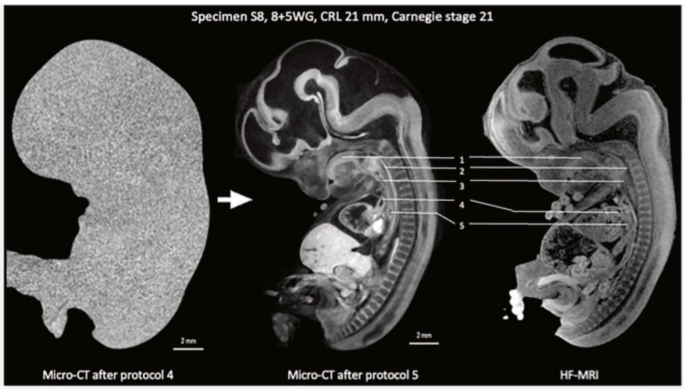

FIGURE 3 Micro-CT sagittal slice after protocol 4 (early fixation without any contrast bath) and protocol 5 (early fixation and 72 h immersion in contrast bath 1:1 ratio of PFA 4% and I2KI/Lugol's iodine made freshly) on specimen S9 (CRL, crown–rump length; WG, weeks of gestation). Using DataViewer (CT) software. (1: tongue; 2: esophagus; 3: trachea; 4: ascending aorta arch; 5 descending aorta). PFA 4%, paraformaldehyde 4%.

RIGHTSLINK

10970223, 2024, 1, Downloaded from https://obgyn.onlinelibrary.wiley.com/doi/10.1002/pd.6489 by Bu Montpellier, Wiley Online Library on [24/10/2024]. See the Terms and Conditions (https://onlinelibrary.wiley.com/terms-and-conditions) on Wiley Online Library for rules of use; OA articles are governed by the applicable Creative Commons License

[5]) can be clearly identified using both micro-CT with protocol 5 and HF-MRI.

Figure 4 shows the median sagittal view with micro-CT using protocol 5 and HF-MRI at different Carnegie stages in a fetus at about 8 WG. The detailed anatomy of these specimens is accessible clinically. Figure 4 presents the thoracic-abdominal sagittal view of specimen S3. Unfortunately, this specimen had a rotation of the head, so the sagittal view of the head is in another plane.

Three different pictures (inter-orbital distance, four-chamber view with pulmonary veins, transversal kidney view) are available from the CNEOF group French guidelines. These reference pictures aim to illustrate ultrasound images obtained during second- and third-trimester ultrasonography. We matched these pictures with slices of micro-CT using protocol 5 and HF-MRI for specimens S5 and S8 (Figure 5). The thorax or abdominal transversal view is more circular during the second and third trimesters and more oval during the first trimester.

We performed quantitative signal evaluation using SNR and CNR. On inter-orbital distance view, the contrast is calculated between the crystalline lens and vitreous body; on four-chamber view, between the right ventricular wall and pericardium and on transversal kidney view, between the renal cortex and perinephric fat. The mean SNR with micro-CT and HF-MRI was 7.6 and 8.9, respectively and the mean CNR was 6.2 and 4.8, respectively (Figure 6). So, our experimental conditions gave high SNR, >5, according to the Rose criterion[54] and good CNR in most of the cases in both micro-CT using protocol 5 and HF-MRI.

3.2 | Histology

Specimen S9 underwent both protocol 3 and 4 and specimen S1 protocol 5. Histology sections were submitted to a pathology specialist who did not find any damage or artifact or distortion. Coloration was homogenous, and quality was compatible with diagnosis. The histology sections were immunostained with CD34, which was positive (Figure 7), despite the preparation protocols and micro-imaging acquisitions. Imaging did not alter the histology, allowing immunostaining and pathological examination.

4 | DISCUSSION

This study shows the feasibility of investigating very early PM human fetal anatomy at 8 WG using whole-body multimodal micro-imaging such as micro-CT using protocol 5 and HF-MRI. The non-destructive morphological visualization of the inner organs as early as 8 WG paves the way to virtual autopsy in the very early stage of the first trimester, which was limited until now.

As previously mentioned, a recent review highlighted the current limitations of imaging after 11 WG[28] except for some micro-CT case reports[40–42] and two small series of 4 cases.[43,44] We report for the first time the largest micro-imaging cohort of very young fetuses, around 8 WG. Several teams focused on a specific organ such as the heart,[55] brain,[56] and sacral artery.[57] As shown in our figures, the whole-body acquisitions can easily be used to focus on the desired

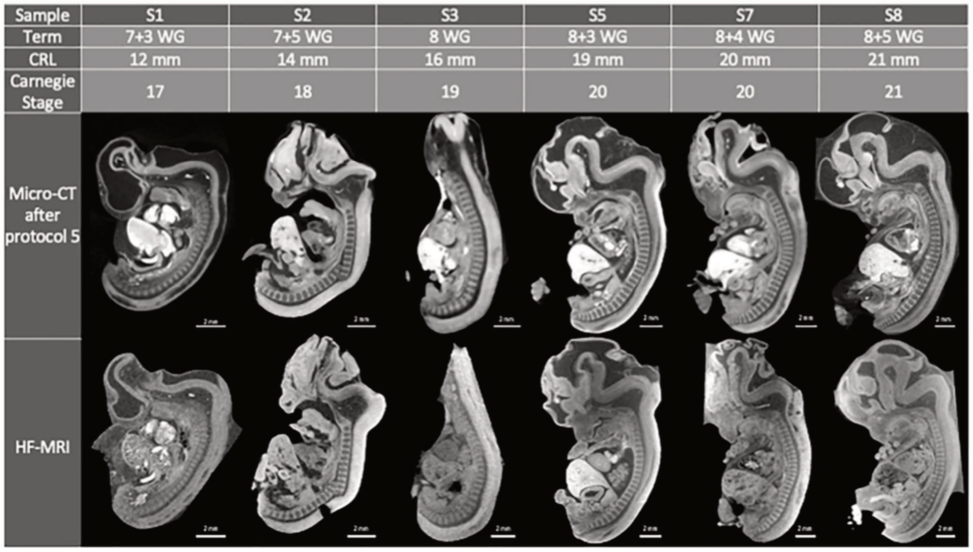

FIGURE 4 Sagittal view of six specimens with both micro-CT after protocol 5 (early fixation and 72 h immersion in contrast bath 1:1 ratio of PFA 4% and I2KI/Lugol's iodine made freshly) and HF-MRI using DataViewer (CT) and Myrian (MRI) software. CRL, crown–rump length; HF-MRI, high-field MRI; PFA 4%, paraformaldehyde 4%; WG, weeks of gestation.

RIGHTSLINK

10970223, 2024, 1, Downloaded from https://obgyn.onlinelibrary.wiley.com/doi/10.1002/pd.6489 by Bu Montpellier, Wiley Online Library on [24/10/2024]. See the Terms and Conditions (https://onlinelibrary.wiley.com/terms-and-conditions) on Wiley Online Library for rules of use; OA articles are governed by the applicable Creative Commons License

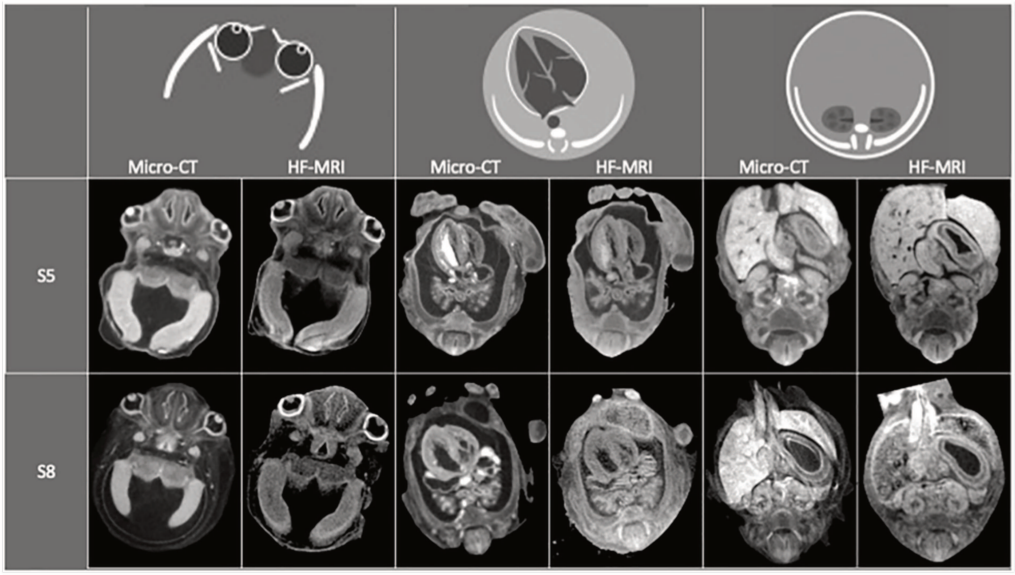

FIGURE 5 Specimens S5 and S8 with both micro-CT after protocol 5 (early fixation and 72 h immersion in contrast bath 1:1 ratio of PFA 4% and I2KI/Lugol's iodine made freshly) and HF-MRI in different slices matched with inter orbital distance view, four-chamber view with pulmonary veins, transversal-kidney view from the CNEOF French guidelines group[52] using DataViewer (CT) and Myrian (MRI) software. CNEOF, Conférence Nationale d'Echographie Obstétricale et Fœtale; HF-MRI, high-field MRI; PFA 4%, paraformaldehyde 4%.

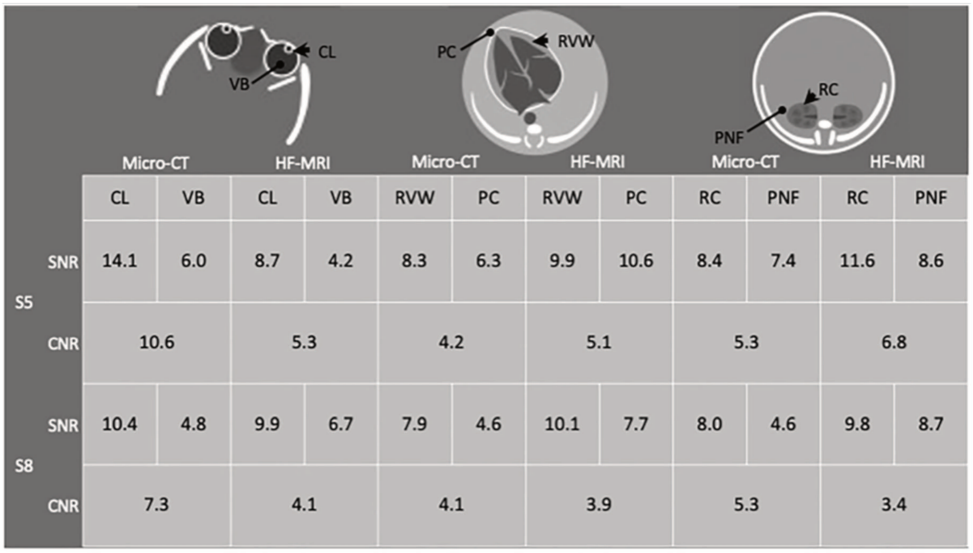

		CL	VB	CL	VB	RVW	PC	RVW	PC	RC	PNF	RC	PNF
S5	SNR	14.1	6.0	8.7	4.2	8.3	6.3	9.9	10.6	8.4	7.4	11.6	8.6
	CNR	10.6		5.3		4.2		5.1		5.3		6.8	
S8	SNR	10.4	4.8	9.9	6.7	7.9	4.6	10.1	7.7	8.0	4.6	9.8	8.7
	CNR	7.3		4.1		4.1		3.9		5.3		3.4	

FIGURE 6 Quantitative signal evaluation of specimens S5 and S8 using SNR and CNR ratio. Arrowheads highlight CL, RVW and RC and round tip arrows highlight VB, PC and PNF. CL, crystalline lens; CNR, contrast to noise; PC, pericardium; PNF, perinephric fat; RC, renal cortex; RVW, right ventricular wall; SNR, signal to noise; VB, vitreous body.

RIGHTSLINK

10970223, 2024, 1, Downloaded from https://obgyn.onlinelibrary.wiley.com/doi/10.1002/pd.6489 by Bu Montpellier, Wiley Online Library on [24/10/2024]. See the Terms and Conditions (https://onlinelibrary.wiley.com/terms-and-conditions) on Wiley Online Library for rules of use; OA articles are governed by the applicable Creative Commons License

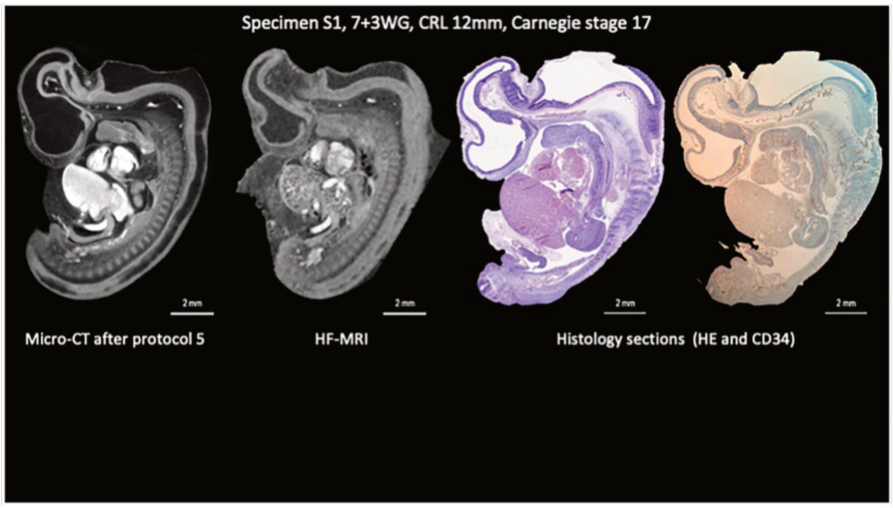

FIGURE 7 Specimen S1 sagittal slice with micro-CT after protocol 5 (early fixation and 72 h immersion in contrast bath 1:1 ratio of PFA 4% and I2KI/Lugol's iodine made freshly), HF-MRI and histology in hematoxylin eosin and CD34 immunohistochemical staining using DataViewer (CT) and Myrian (MRI) software. HF-MRI, high-field MRI; CRL, crown–rump length; PFA 4%, paraformaldehyde 4%; WG, weeks of gestation. [Colour figure can be viewed at wileyonlinelibrary.com]

organ. As shown in Figure 5, PM micro-imaging allows an anatomical examination with better accuracy than second or third trimester prenatal ultrasonography as early as 8 WG. Micro-CT and HF-MRI were found useful for virtual autopsy before 20 WG,[10,28] and here we demonstrate that it can be reasonably extended to 8 WG.

Limitations of the present work are the small sample size for each of the modalities and the unicentric experience with only local expertise.

As compared with other protocols, iodinated micro-CT (using protocol 5) results in well-contrasted images, as shown in Figure 3. Our results are in favor of the need for early fixation before any contrast bath.[50] Therefore, the protocol 5 preparation should be freshly made just before use.[37] This protocol is specific because of its mixed character using a conservative solution (PFA 4%) and contrast solution (potassium triiodide I2KI/Lugol's iodine solution).[35] A study comparing different previously published contrast baths might help support these observations.

Both iodinated micro-CT using protocol 5 and HF-MRI are valuable and result in great signal (SNR >5 according to the Rose criterion[54]) and comfortable CNR. The spatial resolution is better with micro-CT, 9–36 µm, as compared with HF-MRI, >50 µm. The scan duration is variable, from about 30 min with micro-CT to 10 h with HF-MRI (Table 2), which favors the clinical use of micro-CT. However, a preparation protocol with contrast bath before micro-CT takes time, about 72 h, whereas no preparation protocol is needed for HF-MRI. HF-MRI is the only technique used in preclinical imaging at present.[10,18] However, micro-CT is now used for virtual autopsy clinically.[18,37,58] HF-MRI machines are more expensive than micro-CT tomographs and are probably less available around the world. Because of the short learning curve for using micro-CT, this technology is probably more accessible to a wider range of practitioners. In contrast, HF-MRI needs specific expertise. In conclusion, each technique has its advantages and limitations, and the choice could probably be guided by the purpose: clinical use or research into embryology or a specific organ.

This study shows non-macerated fetuses without any malformation, which enables high-quality anatomical analysis. The use of these imaging techniques in clinical practice will need to take account of and adapt to fetal maceration. Maceration may create artefacts even though anatomical examination remains possible.[59]

Others considered that micro-CT has better diagnostic value and quality of imaging on quantitative and qualitative outcomes than HF-MRI.[45] Figure 4 highlights the high liver absorption of the iodine contrast. This high absorption might be due to the sponge aspect of the liver, which pooled systemic and portal vascularization and the bile duct. This turns difficult the study of the liver using iodinated micro-CT with protocol 5. If we were to carry out a study focusing on the liver, we would probably use HF-MRI. We could also carry out a preliminary micro-CT study with a lower dilution of lugol or a shorter bath duration or rinsing techniques[60] more adapted for examining liver abnormalities. The cerebral cortex appears with different gray layers on HF-MRI, so HF-MRI seems better than micro-CT for examining the central nervous system. Future study should focus on the best imaging modalities to study each organ. When the prenatal diagnosis unit identifies an abnormality in a specific organ, the question is which imaging modality is the most pertinent for non-invasive PM examination: HF-MRI, micro-CT, or PM ultrasonography.

RIGHTSLINK

10970223, 2024, 1, Downloaded from https://obgyn.onlinelibrary.wiley.com/doi/10.1002/pd.6489 by Bu Montpellier, Wiley Online Library on [24/10/2024]. See the Terms and Conditions (https://onlinelibrary.wiley.com/terms-and-conditions) on Wiley Online Library for rules of use; OA articles are governed by the applicable Creative Commons License

Fetal pathology, PM exploration and autopsy described in Figure 1 is currently the gold standard reference protocol. In fetuses <11 weeks, invasive procedures are rarely performed because of microdissection difficulties and fast maceration. However, as previously mentioned, early fetal loss should not be downplayed because they are common, with 23 million occurring each year.[46] Miscarriage PM exploration is valuable both in the clinic and in research.[46,47] Consequently, we propose a feasible management circuit to perform early virtual autopsy in a fetus during the first trimester, before the fetus is released to the family (Figure 1).

External examination is needed and is of central relevance. The paucity of scientific literature on this subject, with only the good study by Abdalla et al.,[61] is at odds with the clinical interest that experts in fetopathology see on a daily basis. Further scientific studies on external examination are needed. Thus, external examination occupies a central place before micro-imaging in the procedure we are proposing for virtual autopsy in the first trimester (Figure 1).

A frozen sample such as a skin biopsy to explore genetics must be taken before iodinated micro-CT because the contrast bath contains PFA and is also not compatible with genetics analysis on biopsy. In case of maceration or other causes of unassessable genetics samples, a placental sample may be frozen and used for genetics exploration if needed. The coupling of micro-CT with biopsy should be able to perform genetic analysis in early pregnancy loss.

We suggest a double benefit of very early virtual autopsy: on the one hand, obtaining a precision phenotype allows a reverse phenotyping to select variants of interest in genome-wide analysis, offering potential genetic counseling for bereaved parents and on the other, medical follow-up and talking about the loss may both have great psychological benefit for the future of the couple.

Micro-imaging and autopsy might be combined if needed. Imaging did not alter the histology, allowing immunostaining and pathological examination. Finally, in most cases, virtual autopsy can be performed when the parents refuse an invasive procedure. A procedure with external examination; biopsy, if possible; micro-imaging; and other alternative procedures (ultrasonography, minimally invasive procedures etc.) might be better than doing nothing.

5 | CONCLUSIONS

PM non-destructive whole-body micro-imaging using iodinated micro-CT and HF-MRI allows for PM human fetal anatomy study as early as 8 WG. It paves the way to virtual autopsy in the very early first trimester. Obtaining a precision phenotype, even regarding miscarriage products, allows a reverse phenotyping to select variants of interest in genome-wide analysis, offering potential genetic counseling for bereaved parents.

ACKNOWLEDGMENTS

We acknowledge the MRI platform member of the national infrastructure France-BioImaging supported by the French National Research Agency (ANR-10-INBS-04, "Investments for the future"), the Labex CEMEB (ANR-10-LABX-0004) and NUMEV (ANR-10-LABX-0020) for using Skyscan 1076 at the beginning of this study. We clarify the contribution of the co-authors Jennifer Salerno (MD), Martha Duraes (MD) and Martin Bertrand (PhD) for histology serial sections of specimen S9 and Valérie Rigau (PhD), Mathieu Gallo (MD), Constance Wells (MD) and Frédérique Lorcy (Biological resource center, Montpellier University Hospital, UM), for histology serial sections of specimen S1 (Figure 7). We are grateful to all the women who gave their consent to this research, making this work possible. We thank the entire obstetrics gynaecology team at the university hospital of Montpellier, France: Florent Fuchs (MD, PhD), Pierre Boulot (MD, PhD). We thank Laura Smales for her careful English-language proofreading. AL is currently funded by Nîmes and Montpellier University Hospital mobility grants.

CONFLICT OF INTEREST STATEMENT

None declared.

DATA AVAILABILITY STATEMENT

Data are available on request to the corresponding author via e mail.

ORCID

Audrey Lamouroux https://orcid.org/0000-0001-7108-9581
Maïda Cardoso https://orcid.org/0000-0001-6149-3695
Martin Bertrand https://orcid.org/0000-0002-9367-9504
Valérie Rigau https://orcid.org/0000-0002-8017-5489
Florent Fuchs https://orcid.org/0000-0003-3530-6328
Eve Mousty https://orcid.org/0000-0002-3648-0304
David Genevieve https://orcid.org/0000-0001-6928-6287
Gérard Subsol https://orcid.org/0000-0002-7461-4932
Christophe Goze-Bac https://orcid.org/0000-0002-9063-4140
Guillaume Captier https://orcid.org/0000-0002-1705-2339

REFERENCES

1. Gilson H. Leonardo da Vinci's embryological drawings of the fetus. *Embryo Project Encyclopedia*. 2008. Accessed November 29, 2022. http://embryo.asu.edu/handle/10776/1929
2. Buklijas T, Hopwood N. Remodelling: publishing in wax and print. *Making Visible Embryos*. 2008. Accessed February 27, 2020. http://www.hps.cam.ac.uk/visibleembryos/s5_3.html
3. Dawood Y, Buijtendijk MFJ, Shah H, et al. Imaging fetal anatomy. *Semin Cell Dev Biol*. 2022;131:78-92. https://doi.org/10.1016/j.semcdb.2022.02.023
4. Ameil M, Delattre JF, Cordobes B, Flament JB. Computerized reconstruction of an anatomical structure based on digitized sections. Preliminary study. *Anat Clin*. 1984;5(4):261-264. https://doi.org/10.1007/bf01798749
5. de Bakker BS, de Jong KH, Hagoort J, Oostra RJ, Moorman AF. Towards a 3-dimensional atlas of the developing human embryo: the Amsterdam experience. *Reprod Toxicol*. 2012;34(2):225-236. https://doi.org/10.1016/j.reprotox.2012.05.087
6. de Bakker BS, de Jong KH, Hagoort J, et al. An interactive three-dimensional digital atlas and quantitative database of human development. *Science*. 2016;354(6315):aag0053. https://doi.org/10.1126/science.aag0053

RIGHTSLINK

10970223, 2024, 1, Downloaded from https://obgyn.onlinelibrary.wiley.com/doi/10.1002/pd.6489 by Bu Montpellier, Wiley Online Library on [24/10/2024]. See the Terms and Conditions (https://onlinelibrary.wiley.com/terms-and-conditions) on Wiley Online Library for rules of use; OA articles are governed by the applicable Creative Commons License

7. Metscher BD. MicroCT for developmental biology: a versatile tool for high-contrast 3D imaging at histological resolutions. *Dev Dynam*. 2009;238(3):632-640. https://doi.org/10.1002/dvdy.21857
8. Labrousse M, Micard E, Tonnelet R, et al. Embryo form project: an original technique for the three-dimensional reconstruction of human embryo morphology. *Reprod Toxicol*. 2015;58:1-7. https://doi.org/10.1016/j.reprotox.2015.07.076
9. Haute Autorité de Santé. [Standard protocol for fetal or perinatal autopsy. Haute Autorité de santé]. *Ann Pathol*. 2014;34:415-433.
10. Shelmerdine SC, Hutchinson JC, Lewis C, et al. A pragmatic evidence-based approach to post-mortem perinatal imaging. *Insights Imaging*. 2021;12(1):101. https://doi.org/10.1186/s13244-021-01042-1
11. Arthurs OJ, Calder AD, Kiho L, Taylor AM, Sebire NJ. Routine perinatal and paediatric post-mortem radiography: detection rates and implications for practice. *Pediatr Radiol*. 2014;44(3):252-257. https://doi.org/10.1007/s00247-013-2804-0
12. Kamphuis-van Ulzen K, Koopmanschap DHJLM, Marcelis CLM, van Vugt JMG, Klein WM. When is a post-mortem skeletal survey of the fetus indicated, and when not? *J Matern Fetal Neonatal Med*. 2016;29(6):991-997. https://doi.org/10.3109/14767058.2015.1029913
13. Man J, Hutchinson JC, Heazell AE, Ashworth M, Levine S, Sebire NJ. Stillbirth and intrauterine fetal death: factors affecting determination of cause of death at autopsy. *Ultrasound Obstet Gynecol*. 2016;48(5):566-573. https://doi.org/10.1002/uog.16016
14. Gitz L, Khung-Savatovsky S, Viot G, et al. Fetopathologic examination for early termination of pregnancy: dogma or necessity? *Am J Obstet Gynecol*. 2011;205(5):467.e1-467.e9. https://doi.org/10.1016/j.ajog.2011.06.066
15. Peyronnet V, Anselem O, Loeuillet L, Roux N, Tsatsaris V. Diagnostic value of fetal autopsy after early termination of pregnancy for fetal anomalies. *PLoS One*. 2022;17(10):e0275674. https://doi.org/10.1371/journal.pone.0275674
16. Lewis C, Simcock IC, Arthurs OJ. Improving uptake of perinatal autopsy. *Curr Opin Obstet Gynecol*. 2021;33(2):129-134. https://doi.org/10.1097/gco.0000000000000691
17. Rankin J, Wright C, Lind T. Cross sectional survey of parents' experience and views of the postmortem examination. *BMJ*. 2002;324(7341):816-818. https://doi.org/10.1136/bmj.324.7341.816
18. Shelmerdine SC, Arthurs OJ. Post-mortem perinatal imaging: what is the evidence? *Br J Radiol*. 2022:20211078. https://doi.org/10.1259/bjr.20211078
19. Thayyil S, Chitty LS, Robertson NJ, Taylor AM, Sebire NJ. Minimally invasive fetal postmortem examination using magnetic resonance imaging and computerised tomography: current evidence and practical issues. *Prenat Diagn*. 2010;30(8):713-718. https://doi.org/10.1002/pd.2534
20. Thayyil S. Less invasive autopsy: an evidenced based approach. *Arch Dis Child*. 2011;96(7):681-687. https://doi.org/10.1136/adc.2009.165704
21. Arthurs OJ, Thayyil S, Olsen OE, et al. Diagnostic accuracy of post-mortem MRI for thoracic abnormalities in fetuses and children. *Eur Radiol*. 2014;24(11):2876-2884. https://doi.org/10.1007/s00330-014-3313-8
22. Arthurs OJ, Thayyil S, Owens CM, et al. Diagnostic accuracy of post mortem MRI for abdominal abnormalities in foetuses and children. *Eur J Radiol*. 2015;84(3):474-481. https://doi.org/10.1016/j.ejrad.2014.11.030
23. Ashwin C, Hutchinson JC, Kang X, et al. Learning effect on perinatal post-mortem magnetic resonance imaging reporting: single reporter diagnostic accuracy of 200 cases. *Prenat Diagn*. 2017;37(6):566-574. https://doi.org/10.1002/pd.5043
24. Arthurs OJ, Guy A, Thayyil S, et al. Comparison of diagnostic performance for perinatal and paediatric post-mortem imaging: CT versus MRI. *Eur Radiol*. 2015;26(7):1-10. https://doi.org/10.1007/s00330-015-4057-9
25. Arthurs OJ, Taylor AM, Sebire NJ. Indications, advantages and limitations of perinatal postmortem imaging in clinical practice. *Pediatr Radiol*. 2015;45(4):491-500. https://doi.org/10.1007/s00247-014-3165-z
26. Shelmerdine SC, Arthurs OJ, Gilpin I, et al. Is traditional perinatal autopsy needed after detailed fetal ultrasound and post-mortem MRI? *Prenat Diagn*. 2019;39(9):818-829. https://doi.org/10.1002/pd.5448
27. Dirnhofer R, Jackowski C, Vock P, Potter K, Thali MJ. VIRTOPSY: minimally invasive, imaging-guided virtual autopsy. *Radiographics*. 2006;26(5):1305-1333. https://doi.org/10.1148/rg.265065001
28. Dawood Y, Strijkers GJ, Limpens J, Oostra RJ, de Bakker BS. Novel imaging techniques to study postmortem human fetal anatomy: a systematic review on microfocus-CT and ultra-high-field MRI. *Eur Radiol*. 2019;30(4):2280-2292. https://doi.org/10.1007/s00330-019-06543-8
29. Kang X, Cos T, Guizani M, Cannie MM, Segers V, Jani JC. Parental acceptance of minimally invasive fetal and neonatal autopsy compared with conventional autopsy. *Prenat Diagn*. 2014;34(11):1106-1110. https://doi.org/10.1002/pd.4435
30. Johnson JT, Hansen MS, Wu I, et al. Virtual histology of transgenic mouse embryos for high-throughput phenotyping. *PLoS Genet*. 2006;2(4):e61. https://doi.org/10.1371/journal.pgen.0020061
31. Wong MD, Maezawa Y, Lerch JP, Henkelman RM. Automated pipeline for anatomical phenotyping of mouse embryos using micro-CT. *Development*. 2014;141(12):2533-2541. https://doi.org/10.1242/dev.107722
32. Dhenain M, Ruffins SW, Jacobs RE. Three-dimensional digital mouse atlas using high-resolution MRI. *Dev Biol*. 2001;232(2):458-470. https://doi.org/10.1006/dbio.2001.0189
33. Ruffins SW, Martin M, Keough L, et al. Digital three-dimensional atlas of quail development using high-resolution MRI. *Sci World J*. 2007;7:592-604. https://doi.org/10.1100/tsw.2007.125
34. Thayyil S, Cleary JO, Sebire NJ, et al. Post-mortem examination of human fetuses: a comparison of whole-body high-field MRI at 9.4 T with conventional MRI and invasive autopsy. *Lancet*. 2009;374(9688):467-475. https://doi.org/10.1016/s0140-6736(09)60913-2
35. Hutchinson JC, Shelmerdine SC, Simcock IC, Sebire NJ, Arthurs OJ. Early clinical applications for imaging at microscopic detail: microfocus computed tomography (micro-CT). *Br J Radiol*. 2017;90(1075):20170113. https://doi.org/10.1259/bjr.20170113
36. Arthurs OJ, Hutchinson JC, Sebire NJ. Current issues in postmortem imaging of perinatal and forensic childhood deaths. *Forensic Sci Med Pathol*. 2017;13(1):58-66. https://doi.org/10.1007/s12024-016-9821-x
37. Simcock IC, Shelmerdine SC, Hutchinson JC, Sebire NJ, Arthurs OJ. Human fetal whole-body postmortem microfocus computed tomographic imaging. *Nat Protoc*. 2021;16(5):2594-2614. https://doi.org/10.1038/s41596-021-00512-6
38. Hutchinson JC, Kang X, Shelmerdine SC, et al. Postmortem microfocus computed tomography for early gestation fetuses: a validation study against conventional autopsy. *Am J Obstet Gynecol*. 2018;218(4):445.e1-445.e12. https://doi.org/10.1016/j.ajog.2018.01.040
39. Votino C, Jani J, Verhoye M, et al. Postmortem examination of human fetal hearts at or below 20 weeks' gestation: a comparison of high-field MRI at 9.4 T with lower-field MRI magnets and stereomicroscopic autopsy. *Ultrasound Obstet Gynecol*. 2012;40(4):437-444. https://doi.org/10.1002/uog.11191
40. Dawood Y, de Bakker BS. Micro-CT of early human development. *Radiology*. 2020;297(1):32. https://doi.org/10.1148/radiol.2020201660
41. Shelmerdine SC, Hutchinson JC, Kang X, et al. Novel usage of microfocus computed tomography (micro-CT) for visualisation of human embryonic development-Implications for future non-invasive

RIGHTSLINK

10970223, 2024, 1, Downloaded from https://obgyn.onlinelibrary.wiley.com/doi/10.1002/pd.6489 by Bu Montpellier, Wiley Online Library on [24/10/2024]. See the Terms and Conditions (https://onlinelibrary.wiley.com/terms-and-conditions) on Wiley Online Library for rules of use; OA articles are governed by the applicable Creative Commons License

post-mortem investigation. *Prenat Diagn*. 2018;38(7):538-542. https://doi.org/10.1002/pd.5281
42. Docter D, Dawood Y, Jacobs K, et al. Microfocus computed tomography for fetal postmortem imaging: an overview. *Pediatr Radiol*. 2022;53(4):632-639. https://doi.org/10.1007/s00247-022-05517-1
43. Lombardi CM, Zambelli V, Botta G, et al. Postmortem micro-computed tomography (micro-CT) of small fetuses and hearts. *Ultrasound Obstet Gynecol*. 2014;44(5):600-609. https://doi.org/10.1002/uog.13330
44. Lhuaire M, Martinez A, Kaplan H, et al. Human developmental anatomy: microscopic magnetic resonance imaging (μMRI) of four human embryos (from Carnegie Stage 10 to 20). *Ann Anat*. 2014;196(6):402-409. https://doi.org/10.1016/j.aanat.2014.07.004
45. Dawood Y, Honhoff C, van der Post A-S, et al. Comparison of postmortem whole-body contrast-enhanced microfocus computed tomography and high-field magnetic resonance imaging of human fetuses. *Ultrasound Obstet Gynecol*. 2022;60(1):109-117. https://doi.org/10.1002/uog.24827
46. Quenby S, Gallos ID, Dhillon-Smith RK, et al. Miscarriage matters: the epidemiological, physical, psychological, and economic costs of early pregnancy loss. *Lancet*. 2021;397(10285):1658-1667. https://doi.org/10.1016/s0140-6736(21)00682-6
47. The Lancet. Miscarriage: worldwide reform of care is needed. *Lancet*. 2021;397(10285):1597. https://doi.org/10.1016/s0140-6736(21)00954-5
48. Wong MD, Dorr AE, Walls JR, Lerch JP, Henkelman RM. A novel 3D mouse embryo atlas based on micro-CT. *Development*. 2012;139(17):3248-3256. https://doi.org/10.1242/dev.082016
49. Gignac PM, Kley NJ. Iodine-enhanced micro-CT imaging: methodological refinements for the study of the soft-tissue anatomy of post-embryonic vertebrates. *J Exp Zool B Mol Dev Evol*. 2014;322(3):166-176. https://doi.org/10.1002/jez.b.22561
50. Gignac PM, Kley NJ, Clarke JA, et al. Diffusible iodine-based contrast-enhanced computed tomography (diceCT): an emerging tool for rapid, high-resolution, 3-D imaging of metazoan soft tissues. *J Anat*. 2016;228(6):889-909. https://doi.org/10.1111/joa.12449
51. Benoist G, Bessis R, Truong Canh MB, et al. Recommandations de la CNEOF 2022 – synthèse. *Gynécologie Obstétrique Fertil Sénologie*. 2023. https://doi.org/10.1016/j.gofs.2023.01.006
52. Lamouroux A, Captier G, Genevieve D. Projet FETTAL, fetal enhanced tridimentional and translationel anatomical landscape. *Morphologie*. 2017;101(335):183-184. https://doi.org/10.1016/j.morpho.2017.07.062
53. Lamouroux A, Genevieve D, Fuchs F, et al. OC18. 01: fetal enhanced tridimensional and translational anatomical landscape: FETTAL Project. *Ultrasound Obstet Gynecol*. 2017;50(S1):37.
54. Hsieh SS, Leng S, Yu L, Huber NR, McCollough CH. A minimum SNR criterion for computed tomography object detection in the projection domain. *Med Phys*. 2022;49(8):4988-4998. https://doi.org/10.1002/mp.15832
55. Sandrini C, Boito S, Lombardi CM, et al. Postmortem micro-CT of human fetal heart—a systematic literature review. *J Clin Med*. 2021;10(20):4726. https://doi.org/10.3390/jcm10204726
56. Lombardi S, Scola E, Ippolito D, et al. Micro-computed tomography: a new diagnostic tool in postmortem assessment of brain anatomy in small fetuses. *Neuroradiology*. 2019;61(7):737-746. https://doi.org/10.1007/s00234-019-02168-2
57. Meignan P, Binet A, Cook AR, Lardy H, Captier G. Fetal median sacral artery anatomy study by micro-CT imaging. *Surg Radiol Anat*. 2018;40(7):735-741. https://doi.org/10.1007/s00276-018-2032-2
58. Shelmerdine SC, Simcock IC, Hutchinson JC, et al. Postmortem microfocus computed tomography for noninvasive autopsies: experience in >250 human fetuses. *Am J Obstet Gynecol*. 2021;224(1):103.e1-103.e15. https://doi.org/10.1016/j.ajog.2020.07.019
59. Simcock IC, Shelmerdine SC, Langan D, Anna G, Sebire NJ, Arthurs OJ. Micro-CT yields high image quality in human fetal post-mortem imaging despite maceration. *BMC Med Imag*. 2021;21(1):128. https://doi.org/10.1186/s12880-021-00658-5
60. Dawood Y, Hagoort J, Siadari BA, et al. Reducing soft-tissue shrinkage artefacts caused by staining with Lugol's solution. *Sci Rep*. 2021;11(1):19781. https://doi.org/10.1038/s41598-021-99202-2
61. Abdalla EM, El Desouky LM, Hassanein NM. Postmortem clinical examination by experienced clinical geneticists as an alternative to conventional autopsy for assessment of fetal and perinatal deaths in countries with limited resources. *Turk J Pediatr*. 2015;57:146-153.

How to cite this article: Lamouroux A, Cardoso M, Bottero C, et al. Micro-CT and high-field MRI for studying very early post-mortem human fetal anatomy at 8 weeks of gestation. *Prenat Diagn*. 2024;44(1):3-14. https://doi.org/10.1002/pd.6489

10970223, 2024, 1, Downloaded from https://obgyn.onlinelibrary.wiley.com/doi/10.1002/pd.6489 by Bu Montpellier, Wiley Online Library on [24/10/2024]. See the Terms and Conditions (https://onlinelibrary.wiley.com/terms-and-conditions) on Wiley Online Library for rules of use; OA articles are governed by the applicable Creative Commons License

RIGHTSLINK

ANNEXE 4

Simcock IC, Lamouroux A, Shelmerdine SC, Sebire NJ, Hutchinson CJ & Arthurs OJ.

Fetal post-mortem imaging using microfocus computed tomography: single centre retrospective clinical experience.

Submitted in American Journal of Obstetrics and Gynecology

American Journal of Obstetrics and Gynecology

Fetal post-mortem imaging using microfocus computed tomography (microfocus-CT): single centre retrospective clinical experience

--Manuscript Draft--

Manuscript Number:	
Article Type:	Original Research
Section/Category:	Imaging
Corresponding Author:	Ian C Simcock, PhD, MSc, BSc Great Ormond Street Hospital for Children NHS Trust London, UNITED KINGDOM
First Author:	Ian C Simcock, PhD, MSc, BSc
Order of Authors:	Ian C Simcock, PhD, MSc, BSc
	Audrey Lamouroux
	Susan C Shelmerdine
	Neil J Sebire
	John Ciaran Hutchinson
	Owen J Arthurs
Manuscript Region of Origin:	UNITED KINGDOM
Abstract:	Background Post-mortem imaging is becoming a more acceptable part of perinatal autopsy, particularly for early gestation or small fetuses where conventional autopsies may be challenging and rejected by parents. Objective(s) The purpose of this study was to establish the relative diagnostic yield of microfocus computed tomography (Micro-CT) as part of less invasive autopsy in fetuses below 24 weeks gestation. Study Design We completed a single center, retrospective study of 7 years of 1007 consecutive unselected perinatal autopsies (2016 - 2023) for fetuses below 300g. Micro-CT was offered as an option to all referred fetuses below 300 g body weight; all parents gave fully informed written consent. Results We imaged 1007 fetuses with mean 17.9 weeks gestation and 92.4g body weight, categorized according to mode of death. A diagnosis was made in 51.1% (515 / 1007), with a fetal cause in 212 / 1007 (21.1%), placental cause in 264 / 1007 (26.2%) and elements of both in 39 / 1007 (3.9%). The single most important diagnostic contributor was the placental examination (353 cases; 35.1%). Micro-CT image quality allowed diagnosis in 598 / 1007 cases (59.4%), higher in miscarriage (80.3%) and termination of pregnancy (74.9%) than in utero deaths (41.4%), reducing in diagnostic contribution with increasing levels of maceration. The overall micro-CT abnormality detection rate was 312 / 1007 (31%), highest in termination of pregnancy (80.7%) vs spontaneous miscarriage (17.9%). Only 43 fetuses required additional invasive autopsy (an autopsy “avoidance rate” of 95.7%; 964 / 1007). Median turnaround time was 18 days (range 13 – 23 days). Conclusion(s) The combination of a routine external examination, placental assessment and micro-CT post-mortem imaging reached a diagnosis in early gestation fetuses in over 50%, similar to historical cohorts. This was achieved within 3 weeks, with an autopsy avoidance rate of 96%, in line with parental consent.

Powered by Editorial Manager® and ProduXion Manager® from Aries Systems Corporation



10 March 2025

To: Dr Catherine Bradley and Dr Roberto Romero
Editor of American Journal of Obstetrics and Gynecology

Dear Editor

Please consider our manuscript titled "**Novel early gestation fetal post-mortem imaging using microfocus computed tomography: single centre retrospective clinical experience**" for publication in the journal Radiology.

The author list is,

Dr Ian C SIMCOCK,

Dr Audrey LAMOUROUX,

Dr Susan C SHELMERDINE,

Prof Neil J SEBIRE,

Dr J Ciaran Hutchinson,

Prof Owen J ARTHURS

Our paper presents a novel method for investigating fetal death as an alternative to invasive autopsy. We have developed and optimised a technique for fetal imaging using Microfocus computed tomography (Microfocus-CT), which we now present the results from over 1000 fetuses, the largest population worldwide imaged with this technique. We contextualize the detection rate against placental and other non-invasive tests so that readers can understand the precise way in which this can be incorporated into a new clinical service in future.

There exists an overlap in the data used for this paper and Shelmerdine SC et al., "*Post-mortem micro-CT for non-invasive autopsies: Experience in > 250 human fetuses*" which was also published in your **American Journal of Obstetrics and Gynecology 2020**, (cited 33 times to date).

In the 2020 study, we reported on 268 patients who underwent a Microfocus-CT examination and compared the findings to conventional autopsy and ante-natal ultrasound. That study demonstrated that Microfocus-CT gave excellent image quality in early gestational fetuses, with high diagnostic accuracy. However, that study recruited parents who consented to invasive autopsy in order to make a comparison, whereas now parents no longer consent to invasive autopsy being performed even within a research study. It is no longer ethical to perform invasive autopsy where no abnormality has been identified on Microfocus-CT.

The current study expands on this work through an increased patient cohort (1007) and different demographic, including parents who would not otherwise have consented to any

autopsy. The current study gives a more real-world pragmatic evidence base by categorizing according to fetal or placental cause of demise, contextualizing how and where Microfocus-CT can be of most benefit to parents.

As American Journal of Obstetrics and Gynecology, you specialize in publishing original reports which are likely to change clinical practice or thinking about a disease, the reduction in parental consent for invasive autopsy together with a decline in perinatal pathologists available to perform autopsy now means that new imaging techniques are desperately needed to help parents following pregnancy loss.

Our manuscript has the potential to change the delivery of perinatal autopsy across the UK and worldwide, and we are grateful for your consideration of the paper. The manuscript has not been published and is not under consideration for publication elsewhere. We have no conflicts of interest or disclosure statements.

There is no conflict of interest or industry support involved in this manuscript, and it has been solely submitted to American Journal of Obstetrics and Gynecology.

Thank you for your consideration,



Prof Owen Arthurs
On behalf of all authors

Author List:
Dr Ian C Simcock
Dr Audrey Lamouroux
Dr Susan C Shelmerdine
Prof Neil J Sebire
Dr J Ciaran Hutchinson
Prof Owen Arthurs

Title page

Article title:

Fetal post-mortem imaging using microfocus computed tomography: single centre retrospective clinical experience

Author names.

Ian C. Simcock, PhD [1, 2, 3,] (ian.simcock@gosh.nhs.uk)

Audrey Lamouroux, MD [4, 5, 6,] (a-lamouroux@chu-montpellier.fr)

Susan C. Shelmerdine, PhD [1, 2,3,] (Susan.shelmerdine@gosh.nhs.uk)

Neil J. Sebire, PhD [2, 3, 7,] (Neil.sebire@gosh.nhs.uk)

J. Ciaran Hutchinson, PhD [2, 3, 7,] (Ciaran.Hutchnson@gosh.nhs.uk)

Owen J. Arthurs, PhD [1, 2, 3] (Owen.arthurs@gosh.nhs.uk)

Affiliations:

[1] Department of Clinical Radiology, Great Ormond Street Hospital for Children; Great Ormond Street, London, WC1N 3JH, UK

[2] UCL Great Ormond Street Institute of Child Health, Great Ormond Street Hospital for Children; London, WC1E 6BT, UK.

[3] Great Ormond Street Hospital NIHR Biomedical Research Centre; London, WC1E 6BT, UK.

[4] Obstetrical Gynecology Department, Nîmes University Hospital; Place du Pr R. Debre, Nimes, 3000, France

[5] Fetopathology unit, Clinical Genetics Department, Montpellier University Hospital; 371 Av. Du Doyen Gaston Giraud, Montpellier, 34090, France.

[6] ICAR research team, LIRMM, CNRS and Charles Coulomb Laboratory, UMR 5221 CNRS-UM, BNIF user facility imaging, University of Montpellier; Building 5-860, Rue de St Priest, Montpellier, 34095, France.

[7] Department of Histopathology, Great Ormond Street Hospital for Children; Great Ormond Street, London, WC1N 3JH, UK

Corresponding author:

Dr Ian C Simcock, Radiology, Great Ormond Street Hospital for Children NHS Foundation Trust, Great Ormond Street, London, WC1N 3JH, UK.

Ian.simcock@gosh.nhs.uk, (+44) 02084059200 ext 0562

Conflict of Interest:

The authors report no conflict of interest.

Funding:

National Institute for Health and Care Research - Clinical Doctoral Research Fellowship ICA-CDRF-2017-03-53 (ICS)

National Institute for Health and Care Research - Development and Skills Enhancement Award NIHR302390 (ICS)

National Institute for Health and Care Research - Career Development Fellowship NIHR-CDF-2017-10-037 (OJA)

National Institute for Health and Care Research - Advanced Fellowship Award NIHR-301322 (SCS)

Mobility funding grant, Nimes university Hospital (AL)

Mobility funding grant, Montpellier University Hospital (AL)

Condensation Page

Tweetable statement

Micro-CT is a non-invasive post-mortem investigation for early pregnancy loss which provides high resolution imaging, with a 96% autopsy avoidance rate.

Short Title

Fetal post-mortem imaging using micro-CT

AJOG at a glance

- A. Why was the study conducted?
- Micro-CT offers high resolution post-mortem fetal imaging following miscarriage, but its yield relative to other autopsy techniques is unknown in a large clinical population.

- B. What are the key findings?
- In an unselected population of over 1000 cases, we made a diagnosis in 51%, identifying a fetal cause (21%), placental cause (26%) or both (4%).
- The single most important diagnostic contributor was the placental examination in 35% of cases, with overall micro-CT abnormality detection rate 31%

- C. What does the study add to what is already known?
- This study demonstrates that micro-CT together with placental examination was associated with an autopsy avoidance rate of 96% and turnaround time

of 18 days, which may influence clinical autopsy service delivery for early fetal death.

Abstract

Background

Post-mortem imaging is becoming a more acceptable part of perinatal autopsy, particularly for early gestation or small fetuses where conventional autopsies may be challenging and rejected by parents.

Objective(s)

The purpose of this study was to establish the relative diagnostic yield of microfocus computed tomography (Micro-CT) as part of less invasive autopsy in fetuses below 24 weeks gestation.

Study Design

We completed a single center, retrospective study of 7 years of 1007 consecutive unselected perinatal autopsies (2016 - 2023) for fetuses below 300g. Micro-CT was offered as an option to all referred fetuses below 300 g body weight; all parents gave fully informed written consent.

Results

We imaged 1007 fetuses with mean 17.9 weeks gestation and 92.4g body weight, categorized according to mode of death. A diagnosis was made in 51.1% (515 / 1007), with a fetal cause in 212 / 1007 (21.1%), placental cause in 264 / 1007 (26.2%) and elements of both in 39 / 1007 (3.9%). The single most important diagnostic contributor was the placental examination (353 cases; 35.1%).

Micro-CT image quality allowed diagnosis in 598 / 1007 cases (59.4%), higher in miscarriage (80.3%) and termination of pregnancy (74.9%) than in utero deaths

(41.4%), reducing in diagnostic contribution with increasing levels of maceration. The overall micro-CT abnormality detection rate was 312 / 1007 (31%), highest in termination of pregnancy (80.7%) vs spontaneous miscarriage (17.9%). Only 43 fetuses required additional invasive autopsy (an autopsy “avoidance rate” of 95.7%; 964 / 1007). Median turnaround time was 18 days (range 13 – 23 days).

Conclusion(s)

The combination of a routine external examination, placental assessment and micro-CT post-mortem imaging reached a diagnosis in early gestation fetuses in over 50%, similar to historical cohorts. This was achieved within 3 weeks, with an autopsy avoidance rate of 96%, in line with parental consent.

Keywords

Autopsy

Microfocus Computed Tomography

Miscarriage

Termination of pregnancy

Main Text

Introduction

Perinatal invasive autopsy is the reference standard for the detection of congenital fetal abnormalities, which may contribute to the diagnosis of cause of pregnancy loss. For example, post-mortem examination as full fetal autopsy (external examination, skeletal radiographs, internal macroscopic examination and histological examination of samples of target organs and macroscopic and microscopic examination of the placenta) can provide additional information in over 75% of cases compared to antenatal ultrasound, and can change genetic counselling in 32.5% of cases.[1]

Despite autopsy providing important information to parents and clinicians on recurrence risk or implications for future pregnancies, many parents now decline invasive autopsy and prefer non-invasive alternatives.[2] Often following an out-of-hospital miscarriage or pregnancy loss, parents are not aware of the range of options available and may avoid coming to medical attention unless there are complications. This population is largely ignored by medical practitioners and the true rate, and determinants of early pregnancy loss is largely unknown, as most studies are based on hospital data.

For those reasons, post-mortem imaging has been developed to provide high resolution 3D imaging datasets which may be able to provide diagnostic information sufficient to avoid an invasive autopsy in most fetal cases. The use of conventional clinical techniques such as MRI is well established for post-mortem imaging of older fetuses, but diagnostic accuracy rates fall with smaller fetal body weight, typically below 300 g,[3-6] with a lack of clinical alternatives for early gestation fetal loss.

Microfocus computed tomography (Micro-CT) is a density-based imaging modality which utilises cone beam radiation and can achieve voxel resolution to 0.001 mm.[7] It has been proposed as a clinical alternative, using iodine to generate high tissue contrast in small fetuses. Initial pilot studies using this technique were promising particularly for early gestation fetal cardiac anomalies[8, 9] and tissue preparation protocols have now been developed.[7, 10] We introduced non-invasive tool, with an initial feasibility study demonstrating lack of additional benefit of progressing to invasive autopsy if micro-CT findings were normal or concordant with antenatal findings.[11]

The aim of this study was to establish the relative diagnostic yield of micro-CT compared to other non-invasive procedures (placental and external examinations) as part of less invasive autopsies in fetuses below 24 weeks gestation.

Materials and Methods

Study design

We completed a single centre, retrospective study of consecutive unselected whole-body iodinated post-mortem micro-CT performed as a part of post-mortem examination over a 7-year period at our tertiary referral centre (October 2016 - October 2023). We obtained ethical approval from the NHS Health Research Authority (HRA) Ethics Committee (IRAS ID: 131395). Previously, data relating to 268 fetuses of the patient cohort reported in this paper, was published in Shelmerdine et al.,[11], which compared micro-CT to conventional autopsy and ante-natal ultrasound, demonstrating that micro-CT provided excellent image quality, with

high diagnostic accuracy. This current investigation instead identifies what micro-CT can provide relating to diagnostic performance as a stand-alone examination within the clinical post-mortem service and the role it can play.

Micro-CT was offered at all referring centres for fetuses to us below <300 g bodyweight, based on predicted maximum tissue preparation time of 14 days.[7, 12] There were no exclusion criteria. Written parental consent was acquired for all postmortem imaging and subsequent autopsy, where performed. All parents gave fully informed written consent allowing for their "ceiling" autopsy type, i.e. maximum invasiveness post-mortem examination to be conducted, from a choice of a) full invasive autopsy, b) minimally invasive autopsy including detailed imaging, with keyhole or laparoscopic approaches permitted, or c) non-invasive autopsy including detailed imaging but no tissue sampling.[4, 6, 13] All parents were informed of the estimated time taken to iodinate and de-iodinate the baby together with possible skin colour changes.[11] All samples were handled in accordance with the Human Tissue Act 2004. Some demographic data was collected as part of routine clinical audit.

Procedures and definitions

All bodies were stored at 4°C in a mortuary following delivery and parental consent was obtained by the referring hospital prior to transfer to our centre.

Specialist paediatric pathologists first evaluated the clinical context with mode of death, estimated gestational age, maternal and familial medical history, consanguinity, ethnicity, first trimester explorations, ultrasound, fetal medicine unit and genetic data if available.

The mode of fetal death was collected and defined as

1. in-utero death: any fetal death which occurred prior to delivery, ("missed miscarriage") irrespective of mode of delivery.

2. miscarriage (spontaneous or "fresh miscarriage") which correspond to spontaneous expulsion or onset of labour irrespective of the theoretical term.

3. termination of pregnancy, defined as induced labour with or without feticide. We further defined termination of pregnancy for fetal reasons into categories including fetal malformation, chromosomal abnormality, twin pregnancy complications, or termination of pregnancy for premature rupture of membrane (PROM), whether there was infection or anhydramnios.

Post-mortem examination contribution to the diagnosis

Post-mortem examination was defined as contributory if a diagnosis (cause of fetal death or diagnosis of main abnormality) was reached overall, sub-categorised further by placental examination, external examination, radiographs, micro-CT or invasive autopsy.

In all cases, an initial whole body skeletal radiograph was performed. Specialist paediatric pathologists then performed an external post-mortem examination with fetal size (i.e. crown – rump and crown – heel lengths, foot length, weight), maceration score (based on a severity scale of 0 (none) to 3 (severe)), gender, facial dysmorphism, external malformation included intrabuccal, choanal, genitalia and anal examination. Placental examination involved macroscopic and later microscopic and immunochemistry if necessary, according to national guidelines.[14]

We divided overall diagnosis (cause of fetal death or diagnosis of main abnormality) into fetal and placental causes. We defined "imaging diagnostic performance" as micro-CT was contributory when the image quality was diagnostic, and non-contributory when severity of maceration rendered the imaging non-diagnostic. We divided micro-CT abnormalities by target organ and organ system, excluding traumatic lesions related to delivery, expulsion, maceration, or obstetric complications, for example abdominal wall disruption in a severely macerated fetus was not termed a congenital abnormality.

Micro-CT Imaging protocol

The detailed study protocol has been published.[7] In brief, the fetus was immersed in a diluted I_2KI solution for several days to allow the contrast agent to diffuse through the body, according to body weight.[7, 12] The fetus was then scanned using set parameters (100 - 130kV, 230-350uA, 250-350ms, 2 frames per projection) for a whole-body low-resolution scan at 21-113 microns, and separate high-resolution brain and body scans at typically 12-63 micron isotropic resolution depending on fetal size.[7] Images were reported by one of two consultant radiologists (OJA or SCS), with 18- and 14-years' radiology experience, and 8- and 5-years micro-CT experience, respectively. The micro-CT reports were reviewed by two researchers (ICS and AL) with 8- and 6-years post-mortem experience respectively. The fetus was then returned to the mortuary following imaging, placed in thiosulphate solution to remove the staining discolouration, and then returned to the referring hospital and the parents.

We collected timing data including dates of delivery, receipt of the body, post-mortem examination, when placed into I_2KI solution ("dipped"), micro-CT performed, micro-CT reported, autopsy final report and body release from our hospital.

Some abnormalities were attributed to delivery, maceration or post-mortem changes, which included brain abnormalities such as cracking of the cerebral hemispheres, or mid-brain disruption due to delivery, and body wall abnormalities such as herniation through an abdominal or thoracic wall defect when the abdominal wall was intact on antenatal imaging.

Invasive autopsy

The decision to perform an invasive autopsy was guided by external post-mortem examination including parental consent, medical history, antenatal context, external post-mortem examination, micro-CT imaging, placental examination, and the pathologist's opinion regarding potential additional benefit of further examination. We applied a clinical policy to do the minimum level of invasive autopsy required to reach a diagnosis (as per standard parental consent). For example, a markedly macerated fetus where the imaging was normal, placenta was normal and antenatal imaging was normal, would not proceed to invasive autopsy, even if the parents had consented.

However, if there was uncertainty regarding the diagnosis on micro-CT or findings that conflicted with the antenatal examination findings, then the pathologist would decide whether to proceed to autopsy on a case-by-case basis, assuming parental consent was provided, and a placental cause was not present. All autopsies were

conducted in line with the standards set by the Royal College of Pathologists.[14] All perinatal autopsies were performed by one of 7 specialist paediatric pathologists with at least 6 years perinatal pathology experience.

Statistical Analysis

The data was inputted into an independent database (Microsoft Excel, Seattle, WA). We performed descriptive statistical tests using R++ software. Qualitative variables are expressed as absolute number and percentage of the effective population. Quantitative variables are expressed as the mean with the corresponding standard deviation. Duration variables are expressed as median with the corresponding first and third quartile.

Results

We imaged 1007 fetuses over the study time period (October 2016 - October 2023). Referrals to our centre increased rapidly following offering the service in 2016, with increase from 37 cases in 2017, to 215 in 2021 (Figure 1). We did not notice a significant effect of COVID disruption on being able to offer the service nor referral patterns (time affected March 2020 – March 2022). Micro-CT numbers were lower for 2023 due to data collection ending in October 2023.

Demographics and referral data is provided in Table 1. We received referrals from 20 different referral hospitals, with no more than 15% of overall numbers from any individual centre. Most cases were born to Caucasian parents with no gender preponderance (Table 1). Mean theoretical term and mean real term (estimate using crown-rump length (CRL) and Robinson formula) were 17.92 weeks of gestation (WG) (SD 2.86) and 10.33 WG (SD 2.09), respectively. Mean CRL and mean body weight were 11.64 mm (SD 3.5) and 92.38g (SD 83.34), respectively. Over half of all fetuses were severely macerated by pathological evaluation (519 / 1007; 51.7%; Table 1).

Performance times

The median times taken for us to receive the baby from the referring hospital was 7 days (range 5 – 10 days), median time taken to scan and report the micro-CT was 9 days (range 6 – 14 days) and overall median time taken from receipt of the body to release from the mortuary was 18 days (range 13 – 23 days; Table 2).

Post-mortem examination contribution

Although many parents consented to a full autopsy including micro-CT, our pathologists did not predict an additional yield from invasive autopsy in most cases (Figure 2). Only 43 fetuses proceeded to additional invasive autopsy to provide diagnostic clarification, implying an autopsy "avoidance rate" of 95.7% (964 / 1007).

Micro-CT contribution

Micro-CT was of acceptable quality in 598 / 1007 cases (59.4%), higher in miscarriage (80.3%) and termination of pregnancy (74.9%) than in in-utero death (41.4%; Table 3). There was a gradual reduction in micro-CT image quality with increasing levels of maceration (Table 3).

Micro-CT was abnormal in 312/1007 (31.0%), which were 223 / 1007 (22.1%) true abnormalities and 89 cases of delivery or maceration related trauma. Abnormality detection excluding trauma was unsurprisingly highest in termination of pregnancy (80.7%) vs spontaneous miscarriage (6.9%) (Table 3). Micro-CT detected the greatest number of abnormalities in the chest (140; 13.9%) such as ventricular septal defect (Figure 3), abdomen (127; 12.6%), such as horseshoe kidney (figure 4) or enlarged bladder with hydronephrosis (Figure 5) and skeletal systems (97; 9.6%) (Table 3).

Overall contribution and cause of death

The single most important contributor to making a diagnosis in the 562 cases where this was possible (55.8%) was placental examination (284 cases; 28.2%; Figure 6). For example, external examination contributed to final diagnosis in 171 cases (17.0%) but was the sole contributor in only 35 cases (3.5%), and whilst micro-CT contributed to the diagnosis in 148 cases (14.7%), it was the sole contributor in only 45 cases (4.5% of our cohort, or 8% of possible diagnoses) (Figure 6).

The cause of death was fetal in 212 / 1007 (21.1%), placental cause in 264 / 1007 (26.2%) and both fetal and placental in 39 / 1007 (3.9%); remained unexplained in 492/1007 (48.9%). There is more unexplained cause of death in in-utero death (69.4%; Table 4), and with increasing levels of maceration (85.5% severe).

Comment

Principal Findings

In this single center retrospective study, we identified that less invasive fetal autopsy including micro-CT reached a diagnosis in 51% of fetal referrals, with 49% unexplained. The single most useful diagnostic contributor was placental examination, followed by external examination and micro-CT examination, which compares favourably with a historic cohort of similar post-mortem examinations carried out at the same centre.[15-17] We conclude that the introduction of micro-CT at our centre has avoided almost all invasive early gestation fetal post-mortem examinations but has a similar overall diagnostic yield.

Results in the Context of What is Known

The collaborative workflow between the perinatal pathologist and the paediatric radiologist now allows different components of post-mortem examinations to be performed that favour minimally invasive investigations. Whilst each part of a post-mortem examination can help identify a clinical diagnosis; we were able to contextualise the relative contributions of non-invasive components across this large cohort of unselected fetuses. Unsurprisingly, and in keeping with fetal autopsy literature, placental examination contributed more commonly to the final diagnosis (cause of fetal death or diagnosis of main abnormality) than fetal imaging in our study. This is in keeping with previous findings, e.g. in individual studies of 512 early in-utero deaths, 23.6% were attributed to placental disease,[18] and a systematic review of 9 studies totalling 1779 stillbirths found that placental pathology was present in 31.5 – 84.0%, with a range of placental diagnosis from 15.4 – 87.0%

depending on criteria.[19] In a similar subgroup of early in-utero deaths before 20 weeks already published, our own group identified a 53% abnormal placental examination rate.[15]

The external examination is known to be an important part of the post-mortem examination, but published evidence is limited with only one paper identifying a diagnostic rate of 57.9% by experienced geneticists.[20] In early termination of pregnancy before 16 weeks, a full autopsy (including external and placental examination, skeletal survey, internal examination and histological examination of the placenta and tissues) provides additional information in 77.5% of cases compared with antenatal first trimester ultrasound and consequently changes genetic counselling in 32.5% of cases.[1]

Micro-CT has previously been shown to have a high concordance with full autopsy of 97.5%,[21] with a high sensitivity of 92.3% and specificity of 98%[11] even in macerated fetuses.[22] Regarding individual organ systems, micro-CT was most accurate at detecting cardiothoracic, abdominal and skeletal abnormalities, but with a high non-diagnostic imaging rate for the brain, largely due to maceration following in-utero death. This is in keeping with other studies showing that post-mortem imaging is affected by prolonged intra-uterine intervals and has a higher diagnostic yield in termination of pregnancies, where the pre-test probability of fetal anomalies is much higher.

Our parent's consent framework allows the perinatal pathologist to proceed with the least invasive components first, before considering invasive autopsy. The documented change in practice at our centre shows that increasingly non-invasive

procedures are being performed, with micro-CT results becoming available within 10 days of receiving the body .A turnaround time of less than 3 weeks from receipt to release of the body [23] may seem an extended time, but this investigation is more acceptable to parents through its non-invasive nature [6] and which compares favourably to report turnaround times of up to 3 months nationally. Further research into reducing the iodination may reduce the turnaround time further.[12]

Clinical Implications

Micro-CT has already demonstrated high concordance with conventional autopsy, through high sensitivity and specificity [11, 21] and in the challenging presence of maceration [22], whilst also demonstrating a high acceptability among parents.[2] By demonstrating within this study that it can also deliver a 96% autopsy avoidance rate, there is growing evidence that this technique should be available on a wider scale so that more parents can take advantage of greater choice in investigating their loss.

Research Implications

Due to the large number of pregnancy losses each year, work is now required to identify when this technique should be employed, and which cases maximum value would be secured. This requires identification of organ system, demographics of the parents and whether individual or multiple abnormalities are identified in each case where a cause for fetal demise is identified.

Strengths and limitations

The strength of this study lies in presenting the use of micro-CT in clinical practice for human fetal post-mortem examination in a large group of unselected cases from several referral hospitals. This reflects how imaging could be used within less invasive autopsy practice in other settings and demonstrates that a high-resolution post-mortem imaging technique when used together with placental and other examinations can help avoid invasive autopsy in line with parental wishes.

The main limitations of this study are its single-centre nature, using expert specialist radiologists and pathologists which may not currently be reproducible in other centres. However, not all centres will wish to offer this level of service: given the dearth of perinatal pathologists in the UK at present, we have provided an example of how a "hub-and-spoke" model could work regarding referrals from a wide number of centres into a single specialist centre for autopsy provision.

A comparative study of micro-CT findings to invasive autopsy was not possible due to parental consent and pathologist ethical decision-making (although this has been done on a subset of earlier cases from our centre); [21] less than 50 autopsies were clinically justifiable in our cohort.

Conclusions

We have demonstrated the clinical utility of micro-CT imaging for early fetal death. In our study, the combination of routine external examination, placental assessment and micro-CT imaging meant an autopsy avoidance rate of 96%, in line with parental

consent. This has the potential to change clinical autopsy service delivery for early fetal death within the NHS.

Acknowledgements

The authors would like to thank the GOSH pathology and mortuary staff for their support in this work.

References

1. PEYRONNET V, ANSELEM O, LOEUILLET L, ROUX N, TSATSARIS V. Diagnostic value of fetal autopsy after early termination of pregnancy for fetal anomalies. PLoS One 2022;17:e0275674.
2. LEWIS C, SIMCOCK IC, ARTHURS OJ. Improving uptake of perinatal autopsy. Prenat Diagn 2021;33:129-34.
3. JAWAD N, SEBIRE NJ, WADE A, TAYLOR AM, CHITTY LS, ARTHURS OJ. Body weight lower limits of fetal postmortem MRI at 1.5 T. Ultrasound Obstet Gynecol 2016;48:92-7.
4. SHELMERDINE SC, HUTCHINSON C, LEWIS C, et al. A pragmatic evidence-based approach to post-mortem perinatal imaging. Insights in Imaging 2021;12.
5. KANG X, CARLIN A, CANNIE M, SANCHEZ TC, JANI JC. Fetal postmortem imaging: an overview of current techniques and future perspectives. American Journal of Obstetrics and Gynecology 2020;223:493-515.
6. SIMCOCK IC, LAMOUROUX A, SEBIRE NJ, SHELMERDINE SC, ARTHURS OJ. Less-invasive autopsy for early pregnancy loss. Prenat Diagn 2023;43:937-49.
7. SIMCOCK IC, SHELMERDINE SC, HUTCHINSON JC, SEBIRE NJ, ARTHURS OJ. Human fetal whole-body postmortem microfocus computed tomographic imaging. Nature Protocols 2021;16:2594-614.
8. LOMBARDI CM, ZAMBELLI V, BOTTA G, et al. Postmortem microcomputed tomography (micro-CT) of small fetuses and hearts. Ultrasound Obstet Gynecol 2014;44:600-9.
9. HUTCHINSON JC, ARTHURS OJ, ASHWORTH MT, et al. Clinical utility of postmortem microcomputed tomography of the fetal heart: diagnostic imaging vs macroscopic dissection. Ultrasound Obstet Gynecol 2016;47:58-64.
10. DAWOOD Y, HAGOORT J, SIADARI BA, et al. Reducing soft-tissue shrinkage artefacts caused by staining with Lugol's solution. Sci Rep 2021;11:19781.
11. SHELMERDINE SC, SIMCOCK IC, CIARAN HUTCHINSON J, et al. Post-mortem micro-CT for non-invasive autopsies: Experience in > 250 human fetuses. American Journal of Obstetrics and Gynecology 2020;224:1-15.
12. SIMCOCK IC, SHELMERDINE SC, HUTCHINSON JC, SEBIRE NJ, ARTHURS OJ. Body weight-based iodinated contrast immersion timing for human fetal postmortem MCT. BJROpen 2024;6:1-5.
13. SHELMERDINE SC, ARTHURS OJ. Post-mortem perinatal imaging: what is the evidence? The British journal of radiology 2022:20211078.
14. PATHOLOGISTS TRCO. Guidelines on autopsy practice: Royal College of Pathologists, 2024.
15. MAN J, HUTCHINSON JC, HEAZELL AE, ASHWORTH M, LEVINE S, SEBIRE NJ. Stillbirth and intrauterine fetal death: factors affecting determination of cause of death at autopsy. Ultrasound Obstet Gynecol 2016;48:566-73.
16. MAN J, HUTCHINSON JC, HEAZELL AE, ASHWORTH M, JEFFREY I, SEBIRE NJ. Stillbirth and intrauterine fetal death: role of routine histopathological placental findings to determine cause of death. Ultrasound Obstet Gynecol 2016;48:579-84.
17. MAN J, HUTCHINSON JC, ASHWORTH M, JUDGE-KRONIS L, LEVINE S, SEBIRE NJ. Stillbirth and intrauterine fetal death: role of routine histological organ sampling to determine cause of death. Ultrasound Obstet Gynecol 2016;48:596-601.
18. GIBBINS KJ, PINAR H, REDDY UM, et al. Findings in Stillbirths Associated with Placental Disease. Am J Perinatol 2020;37:708-15.
19. GRAHAM N, HEAZELL AEP. When the Fetus Goes Still and the Birth Is Tragic: The Role of the Placenta in Stillbirths. Obstet Gynecol Clin North Am 2020;47:183-96.
20. ABDALLA EM, EL-DESOUKY LM, HASSANEIN NM. Postmortem clinical examination by experienced clinical geneticists as an alternative to conventional autopsy for assessment of fetal and perinatal deaths in countries with limited resources. The Turkish Journal of Pediatrics 2015;57:146-53.

21. HUTCHINSON JC, KANG X, SHELMERDINE SC, et al. Postmortem microfocus computed tomography for early gestation fetuses: a validation study against conventional autopsy. American Journal of Obstetrics and Gynecology 2018;218:445.e1-45.e12.
22. SIMCOCK IC, SHELMERDINE SC, LANGAN D, ANNA G, SEBIRE NJ, ARTHURS OJ. Micro-CT yields high image quality in human fetal post-mortem imaging despite maceration. BMC Medical Imaging 2021;21.
23. SIMCOCK IC, ARTHURS OJ, HUTCHINSON JC, et al. Impact of non-invasive post-mortem micro-CT imaging on a fetal autopsy service: a single centre retrospective study. Clin Radiol 2024;79:791-98.

Tables

Table 1 Referral pattern and demographics

		Overall 1007 (100%)	In Utero Deaths 517 (51.34%)	Miscarriage or termination of pregnancy for SROM 319 (31.68%)	Termination of pregnancy for fetal malformations or other 171 (16.98%)	Missing data
GENDER	Male	497 (49.35%)	266 (51.45%)	157 (49.22%)	74 (43.27%)	0
	Female	439 (43.59%)	202 (39.07%)	156 (48.90%)	81 (47.37%)	
	Undetermined	71 (7.05%)	49 (9.48%)	6 (1.88%)	16 (9.36%)	
MOTHER ETHNICITY	White	425 (66.10%)	240 (70.38%)	105 (55.85%)	80 (70.18%)	364
	Black	97 (15.09%)	42 (12.32%)	45 (23.94%)	10 (8.77%)	
	Indian	57 (8.86%)	26 (7.62%)	19 (10.11%)	12 (10.53%)	
	Other	64 (9.95%)	33 (9.68%)	19 (10.11%)	12 (10.53%)	
FATHER ETHNICITY	White	427 (66.41%)	246 (70.89%)	103 (56.91%)	78 (67.83%)	364
	Black	84 (13.06%)	44 (12.68%)	30 (16.57%)	10 (8.70%)	
	Indian	74 (11.51%)	32 (9.22%)	26 (14.36%)	16 (13.91%)	
	Other	58 (9.02%)	25 (7.20%)	22 (12.15%)	11 (9.57%)	
Theoretical-term (weeks of gestation) : Mean (SD)		17.92 (2.86)	18.46 (2.9)	17.7 (2.3)	16.75 (3.19)	308
Term according to Crown-rump length according to Robinson formula (weeks of gestation) : Mean (SD)		10.33 (2.09)	9.83 (2.01)	11.16 (1.81)	10.32 (2.31)	3
Crown-Rump length (mm) : Mean (SD)		11.64 (3.5)	10.79 (3.37)	13.02 (3.04)	11.62 (3.88)	3
Crown to Heel Length (mm) : Mean (SD)		16.18 (5.18)	14.9 (4.93)	18.28 (4.61)	16.06 (5.67)	8
Foot Length (mm) : Mean (SD)		1.83 (0.84)	1.6 (0.79)	2.17 (0.79)	1.9 (0.85)	29
Post mortem weight (g) : Mean (SD)		92.38 (83.34)	61.72 (64.88)	131.77 (84.13)	111.59 (94.55)	0
MACERATION ACCORDING TO PATHOLOGICAL EXAMINATION	None	302 (30.11%)	7 (1.35%)	195 (61.32%)	100 (59.52%)	4
	Mild	118 (11.76%)	27 (5.22%)	53 (16.67%)	38 (22.62%)	
	Moderate	64 (6.38%)	41 (7.93%)	13 (4.09%)	10 (5.95%)	
	Severe	519 (51.74%)	442 (85.49%)	57 (17.92%)	20 (11.90%)	

Table 2 Turnaround times

Duration in days Median (Q1, Q3)	Overall 1007 (100%)	In Utero Deaths 517 (51.34%)	Miscarriage or termination of pregnancy for SROM 319 (31.68%)	Termination of pregnancy for fetal malformations or other 171 (16.98%)
Birth to Receipt	7 [5, 10]	7 [5, 10]	7 [5, 10]	6 [5, 10]
Receipt to Post mortem examination	1 [1, 3]	1 [1, 3]	1 [1, 2.75]	1 [1, 2]
Receipt to Iodination	1 [1, 2]	1 [1, 3]	1 [1, 2]	1 [1, 2]
Receipt to micro-CT	8 [6, 12]	7 [5, 11]	10 [6, 13]	8 [5.75, 13]
Receipt to micro-CT Report	9 [6, 14]	8 [6, 13]	10 [7, 14]	11 [6, 14]
Receipt to Final report	15 [12, 23]	15 [11, 22]	16 [13, 23]	16.5 [12, 25.25]
Receipt to Release	18 [13, 23]	15 [12, 22]	20 [15, 26]	19 [14, 23]

Table 3 Contribution of micro-CT to the final diagnosis image quality and abnormalities identified.

			Overall 1007 (100%)	In Utero Deaths 517 (51.34%)	Miscarriage or termination of pregnancy for SROM 319 (31.68%)	Termination of pregnancy for fetal malformations or other 171 (16.98%)
(Missing data on micro-CT image quality)			43 (4.27%)	6 (1.16%)	20 (6.27%)	17 (9.9%)
Micro-CT IMAGE QUALITY	Diagnostic micro-CT image quality		598 (59.38%)	214 (41.39%)	256 (80.25%)	128 (74.85%)
		No maceration	249 (24.73%)	25 (4.84%)	148 (46.39%)	76 (44.44%)
		Mild maceration	134 (13.31%)	35 (6.77%)	70 (21.94%)	29 (16.96%)
		Moderate maceration	106 (10.53%)	70 (13.54%)	21 (6.58%)	15 (8.77%)
		Severe maceration	109 (10.82%)	84 (16.25%)	17 (5.33%)	8 (4.68%)
	Non-diagnostic micro-CT image quality		366 (36.35%)	297 (57.45%)	43 (13.48%)	26 (15.2%)
		Brain non-diagnostic	295 (29.29%)	240 (46.42%)	34 (10.66%)	21 (12.28%)
		Abdomen and brain non-diagnostic	61 (6.1%)	49 (9.48%)	8 (2.51%)	4 (2.34%)
		Whole body non-diagnostic	10 (1%)	8 (1.55%)	1 (0.31%)	1 (0.58%)
Micro-CT FINDINGS	Micro-CT findings per organ system					
		CNS	78 (7.75%)	13 (2.51%)	15 (4.92%)	50 (29.24%)
		Chest	140 (13.9%)	57 (11.03%)	14 (4.40%)	69 (40.35%)
		Abdominal	127 (12.61%)	60 (11.61%)	22 (6.92%)	45 (26.32%)
		Urinary tract	71 (7.10%)	20 (3.87%)	7 (2.20%)	44 (25.73%)
		Skeletal or Soft tissue	97 (9.63%)	22 (4.26%)	7 (2.20%)	68 (39.77%)
	Micro-CT findings per case					
		Overall abnormal case number	312 (30.98%)	117 (22.63%)	57 (17.92%)	138 (80.70%)
		Overall abnormal cases excluding delivery trauma	223 (22.14%)	63 (12.19%)	22 (6.92%)	138 (80.70%)

Table 4 Contribution from post-mortem examination

			Overall 1007 (100%)	In Utero Deaths 517 (51.34%)	Miscarriage or termination of pregnancy for SROM 319 (31.68%)	Termination of pregnancy for fetal malformations or other 171 (16.98%)
POST MORTEM EXAMINATION CONTRIBUTION TO THE FINAL DIAGNOSIS	ANY CONTRIBUTION	None	445 (44.23%)	317 (61.43%)	112 (35.11%)	16 (9.36%)
		Any	562 (55.81%)	200 (38.68%)	207 (64.89%)	155 (90.64%)
		Placenta examination	353 (35.05%)	137 (26.50%)	188 (58.93%)	28 (16.37%)
		External examination	206 (20.46%)	61 (11.80%)	31 (9.72%)	114 (66.67%)
		Skeletal survey	63 (6.26%)	7 (1.35%)	3 (0.94%)	53 (30.99%)
		Micro-CT	193 (19.17%)	49 (9.48%)	21 (6.58%)	123 (71.93%)
		Autopsy	10 (0.99%)	1 (0.19%)	0 (0%)	9 (5.26%)
	SOLE CONTRIBUTION	Placenta examination alone	284 (28.20%)	112 (21.66%)	168 (52.66%)	4 (2.34%)
		External examination alone	35 (3.48%)	21 (4.06%)	4 (1.25%)	10 (5.85%)
		Skeletal survey alone	8 (0.80%)	2 (0.39%)	1 (0.31%)	5 (2.92%)
		Micro-CT alone	45 (4.47%)	20 (3.87%)	4 (1.25%)	21 (12.28%)
		Autopsy alone	None	None	None	None
CAUSE OF DEAT	Unexplained		492 (48.86%)	359 (69.44%)	124 (38.87%)	9 (5.26%)
	Fetal		212 (21.05%)	53 (10.25%)	12 (3.76%)	147 (85.96%)
	Placenta		264 (26.22%)	83 (16.05%)	174 (54.55%)	7 (4.09%)
	Both fetal and placenta		39 (3.87%)	22 (4.26%)	9 (2.82%)	8 (4.68%)

Figure Legends

Figure 1 Number of micro-CT imaging cases performed per year according to the subgroup.

Key – dark bars – In utero deaths; grey bars – miscarriage or termination of pregnancy for SROM; white bars – termination of pregnancy for fetal malformation or other reason.

Figure 2 Post-mortem examination by parental consent vs type of post-mortem performed, categorized by subgroup (in-utero death, miscarriage, termination of pregnancy).

Key: dark squares = full autopsy; grey = minimally invasive autopsy MIA or less invasive autopsy approaches; white = external examination only

Figure 3 Axial micro-CT image of a 13-week gestation fetus demonstrating ventricular septal defect (arrow) in a moderately macerated fetus. Note reduced overall greyscale and loss of tissue boundaries caused by maceration.

Figure 4 Axial (a and b) and coronal (c and d) micro-CT of renal abnormalities: this case at 14 weeks gestation was diagnosed antenatally with malrotated kidneys (closed white arrow), with the isthmus of a horseshoe kidney (closed white arrow) demonstrated on micro-CT.

Figure 1

Click here to access/download;Figure #;Supplementary Figure 1.jpg

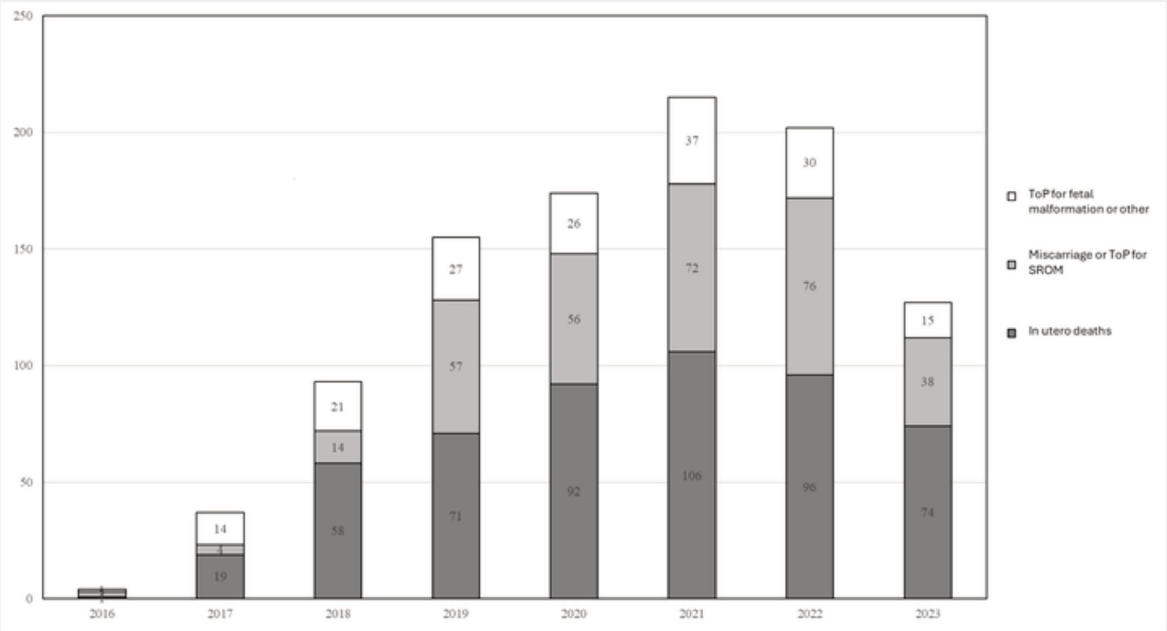

Figure 2

Click here to access/download;Figure #;Figure 2.jpg

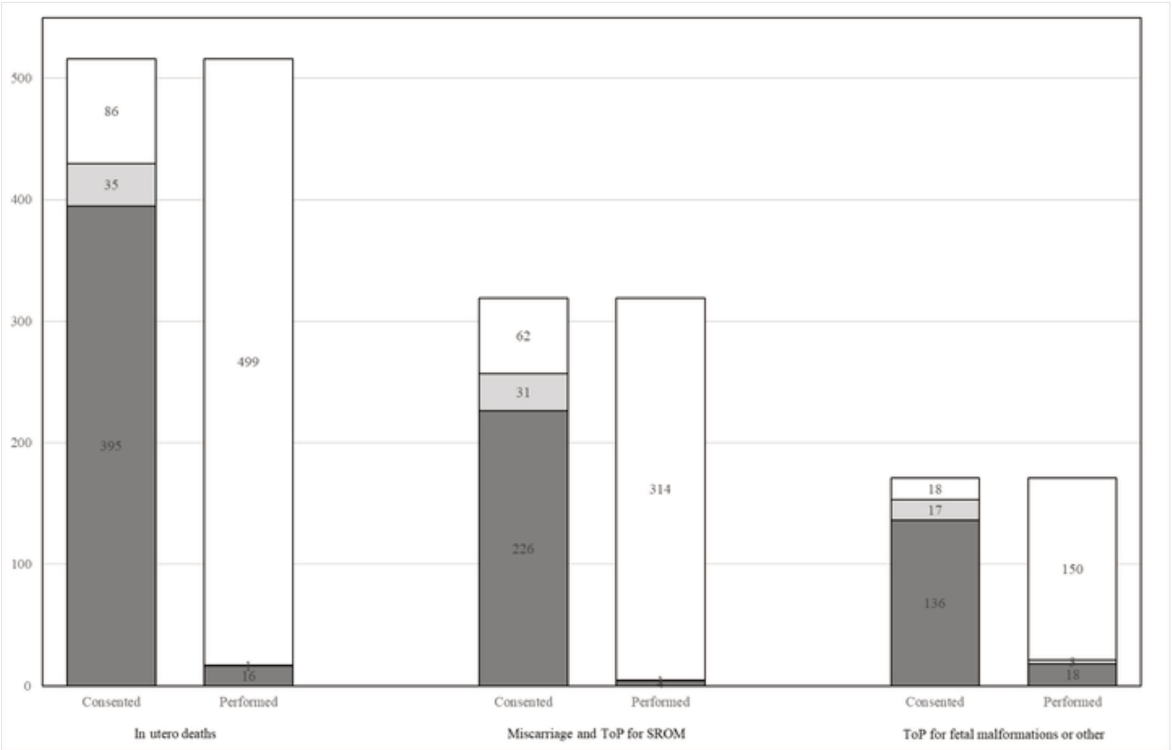

Figure 3

Click here to access/download;Figure #;Figure 3.jpg



Figure 4

Click here to access/download;Figure #;Supp Figure 4.jpg

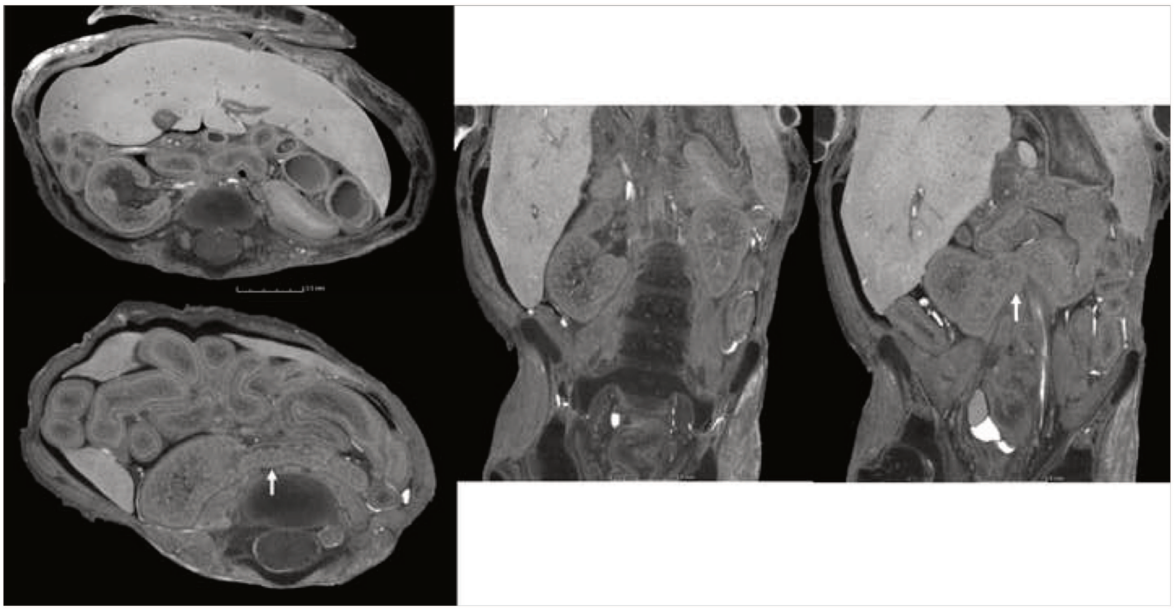

Figure 5

Click here to access/download;Figure #;Figure 5.jpg

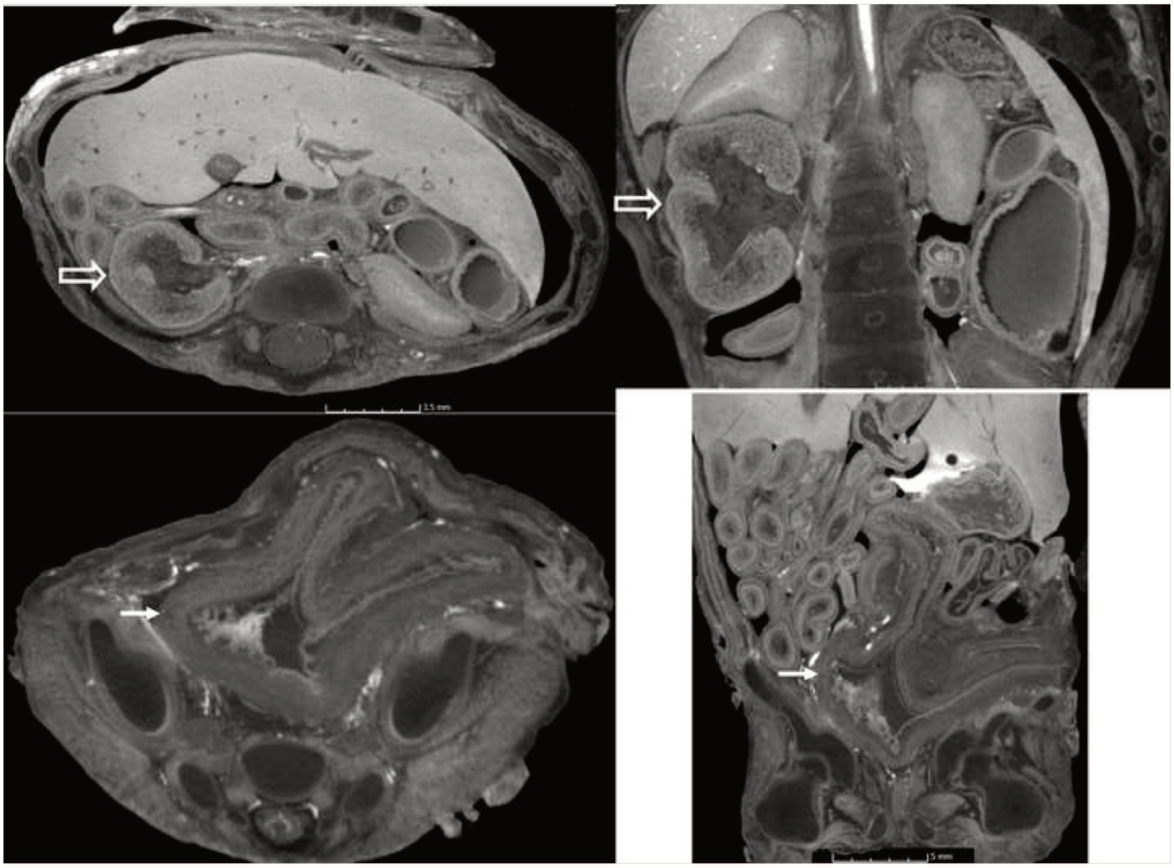

Figure 6

Click here to access/download;Figure #;Figure 6.jpg

